Exploiting reversible interactions: hydrogels and protein cross-linkers

By

Adam Belsom

Thesis for the Degree of Doctor of Philosophy

UNIVERSITY OF EDINBURGH

COLLEGE OF SCIENCE AND ENGINEERING
SCHOOL OF CHEMISTRY

July 2010

UNIVERSITY OF EDINBURGH

COLLEGE OF SCIENCE AND ENGINEERING
SCHOOL OF CHEMISTRY

Abstract for Doctor of Philosophy

Exploiting reversible interactions: hydrogels and protein cross-linkers

By Adam Belsom

A series of low molecular weight thermoreversible cystine hydrogelators were synthesised *via* solid-phase chemistry. Novel hydrogels were found to gelate at concentrations of <2 mM using microwave super-heating. Benzoyl cystine amide derivative hydrogel, which could form at a concentration of 0.5 mM, equivalent to 0.022% w/w of gelator with respect to water (an incredible 111,000 molecules of water gelated per single molecule of gelator), was applied to cell culture of cervical cancer (HeLa) cells, which were found to distribute within the gel. Hydrogels were produced on a microarray format using a novel strategy involving deposition of hydrogel solutions by inkjet printing. The incorporation of fluorescent dye (Rhodamine B) into hydrogels provided a novel means for studying hydrogel morphology.

Reversible boronate chemistry was implemented for the capture and release of proteins and peptides onto a solid-support as part of a modified peptide enrichment strategy. The strategy was proven following synthesis of hydroxamic acid and catechol modified peptides and a study of their interaction with solid-supported phenylboronic acid. NHS active ester affinity tags and cross-linkers were synthesised and applied to a 3D proteomics cross-linking analysis pipe-line. The introduction of a PEG unit led to a cross-linker with increased hydrophilicity and improved observation of both inter and intra-protein cross-links by mass spectrometry.

Declaration of Authorship

The research described in this thesis was carried out by the author under the supervision of Prof. Mark Bradley at the University of Edinburgh between May 2006 and January 2010. No part of this thesis has been previously submitted at this or any other university for any other degree or professional qualification.

Acknowledgements

I would like to thank my supervisor, Professor Mark Bradley for giving me this opportunity and for his continuous support and encouragement throughout my PhD. The patience, knowledge, enthusiasm and understanding have been greatly appreciated. I would also like to thank Dr Juri Rappsilber for his invaluable support and contributions towards the cross-linking project.

Then I would like to thank all members of both the Bradley and Rappsilber groups (past and present) who I have learnt huge amounts from and who have coloured the whole PhD experience. They are too numerous to list individually, but in particular, warm thanks to Dr. Juanjo Díaz-Mochón and Dr. Rosario Sánchez-Martín who have constantly been there for me and to Dr. Asier Unciti-Broceta who has always kept me in good spirits. Big love goes to Lois. Special thanks to Mariona, Frank, Juanma and Nicos for the banter.

I would like to acknowledge my collaborators Lau and Helena for their contributions to the work on cross-linking.

And finally thanks to my family, most importantly my long-suffering Mum and Dad who I know would do anything to help me.

Abbreviations

AMP	adenosine monophosphate
ANS	1-anilino-8-naphthalene sulfonate
BA	Boronic Acid
BAMG	(bis(succinimidyl)-3-azidomethyl glutarate)
BEN	*N,N'*-Di(benzoyl)-L-cystine diamide
BRO	*N,N'*- Di(*p*-bromobenzoyl)-L-cystine diamide
CBZ	carboxybenzyl
CPG	controlled pore glass
DCC	dicyclohexylcarbodiimide
DIC	diisopropylcarbodiimide
DIPEA	diisopropylethylamine
DMAP	4-dimethylaminopyridine
DMF	dimethylformamide
DMSO	dimethyl sulfoxide
DNA	deoxyribonucleic acid
DTT	dithiothreitol
EDC	1-ethyl-3-(3-dimethylaminopropyl) carbodiimide hydrochloride
EEDQ	2-ethoxyl-1-ethoxycarbonyl-1,2-dihydroquinoline
ELSD	evaporative light scattering detector
eq	equivalent
ES	electrospray mass spectrometry
ESI	electrospray ionisation mass spectrometry
FLU	*N,N'*-Di(*p*-fluorobenzoyl)-L-cystine diamide
Fmoc	9-fluorenylmethoxycarbonyl
FT-MS	Fourier-transform mass spectrometer
g	grams
GFP	green fluorescent protein
GLY	*N,N'*-Di(napthoyl)-L-cystine *N'',N'''*-Di(glycine) diamide
h	hours
HBSS	Hank's balanced saline solution
HBTU	*O*-benzotriazole-*N,N,N',N'*-tetramethyl-uronium-hexafluoro-phosphate
HEPES	4-(2-hydroxyethyl)-1-piperazineethanesulfonic acid
HOBt	1-hydroxybenzotriazole
HPLC	high-performance liquid chromatography

IIDQ	1-isobutoxycarbonyl-2-isobutoxy-1,2-dihydroquinoline
IPN	interpenetrating polymer network
IR	infrared
J	scalar coupling constant (NMR assignment)
L	litres
LC	liquid chromatography
λ	wavelength
m	multiplet (NMR assignment), metres, medium (IR assignment)
MALDI-TOFMS	matrix-assisted laser desorption/ionisation time-of-flight mass spectrometry
min	minutes
MOB	*N,N*'-Di(*p*-anisoyl)-L-cystine diamide
mol	moles
mp	melting point
MS	mass spectrometry
mw	molecular weight
m/z	mass to charge ratio
NAP	*N,N*'-Di(2-naphthoyl)-L-cystine diamide
NHS	*N*-hydroxysuccinimide
NHSS	*N*-hydroxysulfosuccinimide
NMM	*N*-methylmorpholine
NMR	nuclear magnetic resonance
NOESY	nuclear Overhauser effect spectroscopy
PBA	phenylboronic acid
Pbf	2,2,4,5,7-pentamethyldihydro-benzofuran-5-sulfonyl
PBS	phosphate buffered saline
PEG	polyethyleneglycol
PHE	*N,N*'-Di(napthoyl)-L-cystine *N'',N'''*-Di(phenylalanine) diamide
PS	polystyrene
Rf	retention factor
RNA	ribonucleic acid
rt	room temperature
RP	reverse phase
s	singlet (NMR assignment), seconds, strong (IR assignment)
SEM	scanning electron microscopy
SHA	salicylhydroxamic acid

t	triplet (NMR assignment)
TEM	transmission electron microscopy
TBA	tetrabutyl ammonium
TCEP	*tris*(2-carboxyethyl)phosphine
TE	tris/EDTA
TEA	triethylamine
TEAB	triethylammonium bicarbonate
TFA	trifluoroacetic acid
TFCS	tridecafluoro-1,1,2,2-tetrahydrooctyl dimethylchlorosilane
THF	tetrahydrofuran
THP	tetrahydropyranyl
TIS	triisopropylsilane
TLC	thin layer chromatography
Trt	trityl
UV	ultraviolet
UV-VIS	ultraviolet-visible spectroscopy
W	weak (IR assignment)

Contents

Chapter 1: *Gels*

1.1 Introduction

It can be said that a gel or jelly is easier to recognise than it is to describe. The first definition by Graham[1] in 1861 was based on the qualitative macroscopic observations that could be made at the time and was "rigidity of the crystalline structure shuts out external impressions, the softness of the gelatinous colloid partakes of fluidity." 80 years ago Lloyd[2] stated that:

> "Only one rule seems to hold for all gels, and that is that they must be built up from two components, one of which is a liquid at the temperature under consideration, and the other of which, the gelling substance proper, is a solid. The gel itself has the mechanical properties of a solid, *i.e.*, it can maintain its form under the stress of its own weight, and under mechanical stress, it shows the phenomenon of strain."

This definition is as true today as it was in 1926 and its tone has been prophetic. Over 100 years after the first definition by Graham, Flory provided an update in order to correlate the microscopic and macroscopic properties of a gel:

> "One may infer from this universal characteristic of those systems regarded as gels that they must possess a continuous structure of some sort, the range of continuity of the structure being of macroscopic dimensions.....If it be granted that the presence of a continuous structure is the feature common to all gels, then it becomes important to differentiate the several kinds of structures occurring in various gels."[3]

Flory then went on to give the four types of gel, classified according to their structural basis; well-ordered lamellar structures, covalent polymeric networks, polymer networks formed through physical aggregation and particulate, disordered structures.

A basic definition of a gel can be given as a material having the structural coherence of a solid but swollen as a result of having a composition with a predominantly liquid content. Gels can be either inorganic or organic in nature. The liquid component in the gel can be water, whereby the gels are referred to as *hydrogels*, or an organic solvent, producing a resulting gel that can be called an *organogel*.

There has always been an enormous amount of interest in gels because their physical and morphological properties are applied in many areas including in foods, as templated materials,[4] drug delivery agents,[5,6] cosmetics,[7,8] lubricants,[9] enzyme immobilization matrices[10] and separation media.[11] In recent years there has been an explosion in interest in organogels[12] while there are increasing demands for biocompatible gels for the study and manipulation of human cells.[13]

Just as there is an enormous scope for applications of hydrogel, the range of chemistries and compounds that are capable of gelating solvent is huge. Most of the gels that are known and familiar to scientists consist of natural polymeric compounds such as gelatine, pectin and agarose. Inorganic gels prepared by swelling silica in organic solvents are very familiar to all modern day organic chemists and swollen organic polymers such as styrene-divinylbenzene have found widespread use in solid phase organic chemistry. Four main classes of gelators can thus be considered: 1) synthetic polymers, 2) natural polymers 3) inorganic materials, and 4) low-molecular weight organic compounds.

1.1.1 Synthetic polymeric hydrogels

The majority of reported gels are three-dimensional networks swollen by solvent and consisting of hydrophilic homopolymers or copolymers.[14,15] In most cases the three-dimensional network is stabilised by polymer chains being either covalently or ionically crosslinked.[16] Wichterle and Lim developed the first polymeric hydrogel network in 1954, a copolymer of 2-hydroxyethyl methacrylate (HEMA) and ethylene dimethacrylate (EDMA) prepared by free radical polymerisation.[17] Work continued

and in the 1960's the enormous commercial potential of versatile synthetic polymeric hydrogels was recognised.

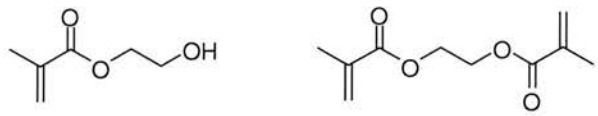

HEMA EDMA

Figure 1.1 Copolymer monomers. Copolymerisation of two monomers 2-hydroxyethyl methacrylate (HEMA) and ethylene dimethacrylate (EDMA) produced the first polymeric hydrogel network.

Gelation occurs in a multiple step process. Firstly the three-dimensional network must be formed and secondly the network must act as a microporous structure that is capable of absorbing water. This results in swelling of the polymer chains to create a hydrogel, with increasing amounts of water becoming incorporated into the gel until a saturation limit. The polymer therefore exhibits solid-like properties because of this network, whereas the liquid-like properties are a result of water being the major constituent (>80%).

The term *hydrogelator* is typically applied to a synthetic polymer if the final mass contains at least 20% water by weight.[18] A classification system that is particularly useful when considering biomedical applications is to classify polymer hydrogels as neutral hydrogels, ionic hydrogels and swollen interpenetrating networks (IPNs).[19] Polymeric hydrogels are also classified according to monomeric composition, which is based on the method of preparation: homopolymeric hydrogels, copolymeric hydrogels and interpenetrating hydrogels. Depending on the ionic charges present on the monomer, the resulting hydrogels can be either neutral, anionic, cationic or ampholytic.

As the name suggests, homopolymers form a polymer network derived from only one monomer and their hydrogels are generally crosslinked. One important category of crosslinked homopolymeric hydrogels are the poly(hydroxyalkyl methacrylates), including poly(3-hydroxypropyl methacrylate) (PHPMA), poly(glyceryl methacrylate) (PGMA) and poly(2-hydroxyethyl methacrylate) (PHEMA).

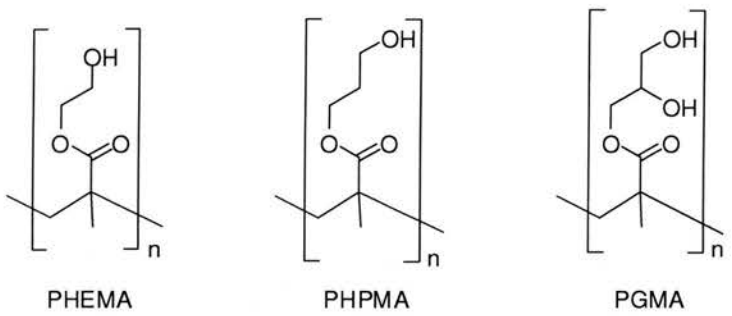

Figure 1.2 Poly(hydroxylalkyl methacrylates). Three examples of homopolymeric hydrogels.

Poly(hydroxyalkyl methacrylates) are important polymers used as materials for drug delivery and contact lenses, with PHEMA hydrogels being amongst the most widely used and studied of all synthetic hydrogel materials.[20,21]

Many commercial applications exist for gels as thickeners and expanders. Such gels include poly(N-vinyl-2-pyrrolidinone (PNVP), poly(acrylamide) (PAM), poly(ethylene glycol) (PEG) and poly(vinyl alcohol) (PVA).[22]

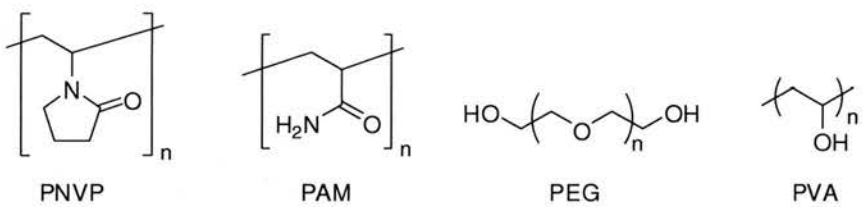

Figure 1.3 Uncrosslinked homopolymers.

PNVP and PVA have proven to be useful in biomedical applications because of increased solubility in water and an acceptable degree of solubility in many other solvents, both polar and non-polar.[23,24] PEG and PAM have found uses in agricultural applications.[25]

A copolymeric hydrogel is formed when two or more different monomer species are used to form the three-dimensional network. One of the components must be hydrophilic for a hydrogel to result but the advantage of using a copolymer is that the other component can be used to improve gel strength. Depending on the purpose of the hydrogel, a copolymeric system can be employed to introduce extra functionality

and usually copolymers are produced to give improved properties. The most successful copolymeric hydrogels include: NVP-co-HEMA, HEMA-co-MMA and HEMA-co-AA.[26]

One study looked at the effect of hydrogel charge density on osteoblast cell attachment.[19] Neutral hydrogels were prepared by polymerization of poly(ethylene glycol) dimethacrylate (PEGDMA) and 2-hydroxyethylmethacrylate (HEMA). Negatively charged hydrogels were produced by addition of sodium 2-sulfoethyl methacrylate (SEMA) and positively charged hydrogels via the addition of [2-(methacryloyloxy)ethyl] trimethyl ammonium chloride (MAETAC).

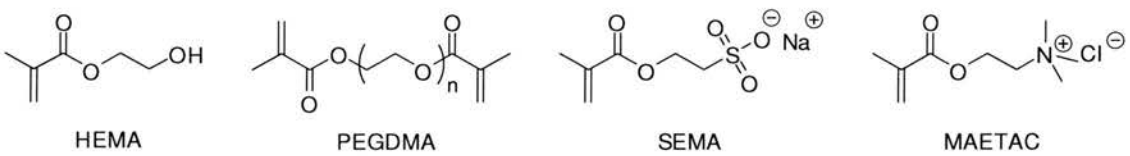

Figure 1.4 Neutral, cationic and anionic monomers used to make copolymeric hydrogels.[19]

A fourth, very important class of polymeric hydrogel materials are the so-called Interpenetrating Polymer Network (IPN) hydrogels. This class is defined as two independent crosslinked synthetic and/or natural polymer components contained in a network.[27] An IPN is typically formed by polymerisation of a second polymer inside a first polymer. This is usually achieved by swelling the first polymer with the second monomer in solution before initiation. An IPN can consist of one crosslinked component and a non-crosslinked polymer, whereby the resulting material is referred to as a *semi-IPN*.[28] A gelatin-bonded dextran based IPN hydrogel was used as a three-dimensional scaffold to encapsulate smooth muscle cells and for the 2-D culture (cell culture on a hydrogel surface) of endothelial cells.[29]

1.1.2 Low molecular weight organogelators

A low molecular weight gelator is roughly defined as a molecule with a molecular mass $\leq$3000 that is capable of reversibly aggregating/gelating a range of organic solvents at low concentrations (less than 5% w/w). Whilst the first commercial

polymeric hydrogels were being produced, low molecular weight organogelators were treated as a mere curiosity.

There is enormous structural diversity of low molecular weight organogelators (Figure 1.5).[15,30]

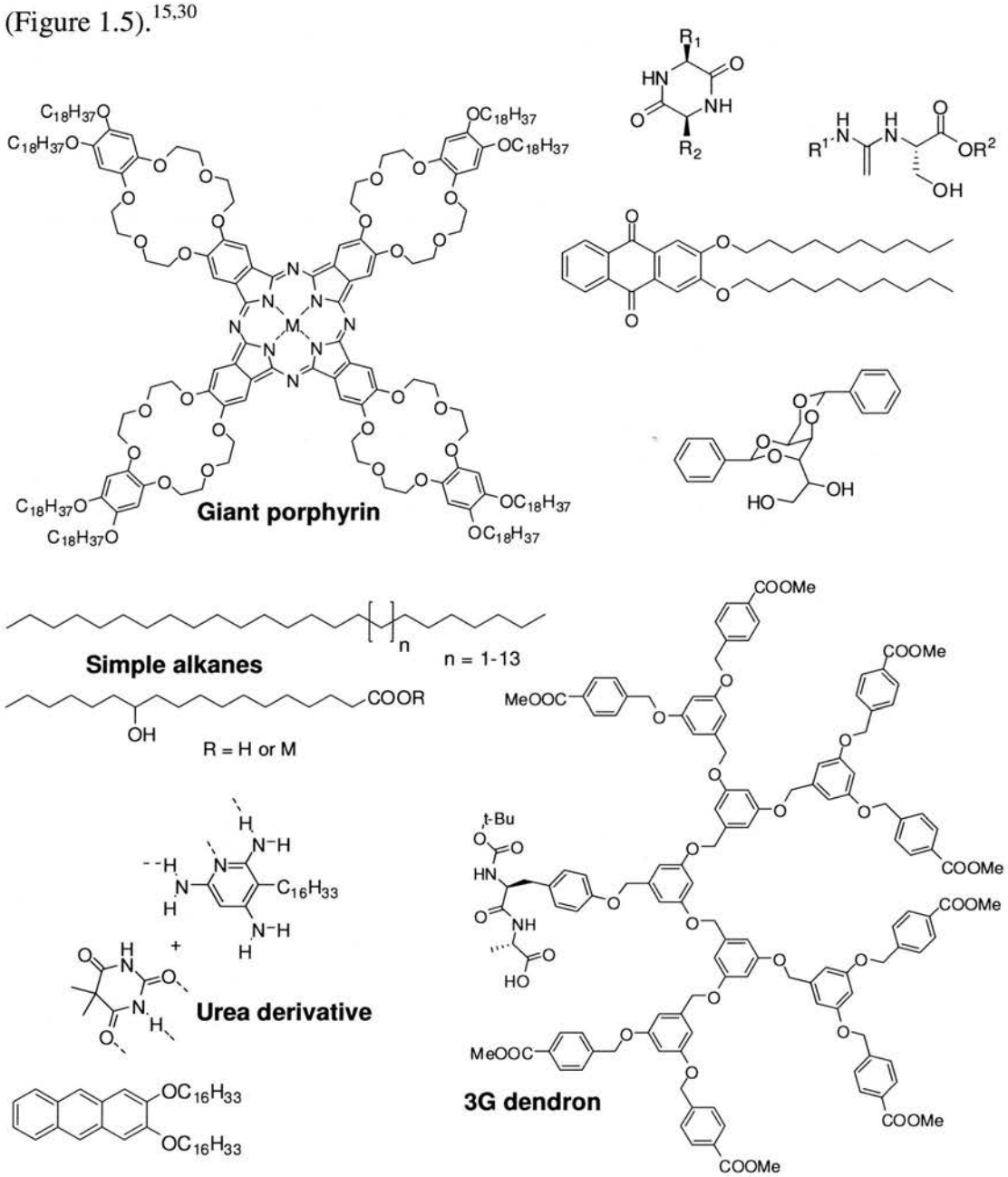

Figure 1.5 Low molecular weight organogelators.

Most low molecular weight organogelators have been discovered serendipitously, with some researchers commenting on the initial annoyance of having formed a gel.[31]

Interest in low molecular weight organogelators however has been developing since the 1990s. In fact low molecular weight hydrogelators appear to offer several advantages over polymeric hydrogels. For biological applications, one of the persistent problems that needs to be overcome for example is to find biodegradable polymers that can be used for controlled drug release.[32] Small molecule hydrogelators could be able to overcome this hurdle as many of them are derived from biocompatible components that the body could degrade. Perhaps more importantly, the huge diversity of functionality in the synthesis of gelators means that it becomes possible to incorporate a drug directly into the gelling component, eliminating the need for a prior drug capturing step.[33]

One intrinsic characteristic of virtually all low molecular weight organogelators is thermo-reversibility. Hence the preparation of an organogel usually involves warming a gelator in solvent until the solid has fully dissolved and then cooling the solution to below the gel transition temperature (T_{GS}). The gel transition temperature is the point where a solution becomes a gel, which means that it is the temperature where flow is no longer discernible over long periods a process analogous to crystallisation. Gelation is governed by the concentration of an organogelator in a specific solvent and the time taken for gelation to occur. Low molecular weight gelators have been shown to gelate a wide variety of organic solvents (such as alcohols, paraffins, aromatic and chlorinated molecules) as well as polysiloxanes, nematic and smectic liquid-crystalline materials, electrolytes and polymerisable liquids amongst others.[12]

1.1.2.1 Gelation Theory – Low molecular weight organo-gelation

Historically, the particular aggregation state of gels formed by low mass organic compounds was defined based on fairly qualitative macroscopic observations of the flow properties of materials. However advances in analytical technology have enabled the study of materials at a microscopic level. This has resulted in a much greater understanding of the chemistry of supramolecular aggregates, which includes organogels, by revealing the organisation and architecture of such materials. A

greater understanding of the nature of a gel and the mechanism of gel formation has shaped the definition of an organogel. Various theories concerning how gel formation occurs have been proposed but there are two main theories.

(I) considers gelation as a form of incomplete crystallisation where the gel consists of 'microcrystalline forms surrounded by solvent'.[34,35]

(II) proposes that gels are formed by non crystalline aggregates that trap solvent *via* surface tension within the micro-regions between them.[3,36,37]

This latter theory suggests that gelator molecules aggregate thermo-reversibly to form fibres or strands (up to micrometers in length). These fibres then form interlocking 3D networks that are capable of containing solvent molecules (Figure 1.6). The fibres or strands are held together by numerous low energy interactions and there is a range of attractive packing interactions that depend on the structure of the gelator. These interactions include London dispersion forces, hydrogen bonding and **π-π** stacking interactions between aromatic groups. The points where fibres cross-link are called 'junction zones' or 'nodes'[38] and they result in the generation of cavities that can contain the liquid component of the gel. This prevents the flow of liquid and results in an apparent thickening of the solvent. The numbers of these nodes ((pseudo)crystalline microdomains) influence both the thickness and the elasticity properties of the material and prevent phase separation into macroscopically separated crystalline and liquid layers.

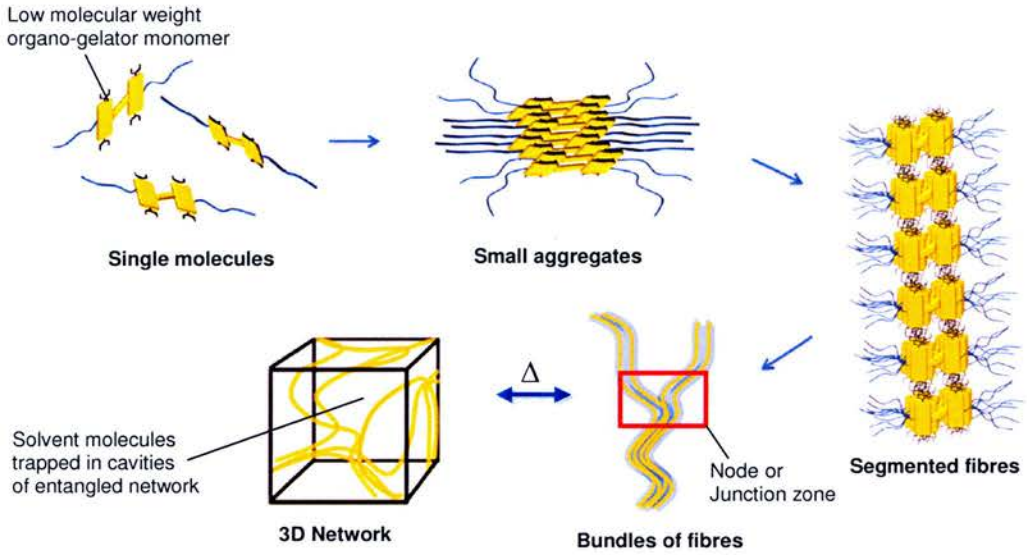

Figure 1.6 Organogel formation mechanism. [39]

Reproduced with permission (copyright American Chemical Society, 2010).

This theory is widely accepted and maintains that gels are multicomponent colloidal systems that are mainly composed of a liquid which retains its physical state at microscopic level despite having a solid-like appearance.

The structure of a gel can be broken down to a primary, secondary and tertiary level, analogous to the structural understanding of proteins (Figure 1.7).[40,41] Molecular level interactions that promote anisotropic aggregation in one or two dimensions determine the primary structure, which is on a nanometer scale with aggregation dependent upon the direction of the molecules. There must be a balance between the tendency for molecules to dissolve or to aggregate in order for gelation to occur. Hydrogen bonding interactions are very influential for organogelator aggregation and such interactions are reduced in water unless they are combined in a cooperative manner and protected from solvent.[42] In aqueous environments hydrophobic forces become more influential than hydrogen bonds in dictating gelation, while the hydrogen bonding interactions are more directing.[43] The secondary structure is defined as the morphology of the aggregates that result from the primary structure, which can be fibres, ribbons, sheets, micelles or vesicles.[44] The types of interactions that occur along the fibres determine the transition from secondary to tertiary structure. Gels can be formed by both physically branched fibres that form

interconnected networks and entangled fibres. Fibres that are physically long, thin and flexible are able to trap solvent better than shorter fibres.[3]

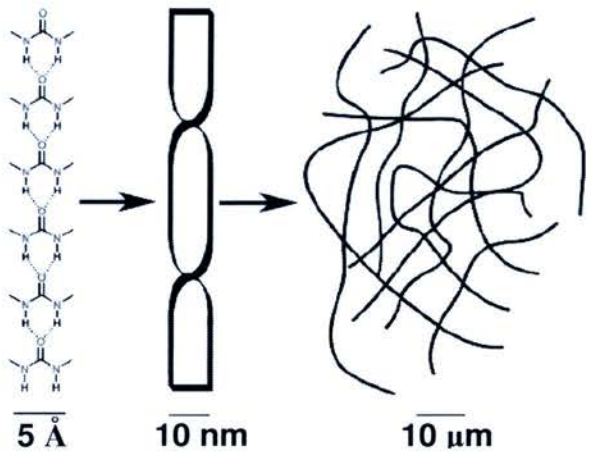

Figure 1.7 Primary, secondary and tertiary structure of a self-assembled physical gel.[14]
Reproduced with permission (copyright American Chemical Society, 2004).

The study of the mechanism of gelation has been facilitated by the use of a range of non-destructive physical techniques ranging from UV-VIS,[45] circular dichroism,[45,46,47] ^{1}H and ^{13}C-NMR,[48,49] IR,[45,50] fluorescence techniques[45,51] and differential scanning calorimetry.[48,50] Spectroscopic methods take advantage of the spectral differences between isolated 'monomeric' units and aggregated states. Electron microscopy techniques (SEM and TEM) are exceptional tools that allow clear identification and imaging of the 3D fibre like superstructures in xerogels (dry gels) (Figure 1.8).

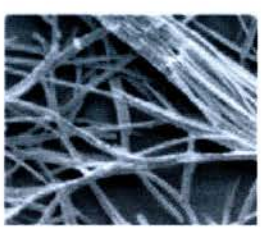

Figure 1.8 SEM of a low-molecular weight organogelator.[52]

The techniques of SANS (small angle neutron scattering) and SAXS (small angle X-ray scattering) have been applied to organogels and can provide information such as dimension and topology (these techniques use high energy X-ray beams and can characterise dilute systems such as organogels without the need for drying them first)

(Figure 1.9). These scattering experiments provide characteristic profiles for materials that are related to the morphology of the sample, to its homogeneity and the composition of the colloidal particles within it.[38,53]

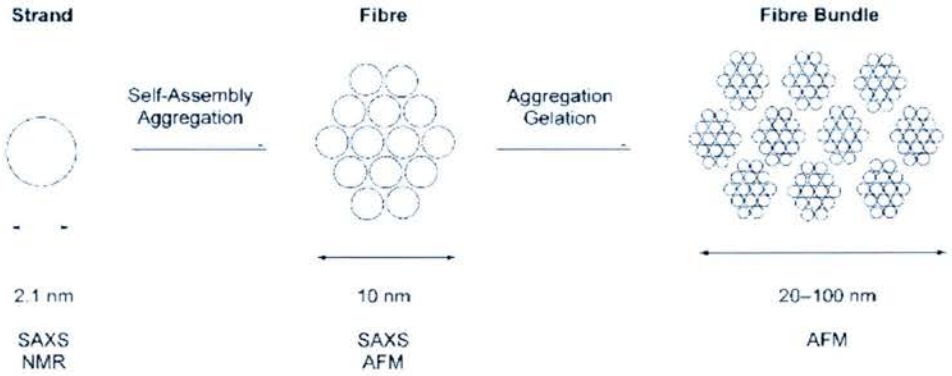

Figure 1.9 Organisation of hydrogel fibres. The three levels of organisation present in phenolic organogels (strand, fibre, fibre bundle), the length of each and the observational method utilised. Reproduced with permission (copyright Elsevier, 2001).[40]

Combining these techniques has allowed an understanding of the supramolecular organisation of self-assembled strands and fibres responsible for gel formation (1 to 1000 nm long) in some cases. However there are many important questions that remain unanswered relating to the interactions of individual gelator monomers at the 0.1-1 nm scale, such as how do assembly processes (of low molecular weight gelators into fibres) occur and how can they be controlled?[54] Studies have been carried out trying to solve the mechanism of the nucleation process[55,56] and to find out what structural features of low molecular weight organogelators are important for gel formation and stabilisation.[57]

1.1.2.2 Characterisation of a gel

A thermoreversible gel can initially be characterised by deducing its gel-to-sol phase transition temperature (T_{GS}). Usually gel melting temperature increases with an increasing concentration of gelator. T_{GS} is considered to be important because it is deemed a "measure of stability of a gel". Early empirical methods to measure gelation temperatures were based on the observation of the temperature at which a gel begins to flow, typically 'inverse flow'[46] and 'ball drop'[46,58] methods. The

'inverse flow' method is performed by forming a gel in a sealed tube and inverting it. It is then immersed and heated in a water bath and increasing its temperature at a fixed rate. The gel melting temperature being the value at which the gel falls to the bottom of the tube or when a continuous flow is observed. The 'ball drop' method is performed by placing a steel ball on top of a gel formed in a sealed tube. The gelation temperature being the temperature at which the ball falls to the bottom of the tube.[51]

Gels can be characterised rheologically and give direct information on elasticity (the ability of a deformed material to return to its original geometry, quantitatively related to a parameter known as the 'storage modulus', ***G'***) and viscosity (the tendency of a material to flow when disturbed, directly linked to a factor ***G''***, the loss modulus), allowing unambiguous evaluation of gel strength.[34] The resistance of the material to deformation is quantified with a 'yield value', defined as the 'minimum stress which has to be applied before a significant flow can occur'.[38] These measurements also allow evaluation of gel-to-sol transition temperatures (T_{GS}), where colloidal contacts and/or colloidal structures are broken, at which point flow begins, by subjecting the gel to small discontinuous oscillating stresses while slowly increasing the temperature. T_{GS} is recorded when the gel breaks. These measurements of T_{GS} depend upon the experimental conditions (the greater the stress, the lower the T_{GS}) and therefore do not represent absolute values.[34]

1.1.3 Applications of hydrogels

The range of applications for both polymeric and low molecular weight gelators, is huge. Polymeric hydrogels have the greatest abundance of applications such as in biomedical coatings,[59] homogeneous materials such as contact lenses,[60] superadsorbent hydrophilic materials found in disposable nappies and personal hygiene products,[61] sustained drug delivery systems and water storage granules in agriculture.[62] Superadsorbent lipophilic gelators can be used to mop up oil spills.[63] Natural hydrogels such as gelatin, agar and gel forming polysaccharides are commonly used as thickening agents in the food industry.[64] Gels exploited for their

separation ability are used in electrophoresis (e.g. DNA agarose gels) and chromatography and the types of gels employed have remained relatively unchanged in composition since they were first introduced.[65]

1.1.3.1 Biomedical applications

There is a growing interest and demand for gels that can be used with cells. The study of cells and cellular processes has been greatly facilitated by the design and development of new tools including great advances in microscopy and the use of fluorescent dye technology. However cells behave differently when they are removed from their native environments and transferred to a Petri dish. This can become an extreme problem in the case of human breast epithelial cells, which proliferate like tumour cells when cultured as a two-dimensional monolayer, but exhibit normal cell growth behaviour when cultured in three-dimensional membranes that resemble their native environment.[66] It has been confirmed that embryonic stem cells differentiate more efficiently into blood-forming stem cells when cultured in three-dimensional scaffolds compared to cells cultured in two dimensions.[67] Therefore new materials that can support and stabilise cells in a 3D manner are greatly needed. Gels have many properties that make them compatible with cells.

1.1.3.2 Hydrogels as three-dimensional scaffolds and drug delivery systems

Hydrogels have great potential as scaffolds for cellular and tissue supports due to their three dimensional nature. Hydrogels also have the advantage of being able to be moulded into shapes and fill cavities. An agarose based gel scaffold employed in the regeneration of damaged spinal cord has been reported.[6] Agarose is particularly useful as a scaffold because it is biocompatible, which means that it does not cause an adverse reaction when implanted *in vivo*. The porosity and mechanical properties of the resulting gel can be manipulated such that maximum axonal outgrowth could be achieved after optimisation. The gel also acted as an embedded drug delivery system for the sustained release of neurotrophins, proteins that induce the survival, development and function of neurons.[68] Moreover, the gel could be applied directly into damaged areas of spinal cord and formed in situ, so the gel perfectly fills the

damaged areas. This allowed maximum contact between the tissues and neurotrophins being delivered to the area.

1.1.4 Discovering new classes of organogelators

There is tremendous interest in organogels and much research is focussed on finding and predicting new classes of organogelators by rational design. Several research groups have used the rationale that there is a relationship between the interactions occurring in a crystal and interactions of the solid component of a gel. X-ray analysis of crystals of organogelators reveals information about the interactions responsible for efficient packing in the solid state. This information can be applied to the design of even better gels that have various structural motifs introduced that are capable of stabilising these packing interactions. This approach has proven successful in some cases,[34,69] however it is limited[70] by the practical difficulties of obtaining crystal structures of most organogelators, due to the nature of crystallisation and gelation processes, which are often competing phenomena. The crystal structure-design approach is also limited because aggregation in solution often results in amorphous aggregates that are not revealed by looking at the solid state. The approach assumes that the only factor that dictates gelation success is the nature of interactions between "solid organogelator" monomers. The fibres in the gel state are part of a 'wet' system and therefore can not be compared with solid state aggregates.

Another approach that has been explored far less than the rational design of new classes of organogelators is the preparation of libraries of compounds. Obviously this approach is limited by the number of experiments that have to be carried out (both synthesis and screening) in order to identify the key interactions which promote and stabilise organogel formation and the functional groups responsible for gel formation occurring.[71,72]

Chapter 2: *Cystine Based Organogelators*

2.1 Introduction

Cystine derivatives are an interesting and potent class of organogelator. The gelation of dibenzoyl-L-cystine was first reported in 1892 but it wasn't until 1921 that its capability of gelating aqueous solutions, at concentrations as low as 2 mM, was studied in any depth.[73]

A key to the study of cystine organogels was the reported crystal structure of di(*p*-toluoyl)-L-cystine, where linear units appeared to be stacked one upon another (Figure 2.1).[74] Hydrogen bonding interactions between the carboxyl carbonyl (acting as the hydrogen-bond acceptor) and the amide-NH (the hydrogen-bond donor) on adjacent molecules were clearly identified. A cystine core is essential for gelation. A study in 1922 showed that replacing –S–S– with $-CH_2CH_2-$ destroyed gelation,[75] presumably because a R–S–S–R dihedral angle of 90° favours hydrogen-bonding contacts, which is backed up by X-ray data.

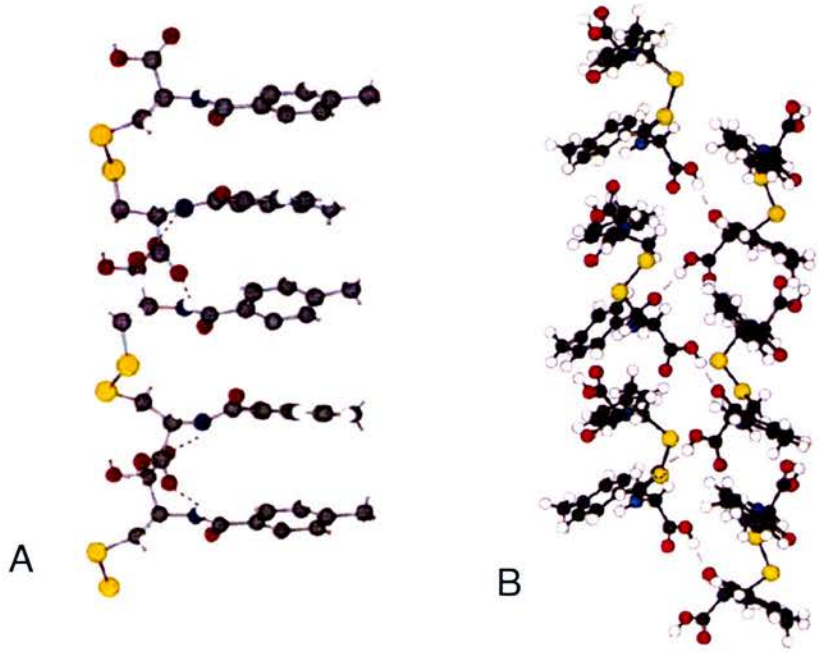

Figure 2.1 X-ray crystal structures of di(*p*-toluoyl)-L-cystine. (A) Showing intermolecular interactions. Red sphere represent oxygen, blue nitrogen and yellow sulphur atoms. The dotted lines represent hydrogen bonds between amide-NH and carboxyl-CO functionalities. (B) Two strands held together by cooperative hydrogen bonds between carboxyl-hydrogen atoms and amide-CO groups. Permission requested (copyright John Wiley and Sons, 2003).[74]

X-ray analysis showed that each unit was connected to the one above and below it by two hydrogen bonds. Aromatic rings were situated one above another, leading to the conclusion that **π-π** stacking interactions contribute to fibre stability.

Di(2-naphthoyl)-L-cystine diamide gelates aqueous solutions at 0.25 mM (ca. 0.01% w/w) in less than 30 s.[34] The incredible propensity for gel formation makes it a particularly remarkable organogelator. The hydrogen bonding interactions that each molecule makes are shown below in Figure 2.2.

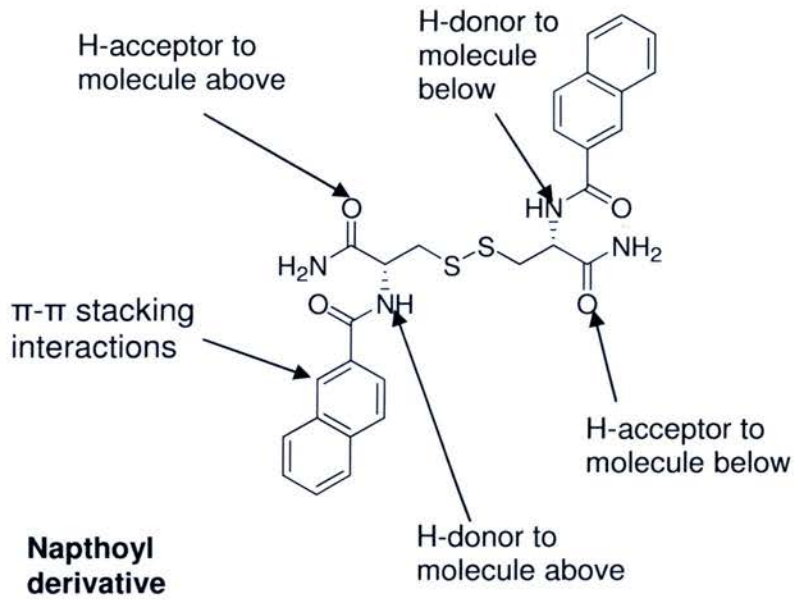

Figure 2.2 *N,N'*-Di(2-naphthoyl)-L-cystine diamide.[34] Showing the low-energy interactions that contribute to gelation.

2.2 Aims

The aims of this work were to: (i) Investigate the prospect of using cystine hydrogels as biodegradable three-dimensional scaffolds for cell culture, (ii) the development of novel ways of forming and studying cystine gelator gels, (iii) to explore further the relationships between gelator structure and subsequent gelation properties and (iv) investigate ways to degrade cystine hydrogels.

2.2.1 Solid-phase synthesis of an organogelator library

Initially a library of substituted cystine based potential organogelators was targeted. Cystine based organogelators can be readily synthesised in solution *via* standard protocols,[34] however in this work a more flexible solid phase strategy was adopted.[76]

Aminomethyl polystyrene resin **2.1** (1.6 mmol/g) and a Rink linker were used, which provides amides when cleaved from the resin. This was considered to be important because cystine amides have been shown to be more potent gelators than the corresponding acids.[34] Fmoc-Cys(Trt)-OH was coupled to the Rink amide PS-resin **2.3** followed by deprotection of the Fmoc group. After a second Fmoc deprotection, resin **2.4** was divided and each portion was coupled with a different carboxylic acid derivative capping group **2.5** to provide the compounds **2.6-2.12** shown in Table 2.1. Disulfide bond formation utilised well documented chemistry,[77] the use of iodine served to cleave the *S*-trityl protection as well as forming an intra resin disulfide bond. Compounds were cleaved from the solid-support using TFA/TIS/CH_2Cl_2 and analysed by RP-LC-MS which indicated purities greater than 95%.

Compounds **2.13** and **2.14** contained a spacer group between the capping group and cystine were synthesised by coupling either Fmoc-protected glycine or β-alanine to cysteine-supported resin **2.4**. After Fmoc deprotection, 2-napthoic acid was coupled to the free amine of **2.4**, followed by formation of an intra resin disulfide bond and cleavage from the resin.

Compounds **2.15-2.20** were synthesised by coupling either Fmoc-Gly-OH or Fmoc-Phe-OH to the free amine of resin **2.3**. Fmoc deprotection was followed by coupling of Fmoc-Cys(Trt)-OH, followed by a second Fmoc-deprotection. The resulting resins were divided and capped with one of each of the following capping groups (benzoic acid, 2-napthoic acid or 4-fluorobenzoic acid). Intra resin disulfide bond formation and cleavage from the resin was carried out as before to provide compounds **2.15-2.20**.

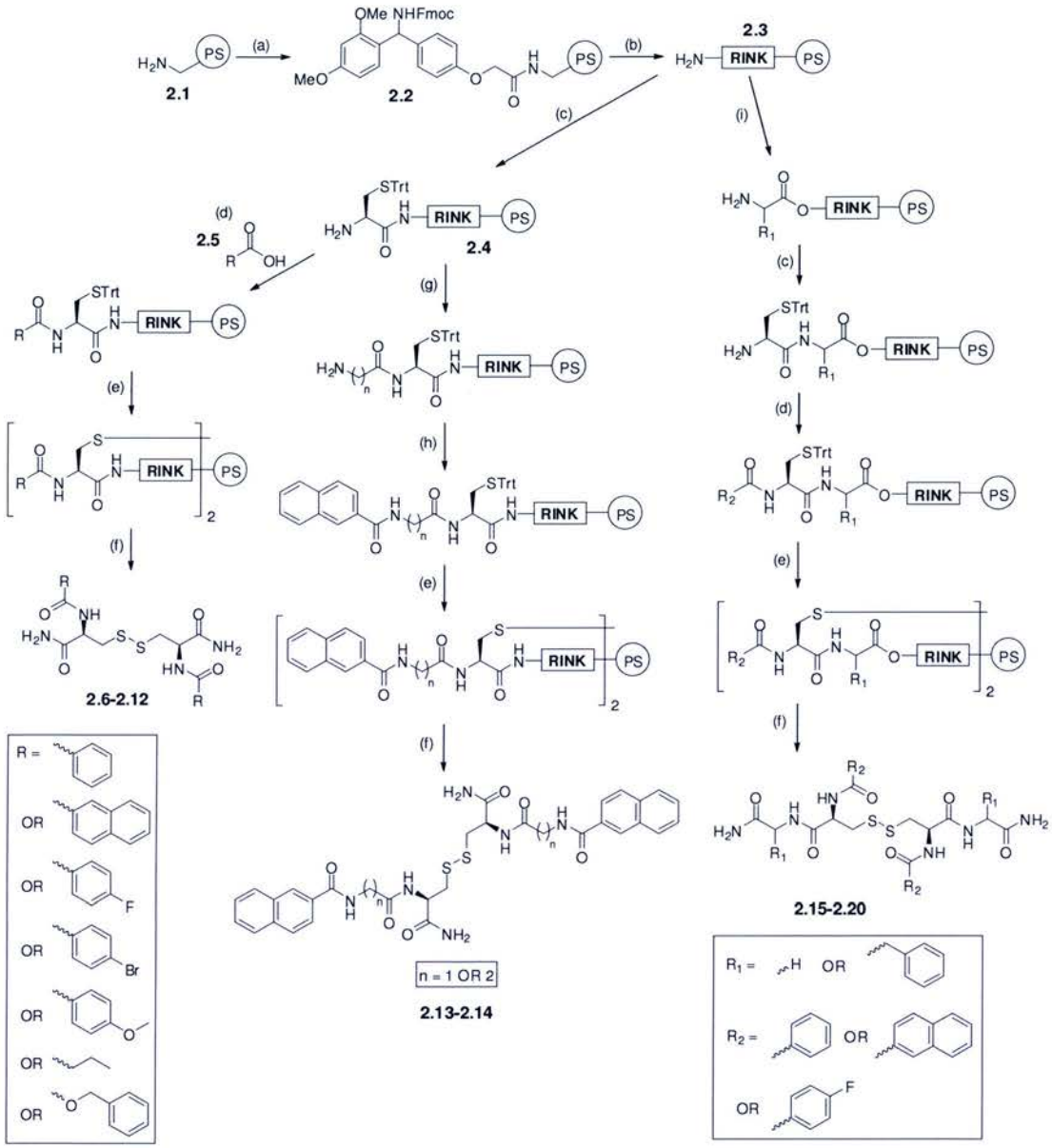

Scheme 2.1 Solid phase synthetic procedure for accessing cystine diamides 2.6-2.20.

(a) 2 eq Fmoc-Rink Amide Linker (4-[(2,4-Dimethoxyphenyl)(Fmoc-amino)methyl]-Phenoxyacetic Acid), 2 eq HOBt, 2 eq DIC, CH_2Cl_2/10% DMF, 2 h; (b) 20% piperidine/DMF, 2 x 20 min; (c) 2 eq Fmoc-Cys(Trt)-OH, 2 eq HOBt, 2 eq DIC, CH_2Cl_2/10% DMF, 2 h, then 20% piperidine/DMF, 2 x 20 min; (d) 2 eq carboxylic acid, 2 eq HOBt, 2 eq DIC, CH_2Cl_2/10% DMF, 2 h; (e) 10 eq I_2, DMF, 1.5 h; (f) TFA/TIS/CH_2Cl_2 (95:2:3), 2 h; (g) 2 eq either Fmoc-Gly-OH or Fmoc-β-Ala-OH, 2 eq HOBt, 2 eq DIC, CH_2Cl_2/10% DMF, 2 h, then 20% piperidine/DMF, 2 x 20 min; (h) 2 eq 2-napthoic acid, 2 eq HOBt, 2 eq DIC, CH_2Cl_2/10% DMF, 2 h; (i) 2 eq either Fmoc-Gly-OH or Fmoc-Phe-OH, 2 eq HOBt, 2 eq DIC, CH_2Cl_2/10% DMF, 2 h, then 20% piperidine/DMF, 2 x 20 min.

Cystine diacids **2.21**-**2.25** (Scheme 2.2) were synthesised to complement the cystine diamides synthesised in Scheme 2.1. Polystyrene Wang resin was used to provide N-terminal carboxylic acid groups following cleavage from the resin.

Compound **2.21** was synthesised by creating an ester between the Wang linker polystyrene resin hydroxyl group and the anhydride of Fmoc-Cys(Trt)-OH, formed using DIC and DMAP. Following Fmoc deprotection, the resulting free amine was capped with 2-napthoic acid, the resin was treated with iodine and the disulfide product cleaved using TFA/TIS/CH_2Cl_2 to provide **2.21**.

Compounds **2.22**-**2.25** were synthesised similarly to compound **2.21** by first coupling either Fmoc-Gly-OH or Fmoc-Phe-OH to Wang linker polystyrene resin. Following Fmoc deprotection, Fmoc-Cys(Trt)-OH was coupled to the free amine followed by a second Fmoc deprotection whereupon the resulting resins were divided and capped with either benzoic acid or 4-fluorobenzoic acid. Intra resin disulfide bond formation and cleavage from the resin was carried out as before to provide compounds **2.22**-**2.25**.

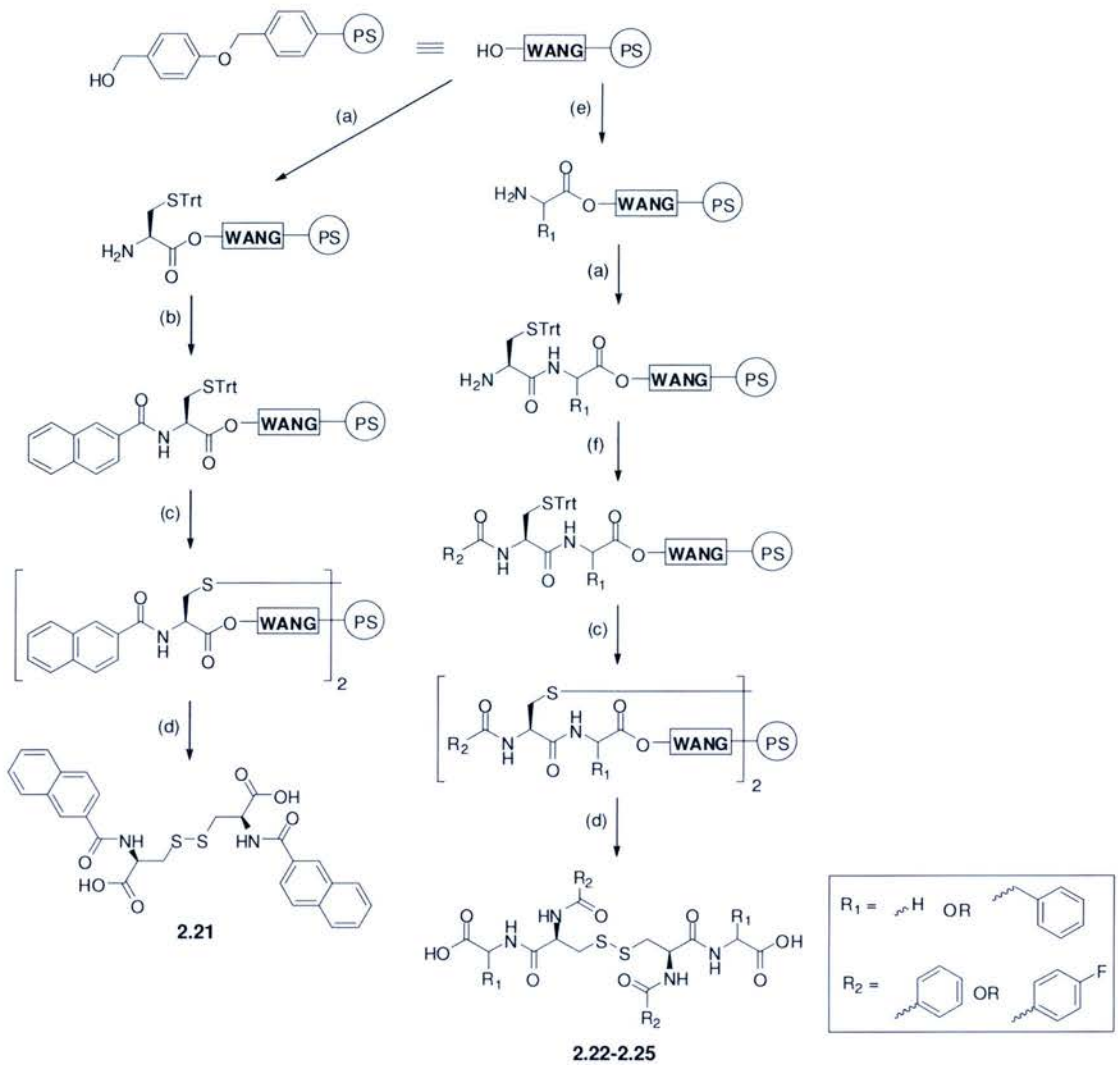

Scheme 2.2 Solid phase synthetic procedure for accessing cystine diacids 2.21-2.25.

(a) 10 eq Fmoc-Cys(Trt)-OH, 5 eq DIC, 0.1 eq DMAP, 2 h, then 20% piperidine/DMF, 2 x 20 min; (b) 2 eq 2-napthoic acid, 2 eq HOBt, 2 eq DIC, CH_2Cl_2/10% DMF, 2 h; (c) 10 eq I_2, DMF, 1.5 h; (d) TFA/TIS/CH_2Cl_2 (95:2:3), 2 h; (e) 10 eq either Fmoc-Gly-OH or Fmoc-Phe-OH, 5 eq DIC, 0.1 eq DMAP, 2 h, then 20% piperidine/DMF, 2 x 20 min; (f) 2 eq carboxylic acid, 2 eq HOBt, 2 eq DIC, CH_2Cl_2/10% DMF, 2 h.

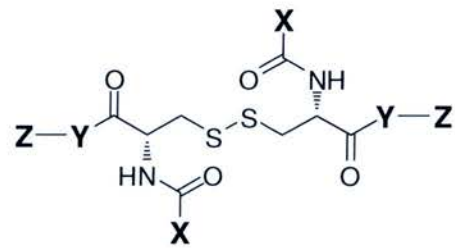

	X	Y	Z
2.6	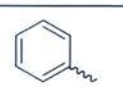		$\sim NH_2$
2.7	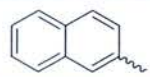		$\sim NH_2$
2.8	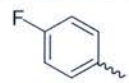		$\sim NH_2$
2.9	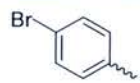		$\sim NH_2$
2.10	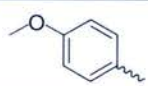		$\sim NH_2$
2.11			$\sim NH_2$
2.12	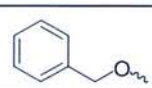		$\sim NH_2$
2.13	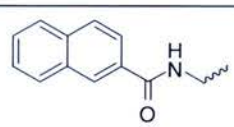		$\sim NH_2$
2.14	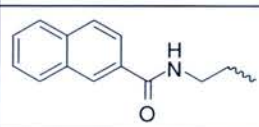		$\sim NH_2$
2.15	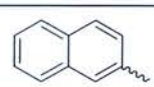	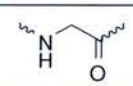	$\sim NH_2$
2.16	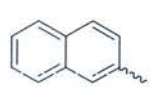	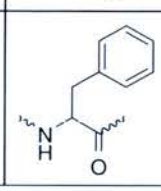	$\sim NH_2$

	X	Y	Z
2.17	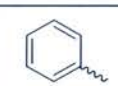	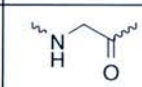	$\sim NH_2$
2.18	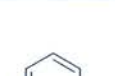	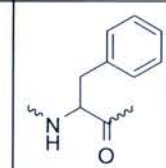	$\sim NH_2$
2.19	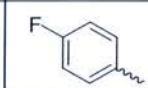	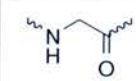	$\sim NH_2$
2.20	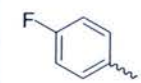	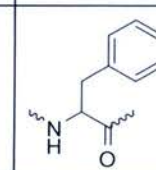	$\sim NH_2$
2.21	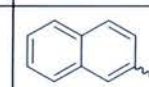		$\sim OH$
2.22	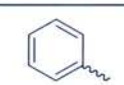	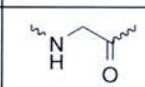	$\sim OH$
2.23	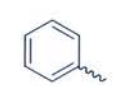	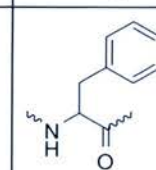	$\sim OH$
2.24	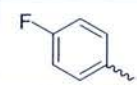	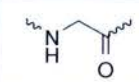	$\sim OH$
2.25	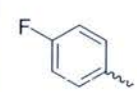	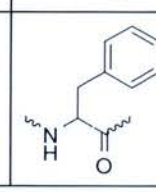	$\sim OH$

Table 2.1 Library of *N,N'*-diacylcystine derivatives.

Water-rich gels of benzoyl **2.6** and 2-naphthoyl **2.7** were made using the hot solvent method according to the literature.[34] Gels were formed by dissolving solid compound in the required volume of hot solvent and allowing the solution to gradually cool down from about 90 °C to room temperature; a process analogous to crystallisation. As before the common problem was insolubility, with crystallisation and precipitation often occurring as the dominant processes over gelation. Gelation of water could only be achieved by dissolving the solid compound in hot DMSO and introducing hot water, the DMSO acting to pre-dissolve the solid.

Crude napthoyl derivative **2.7** was screened in 25% DMSO/75% H_2O and was found to gelate the water rich mixture at the amazingly low concentration of 0.5 mM (0.03% w/w), shown in Figure 2.3. Upon addition of hot water to compound pre-dissolved in DMSO, the napthoyl derivative **2.7** formed a gel almost instantaneously and furthermore the resulting gel was completely transparent and homogeneous.

Figure 2.3 0.5 mM *N,N'*-Di(2-naphthoyl)-L-cystine diamide gel 2.7. 25% DMSO/H_2O gel.

Various concentrations of DMSO (5-25% v/v) were examined in order to qualitatively assess the effect of co-solvent upon gelation (see Figure 2.4).

For each concentration of DMSO, a final gelator concentration of 2 mM (0.11% w/w) was used, with the solid compound dissolved in hot DMSO, heated in a water bath at 90 °C, followed by the addition of hot water. This corresponded to a ratio of 22,765 molecules of solvent for every molecule of gelator!

Gel formation was defined by the ability to rigidify the solvent such that it was self-supporting upon inversion of the vial containing the gel. Jelly was defined as an inhomogeneous mixture of "gel lumps" and solution, which in most cases had increased viscosity compared with the solvent without gelator. The gelation process was heavily influenced by the percentage of DMSO used. Gel formed so rapidly that in many instances it was not possible to add the volume of water required to reach the desired concentration. The result was formation of a dense lump of gel and a separate liquid phase composed almost entirely of unincorporated water.

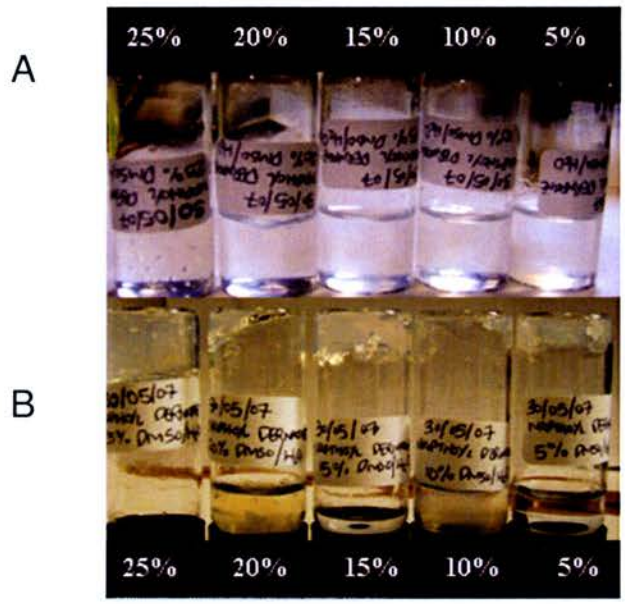

Figure 2.4 Different DMSO/H_2O ratios gelated by *N,N'*-Di(2-naphthoyl)-L-cystine diamide 2.7. 2 mM concentration (percentage of DMSO is shown). (A) Gel prior to inversion. (B) Inverted gel.

With 25% DMSO/H_2O there was evidence of randomly distributed air bubbles within the gel that had been incorporated with the addition of water, which was evidence that gel formation had occurred very rapidly. Reducing the percentage of DMSO from 25% to 20% resulted in a destabilisation of the gel upon inversion with the gel collapsing under gravity. Reducing the percentage of DMSO further to 15% resulted in definite phase separation, where half the matter was composed of a dense, rough gel and approximately half the water had failed to become incorporated in the gel. This trend continued as the percentage of DMSO was decreased. 25% DMSO/H_2O formed the most uniform gel in the series, which was the least cloudy with the smoothest consistency. This experiment demonstrated the inherent

difficulties in making qualitative definitions regarding gel formation. Subtle differences in the dimensions of the vial used also influenced the outcome of each experiment.

2.3 Microwave-assisted hydrogelation

Sonication and traditional oil/water bath heating both failed to produce consistent results, in most instances precipitation was favoured over gelation and in many cases inhomogeneous/inconsistent gels formed. A method was required to remove the need for using DMSO in order to solubilise the gelator.

Since microwave heating was introduced to the chemical laboratory there have been a surge of papers touting the benefits of using microwaves over conventional oil bath heating. Microwave heating allows heating at temperatures that far exceed the boiling points of solvents at increased pressure. Microwave heating doesn't involve temperature hot-spots that occur with conventional heating systems due to the inside-to-out nature of microwave energy transfer, and it has been proven that temperature ranges within a microwave reaction vessel are much lower than variations that occur with oil-bath heating.[78]

At 250 °C, water has a density and polarity similar to that of acetonitrile at room temperature.[79] The dielectric constant of water (ε') drops rapidly with temperature and at 250 °C it has fallen from 78.5 (at 25 °C) to 27.5.[80] This means that the solubility of organic compounds increases as the temperature is increased.

Gelation of napthoyl cystine amide derivative **2.7** in pure water was attempted using a single-mode microwave. A range of temperatures was used between 100 °C and 200 °C with a series of different concentrations to investigate the effect of microwave heating. Above 180 °C the measured internal pressure began to reach and exceed the safety level set on the machine. Figure 2.5 shows the result from 2 mM napthoyl cystine amide gelator **2.7**. After cooling it was observed that at 100 °C there was un-dissolved compound. At 120 °C and 140 °C the solution became increasingly

cloudy but still there was a large degree of insolubility and precipitation. Gel formed at 160 °C and 180 °C but was heterogeneous; a large volume of water had not been incorporated into the gel phase. The gels were stable to inversion at these temperatures but were cloudy and inhomogeneous.

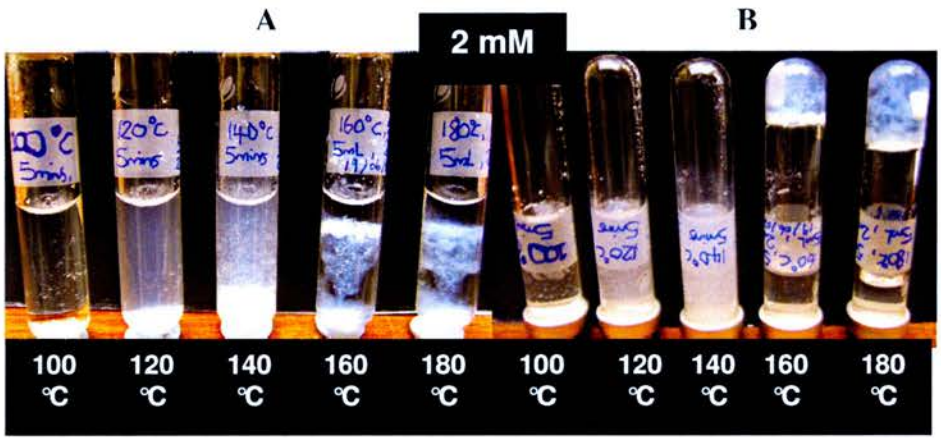

Figure 2.5 Microwave-assisted hydrogel formation. 2 mM *N,N'*-Di(2-naphthoyl)-L-cystine diamide **2.7**. Microwave heating for 5 mins at temperatures between 100-180 °C.

The result of 1 mM **2.7** is shown in Figure 2.6. Again it was observed at 100 °C and 120 °C that gelation had not occurred. Upon inversion, a self-supporting gel was produced at 140 °C but with evidence of a clear gel with a large amount of un-dissolved compound. At 160 °C and 180 °C all compound had dissolved with a more homogeneous gel formed at the higher temperature.

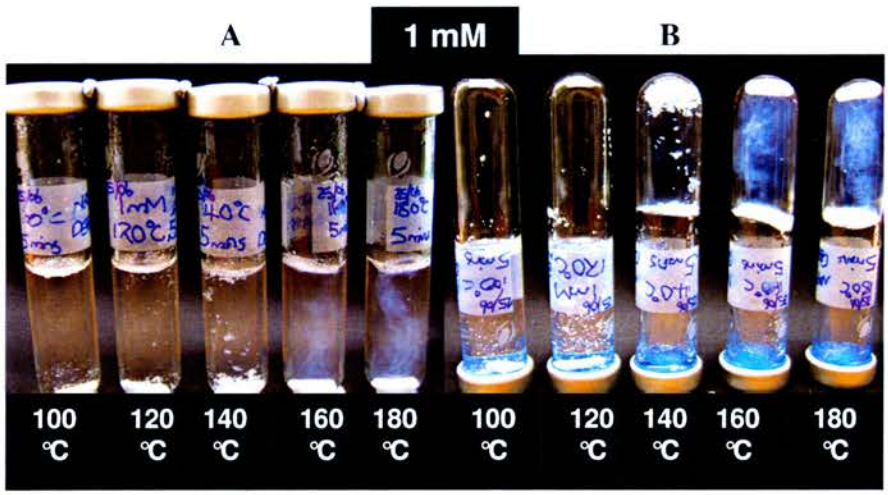

Figure 2.6 Microwave-assisted hydrogel formation. 1 mM *N,N'*-Di(2-naphthoyl)-L-cystine diamide **2.7**. Microwave heating for 5 mins at temperatures between 100-180 °C.

Very similar results were produced when the concentration of napthoyl cystine amide gelator was reduced to 0.5 mM (Figure 2.7).

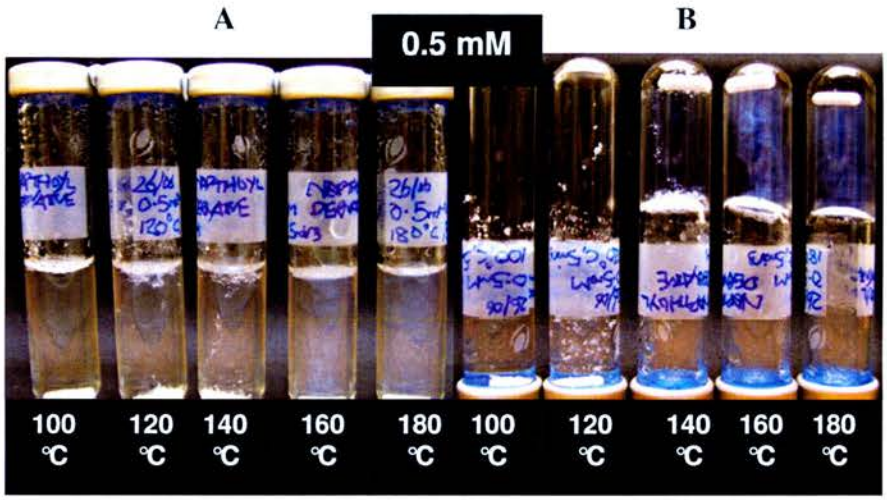

Figure 2.7 Microwave-assisted hydrogel formation. 0.5 mM *N,N'*-Di(2-naphthoyl)-L-cystine diamide **2.7**. Microwave heating for 5 mins at temperatures between 100-180 °C. (A) Before vial inversion. (B) After vial inversion.

A self-supporting gel was formed at 140 °C, which was equivalent to 111,000 molecules of water per molecule of gelator. However at 140 °C there was still evidence of incomplete solubility whereas at 160 °C and 180 °C there was no evidence of solid, which meant that all compound had been dissolved at these temperatures, although the resulting gel was not clear. 0.5 mM was the lowest concentration that could form a gel.

The optimum conditions for gelation were heating at 180 °C for 5 minutes followed by an unassisted cooling procedure to room temperature. Increasing the heating time had little effect on the solubility of gelator at different temperatures however heating for times longer than 30 minutes were found to destroy the ability to form a gel with the compound. Heating at high temperature for a long period altered the gelator such that it didn't form a gel after cooling, which is a phenomenon that needs to be investigated further.

The benzoyl cystine amide derivative **2.6** was also analysed using the microwave heating method. A range of concentrations of **2.6** in water were investigated (see

Figure 2.8), and it was observed that increasing the concentration resulted in a gradual increase in turbidity but in all cases a completely homogeneous gel. Gel formed at the low concentration of 0.5 mM (equivalent to 0.022% w/w). This was far lower than previously reported concentrations for this gelator,[34] which meant that gelation in pure water (using microwave super-heating and cooling) resulted in a far stronger gel than the gel dissolved in water and co-solvent using the traditional method. Below 0.5 mM the gel was too weak to be self-supporting and collapsed.

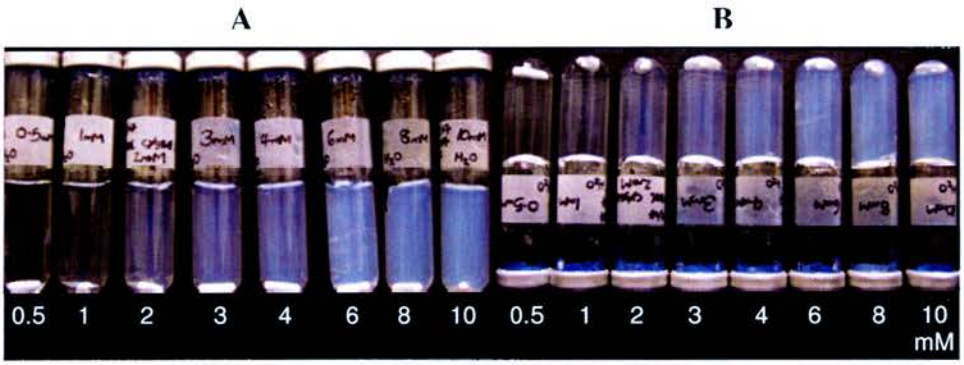

Figure 2.8 Microwave-assisted hydrogel formation of *N,N'*-Di(benzoyl)-L-cystine diamide 2.6. Microwave heating for 5 mins at 180 °C. Concentrations from 0.5-10 mM. (A) Before vial inversion. (B) After vial inversion.

2.4 Series of modified hydrogels

The gelation by microwave heating method allowed qualitative comparisons to be made of gels formed after making subtle changes in the structure of gelators.

To investigate the significance of the role of the primary amide groups on the napthoyl cystine derivative **2.6** the compound was synthesised using Wang resin (affording carboxylic acid groups after cleavage) to give compound **2.21**. The result (shown in Figure 2.9) was that there was no gel formation when the amide groups were exchanged.

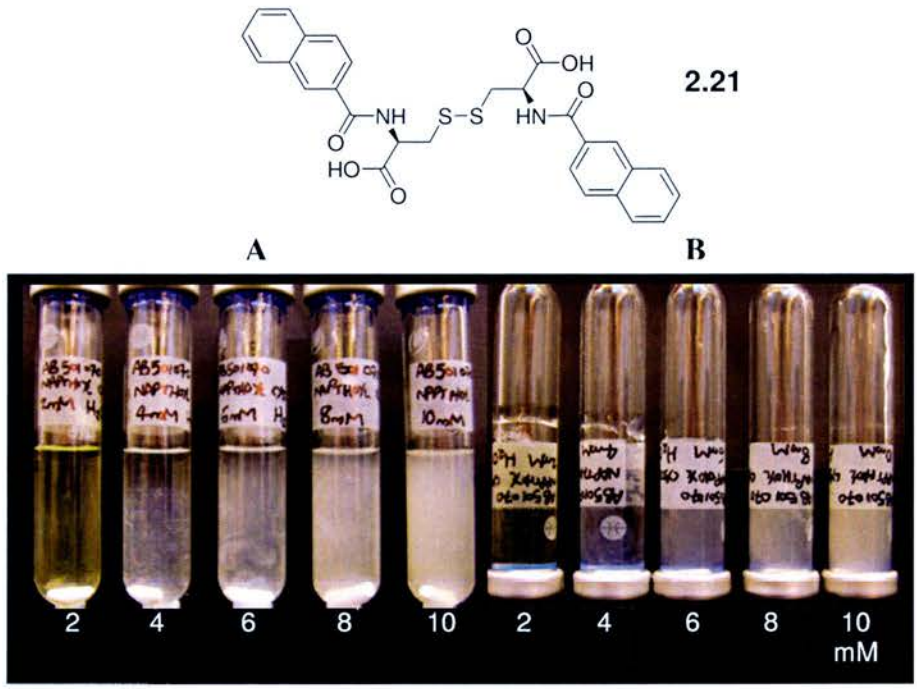

Figure 2.9 Attempted hydrogelation of *N,N'*-Di(2-naphthoyl)-L-cystine 2.21. Microwave heating concentrations between 2-10 mM for 5 mins at 180 °C. (A) Before vial inversion. (B) After vial inversion.

There is interest in gelators that have extra amino acids added to the core cystine or between the cystine core and the capping groups because these gelators could be enzymatically cleaved.

Two gelators were synthesised using Rink Amide resin, which afforded primary amide derivatives after cleavage from the resin, one with glycine **2.15** and one with phenylalanine **2.16** coupled to Rink Amide resin followed by Fmoc deprotection and cysteine coupling. The amine group from the cysteine was capped with 2-napthoic acid.

The results are shown in Figure 2.10. After cooling to room temperature, phenylalanine derivative **2.16** formed a fine precipitate.

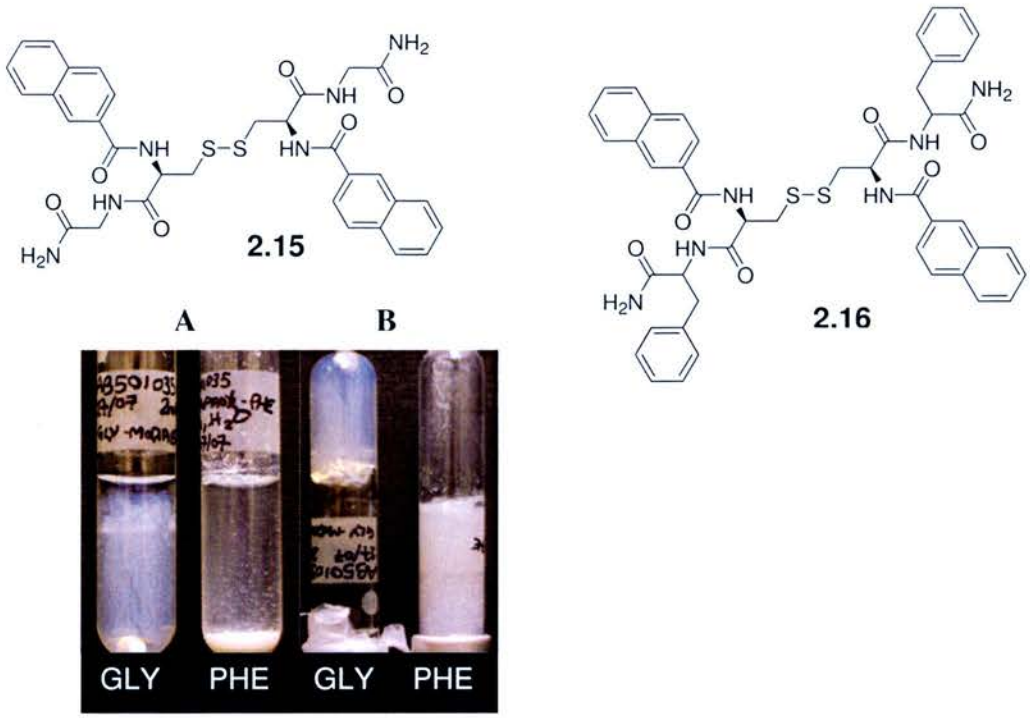

Figure 2.10 Addition of di-glycine 2.15 (GLY) and di-phenylalanine 2.16 (PHE) to di-napthoyl cystine gelators. 2 mM hydrogel. (A) Before vial inversion. (B) After vial inversion.

In contrast, glycine derivative **2.15** was able to form a waxy gel. This suggested that adding two secondary amide bonds did not significantly reduce gelation ability but adding two extra phenyl groups to the gelator **2.16** completely destroyed gelation ability.

Two compounds were synthesised, one with a two carbon spacer between the cystine and the capping group **2.13** and the other with a three carbon spacer **2.14** (Figure 2.11).

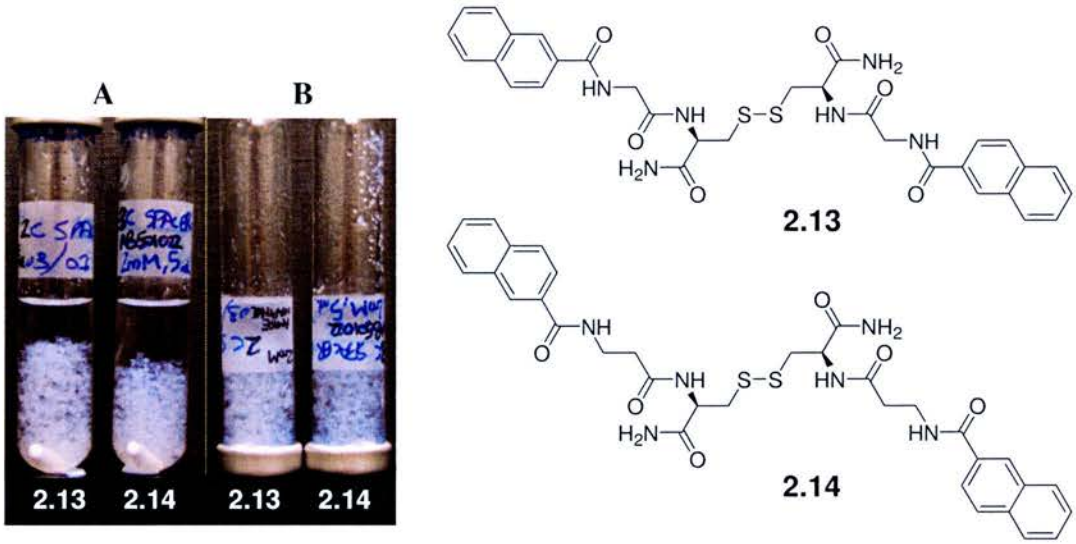

Figure 2.11 Addition of alkyl spacers to di-napthoyl cystine gelators. 2 mM **2.13** and **2.14** in H_2O. (A) Before vial inversion. (B) After vial inversion.

In both cases a fluffy white precipitate was produced. The length of spacer inserted between the cystine and the terminal capping group clearly influencing gelation ability and affecting solubility.

For subsequent compounds it was decided to change the napthoyl capping group to the less bulky benzoyl group and a second series with a 4-fluorobenzoyl capping group. Series of compounds with these capping groups were synthesised using Rink Amide resin to afford primary amide groups after cleavage from resin and Wang resin to afford carboxylic acid groups. Also the two different amino acids (glycine or phenylalanine) were again coupled. All compounds were subjected to the microwave gel forming protocol at different concentrations in water.

Derivative **2.22** with benzoyl capping groups and substituted glycine produced a self-supporting uniform gel in water at concentrations between 4-10 mM (Figure 2.12). At 2 mM the resulting gel was too weak to withstand vial inversion and there was a partial collapse from the bulk and lowering the concentration to 1 mM resulted in a clear solution. As the concentration was increased the strength of gel increased but there was also an increase in gel turbidity.

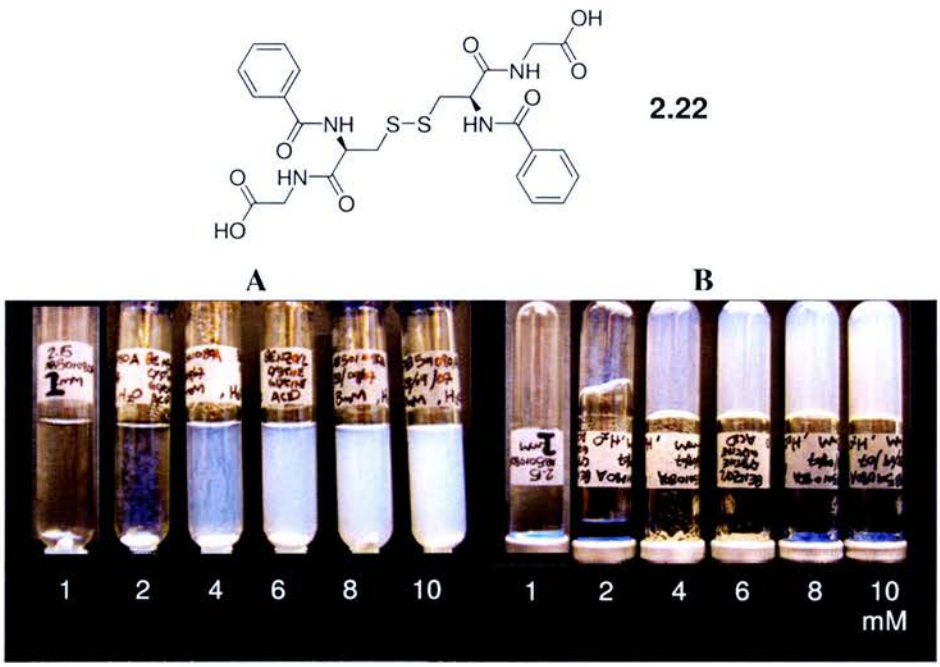

Figure 2.12 Hydrogelation of 2.22. Microwave heating concentrations between 1-10 mM for 5 mins at 180 °C. (A) Before vial inversion. (B) After vial inversion.

When the carboxylic acid group was changed to a primary amide to give derivative **2.17** there was a marked decrease in solubility in water but at 8 and 10 mM concentrations a self-supporting gel was formed (Figure 2.13). There was an increase in the amount of gelator that precipitated from solution. The resulting gel was inhomogeneous but a gel nonetheless, with 10 mM concentration corresponding to 0.74% w/w, which is still well within the 5% w/w concentration that is considered to be the limit for classification as a low molecular weight organogelator.[30]

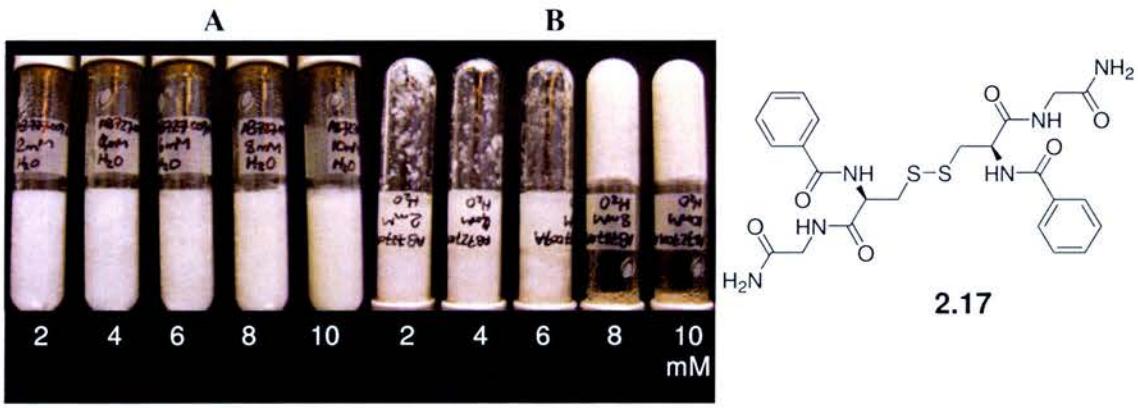

Figure 2.13 Hydrogelation of 2.17. Microwave heating concentrations between 2-10 mM for 5 mins at 180 °C. (A) Before vial inversion. (B) After vial inversion.

After inserting phenylalanine rather than glycine between Wang resin and cystine to give **2.23**, a waxy, heterogeneous gel was formed (Figure 2.14).

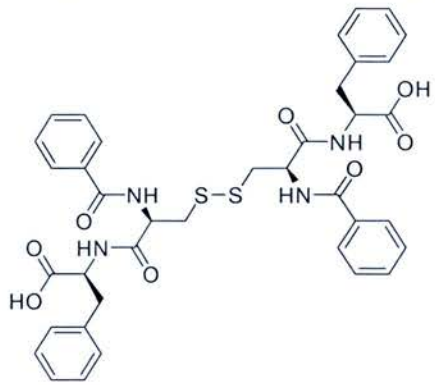

2.23

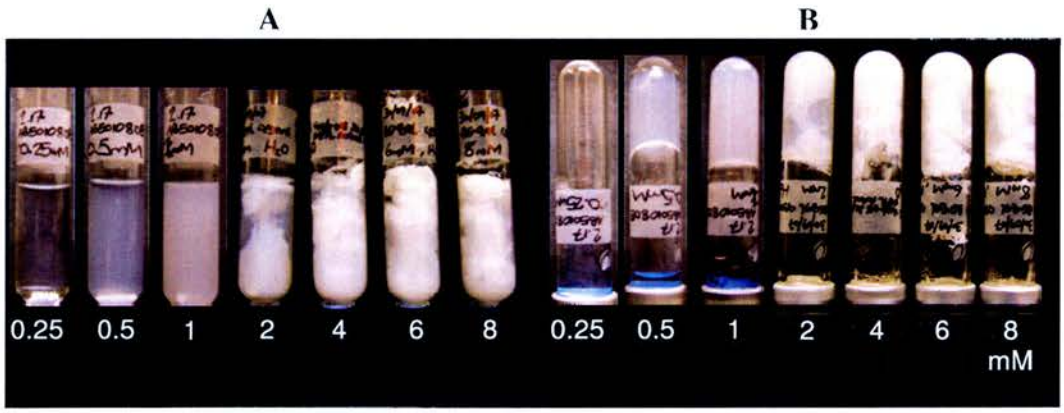

Figure 2.14 Hydrogelation of 2.23. Microwave heating concentrations between 0.25-8 mM for 5 mins at 180 °C. (A) Before vial inversion. (B) After vial inversion.

The resulting system had a large degree of aggregation in competition with gelation at 2-8 mM, compared with glycine derivative **2.22**, thus the addition of phenyl groups resulted in an increase in aggregation. Lowering the concentration to 1 mM produced a robust, albeit cloudy, gel and a partial gel resulted at 0.5 mM.

Changing the carboxylic acid groups to primary amides **2.18** resulted in a complete loss of gel formation and instead resulted in formation of waxy precipitate, with little difference between the concentrations of **2.18** (Figure 2.15).

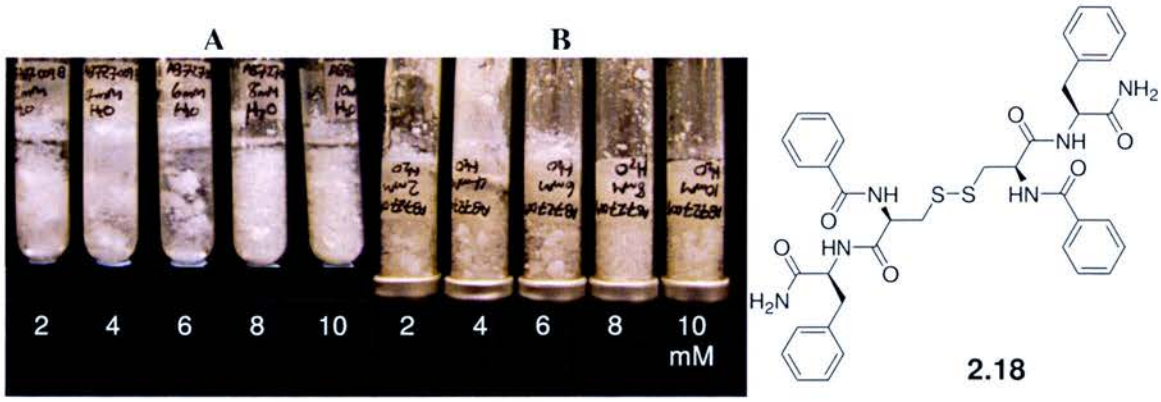

Figure 2.15 Attempted hydrogelation of 2.18. Microwave heating concentrations between 2-10 mM for 5 mins at 180 °C. (A) Before vial inversion. (B) After vial inversion.

A cystine derivative with 4-fluorobenzoyl capping groups and substituted glycine **2.24** was synthesised. The result was a new "super-gelator", with a very robust, clear gel being produced at 2 mM (Figure 2.16).

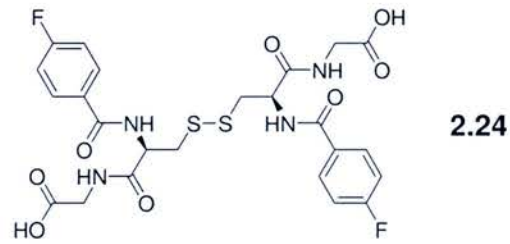

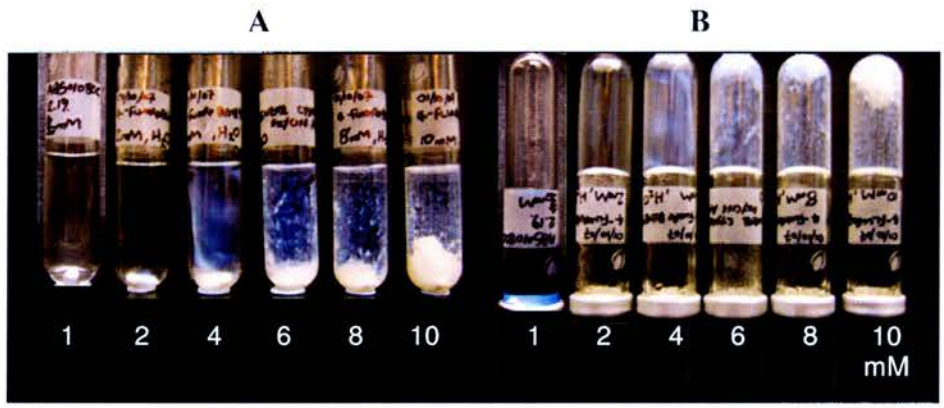

Figure 2.16 Hydrogelation of 2.24. Microwave heating concentrations between 1-10 mM for 5 mins at 180 °C. (A) Before vial inversion. (B) After vial inversion.

When the concentration was increased above 2 mM there was evidence of undissolved compound. Gel did not form when the concentration was reduced to 1 mM.

Remarkably, when the carboxylic acid groups were changed for primary amide groups with the diamide cystine derivative **2.19**, all gelation ability was lost and there was only evidence of "fluffy precipitation" (Figure 2.17).

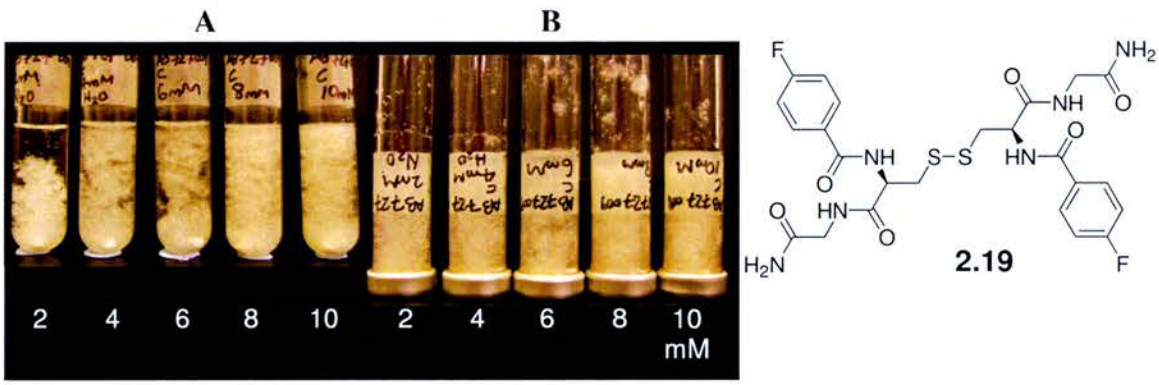

Figure 2.17 Attempted hydrogelation of 2.19. Microwave heating concentrations between 2-10 mM for 5 mins at 180 °C. (A) Before vial inversion. (B) After vial inversion.

For gelation to occur with the addition of the glycine moiety, a terminal carboxylic acid was required to increase the solubility of the compound enough to allow gelation.

4-fluorobenzoyl cystine phenylalanine acid derivative **2.25** gave gel that was increasingly turbid across the concentration range (Figure 2.18).

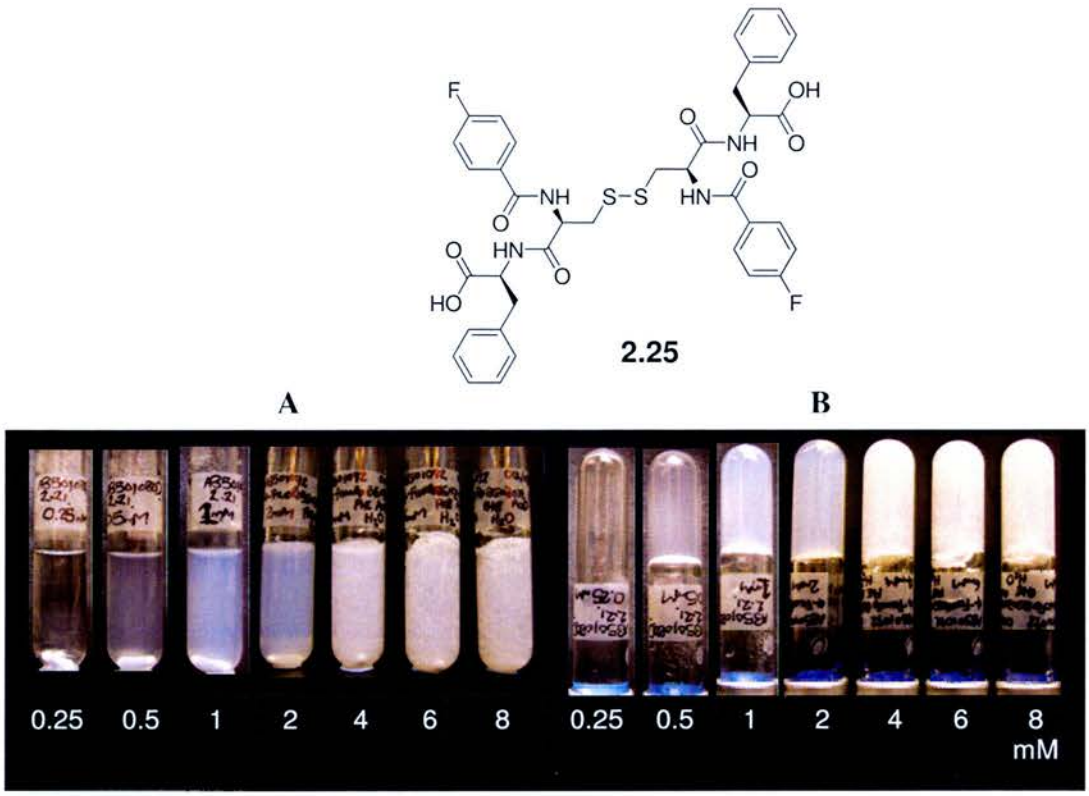

Figure 2.18 Hydrogelation of 2.25. Microwave heating concentrations between 2-10 mM for 5 mins at 180 °C. (A) Before vial inversion. (B) After vial inversion.

It was evident that addition of phenyl groups resulted in a decrease in compound solubility and the result was a waxy gel, a common feature for all gelators with additional phenyl groups.

When the terminal carboxylic acid groups were changed to primary amide groups giving **2.20** (Figure 2.19), gelation ability, that had been evident with the former compound **2.25**, was lost. Although after vial inversion the water remained in the bottom of the vial, this was due to the formation of a "plug" of compound, possibly as a result of compound remaining insoluble despite heating at high temperature and pressure.

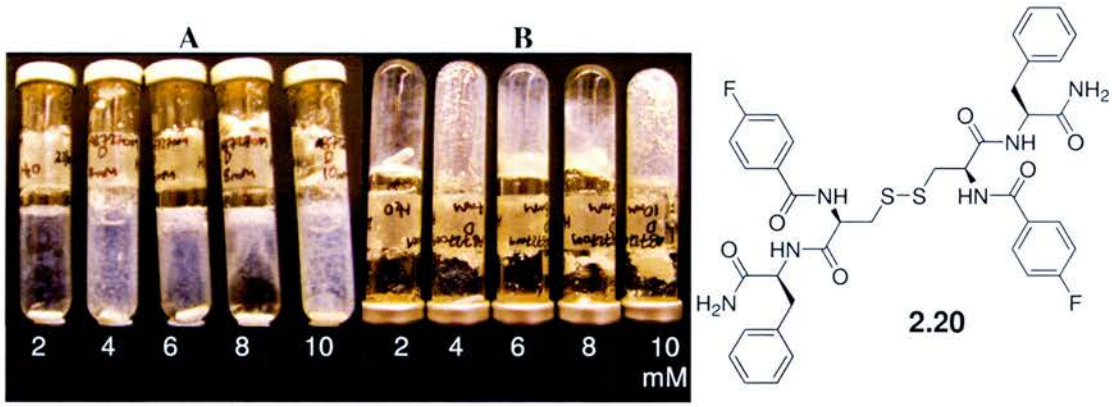

Figure 2.19 Attempted hydrogelation of 2.20. Microwave heating concentrations between 2-10 mM for 5 mins at 180 °C. (A) Before vial inversion. (B) After vial inversion.

A further modification on the original basic structure of cystine low molecular weight gelators was the introduction of a carbamate group between the cystine and the capping group **2.12**. The CBZ group was coupled onto the free amine group from the cystine. At all concentrations a turbid self-supportive gel was formed, which meant that the addition of a carbamate group could be tolerated in a gel (Figure 2.20).

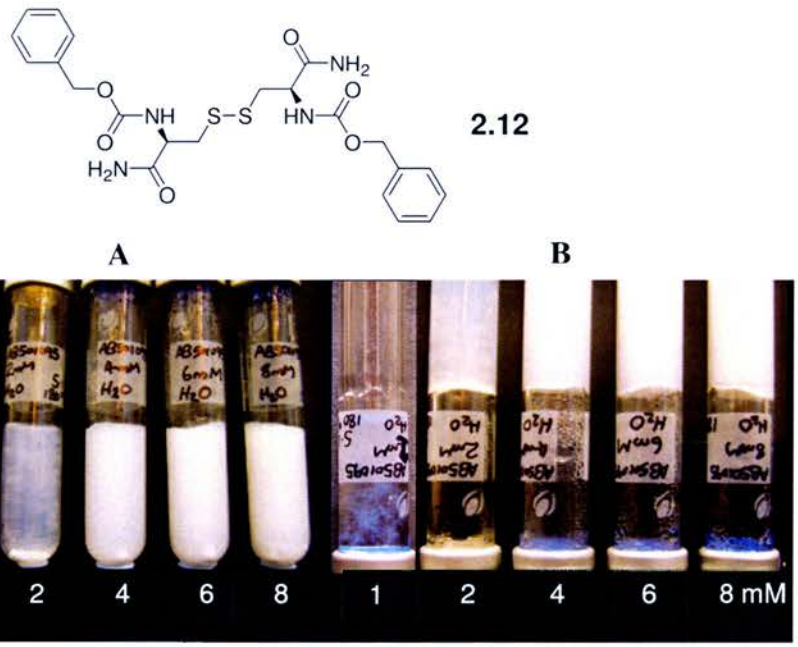

Figure 2.20 Hydrogelation of 2.12. Microwave heating concentrations between 2-8 mM for 5 mins at 180 °C. (A) Before vial inversion. (B) After vial inversion.

2.5 Practical application of benzoyl cystine amide derivative **2.6**

Although cystine based organogelators can be considered extremely fascinating and worthy of investigation in their own right, their development is important for practical use as three-dimensional cellular supports.

Benzoyl cystine diamide derivative **2.6** was chosen for this work because it forms a clear, robust and quick-forming gel.

The HeLa-GFP cell line was selected for investigation because it had the advantage of producing a fluorescent protein when cultured, which could be used as an indicator of the suitability of the environment.

Cells require buffers rather than pure water and therefore attempts were made to gel buffered solutions. Four different buffers: tris/EDTA (TE), 4-(2-hydroxyethyl)-1-piperazineethanesulfonic acid (HEPES), Hank's balanced saline solution (HBSS) and phosphate buffered saline (PBS), all at 50 mM and pH 7.4, were used for the first gelation experiment to produce a 2 mM gel with derivative **2.6**. The result is shown in Figure 2.21, and it was observed that TE formed the strongest gel followed by HEPES, whereas HBSS and PBS were not gelated. Additional experiments showed that phosphate inhibited gel formation.

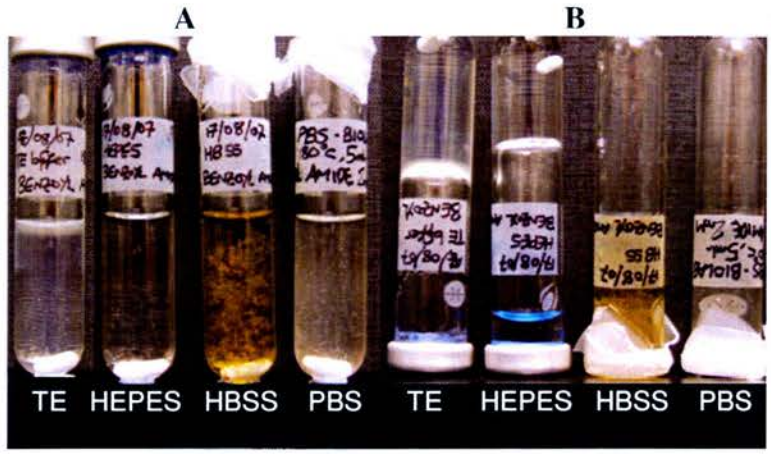

Figure 2.21 Attempts to gelate four different buffers (pH 7.4, 50 mM): TE, HEPES, HBSS and PBS. 2 mM *N,N'*-Di(benzoyl)-L-cystine diamide **2.6**. (A) Before vial inversion. (B) After vial inversion.

The effect of varying pH was investigated with HEPES with a range of pH's between 6-8, the result of which can be seen in Figure 2.22, with clear gel formation at pH 6 and 7, which ceased at pH 8.

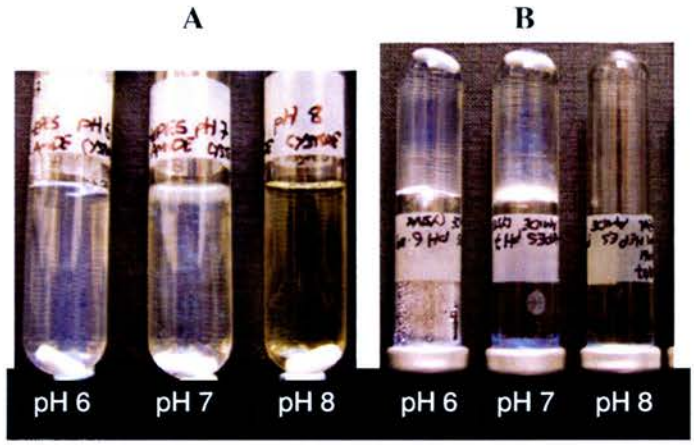

Figure 2.22 Attempted gelation of HEPES buffers at pH's 6, 7 and 8 (50 mM): 2 mM *N,N'*-Di(benzoyl)-L-cystine diamide **2.6**. (A) Before vial inversion. (B) After vial inversion.

Benzoyl cystine amide derivative **2.6** gel could be "broken up" into a clear, viscous solution by shaking. However, this "gel solution" could be reheated (>90 °C) and cooled to give a clear gel that was stable again to inversion. Thus, once the gelator had dissolved (at high temperature and pressure), a much lower temperature was needed to reform gel.

Three different 2 mM benzoyl cystine amide derivative **2.6** gel solutions were produced in water, 50 mM HEPES (pH 7.4) and 50 mM TE (pH 7.4). "Gel solution" (50 µl) was added to the wells in a 96-well plate. The gel was reformed in 96-well plates by heating using a domestic microwave and the well-plate was checked under a light microscope to look for gelation. The gel was seeded using HeLa-GFP cells in media and incubated for 24 hours at 37 °C and examined using a pseudo-confocal microscope (Figure 2.23).

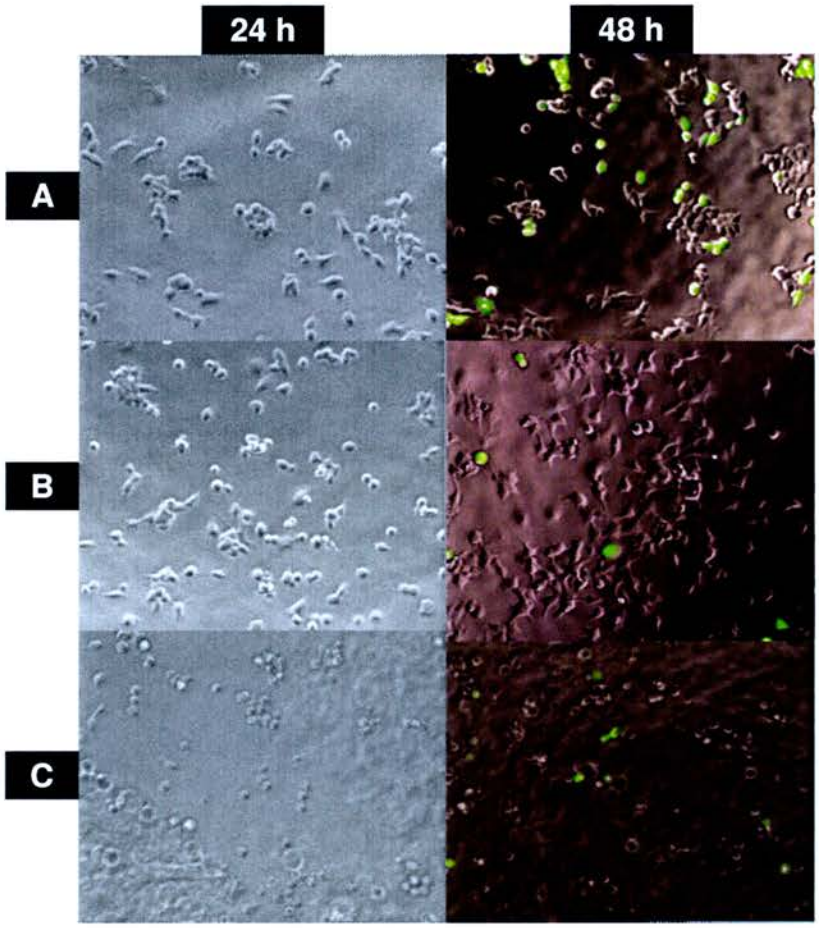

Figure 2.23 Brightfield microscopy images. Well-plates containing three different gels in A. water, B. HEPES (50 mM, pH 7.4) and C. TE (50 mM, pH 7.4) seeded with HeLa-GFP cells and media. (Left) 24 h after seeding. (Right) 48 h after seeding.

In gels with TE buffer, cells were either dead or unhealthy. However with pure water the cells appeared to be very healthy and were spreading and attaching. Cells were also healthy in HEPES buffered gel.

These preliminary studies show that the benzoyl cystine amide **2.6** gel was not only non-toxic but supported cell division.

A pseudo-confocal microscope was used to capture three-dimensional images through the gels. HeLa-GFP cells were present throughout the gel (Figure 2.24). Cells seeded in the gel had penetrated through the gel to a depth of 30 μm.

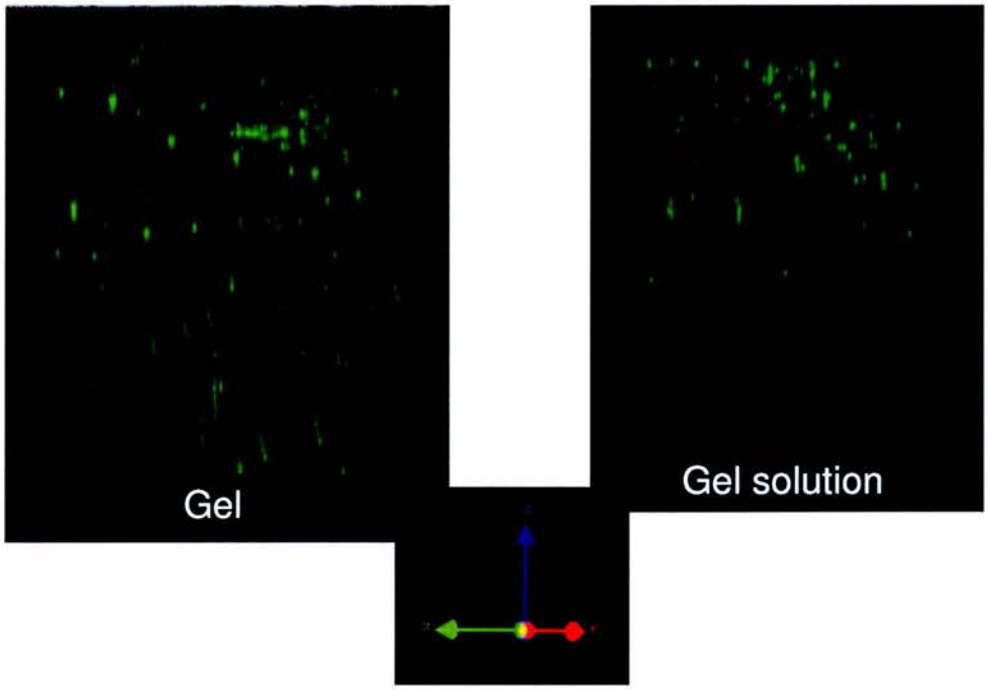

Figure 2.24 Pseudo-confocal microscopy images. Three-dimensional slices through HeLa-GFP seeded in gel and gel solution. (Taken through a depth of 30 μm from the surface.)

2.6 Gel study on a microarray format

A principle test for the assessment of gel formation is a study at the macroscopic level, where a gel is defined by its ability to be gravitationally self-supporting. There are numerous reasons why the inversion test is a fairly poor method of evaluation. For a start it is obvious that the ability of a gel to be self-supporting depends upon the cross-section of the vial in relation to the mass of the bulk gel. The irreproducibility of forming gel in glass vials is also contributed to by irregularities in the glass used. For example, the vial may have a slightly concave form upon which a weaker gel could form and remain self-supporting. An analogy would be two identical beam bridges, one having a purely linear structure crossing two points in a straight fashion, the other with several support trusses. The bridge with the support is obviously going to be stronger. The same principle applies to the effect of the container on the gel. In some publications[33,81] gels are displayed horizontally, most likely because the gel is too weak to be a fully self-supporting gel when in a vertical position.

If novel gels are to be developed through a parallel library approach,[71] a higher throughput screening method is required if a very significant bottle-neck is to be avoided. The microarray format[82] has been adapted to many novel applications and the basic philosophy remains that small molecules, biomaterials, enzymes or cells can be printed onto a 2D surface at defined locations in tiny amounts.[83] A high-throughput gelation study on a microarray format has the potential to allow hundreds of gelation experiments to be investigated on one glass chip. The advantages of using a microarray format are obvious: high-throughput, only very small amounts of material are required and potential savings in time of analysis.

There are several practical considerations that must be developed in order for gelation to be achieved on a microarray. The major problem is determining whether a gel has been formed or whether there is solution or even a precipitation. Microarrays means a decrease in the amount of material involved in each sample but this means that it is no longer possible to see macroscopic results, although it is still possible to do an "inversion test". It is extremely difficult to subject a gel on the surface of a glass substrate to any kind of physical analysis. Volumes that are very small are vulnerable to evaporation due to a large surface area to volume ratio, making it difficult to ascertain the precise concentration that is being dealt with. One of the issues inherent with microarray printing is how to control rates of evaporation or even to exploit it to achieve better results.[84] A second problem inherent with the transfer of gelation from a glass container to the surface of a glass substrate is the process that is used to form the gel. Gelators produce thermoreversible gels, which means to form a gel the gelator needs to be heated until fully dissolved and then the solution allowed to cool down. A primary concern when switching gel formation from a vial to a glass surface is dissolving the gelator. The secondary problem is then how to prevent the solution from completely evaporating before the molecules of gelator can organise themselves.

2.6.1 Environmental dyes

Environmental chromophoric probes were first applied around 50 years ago to study the polarity of internal protein environments.[85] One of these chromophores was 1-anilino-8-naphthalene sulfonate (ANS), particularly interesting as it emits only very weak green fluorescence in water but intense blue fluorescence when present in a highly hydrophobic environment (e.g. adsorbed by serum albumin).[86] In the case of ANS, dependence of the λ_{max} on the polarity of the solvent results from a reorientation of the solvent shell around the chromophore when it is excited. The excited state of ANS has more dipolar character than the ground state and interacts with a polar solvent so that the solvent dipoles are aligned. In a nonpolar solvent the solvent shell is less disturbed. This means that in a polar solvent some of the solvation energy of the excited state of ANS is lost when the chromophore returns to the ground state, which results in a lower energy photon being emitted than in a nonpolar solvent where there has been no reorientation of solvent molecules.[85]

ANS has been used as a chromophoric environmental probe for the study of hydrogels.[87,88] Changes in emission wavelength and intensity of ANS being directly correlated with the formation of fibres in the hydrogel.[88]

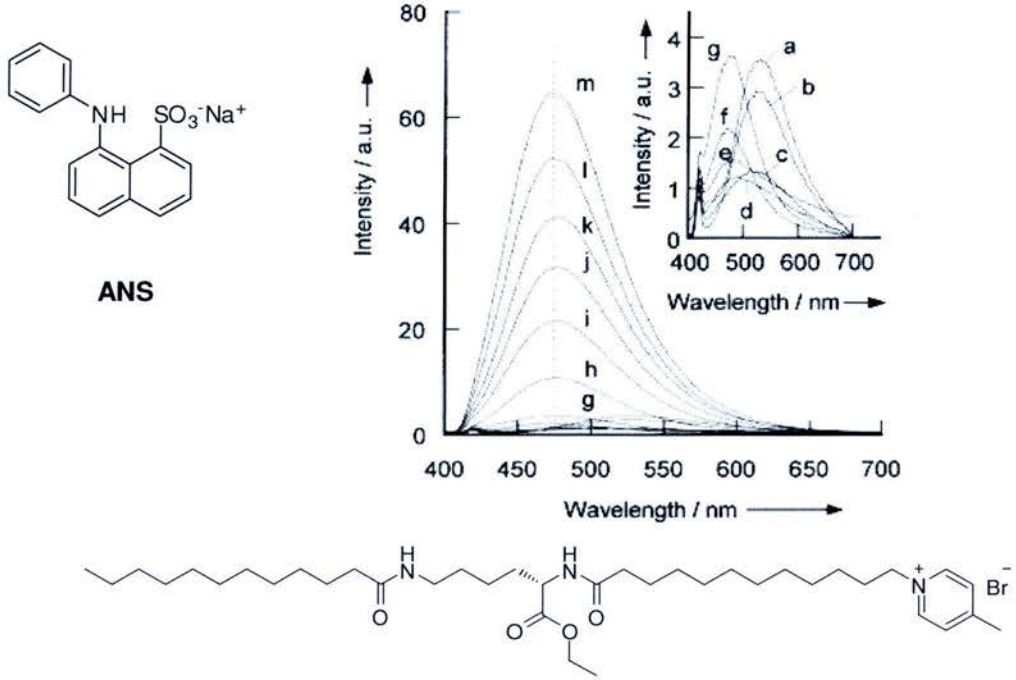

Figure 2.25 Luminescence spectra of 8-anilino-1-naphthalenesulfonic acid (ANS) (10 μM) in aqueous solutions containing various concentrations of **2.27**, where [**2.27**] (mM): **a**: 0; **b**: 0.01; **c**: 0.05; **d**: 0.1; **e**: 0.15; **f**: 0.5; **g**: 1.00; **h**: 1.50; **i**: 2.00; **j**: 3.00; **k**: 5.00; **l**: 7.00; **m**: 10.0. [88]

Figure 2.25 shows the luminescence spectra obtained after increasing the concentration of low molecular weight organogelators up to 0.5 mM and showing a gradual decrease in λ_{max}, after which there was an increase in emission fluorescence intensity but little change in λ_{max}.

The theory proposed to explain this phenomenon was that the ANS dye was incorporated into the hydrophobic interior of the strands of self-assembled nanofibres as they were forming. The fact that there was a decrease in maximum emission wavelength followed by an increase in intensity suggested that there were two stages involved. The initial sharp blue-shift occurred as the concentration of gelator was increased up to 0.5 mM and the explanation for this was that gelator molecules pre-self-assembled into aggregates that had hydrophobic pockets. The concentration at which luminescence intensity began to increase was around 1 mM, where the gelator self-assembled into completely closed aggregates where there was no exposure to

surrounding water. This theory correlates closely with luminescence behaviour around the critical micelle concentration of surfactant systems.[89]

For the purposes of this work, it was decided to see what happens when dyes are incorporated into gels. The first experiments performed were attempts to form gels on a relatively large scale in glass vials along with each of the dyes chosen (Figure 2.26), to ascertain if gelation tolerated the presence of dyes. The napthoyl cystine amide was selected for these initial experiments on the basis of its ability to rapidly form a gel and because it forms a weak gel, it can be considered to be sensitive to the addition of other compounds. The concentration of gel was kept constant at 2 mM with a final solvent composition of 25% DMSO/H_2O. A range of dyes were used to give final concentrations between 0-0.5 mM. A gel was formed at every concentration of both the dyes studied (Rhodamine B and Cy5), meaning that gelation was dye independent.

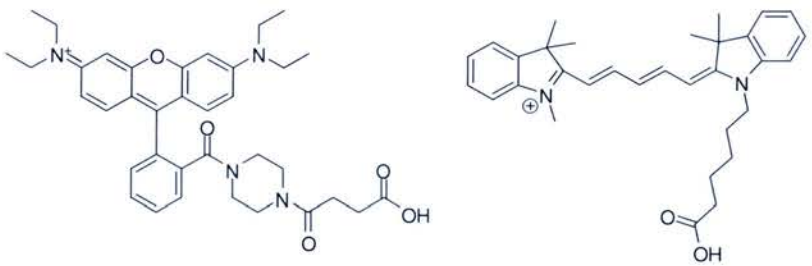

Figure 2.26 Fluorescent dyes. Rhodamine B (Left) and Cy5 (Right).

2.6.2 Gel formation on glass slides

Napthoyl cystine amide gelator **2.7** (2 mM) along with Rhodamine B (0.5 μM) were dissolved in DMSO (2 μL) and spotted onto oxygen plasma treated plain glass slides. The glass slides were then placed in an incubation chamber, which was then sealed with water (2 mL) in the base-well, and the chamber placed in an oven at 80 °C for 1 h (Figure 2.27). This system provided a means of introducing the water component that would form the gel. It also allowed the gradual cooling required for gelation.

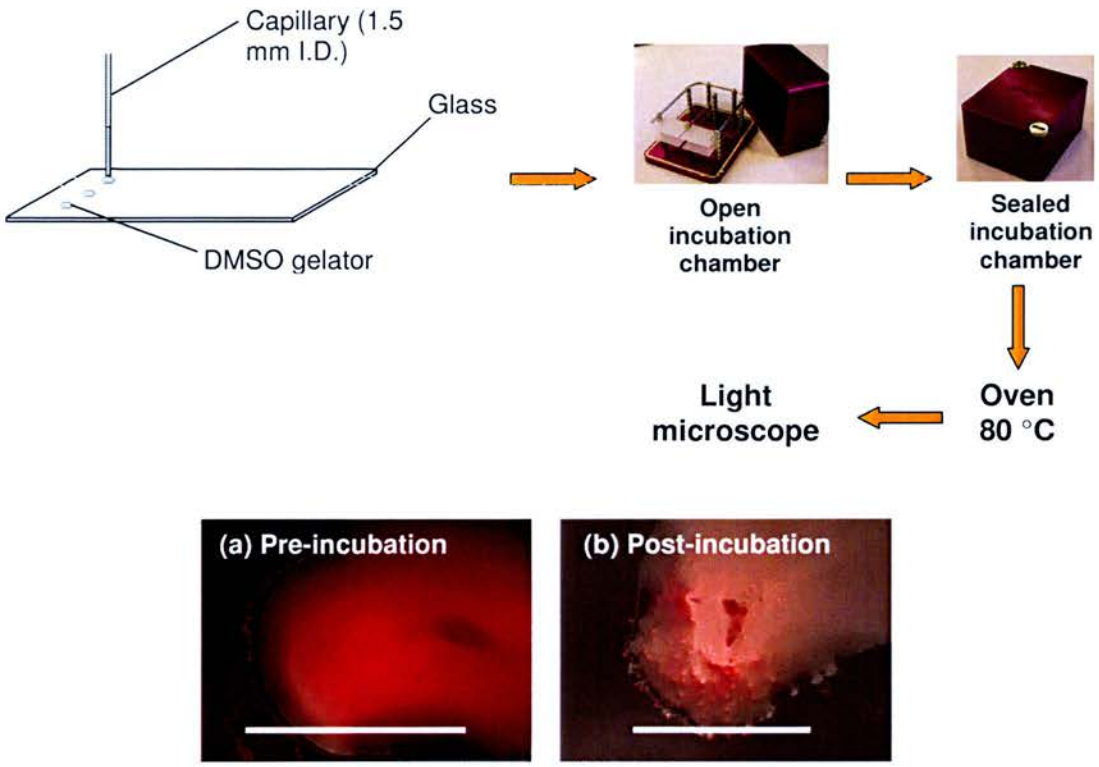

Figure 2.27 Gelation of *N,N'*-Di(2-naphthoyl)-L-cystine diamide 2.7. Light microscopy images: (a) gelator dissolved in DMSO, prior to incubation and (b) following incubation (80 °C, 1 h.) in the presence of water. Scale bars 2 mm.

The first observation was that the original gelator spots were non-uniform and the majority had spread across the surface of the slide. There was also condensation across the surface of the slide. When the slides were examined under a light microscope it was clear that a transformation had occurred in the gelator spots.

These initial results suggested that gelation could be studied on a microarray format but the system obviously needed to be optimised further with the principle requirement for a much more robust system for containment of gelator spots.

2.6.3 Hydrophobic printed slides

Thermo Scientific produce microscope slides coated with a hydrophobic Teflon mask that are designed to eliminate cross contamination by keeping fluids within "wells" (Figure 2.28).

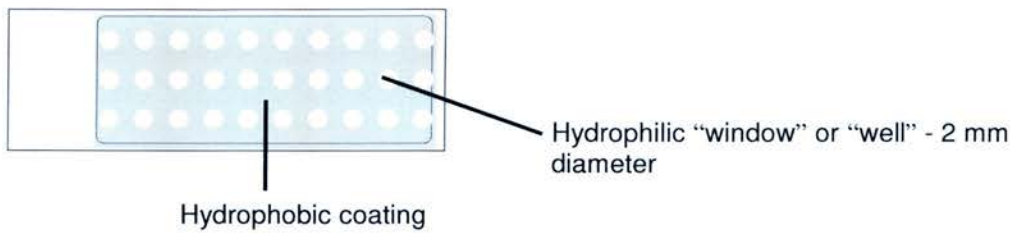

Figure 2.28 Teflon coated microarray slide (26x76 mm).

When applied, wells prevented DMSO spots from spreading across the surface of the chip, effectively containing the spotted material. Another advantage was that the hydrophobic coating surrounding each well would contain a controlled volume (3 μL). Mixtures of napthoyl cystine amide derivative **2.7** and Rhodamine B in DMSO were spotted into the hydrophilic wells on the Teflon coated microarray slides. In order to optimise the process the slides were incubated in the chamber using different conditions, with different volumes of water in the incubation well and by varying the incubation temperature. Qualitative observation of the slides and fluorescence analysis showed the best results were obtained at 80 °C. Incubation at 90 °C gave higher background fluorescence on the slide, suggesting that the hydrophobic coating was not stable at this temperature. Between 80-60 °C spot morphology became less pronounced as the temperature decreased and below 60 °C there was no difference between the morphology of spots on an incubated slide and a slide immediately after printing. A range of dye concentrations was investigated and it was found 0.5 μM gave a fluorescence intensity that could be measured by the fluorescence scanner, above this fluorescence intensity was saturated.

Figure 2.29 shows the fluorescence image resulting from a slide incubated in optimised conditions. The first observation was that after incubation there was a massive change in the morphology of printed spots with gelator added. It was clear that the dye became incorporated into the gelled state.

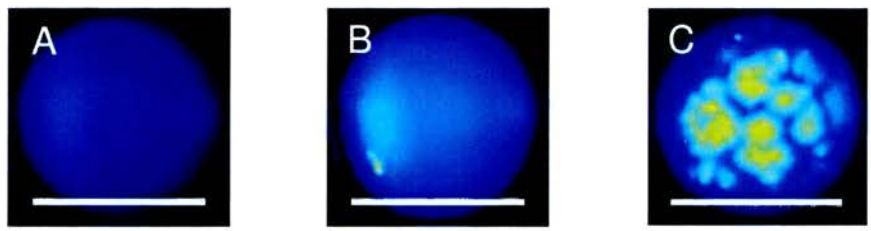

Figure 2.29 Glass slide gelation of *N,N'*-Di(2-naphthoyl)-L-cystine diamide 2.7. Fluorescence imaging: **A.** DMSO; **B.** 0.5 μM Rhodamine B; **C.** Mixture of 2 mM gelator and 0.5 μM Rhodamine B. Scale bars 2 mm.

Figure 2.30 shows an experiment performed when different concentrations of napthoyl cystine amide derivative **2.7** were spotted onto an array. After incubation there was a very significant change in morphology across the range of concentrations of gelator (it was noteworthy that the morphology of duplicates at each concentration showed similar features that were characteristic for the printed concentration). The 4 mM material showed evidence of faint fluorescent fibres, which became more pronounced at 8 mM. At 8 and 10 mM concentrations the fluorescence intensity was spread evenly across the fibrous network, whereas at 15 mM the fluorescence was much more irregular. These qualitative observations suggested that a fibrous network was clearly forming at around 4 mM, with the fluorescence intensity of fibres increasing as the spotted concentration increased. This correlated with theoretical expectations that fibre formation is stronger at higher gelator concentration. At >15 mM a blotchy fluorescence intensity suggested that precipitation was occurring.

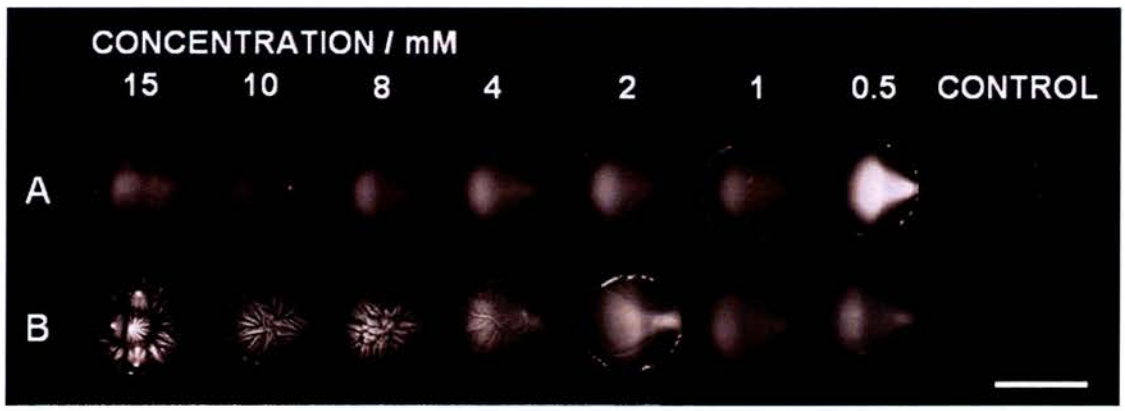

Figure 2.31 Different concentrations of *N,N'*-Di(2-naphthoyl)-L-cystine diamide 2.7 spotted on an array. Initial spotted concentrations of gelator (0-15 mM) with 0.5 μM Rhodamine B. Control = DMSO. **A.** Before gelation; **B.** After gelation. Scale bar 2 mm.

Figure 2.31 shows an investigation of the behaviour of a known non-gelator (di(butyryl)-L-cystine diamide **2.11**) compared with the napthoyl cystine amide derivative **2.7**. After incubation the fluorescence intensity of the butyl derivative **2.11** was almost identical to the dye only, as was morphology. The napthoyl derivative **2.7** at the same concentration showed the formation of a fibrous network. When there was no molecular aggregation, the dye was not concentrated into the hydrophobic network that results whereas when aggregation was occurring dye concentrated in the structures formed.

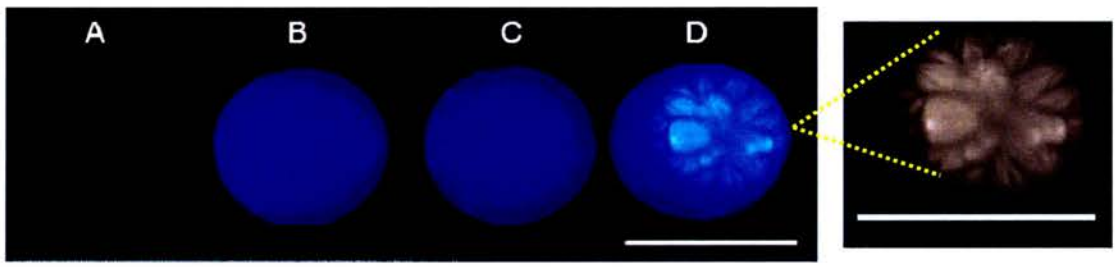

Figure 2.31 Scanning of a non-gelator and a gelator. A. DMSO; **B.** 0.5 μM Rhodamine B; **C.** 10 mM di(butyryl)-L-cystine diamide **2.11** and 0.5 μM Rhodamine B; **D.** 10 mM di(2-naphthoyl)-L-cystine diamide **2.7** and 0.5 μM Rhodamine B (shown enlarged and in greyscale). Scale bars 2 mm.

However, experiments were carried out repeatedly using Teflon coated slides there were obvious inconsistencies with the levels of fluorescence intensities achieved (see Figure 2.32) with the coating/its adhesion influencing fluorescence. An alternative to Teflon coated slides was desirable that could answer these problems.

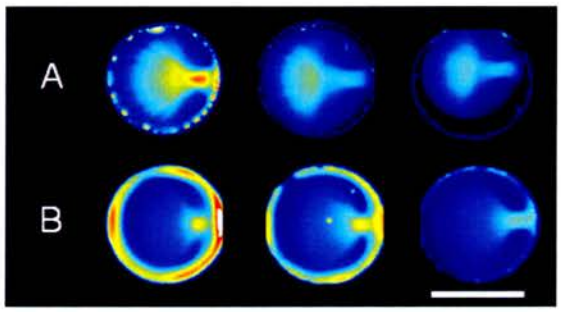

Figure 2.32 Inconsistencies in printed spots of di(butyryl)-L-cystine diamide 2.11. 10 mM cystine derivative and 0.5 μM Rhodamine B. **A.** Before incubation; **B.** After incubation. Scale bar 2 mm.

2.6.4 In-House micro-patterned slides production

Hydrophobic glass slides patterned with hydrophilic areas were produced by printing a sucrose masking solution onto areas of slides where a hydrophilic surface was required, followed by the application of a hydrophobic slide coating.

2.6.4.1 Mask application - Ink-jet printing vs contact printing

Two methods were considered for printing sucrose in defined arrays on glass substrates. The first method employed contact-printing using pins to physically transfer sucrose solution from a well plate to the surface of the glass substrate. This approach proved to be problematic due to evaporation effects. Different concentrations of sucrose solution were investigated but when the concentration was low, the resulting film that was deposited was inconsistent and produced features that lost their shape upon drying. When the concentration of sucrose was increased to achieve a better coverage the solution became increasingly viscous during the printing procedure resulting in trails of sucrose between the contact pins and the substrate. Sucrose solution drying on the pins during printing resulted in a loss of precision producing very inconsistent and unsatisfactory results.

The second approach involved inkjet printing sucrose solutions using a piezo-electric nozzle, with no contact between the print head and the substrate, to form dried patterns following solvent evaporation. In 2007 Cull demonstrated how inkjet printing could be used to produce liquid crystal libraries using three liquid crystals, mixed *in situ* in ratios controlled *via* the number of drops deposited by the nozzle at each position on the matrix.[90] 231 different liquid crystal formulations were fabricated on a 30 x 30 mm substrate with 1.9 mm spacing between spots (100 drops per spot).

Stroboscopic cameras can be used to monitor droplet formation. This allows accurate control of the volume of deposited materials according to the number of drops printed in any given location. In a review of inkjet printing platforms, De Gans and Schubert concluded that the Autodrop platform possesses a drop volume error of less

than 1% and a positional accuracy of (10±3) μm,[91] which is accurate enough for spot-on-spot printing.

The resolution of a printed pattern is determined by the density of printed spots, where the distance between each spot printed in the X and Y directions can be reduced until individual spots merge with each other. Sucrose solutions are generally very viscous and this can be problematic for printing. A high sucrose concentration was desirable because at a higher concentration evaporative effects cause fewer problems. This meant that when a high sucrose concentration was printed the droplet remained at the position it was printed and had less inclination to "bleed" into adjacent spots and areas on the glass substrate surface. The effect of varying the sucrose concentration was investigated and it was found that the most reliable results were produced with 40% sucrose w/v. Figure 2.33 shows the generation of an individual droplet of sucrose and it is notable that the droplet that is produced is spherical with neither tail nor any satellites.

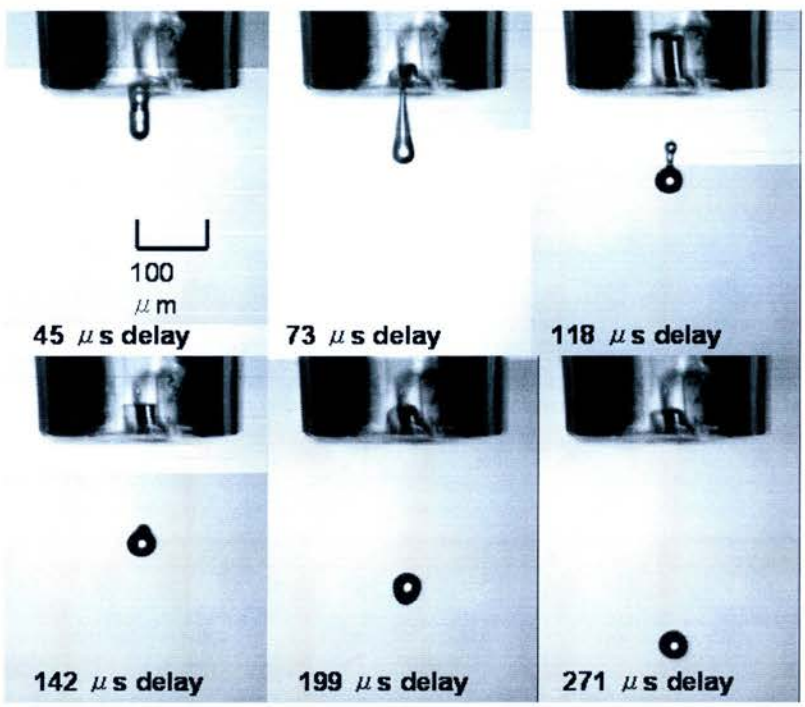

Figure 2.33 Inkjet printing. Generation of an individual droplet of 40% sucrose in water by inkjet printing.

In-house arrays were fabricated according to the following protocol (Figure 2.34). Glass microscope slides (76 x 25 mm) were first rinsed in solvents to remove manufacturing debris and etched using an oxygen plasma (Europlasma NV Junior System, Frequency: 50 Hz, R_f Power: 100 W). A sucrose mask (40% w/v sucrose in H_2O) was printed with defined locations on the array using an inkjet printing system (Microdrop Technology, Norderstedt, Germany). This printing system consisted of a piezo-electric printing nozzle (70 μm diameter), an automated XYZ stage and a stroboscopic video camera. Printing parameters and printing density were optimised to achieve homogenous patterning of uniform squares printed in organised arrays. Following printing, slides were dried at 60 °C for 1 h and coated with tridecafluoro-1,1,2,2-tetrahydrooctyl dimethylchlorosilane (TFCS) using a K bar coater (0.05 mm diameter wire, 2.5 cm/sec). Slides were then washed with H_2O to remove the mask along with excess TFCS and dried under a stream of nitrogen leaving a chip with defined hydrophilic and hydrophobic areas.

Slides with the following sizes of hydrophilic squares were produced and tested: 4.5 x 4.5 mm, 1.5 x 1.5 mm and 0.75 x 0.75 mm.

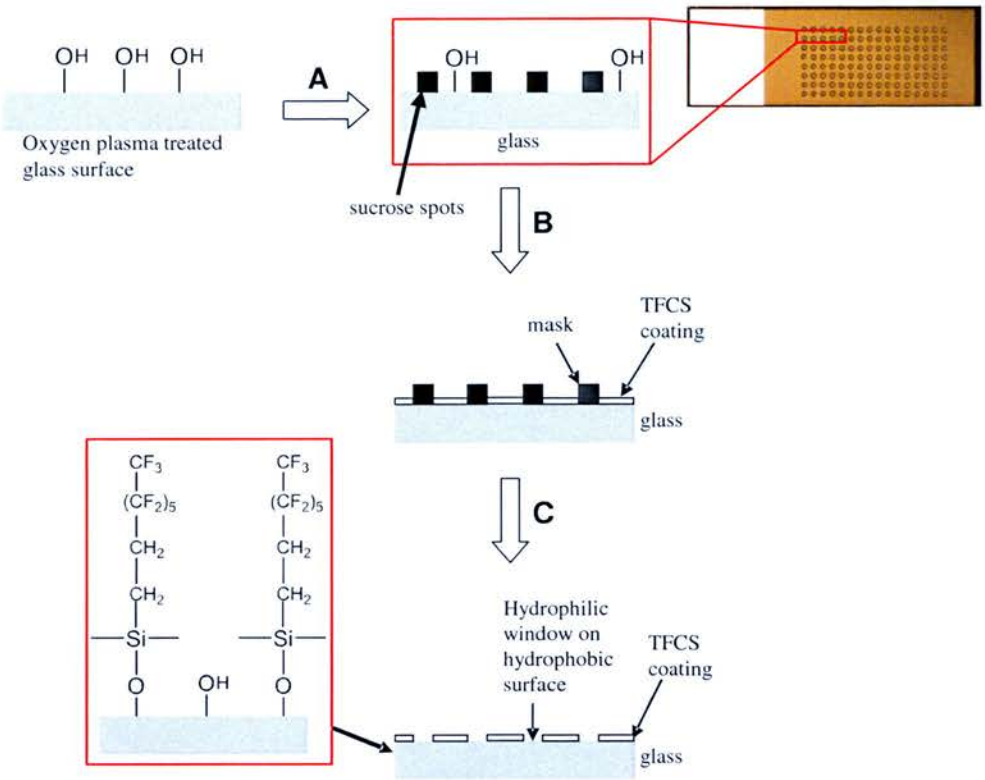

Figure 2.34 Slide patterning. (A) Sucrose (40% in H_2O) mask printing; (B) Glass surface modification with tridecafluoro-1,1,2,2-tetrahydrooctyl dimethylchlorosilane; (C) Mask dissolution.

Figure 2.35 shows the corner of a sucrose printed region that has dimensions of 1.5 x 1.5 mm (it is possible to see the individual droplets that were printed at the print edge).

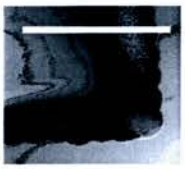

Figure 2.35 Corner of a sucrose masked printed area. Scale bar 1 mm.

Figure 2.36 shows examples of how water can be "contained" within the hydrophilic regions generated by the masking/coating method even when an excessive volume of water is added.

Figure 2.36 Hydrophilic "window" filled with H_2O. Scale bar 0.75 mm.

Figure 2.37 shows images of a chip containing 21 sucrose printed squares (each of 4.5 x 4.5 mm).

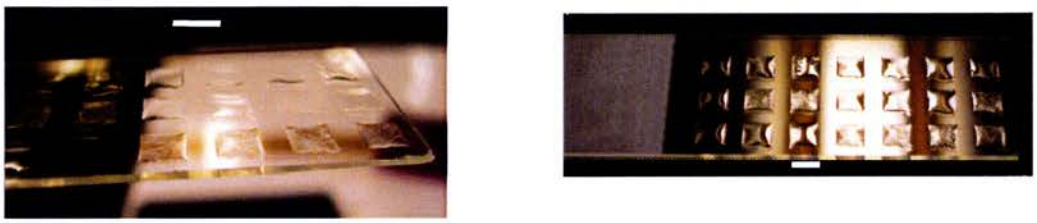

Figure 2.37 Images of a sucrose array. Taken from different perspectives. Scale bars 4.5 mm.

It was possible to comfortably accommodate 100 1.5 x 1.5 mm sucrose squares, and these gave the best results initially so were used in subsequent experiments.

A series of experiments were performed using the hydrophobic/hydrophilic patterned arrays. An experiment was carried out with 14 varying concentration of napthoyl cystine amide derivative gelator **2.7** printed on one chip (Figure 2.38). DMSO solutions containing the dissolved gelator and Rhodamine B were printed rapidly in precise and reproducible volumes into the hydrophilic areas on modified slides. The printing parameters were optimised to ensure that the printing time could be reduced to a bare minimum (the aim was to print an entire chip in less than 10 minutes). This was very important to prevent evaporation.

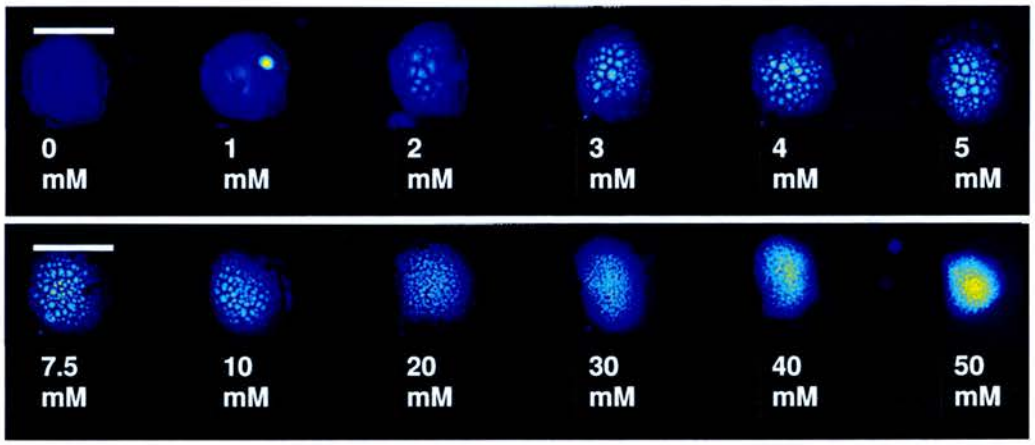

Figure 2.38 Different concentrations of *N,N'*-Di(2-naphthoyl)-L-cystine diamide 2.7 printed on a patterned glass slide. 0-50 mM of gelator and 0.5 μM Rhodamine B. Scale bars 1.5 mm.

A gradual increase in fluorescence intensity was observed as the concentration of napthoyl derivative **2.7** increased. At 40 mM and 50 mM the overall fluorescence intensity was much greater than the control, thus Rhodamine B is clearly acting as an environmental sensor regarding gelation.

Relative fluorescence intensities of gel spots were measured and plotted (Figure 2.39).

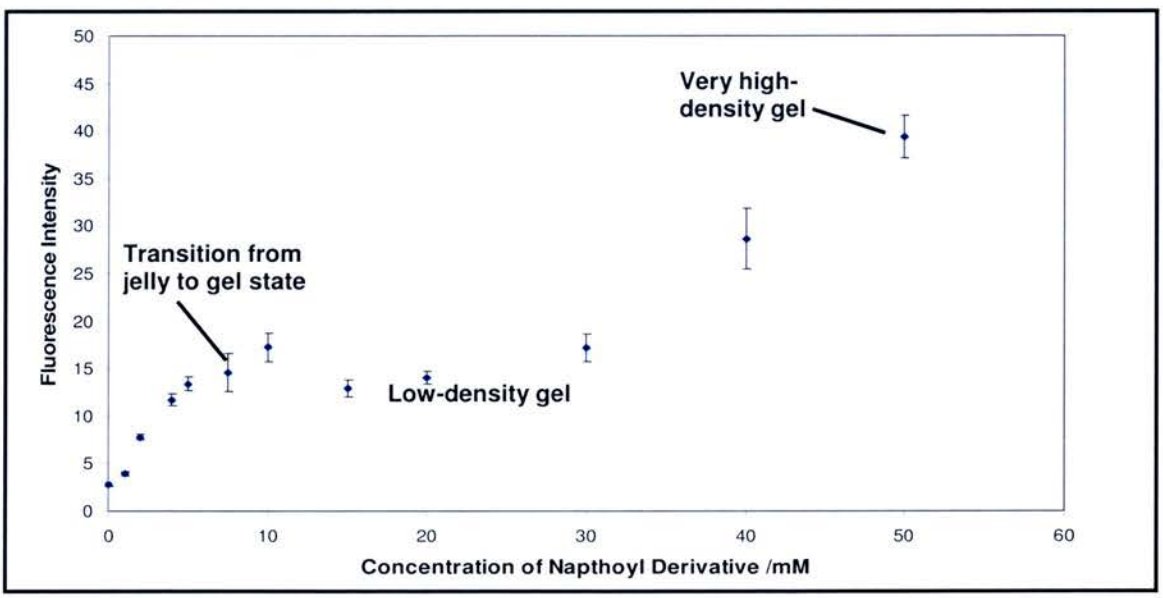

Figure 2.39 Influence of changing gelator 2.7 concentration on fluorescence intensity of Rhodamine B.

Between 0-7.5 mM napthoyl gelator **2.7** there was a rapid increase in fluorescence intensity corresponding to a transition from a liquid state through a jelly state to a low-density gelled state. Above 7.5 mM the rate of increase of fluorescence intensity levelled off. Above 30 mM there was a second increase in fluorescence intensity. The initial increase in fluorescence intensity was caused by increasingly more complete gel fibre formation. Between 10-30 mM I hypothesise that complete fibre formation has occurred and that there is no further arrangement of fibre molecules; a tertiary structured fibre has been achieved. Between 30-50 mM concentration there was a further transformation occurring in the gelled state going from a low-density gelled state to a high-density gel.

As a comparison to a microarray gelation investigation, a range of concentrations of napthoyl cystine amide derivative **2.7** were made in glass vials on a macro-scale, the result (Figure 2.40).

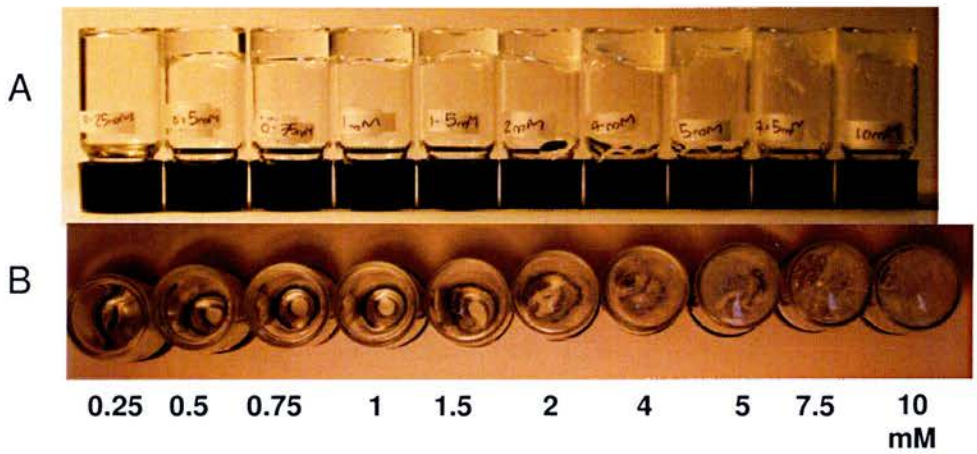

Figure 2.40 Range of *N,N'*-Di(2-naphthoyl)-L-cystine diamide 2.7 concentrations in vials. Gels consisting of 25% DMSO, 75% water. A. Inverted vials side-view. B. Inverted vials seen from above.

At 0.25 mM the gel was too weak to be self-supporting and collapsed under gravity. At 0.5 mM a weak gel was formed that was self-supportive. The resulting gel appeared to be clear up to a 1.5 mM, after which point the resulting gel became increasingly opaque as the concentration increased. Between 1.5-4 mM the gel became more inhomogeneous. This was believed to be because of difficulties in the practical handling of the gel. The gel forms very rapidly, in less than one second upon adding water and so it was possible that a gel was formed from the water that

made first contact with the gelator solution in DMSO, followed by disruption of this primary gel by the addition of the last portion of water. It could be that when the gel was made in large volumes with 10% DMSO/H_2O it was not possible to add the full aliquot of water to give the desired concentration. In these cases a small volume of dense gel was formed followed by water that failed to incorporate. I hypothesise that the weakening effect seen on a macro-scale (1.5-4 mM gelator) can be correlated with what was seen on the microarray between an initial print concentration of 10-30 mM. Between 5-10 mM an increasingly "lumpy gel" was formed that become more solid-like and precipitous rather than liquid in nature.

2.6.5 Effect of dye on gel morphology

An experiment was performed using three different dyes on the microarray with two different initial print concentrations of napthoyl cystine amide gelator **2.7**. The concentration of each dye used was optimised by printing concentration ranges of dye in DMSO. In the case of Rhodamine B and Cy5 dyes, the morphology was the same for both dyes at identical concentrations of gelator (see Figure 2.41). This suggested that the mechanism for incorporation of dye into a gel was the same for both types of dye.

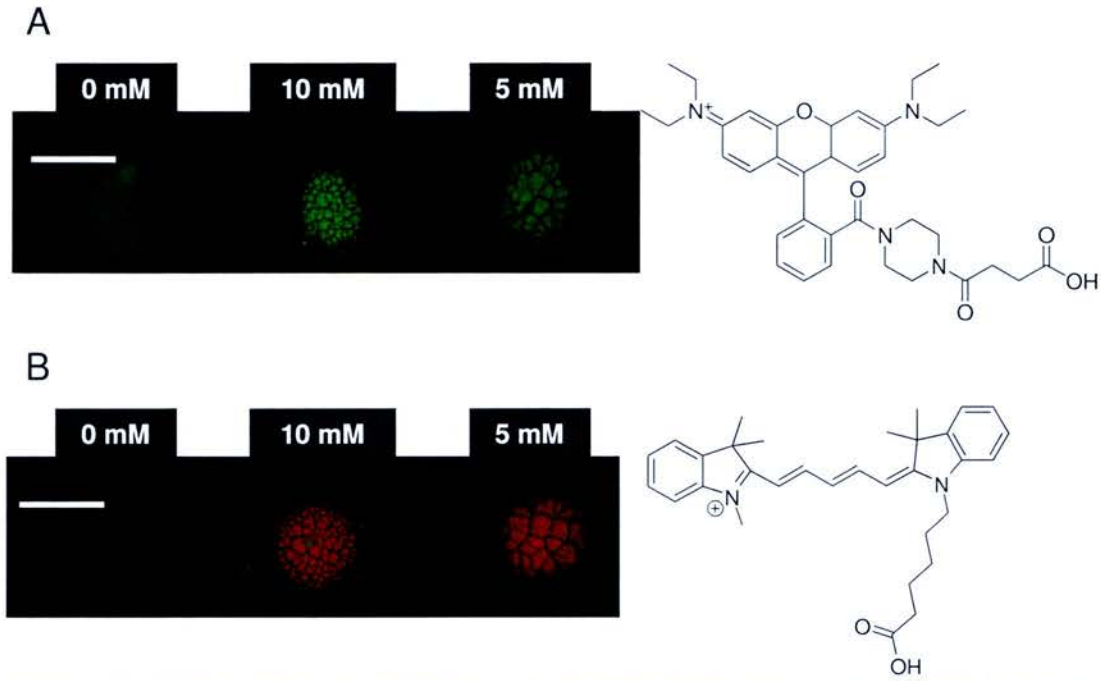

Figure 2.41 Gelation attempted with two different fluorescent dyes: A. Rhodamine B (0.5 μM); B. Cy-5 (5 μM). Initial concentration of *N,N'*-Di(2-naphthoyl)-L-cystine diamide **2.7** either 0, 5 or 10 mM. Scanned using BioAnalyzer 4F/4S white light scanner using: A. Cy3 filter and B. Cy5 filter. Scale bars 1.5 mm.

2.6.6 Mixed gelators on an array

It was thought that the disulfide bond from the cystine could be exploited by encouraging disulfide exchange between cystine derivatives with different capping groups to study the effects of mixed disulfides on gelation morphology. By performing this study on a microarray an enormous amount of information concerning the morphology of mixed gelators could be gathered in just a few experiments. Ink-jet printing enabled printing of a set number of droplets of the first gelator into hydrophilic areas on a hydrophilic/hydrophobic masked chip, followed by printing of an identical number of droplets of the second gelator directly on top of the first set. Three different conditions were employed for the series of experiments. In one experiment, a stoichiometric quantity of dithiothreitol (DTT) was printed on the mixture of cystine derivatives and the chip was incubated for one week. The chip was then incubated in the usual way in the presence of water for 1 h at 80 °C. DTT was printed onto mixtures of cystine derivatives on another chip but was introduced into the incubation chamber immediately in the presence of water for 1 h at 80 °C.

Another chip was prepared with mixtures of cystine derivatives but this time pure DMSO was printed onto the mixed cystine derivative spots and the chip was incubated. The general principle is shown in Figure 2.42.

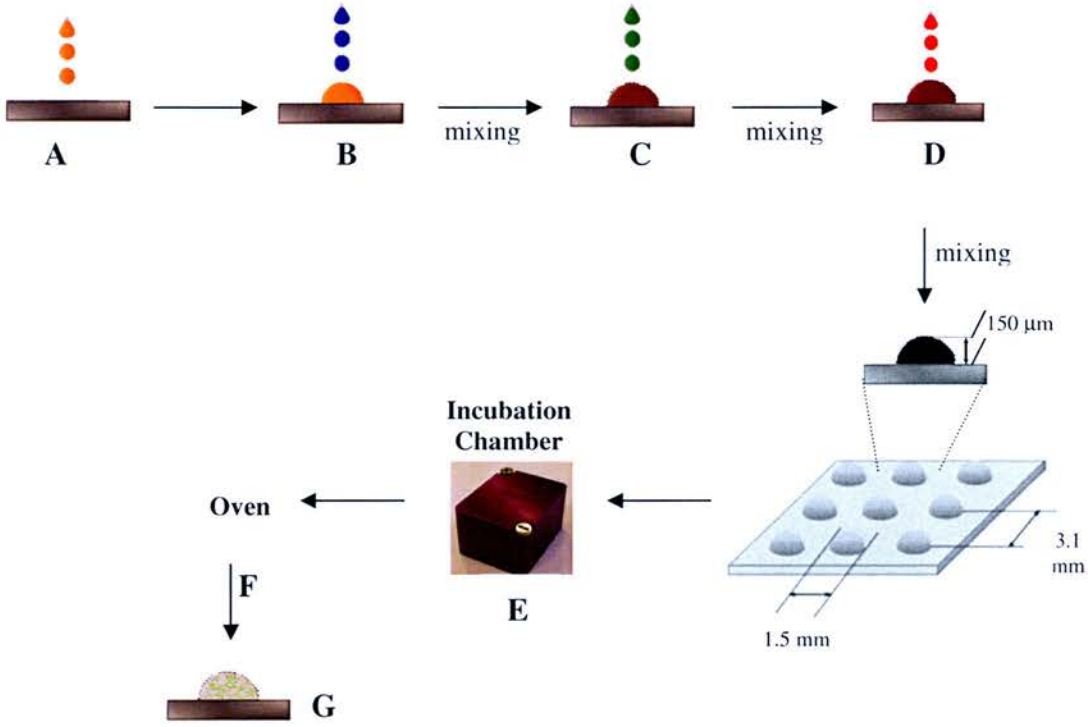

Figure 2.42 Scheme of mixed gelator production on a microarray. A. Glass slides printed with Gelator A dissolved in DMSO (100 drops, 35 mM). **B.** Gelator B dissolved in DMSO (100 drops, 35 mM) spots printed on top of Gelator A spots. **C.** Printing of DTT in DMSO (100 drops, 210 mM) spots on top of mixed gelator spots (DMSO only printed for experiments excluding DTT). **D.** Rhodamine B in DMSO (50 drops, 3.5 µM) printed on top of mixed gelator spots with DTT. **E.** Incubation at 80 °C for either 1 h. or 6 days. **F.** Incubation chamber allowed to cool to 20 °C. **G.** Slides scanned using BioAnalyzer 4F/4S white light scanner, Cy3 filter.

The five capping groups chosen are given in Figure 2.43 along with the results from the experiments. The methoxybenzoyl derivative **2.10** was selected because it had previously been shown to precipitate in DMSO/H_2O and form a lumpy gel so it was interesting to see the resulting morphology in comparison to the known good gelators. The napthoyl derivative **2.7** formed a gel rapidly and had been studied in previous experiments. The benzoyl **2.6**, 4-fluorobenzoyl **2.8** and 4-bromobenzoyl derivatives **2.9** had all proven to have different gelation abilities when studied on a macro-scale.

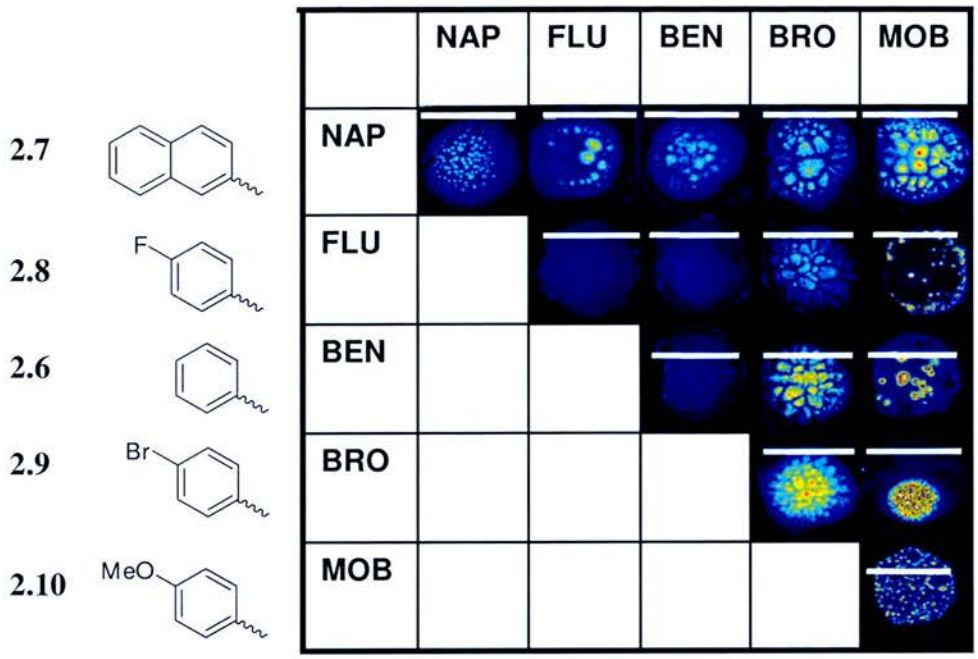

Figure 2.43 Set of mixed gelators. Gelator (NAP **2.7**, FLU **2.8**, BEN **2.6**, BRO **2.9**, MOB **2.10**) (20 mM) and Rhodamine B (0.5 μM). Gelation conditions: 80 °C, 1 h.; Scale bars 1.5 mm.

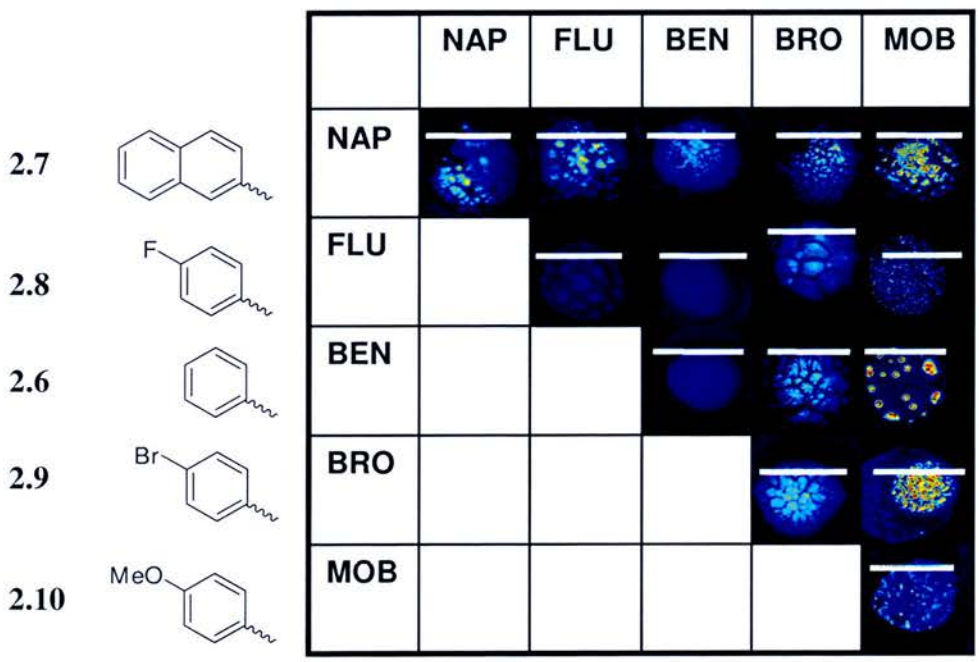

Figure 2.44 Set of mixed gelators with DTT added. Gelator (NAP **2.7**, FLU **2.8**, BEN **2.6**, BRO **2.9**, MOB **2.10**) (20 mM), Rhodamine B (0.5 μM) and DTT (60 mM). Gelation conditions: 80 °C, 1 h.; Scale bars 1.5 mm.

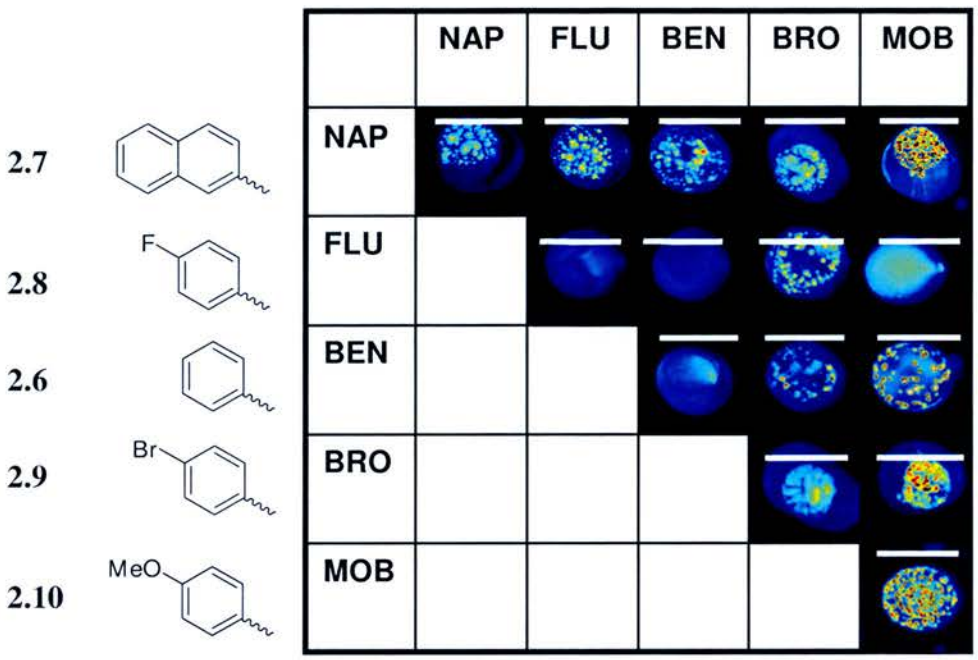

Figure 2.45 Set of mixed gelators with DTT added with incubation. Gelator (NAP **2.7**, FLU **2.8**, BEN **2.6**, BRO **2.9**, MOB **2.10**) (20 mM), Rhodamine B (0.5 μM) and DTT (60 mM). Gelation conditions: 80 °C, 6 days.; Scale bars 1.5 mm.

Figures 2.43-2.45 show a selection of results with the fifteen different possible combinations of cystine derivatives at three different conditions; a total of 45 different types of gel. An observed general trend from the morphology of spots after incubation with no DTT was the absence of any evidence of fibrous morphology in spots with methoxybenzoyl derivative **2.10**, apart from the mixture with napthoyl derivative **2.7**. The napthoyl derivative **2.7** formed a highly fluorescent gel in all cases after incubation where no DTT had been used, which indicated that gel formation between molecules of napthoyl derivative **2.7** was the overriding process when it was mixed with other gelators. There was evidence of a strongly fluorescent fibrous morphology when napthoyl derivative **2.7** was combined with 4-bromobenzoyl derivative **2.9** and the fluorescent gel pattern that resulted could be considered to be a compromise between the morphologies formed by the individual unmixed gelators (shown in Figure 2.46).

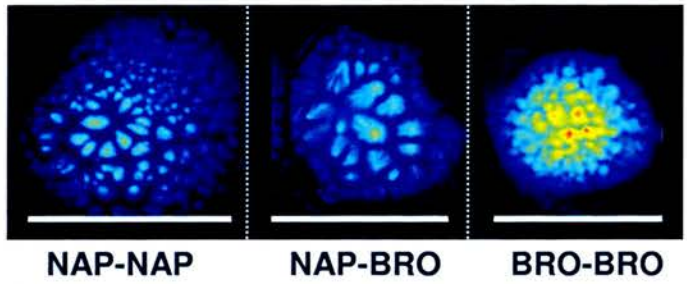

Figure 2.46 Mixed cystine derivative (NAP-BRO) compared with single gelators on microarray. Scale bars 1.5 mm.

The 4-bromobenzoyl derivative **2.9** formed a strong fluorescent fibrous network in all mixtures and when mixed with the methoxybenzoyl derivative **2.10** the gel was very dense and compact, indicated on the microarray by a small, round, highly fluorescent spot with the media surrounding the gel spot having a background level fluorescence intensity.

Gel mixtures that didn't contain DTT had more intense fluorescent patterns than those that did. Incubating gel mixtures with DTT for 6 days generally resulted in a complete loss of morphology from gel spots that showed strong gel morphology in the absence of DTT. When DTT was added directly prior to gelation there was evidence of a reduction in the intensity of the fluorescent network compared with gels that contained no DTT. However, when DTT was mixed with gelator solutions with no incubation period, there was no loss of the resulting fluorescent gel pattern.

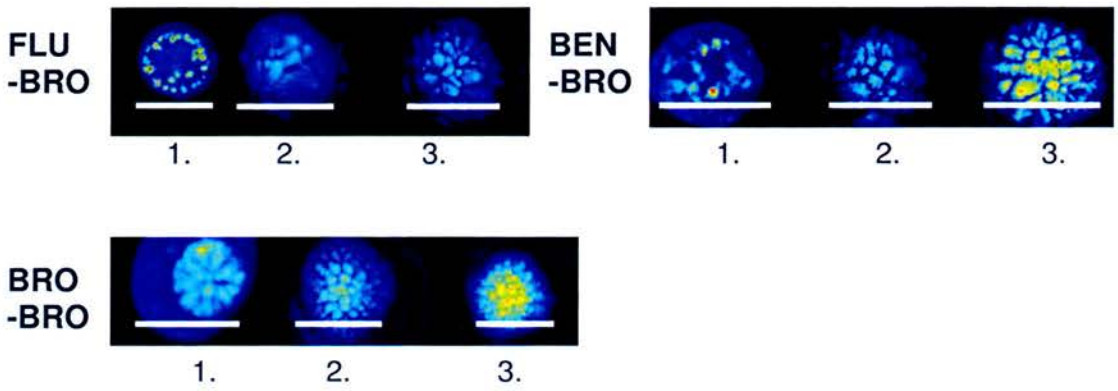

Figure 2.47 Mixed gelator combinations (20 mM) and Rhodamine B (0.5 μM) treated with three different conditions: 1. DTT (60 mM), 80 °C, 6 days; 2. DTT (60 mM), 80 °C, 1 h.; 3. No DTT, 80 °C, 1 h.; Scale bars 1.5 mm.

In the case of mixed FLU-BRO derivative and mixed BEN-BRO there was a complete loss of morphology when DTT was present and left over an incubation period (Figure 2.47). When DTT was added and gelation was induced immediately with no incubation period morphology characteristic of formed gel was observed. Fibres appeared to be longer in mixed FLU-BRO derivative when DTT was added without incubation compared with gelator in the absence of DTT. This was also seen in BRO-BRO derivative.

A "mixed-cap" (BEN-BRO) cystine derivative **2.26** was synthesised to confirm the microarray observation on a macro-scale. Cystine **2.26** was synthesised according to the synthetic scheme outlined earlier, by coupling Fmoc-Cys(Trt)-OH with a polystyrene Rink amide resin and capping with a 1:1 mixture of benzoic acid and 4-bromobenzoic acid. The attempt to gelate water using 2 mM **2.26** is shown in Figure 2.49. The result was a fine lumpy precipitate in solution with no evidence of fibre formation, which is consistent with the morphology observed in the mixed gelator combination (BEN-BRO) incubated with DTT (shown in Figure 2.48).

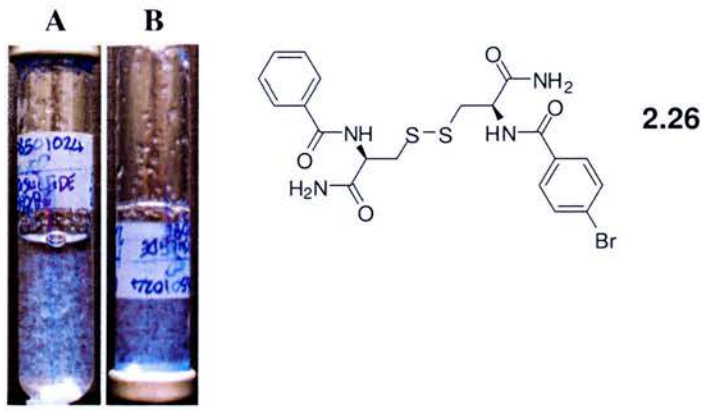

Figure 2.48 Attempted hydrogelation of "mixed-cap" cystine derivative 2.26. 2 mM BEN-BRO derivative **2.26** in H_2O following microwave heating at 180 °C for 5 mins. (A) Before vial inversion. (B) After vial inversion.

2.7 Degradation of cystine-based hydrogels

Cystine-based hydrogels were remarkably stable when handled carefully, surviving intact for over 2 years in the majority of cases. Gels liquefied in seconds when subjected to mechanical agitation. Gel stability was studied using the "ball drop"

method. Benzoyl cystine diamide **2.6** (2 mM) hydrogel was formed using microwave heating and a steel ball bearing (diameter = 4 mm, 84 mg) was placed onto the gel surface. Addition of DTT solution (1 M, pH 8.2) resulted in complete liquefaction after 7 days by which time the ball fell a distance of 40 mm. Without the addition of DTT the ball fell 3 mm in the same time. When the concentration of DTT solution added was increased (4 M, pH 8.2), complete liquefaction occurred in a little over 4 hours.

The possibility of proteolytically degrading modified cystine hydrogels was investigated by adding trypsin to napthoyl cystine glycine **2.15** (2 mM) hydrogel but no degradation was observed.

2.8 Conclusions

A structurally diverse library of cystine derivatives has been accessed using an efficient and straightforward solid phase route. Microwave heating at high temperatures and pressures has allowed the production of novel hydrogels at remarkably low concentrations and the study of gelation ability in relation to compound structure. Preliminary experiments have shown that cells can be successfully incorporated into these hydrogels.

A novel method of visualising gels from low-molecular weight gelators has been demonstrated for the first time. Low-molecular weight gelators were inkjet-printed as arrays onto hydrophobic glass slides modified with defined hydrophilic areas and gelated in the presence of a fluorescent dye, allowing subsequent gel morphology to be directly observed. This high-throughput technique has enormous potential for the future study of low-molecular weight gelators.

Chapter 3:

Protein and Peptide Chemical Cross-linking Reagents

3.1 Introduction

Protein-protein interactions play a key role in a multitude of cellular and biological processes, with abnormal protein-protein interactions having been implicated in various disease states. Some cervical cancers are caused by specific human papillomavirus infections[92], where viral E2 proteins target the cellular protein Brd4, forming a physical tether between the viral "plasmid" and the host cell mitotic chromosomes. This leads to the virus persisting for a long time, maintaining the transformation status of affected cells.[93]

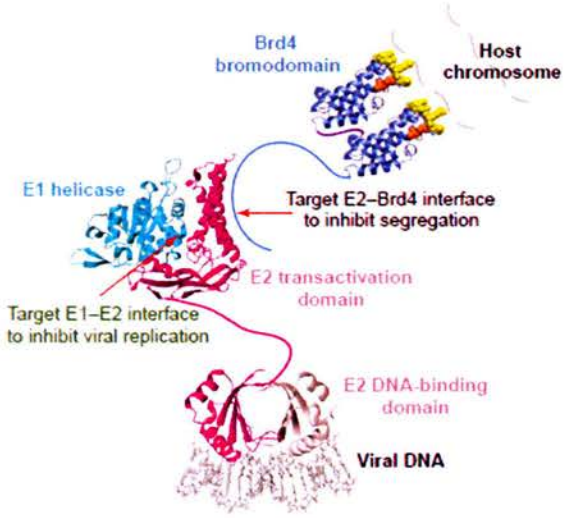

Figure 3.1 Potential targets for papilloma virus E2 inhibition. Arrows indicate potential targets for inhibition of papilloma virus infection.[94]
Reproduced with permission (copyright Elsevier, 2005).

Staphylococcus aureus and *Streptococcus pyogenes* are two important human pathogens that adhere to and invade host cells *via* a protein-protein interaction between fibronectin-binding proteins anchored in the bacterial cell wall and host fibronectin.[95] Protein-protein interactions are implicated in T-cell leukaemia and breast cancer. LIM domains are protein structural domains, named after their initial discovery in the proteins **L**in11, **I**sl-1 and **M**ec-3.[96] LIM-domain containing proteins play roles in cytoskeletal organisation, organ development and oncogenesis. LIM-

domains mediate protein-protein interactions critical to cellular processes. The key targets of the LIM-domain-binding protein ldb1 are the LIM-only (LMO) and LIM-homeodomain proteins. A direct link has been made between overexpression of LMO2 in T cells and the onset of T-cell acute lymphoblastic leukaemia in children, due to competition for ldb1 by ectopically expressed LMO2 and endogenous LMO4 in T cells.[97] Huntington's disease is one of several neurodegenerative poly-glutamine (polyQ) disorders, where the abnormal expansion of polyQ regions in proteins causes the proteins (huntingtin in the case of Huntington's disease) to associate, forming insoluble protein deposits in the brain.[94] Due to this fact there is a desire not just to understand which proteins are interacting with each other but to be able to develop small molecules that are capable of blocking specific protein-protein interactions.[98]

Determining the protein interaction network is one of the major problems facing functional proteomics and one of the most challenging problems of the post-genomic era. There is a huge amount of information available concerning protein structures and this is steadily increasing with regards to protein-protein interactions. However, the rate of structure determination of protein-protein complexes using experimental methods such as X-ray crystallography and NMR spectroscopy is seriously lagging behind that for conventional single protein structures.[99] X-ray crystallography and NMR spectroscopy both yield detailed information on protein structure however NMR spectroscopy requires large quantities of pure protein and for X-ray studies the protein has to be crystallised, which demands considerable skill and a large time investment. Another limitation of these techniques is that they are considered to have a low throughput. A large-scale study designed to obtain 3D protein structures from across the human genome using X-ray or NMR analysis resulted in a success rate of only 3-5%.[100] Sensitive techniques are thus required to perform large-scale protein and protein-protein analysis, ideally in a high-throughput manner, because sample amounts are often limited. Mass spectrometry is a fantastically powerful tool for these studies and has the potential to fulfil such a role.[101] Indeed, there are a growing number of mass spectrometric techniques that are being used for structural studies of proteins: hydrogen-deuterium exchange,[102] analysis of intact non-covalent complexes in the gas phase[103] and chemical cross-linking.[104]

3.2 Chemical Cross-linking

Chemical cross-linking is a well established method in protein chemistry. The aim of performing intramolecular chemical cross-linking is to gain knowledge and clarification of how a protein folds and an understanding of site-site interactions. The objective of intermolecular cross-linking between different proteins is to simultaneously identify which components interact and how and where they are physically connected to each other by residue-residue contacts between interacting proteins. This means that chemical cross-linking can be considered as a low-resolution complimentary approach to NMR spectroscopy and X-ray crystallography based methods. The advantages of chemical cross-linking coupled with mass spectrometry however are huge: Unlike other techniques, it can be used on analytes at low concentrations, it does not require protein crystals or proteins in a specific solvent and it is fast because data analysis can be automated, all benefits that allude to greater throughput.

Figure 3.2 Chemical cross-linking of a model protein. Bovine basic fibroblast growth factor ((FGF)-2) cross-linked with the lysine-specific cross-linking agent bis(sulfosuccinimidyl) suberate (BS3) (the 14 lysines of (FGF)-2 are shown in red, observed cross-links are indicated by yellow dashes.).[105]

The nature of protein-protein interactions can vary depending on the function of the proteins involved and the biological process that they are involved in. A requirement of multiprotein complexes is that the interactions between intracellular proteins are stable, whereas when two or more proteins associate in the catalytic step of a biosynthetic or signal-transduction pathway, the interactions involved are more

commonly transient.[106] Chemical cross-linking is a direct method of identifying both transient and stable interactions. Chemical cross-linking involves the formation of covalent bonds either between two or more proteins in the case of inter-molecular cross-linking or one protein that has been intra-molecularly cross-linked. Chemical cross-linkers are usually bifunctional reagents containing two reactive end groups that react with two functional groups from amino acid residues that are present throughout proteins, most commonly primary amines and thiols. Two proteins can only be covalently cross-linked together if they are physically interacting. Observing cross-links between two distinct proteins is direct evidence that the proteins must be in close proximity to each other.

Cross-linking of proteins began with Mother Nature; cross-linking imparts rigidity on loosely folded, floppy proteins or flimsy protein complexes.[107] Man also had the same intentions; Quiocho and Richards showed that cross-linking of enzyme crystals with gluteraldehyde increased their mechanical stability.[108] The first identification of a cross-link with regards to interest in protein structure was carried out by Zahn in 1958, cross-linking the N-terminal groups of the two peptide chains of insulin.[109] The next advance in the field came in 1966, with the introduction of bis-alkyl imidates as a reactive cross-linking chemistry,[110] followed by a demonstration in 1970, of how SDS gel analysis of cross-linked proteins could indicate the quaternary structures of proteins quickly and simply.[111] A breakthrough in proteomics came in 1988 with the introduction of new mass spectrometry techniques for introducing large, intact molecules into the gas phase.[112] Reported examples of the application of chemical cross-linking in conjunction with mass spectrometry to protein complexes followed. One of the first examples involved the identification of members of the yeast nuclear pore complex, in which the complex component Nup85p was tagged and a six-membered complex identified following analysis using matrix-assisted laser desorption/ionisation time-of-flight mass spectrometry (MALDI-TOF-MS).[113] Another seminal work involved mapping molecular interfaces between homodimeric DNA binding protein ParR and the glycoproteins CD28 and CD80.[114] These demonstrations of the potential of the cross-linking approach were followed up with a determination of the interaction regions in complexes between calmodulin and a

cloned fragment of the giant muscle protein nebulin[115] and the interacting regions in complexes of microtubule-destabilising protein Op18 and tubulin.[116] Interaction sites have been identified in the light-activated complex between transducin and a number of single cysteine rhodopsin mutants,[117,118] in the yeast mitochondrial prohibitin complex consisting of subunits PHB1 and PHB2,[119] in assembled tubes of capsid protein of HIV-1[120] and in homodimers of apolipoprotein A1 in reconstituted HDL particles.[121] Interacting regions were identified between the HIV envelope protein gp120 and its cellular receptor CD4[122] and between paxillin and its binding partners.[122] Further reports have identified intermolecular contact regions between interleukin-6 (IL-6) chains in interleukin-6-dimer,[123] between two DNA repair proteins Rad6/Rad18,[124] between monomeric subunits in the homodimer of aminoacylase 1[125] and between components of the heterodimeric protein complex negative cofactor 2.[126]

There is now no question that the chemical cross-linking combined with mass spectrometry approach is of tremendous value to proteomics, enabling low-resolution three-dimensional protein mapping. Thus it has been used to determine the low-resolution three-dimensional structure of fibroblast growth factor (FGF)-2, revealing the folding patterns of the protein family.[105] A number of publications have reported amino acid distance constraints within cytochrome c,[127,128] lysozyme,[128] ribonuclease A[127] and ubiquitin.[129,130] Cross-linking products have been identified in haemoglobin,[131] neurofibrillary tangles from the brain of an Alzheimer's disease patient,[131] tyrlysbradykinin[132] and neurotensin.[132]

3.2.1 Mass spectrometric analysis of cross-linking products

Mass spectrometry is now the method of choice for detecting tiny quantities of proteins.[107] The power of the field has been enabled by the advent of the soft ionisation techniques MALDI[133] and ESI[134] that can be applied to either large biomolecules or to allow accurate MS analysis of smaller peptides.

(i). MALDI-TOFMS - Matrix-assisted laser desorption/ionisation time-of-flight mass spectrometry is a very sensitive method for analysing proteins and gives solid, reproducible results. Interestingly the mechanisms of ion formation in MALDI are still being debated.[135,136,137,138] Sample (analyte) is deposited on a probe by co-crystallisation with a matrix (typically aromatic acids, of which the most commonly used being: 3,5-dimethoxy-4-hydroxycinnamic acid (sinapinic acid)[139], α-cyano-4-hydroxycinnamic acid (alpha-cyano or alpha-matrix)[140] and 2,5-dihydroxybenzoic acid (DHB)[141] and then introduced to the vacuum chamber. Ionisation is induced by firing short pulses of laser light focussed on the sample probe. MS/MS experiments of cross-linked peptides, where post-source decay (PSD) analysis can be performed,[142] can reveal primary structure information of proteins as well as abundant fragment ions directly at the site or sites of cross-linker modification.[105] MALDI-TOFMS has been used for the analysis of a number of cross-linking studies.[105,113-119,122,124-126,143]

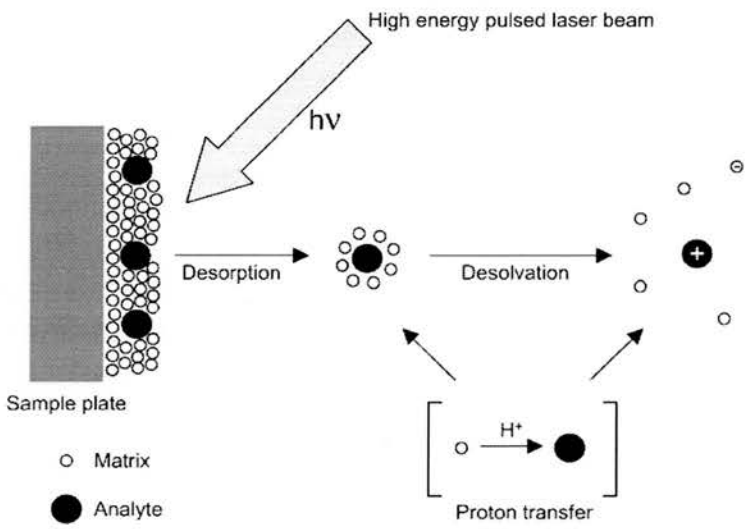

Figure 3.3 The MALDI process. Laser induced desorption is followed by ionisation, the exact mechanism is not fully understood.

(ii). ESI-MS - The principle of ESI is that liquids are sprayed through a needle with a carrier gas in the presence of a strong electric field, such that they form small and highly charged droplets. The droplets undergo desolvation, which decreases the diameter of the droplets. This leads consequentially to charge density increasing on the surface of the droplet, until Coulombic repulsion becomes the same order as surface tension. At this point there is a "Coulombic explosion" whereby the droplet

becomes unstable and splits to form daughter droplets that also begin to evaporate and decrease in size. This sequence of events is repeated until the electric field generated by the surface charge density of the droplet is strong enough to desorb ions from the droplet into the ambient gas. There have been massive developments in mass spectrometer technology resulting in improved sensitivity, reduced flow rates and miniaturisation of the electrospray technique by using narrower spray capillaries to introduce smaller droplets into the mass spectrometer.[144]

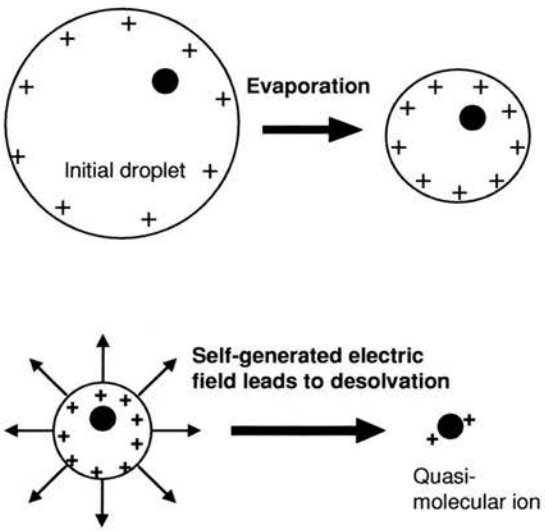

Figure 3.4 Electrospray mass spectrometry.[134] Ion formation occurs following evaporation of the initial droplet solvent followed by desolvation in a sequence of Coulomb explosions.

A peptide mixture is normally introduced into a mass spectrometer following application of a separating technique such as liquid chromatography (LC) or capillary electrophoresis (CE). Complex mixtures of peptides are commonly separated prior to analysis using RP-HPLC or by 2D-HPLC, which is usually the combination of a strong cation-exchange step and an RP chromatographic step.[145] ESI-MS/MS is usually used to obtain amino acid sequence information that is of high-quality and provides structural information. MS/MS, also known as tandem mass spectrometry, involves two stages of mass analysis. In the first stage an ion is isolated by separating it in time in a single mass spectrometer or separating it in space where individual mass spectrometer elements are separated. Ion separation can be achieved in an ion trap, a triple quadrupole (QqQ) or quadrupole time-of flight

(QqTOF) instruments.[146] After the first stage of analysis, isolated ions are subjected to ion activation whereby energetic gas-phase collisions are applied, which leads to fragmentation of the peptide ions. The second stage of analysis measures *m/z* values of the fragmentation products. Cross-linked protein products have been analysed many times using ESI-QIT (quadrupole ion trap), ESI-QqTOF or ESI-TOF (time-of-flight) instruments.[157,147,148,149]

3.2.2 Cross-linking strategies

Intra and intermolecular cross-linking – low-resolution 3D structure mapping of proteins and mapping protein interfaces

3.2.2.1 The strategy

A cross-linking reaction can be performed using either homobifunctional or heterobifunctional cross-linkers. These cross-linkers provide intramolecular distance constraint information because they will only bridge defined distances through space, as opposed to so-called (see later) zero-length cross-linkers that merely show direct contacts. The value and great potential of chemical cross-linking does not lie solely with the ability to elucidate the three-dimensional folding patterns of proteins. The technique is remarkably powerful for mapping molecular interfaces in protein complexes if intermolecular cross-linking products between two proteins are targeted.

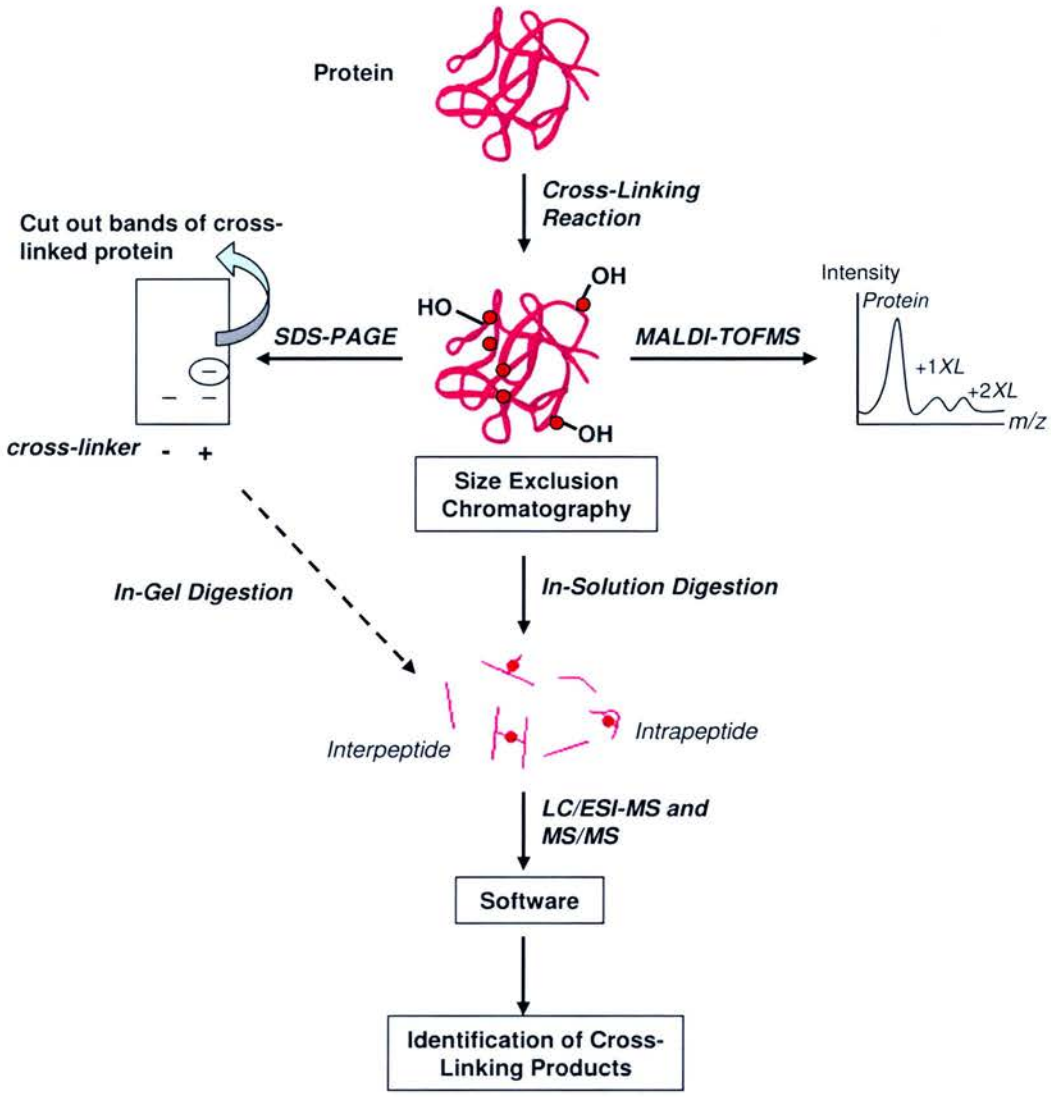

Figure 3.5 General cross-linking analytical strategy.[150] Mapping three-dimensional structures of proteins by intramolecular cross-linking.

The process of intramolecular cross-linking and analysis proceeds according to the following steps:

(i) Cross-linking reaction: Usually cross-linker concentrations, reaction times and buffer pH must be optimised to get a high yield of cross-linked product.

(ii). Assessment of cross-linking products: One-dimensional gel electrophoresis as well as matrix-assisted laser desorption/ionisation time-of-flight mass spectrometry (MALDI-TOFMS) are used to assess whether high molecular mass aggregates have

been formed by intermolecular cross-linking, thus also giving an indication of cross-linking reaction efficiency. Size-exclusion chromatography can be applied, as an alternative to gel electrophoresis, in order to separate intramolecular cross-linking products from the higher molecular mass aggregates that are made by intermolecular cross-linking.

(iii). Processing of cross-linking products: Gel bands containing the desired cross-linked proteins are excised from the gel and in-gel proteolytic digestion performed using trypsin. The peptide mixture that results from digestion with trypsin is typically complex in nature. It consists of peptides that remain unmodified by cross-linking, intramolecular cross-linking products, that are both inter- and intrapeptide cross-linked, as well as intermolecular cross-linking products (cross-links between two proteins); all types of cross-linking products present in a large range of different combinations. Intramolecular cross-links give valuable information on how the proteins fold within a complex. Intermolecular cross-linked products give information on protein-protein interactions.

After a cross-linking reaction there are a huge number of cross-linked products. A cross-linker (depending on its structure) can react at one or two different amino acid side chain groups as well as the amino and carboxyl termini of the protein. There are three main types of cross-linked peptide that can be formed:

1. One end of the cross-linker reacting with an amino acid side chain or protein termini, with the other end having hydrolysed. This type of "cross-linked" product has been referred to as 'dead-end', 'decorated', 'end-capped' or 'hanging'. Peptides that are modified by hydrolysed cross-linker are considered to be undesirable because they do not yield any information concerning distance constraints within a protein, however they can still be of use because they do provide information on surface accessibility.

2. Both ends of the cross-linker have reacted and an intrapeptide cross-link has been formed where two amino acid side chain groups from the same peptide have reacted.

3. Both ends of the cross-linker have reacted and two independent peptide chains have been united to produce an interpeptide cross-link.

Of course the cross-linked peptide product mixture can be complicated further with multiple modifications. It is quite possible for a peptide to contain more than one hydrolysed cross-linker molecule. It is also possible for a peptide to contain a hydrolysed cross-linker and either an inter- or intrapeptide cross-link. Every cross-linking experiment produces such an enormous range of outcomes; the subsequent data analysis and interpretation is a daunting task.

(iv). Analysis: The peptide mixture is analysed by combinations of liquid chromatography and electrospray ionisation mass spectrometry (LC/ESI-MS) and by MALDI-TOFMS.

(v). IT solutions: Finally, sophisticated computer software processes the data and compares the signals that are present in the mass spectra of cross-linking products but that are not present in non-cross-linked proteins. When cross-links have been identified they can be assigned to parts of the proteins. This leads to the determination of intramolecular distance constraints within the protein.

3.2.3 Cross-linking reagents

3.2.3.1 Homobifunctional cross-linkers

Homobifunctional cross-linking reagents, in particular cross-linkers that react specifically with primary amine groups, have been used extensively. They are typically soluble in aqueous solvents and are able to form stable inter- and intra-subunit covalent bonds. Over the past 20 years the variety of available homobifunctional cross-linking reagents has greatly increased and now a wide range

of reagents, with different spacer lengths and reactivities, are available commercially, to suit particular cross-linking requirements. Some cross-linkers have "cleavable" linkages whereas others are non-cleavable, which means that cross-links are irreversible.

One major drawback intrinsic with homobifunctional reagents is that a large range of poorly defined products are generated, because homobifunctional reagents will react with every reactive group available.

Disulfosuccinimidyl tartarate
(sulfo-DST)
Spacer length = 6.4 Å

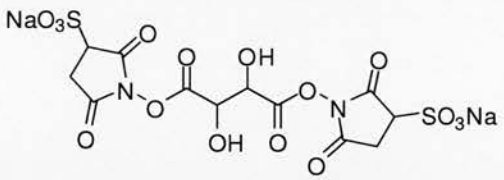

Bis(sulfosuccinimidyl)
suberate (BS3)
Spacer length = 11.4 Å

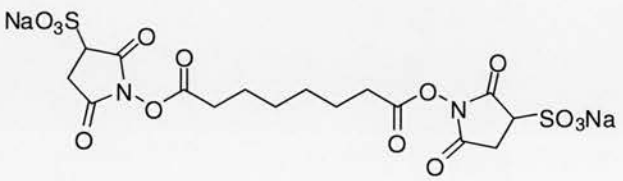

Ethylene glycol bis
(sulfosuccinimidyl succinate)
(sulfo-EGS)
Spacer length = 16.1 Å

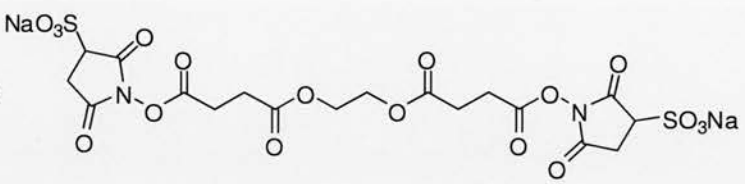

Figure 3.6 Homobifunctional cross-linking reagents. Examples of three such cross-linking reagents: sulfo-DST, BS3 and sulfo-EGS.

3.2.3.2 Heterobifunctional cross-linkers

Heterobifunctional conjugation reagents contain two different reactive groups that can couple to two different functional groups on proteins.[151] For example, one part of a cross-linker may contain an amine-reactive group while the other end may consist of a sulfhydryl-reactive group. The main benefit that comes from the different reactivities of heterobifunctionality is that the cross-linking process can be

controlled. This means that whereas with homobifunctional cross-linkers there is the possibility that everything gets conjugated and there is a large degree of high molecular mass aggregate formation, the use of heterobifunctional cross-linkers makes cross-linking a more controlled process. When using a heterobifunctional cross-linker, one reactive group can be allowed to react and a purification step can be performed. Then the reaction conditions can be changed so that a coupling with the other reactive group is favourable. Heterobifunctional cross-linkers can contain a photoreactive group that is non-selective to target molecules and is only fixed with UV light. The non-selective nature of photoreactive groups makes their use suitable for characterising binding sites between receptors and ligands because the photoreactive groups will not react prior to UV treatment, allowing equilibrium to establish before being fixed for analysis. In contrast, amine-reactive cross-linkers will typically react with the first reactive target group that they encounter.

3.2.3.3 Zero-length cross-linkers

So-called zero-length cross-linkers are the smallest type of cross-linkage that can exist because they simply mediate direct cross-linking between/in proteins. The most common zero-length cross-linking system utilises a carbodiimide (such as 1-ethyl-3-(3-dimethylaminopropyl) carbodiimide hydrochloride (EDC)) to provide an amide linkage between a carboxylate and an amine or a phosphoramidate linkage between a phosphate and an amine.[152] Zero-length cross-linkers are apparently excellent tools for mapping contact regions in/between proteins.[153]

3.3 Current cross-linker chemistry

Although there are now hundreds of reported cross-linkers in the literature[151] and a wide range of commercially available reagents, their action is based on a small number of reactions. Consequently the protein functionalities that react with such cross-linkers are equally small. The most common cross-linker target functionality is the amino group, present on the side chain of lysines and the free *N*-termini of proteins. Sulfhydryl groups are the second most common cross-linker functionality targeted, especially in the design of heterobifunctional cross-linkers. Photoreactive

cross-linkers which react after exposure with UV light and insert non-specifically into the chemical bonds of target molecules are much less common and typically target double bonds, where an addition reaction can occur, and C-H and N-H sites whereby the photoreactive moiety undergoes an insertion reaction.

3.3.1 Amine-reactive cross-linkers

3.3.1.1 N-hydroxysuccinimide (NHS) esters – The concept of using NHS esters on the reactive ends of a homobifunctional cross-linker was first introduced in the mid-1970s.[154,155] NHS esters react readily with nucleophilic amines at physiological pH (Figure 3.7), which is one of the reasons why they are used today in the vast majority of cross-linkers.

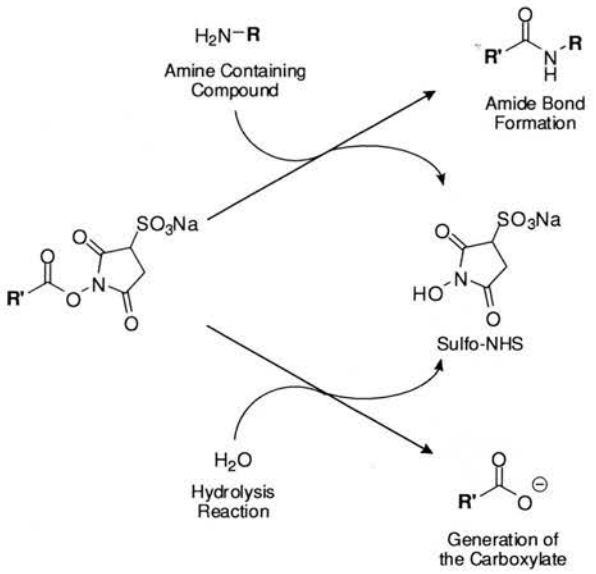

Figure 3.7 NHSS active ester reactions. Hydrolysis of the NHSS ester competes with nucleophilic attack by free amine containing compounds.

NHS esters react to produce stable amide bonds with primary or secondary amines and the NHS group released (as a good leaving group). Many NHS esters are insoluble in aqueous buffers, which often means that they must be first dissolved in DMSO. Sulfo-NHS esters are water soluble alternatives that allow a cross-linker to be dissolved directly into an aqueous buffer. NHS esters have half-lives in the order of hours at physiological pH but when the pH is increased, so is the rate of hydrolysis and amine reactivity. It has been reported that NHS esters can react with the

sulfhydryl groups of cysteines and with hydroxyl groups such as those found in serine and threonine, and that the products are unstable and the subsequent thioester or ester products hydrolyse very quickly in aqueous solution.[156] Studies have demonstrated that while sulfo-NHS esters react with lysine residues and the *N*-terminus, they also react with ammonium ions (*via* NH_3) that can contaminate buffers, as well as with serine and tyrosine residues.[157] Another study showed that although NHS esters preferentially react with primary amines, unexpected side reactions with the hydroxyl groups of tyrosine, threonine and serine can be detected.[158] The reactivity of amino acid hydroxyl groups is dependent on pH and the amino acids in proximity. Histidine and arginine both increase reactivity of neighbouring serine, threonine and tyrosine by formation of an intermediate cross-link.[159] In acidic conditions (pH 6.0) the yields of the side reactions can be greater than the reaction with lysine. In basic conditions (pH 8.4) the preference is for reactions involving the *N*-terminus and the amino groups present on lysine residues.

3.3.1.2 Imidoesters – The application of imidoesters in homobifunctional amine-reactive cross-linkers predates the use of NHS esters.[110] Imidoesters are the most specific acylating agents available for modifying primary amines and have minimal reactivity with other nucleophiles in comparison with most other cross-linking reagents. The *N*-termini primary amines and lysine side chains of proteins are targeted by imidoesters and reaction occurs at between pH 7-10, with optimal reaction occurring at a pH between 8 and 9. The product of the reaction is an imidoamide (also known as an amidine), which is protonated at physiological pH. The major reason why imidoesters have fallen out of favour in recent years is their slow and modest cross-linking efficiency compared with NHS esters. NHS esters are much more reactive than imidoesters and give much better cross-linking efficiency.

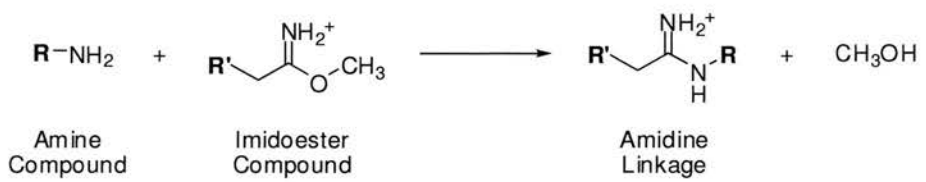

Figure 3.8 Imidoesters. Reaction between an amine and imidoester compound producing an amidine.

3.3.2 Sulfhydryl-reactive cross-linkers

The second most commonly exploited reactive groups used for cross-linking and modification are those that target sulfhydryl-containing molecules. Sulfhydryl-reactive groups are frequently present as one of the two reactive ends of heterobifunctional cross-linkers, with the other end usually being an amine-reactive group rather than being the sole functionality in a homobifunctional cross-linker. Most of the reagents that undergo reaction with sulfhydryl groups are stable in aqueous environments, allowing a two-step conjugation strategy to be used. The major coupling reactions involving sulfhydryl reactive groups are either by alkylation or disulfide exchange, resulting in stable thioether or more labile disulfide bonds. One of the problems with sulfhydryl-reactive groups is that while they target and react with the free thiol groups of cysteines, reduction of disulfide bonds in order to create the necessary free thiol groups carries the inherent risk of distorting the three-dimensional structure of a protein.[160,161]

3.3.2.1 Maleimides – Maleimides, also known as maleic acid imides, target sulfhydryl groups and are widely used in heterobifunctional cross-linkers. The thiolate anion is added to the maleimide in a 1,4-addition and the reaction is specific for thiols in the pH range of 6.5-7.5.[162]

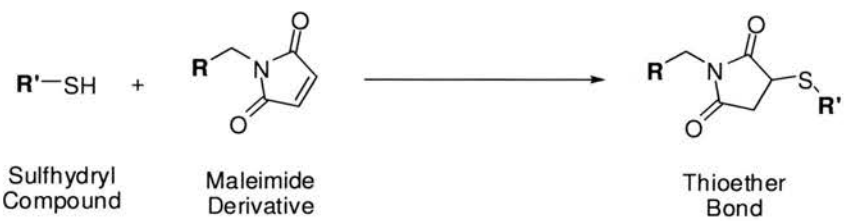

Figure 3.9 Maleimides. Reaction between a thiol and a maleimide producing a thioether bond.

At pH 7.0, the reaction of the maleimide with sulfhydryls proceeds at a rate 1000 times faster than its reaction with amines. However at more basic pH, there is some cross-reactivity with amino groups and above pH 8 hydrolysis of the maleimide group can occur, creating an open maleamic form, which is non-reactive towards sulfhydryl groups.[163]

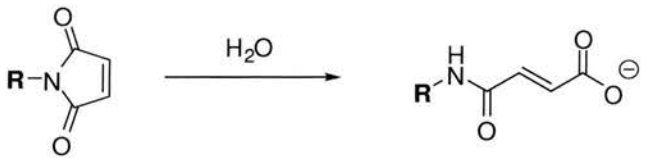

Figure 3.10 Maleimide hydrolysis.

3.3.3 Photoreactive cross-linkers

Photoreactive groups can be used in highly controlled reactions, because they do not react with target molecules until they are exposed to UV light, and prior to exposure they are typically non-reactive in usual thermochemical processes. Photoreactive groups are normally very reactive and insert indiscriminately into any type of residue. The groups used have to be stable in the dark and must become reactive when exposed to light of a wavelength that does not induce photolytic damage in biological samples. The vast majority of photoreactive reagents are based on nitrene or carbene chemistry where the photolabile precursors are azides, diazirines, diazo compounds and benzophenones.

3.3.3.1 Aryl azides – Aryl azides are the most popular type of photosensitive functional group. Following photolysis of an aryl azide, a short-lived nitrene is formed that is able to insert non-specifically into the chemical bonds of a target molecule, including undergoing addition reactions with double bonds and insertion reactions into active hydrogen bonds at C-H and N-H sites.[164] Evidence has shown that after an aryl nitrene has formed it immediately undergoes ring expansion creating a dehydroazepine intermediate that reacts with nucleophiles, in particular with amines.

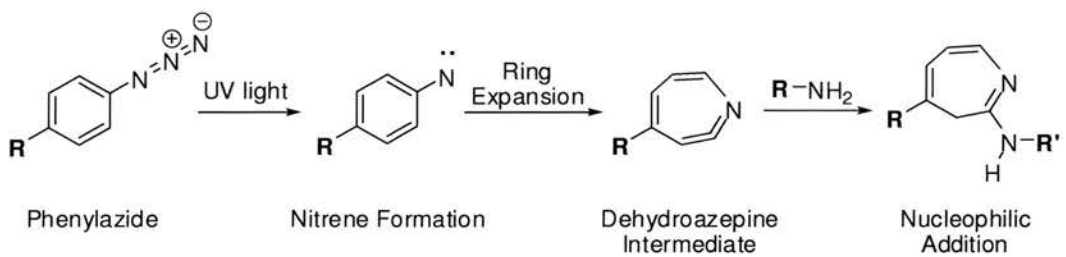

Figure 3.11 Aryl azides. Photo-activation of an aryl azide and subsequent nucleophilic addition by an amine.

Aryl azides that contain a perfluorinated ring structure form the desired nitrene more efficiently so that the addition and insertion reactions occur in preference to nucleophilic addition.[165] The major disadvantage of aryl azides is that once they have been activated, the created nitrene reacts with everything.

3.3.3.2 Diazirines – Diazirines display similar photoreactivity to diazo groups. The photosensitive diazirine consists of a three-membered ring system that contains two nitrogen atoms connected through a double bond. Diazirines come second in terms of the popularity of photoreactive cross-linking reagents after the aryl azides and were developed slightly later.[166]

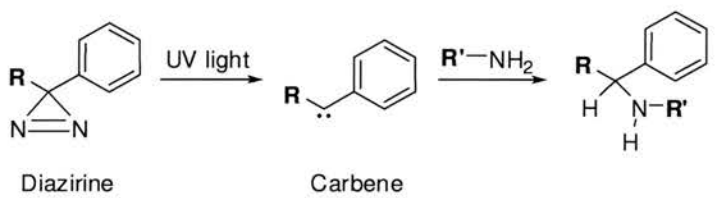

Figure 3.12 Diazirines. Photo-activation of a diazirine results in formation of a carbene, which inserts into an N-H bond.

The diazirine is photolysed at wavelengths of around 360 nm, which generates a carbene that is highly reactive and capable of inserting into C-H or N-H bonds. The major problem with diazirines is that photolysis can lead to diazo isomers that are strongly alkylating and are responsible for undesired reactions in the dark.[167] Despite this flaw, diazirines have been successfully used in heterobifunctional crosslinkers to attach macromolecules to surfaces such as polystyrene and glass (Figure 3.13).[168] Photoreactive active amino acid analogs (photo-leucine and photo-methionine) that exploit diazirine groups have been used to study protein interactions within cells.[169]

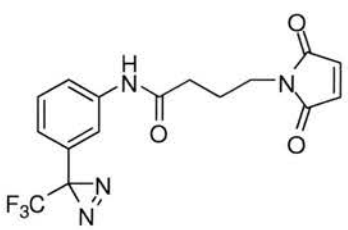

Figure 3.13 Diazirine containing heterobifunctional cross-linker. Structure of MAD (N-(4-maleimidobutyryl)-*N*-[3-(trifluoromethyl)diazirin-3-yl]phenyl amide) cross-linker.[168]

3.3.3.3 Benzophenones – A benzophenone photoreactive group after exposure to UV light, gives a triplet-state ketone intermediate (production of a biradical) that is highly reactive.[170] The resulting radicals can insert into C-H bonds and other groups to give covalent linkages with target molecules. Whereas decomposition or decay of the photoactive species leads to deactivation of aryl azides, benzophenones that have become deactivated without forming a covalent bond with a target can be reactivated by photolysis to the active state. Activation of benzophenones does not follow a photo-dissociative mechanism, which makes its activity reversible. This means that benzophenones have more chance to react with the intended targets than aryl azides, which lead to higher yields of photo-cross-linking compared to phenyl azide cross-linkers.[171]

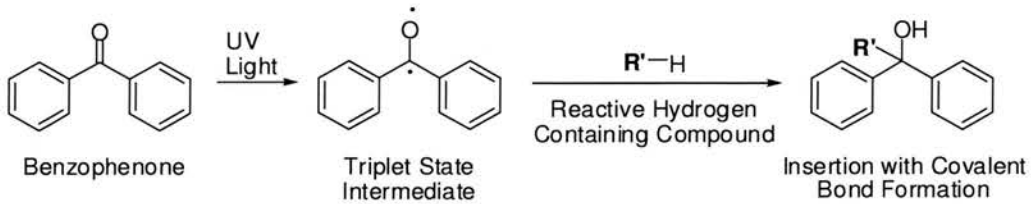

Figure 3.14 Benzophenones. Photo-activation of benzophenone followed by insertion into a reactive hydrogen containing compound.

3.4 Problems with the chemical cross-linking approach

The sheer complexity of digested cross-linked material poses a huge problem. One of the greatest challenges that needs to be answered, before chemical cross-linking of proteins can be considered to be a truly effective tool, is how to identify cross-linked peptides amongst an ocean of non-cross-linked or partially linked background peptides. It is the question of how to find the 'needles in the haystack'. Figure 3.15 shows a FT-MS scan of a cross-linked digest of just the yeast 20S proteasome that demonstrates the gravity of the problem. Cross-linked peptides are generally low-intensity and have a limited elution window. The likelihood of them being sequenced in a complex sample is low because in practical terms cross-linked peptides will be over-looked.

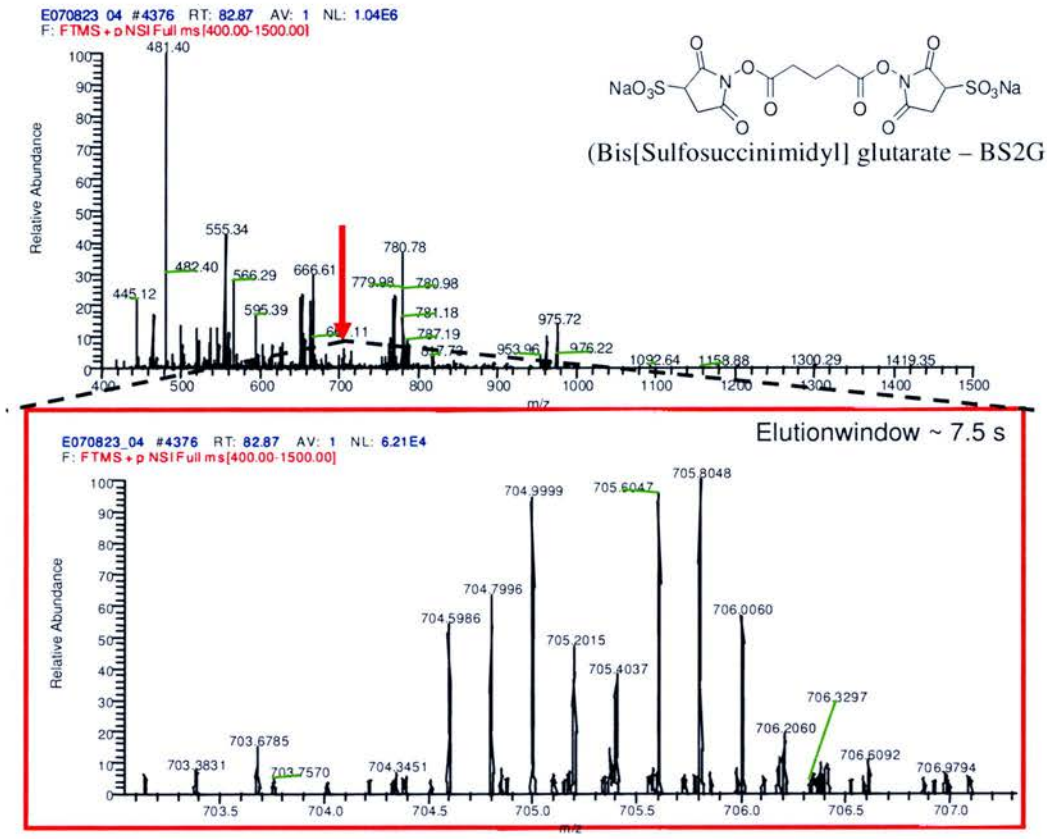

Figure 3.15 Mass spectrum showing a cross-linked peptide. Cross-linking of a yeast 20S proteasome digest, carried out using (deuterated Bis[Sulfosuccinimidyl] glutarate – BS2G-d_0/d_4). Top pane: Red arrow indicates position of a cross-link fragment at 706.33 with the elution window of 7.5 s. Bottom pane: Zoom of double isotope cluster corresponds to cross-linked peptides.

There are two approaches that can be taken to help to pick-out only the cross-linked peptides:

(i). Introducing a discriminating feature on the cross-linked products to make identification of cross-linked peptides easier.

(ii). Develop an enrichment strategy to filter out or even remove any undesired, non-cross-linked background product.

3.4.1 Strategies to improve detection of cross-linking products

3.4.1.1 Cleavable cross-linkers

The cleavable cross-linkers that are currently available can either be cleaved chemically or during MS/MS experiments if they contain bonds that fragment using low-energy activation. Such cleavable cross-linkers facilitate the identification of a cross-linked product but only if it is not obscured by background data from the experiment. In other words, cross-linked products will only be identified if they are in very high proportion with respect to the total sample. The principle is that spectra can be compared before and after the cross-linker is cleaved and following cleavage, the disappearance of a peak can mark it out as a cross-linked product.

(i). Chemical cleavage with periodate - Cross-linkers that contain a diol such as disuccinimidyl tartrate (DST) can be cleaved using periodate with each hydroxyl group being oxidised to an aldehyde.

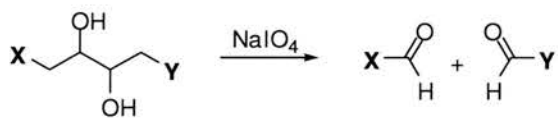

Figure 3.16 Periodate cleavage. Diol is cleaved producing two aldehydes.

One drawback of this chemistry is that it is then possible for the resulting aldehydes to produce secondary unwanted reactions, especially Schiff base formation with any free amine groups that are available. Another disadvantage is that sodium periodate is also capable of oxidising other amino acids, in particular tryptophan and methionine residues. A benefit of employing periodate as a cleavage agent is that disulfide bonds are preserved, which means that tertiary structure of proteins and other molecules is usually unaffected so that any protein bioactivity can be retained.

(ii). Chemical cleavage of disulfide bonds – Formation of disulfide bonds between cross-linked molecules is an important feature in many conjugation chemistries and two examples of cross-linkers that can be cleaved *via* their disulfide bonds following peptide cross-linking are shown in Figure 3.17.

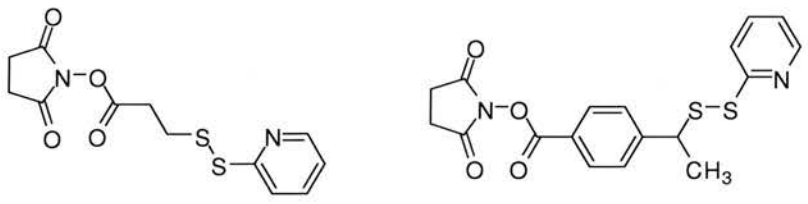

Figure 3.17 Disulfide cleavable hetero-bifunctional cross-linkers. SPDP (*N*-succinimidyl-3-(2-pyridyldithio)propionate) and SMPT (succinimidyloxycarbonyl-α-methyl-α-(2-pyridyldithio)toluene).

The NHS ester reacts with a primary amine. The other end of the cross-linker then reacts with a free thiol (with the release of pyridine-2-thione) (Figure 3.18).

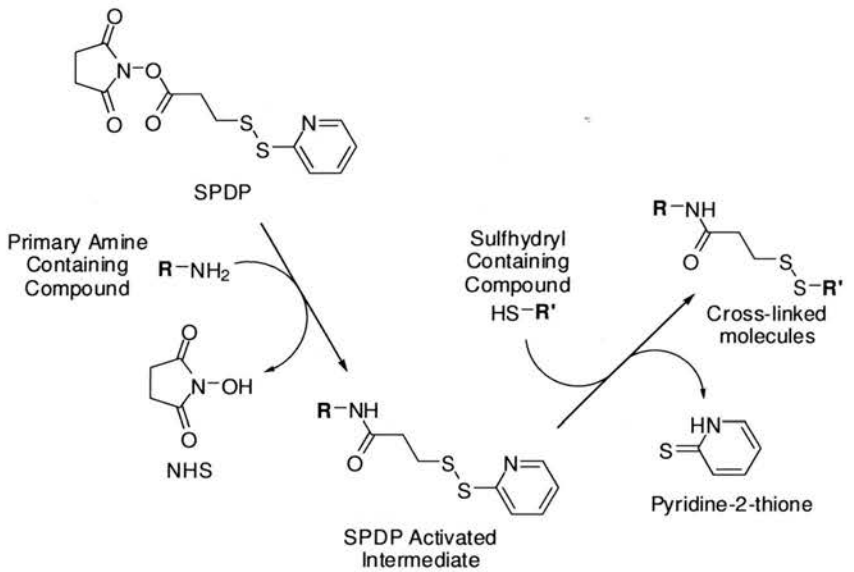

Figure 3.18 Reaction of SPDP. SPDP cross-links two molecules *via* a disulfide and an amide.

The incorporation of a disulfide into the cross-linker means that the cross-linker can be specifically cleaved after conjugation by either a strong reductant such as sodium borohydride or through disulfide interchange with a compound containing one or more free thiols.

The thiol-cleavable cross-linker DTSSP (3,3'-dithio-*bis*(succinimidylpropionate)) has been used to map interfaces of a number of protein complexes[119,121,172] and to map the three-dimensional structure of a number of proteins.[173,174] MALDI-TOF-MS and ESI-QTOF-MS were used to produce peptide maps of digested reaction mixtures

before and after reduction and the masses were compared. Cross-links were confirmed on the basis of observing the corresponding peptide 'halves' of cross-linked products that had been previously identified prior to reduction. However there are major limitations with this technique as sometimes it is possible to see peptides before reduction but not after, suggesting that actual cross-links are not present, and vice-versa. The biggest concern with the technique is that cross-linked peptide products may still be obscured amongst a huge amount of background material.

(iii). MS/MS cleavage – An amine-reactive homobifunctional cross-linker *N*-benzyliminodiacetoyloxysuccinimide (BID) was used to cross-link model peptides as well as components of a protein complex. The cross-linker aided detection of cross-linked products due to a marker ion being produced (*m/z* 91) during triple-quadrupole and QTOF tandem MS experiments (Figure 3.19),[131] with observation of the marker ion indicating that cross-linking had occurred.

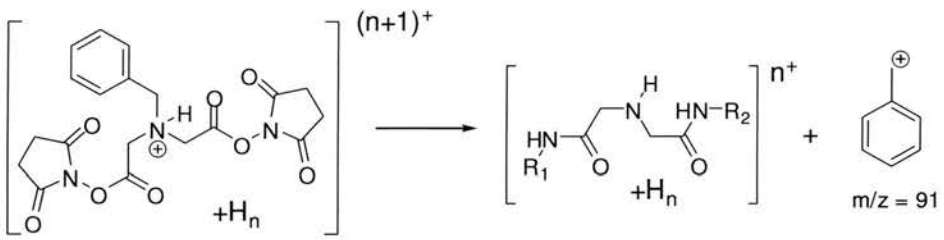

Figure 3.19 *N*-benzyliminodiacetoyloxysuccinimide (BID) cross-linker. Production of a marker ion indicates that cross-linking has occurred.[131]

A novel type of cross-linker was synthesised that has two MS/MS cleavable bonds within the spacer chain. The cross-linker system was named PIR (protein interaction reporter) was synthesised using solid-phase chemistry exploiting lysine chemistry and the Rink linker.[106] After MS/MS cleavage, a reporter ion was released of *m/z* 711 that indicated that a cross-linked product was present. The PIR cross-linker was used to cross-link ribonuclease S (RNase S), a non-covalent complex of S-peptide 1-20 and S-protein 1-104 that are the hydrolysis products from ribonuclease A (RNase A) following cleavage by the serine protease subtilisin.

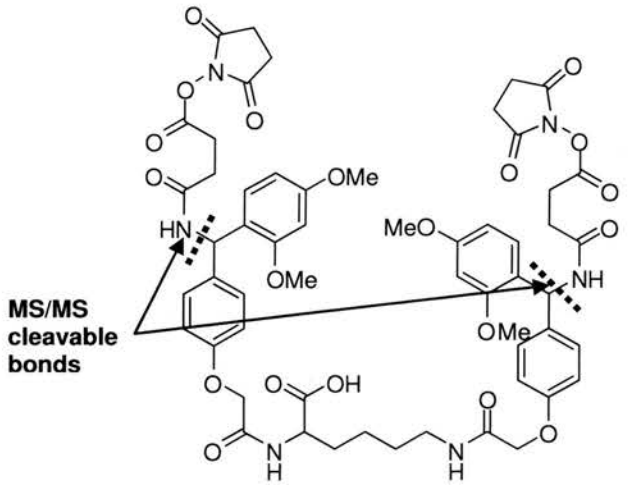

Figure 3.20 PIR (protein interaction reporter) cross-linker. Contains two MS/MS cleavable bonds that release a reporter ion indicating cross-linking upon MS/MS cleavage.

Perhaps the biggest downfall of the PIR cross-linking system is that its spacer chain length is 43 Å in its most extended conformation and this coupled with its high flexibility casts doubts over whether any structurally meaningful information can be obtained.

3.4.1.2 Affinity enrichment systems

Probably the best way to solve the problem of the complexity of the cross-linked product mixtures is to isolate cross-linked products from the enormous background. Using an affinity enrichment system to specifically isolate products probably holds the greatest potential for solving the complexity issue.

(i). Enrichment via biotin – The extremely strong noncovalent conjugation between (strept)avidin and biotin has been exploited in a number of enrichment strategies.

Avidin interacts with biotin with one of the strongest noncovalent affinities known, with a dissociation constant of about 1.3×10^{-15} M.[175] Avidin is a tetrameric protein and when biotin is bound to avidin, the interaction promotes even greater stability to the complex. In fact the interaction in the avidin-biotin complex (ABC) is resistant to break down in the presence of up to 8 M guanidine, to achieve complete dissociation 6-8 M guanidine at pH 1.5 is required. The ability of biotinylated molecules and

avidin conjugates to "find" each other and subsequently bind and complex together under extreme conditions is remarkable.

The great interaction between avidin and biotin has been capitalised on for the synthesis of some trifunctional cross-linkers, composed of biotin containing heterobifunctional cross-linkers, which allowed enrichment of cross-linked products by affinity purification on monomeric avidin beads.[176,177] Cross-linkers (Figure 3.21) containing aryl azide photoactivatable groups such as sulfo-SBED (sulfosuccinimidyl-2-[6-(biotinamido)-2-(*p*-azidobenzamido)hexanoamido]ethyl-1,3'-dithiopropionate) have been developed commercially (Fujimoto) and used to map the interface regions between calmodulin and its target peptide, derived from the skeletal muscle myosin light-chain kinase.[177]

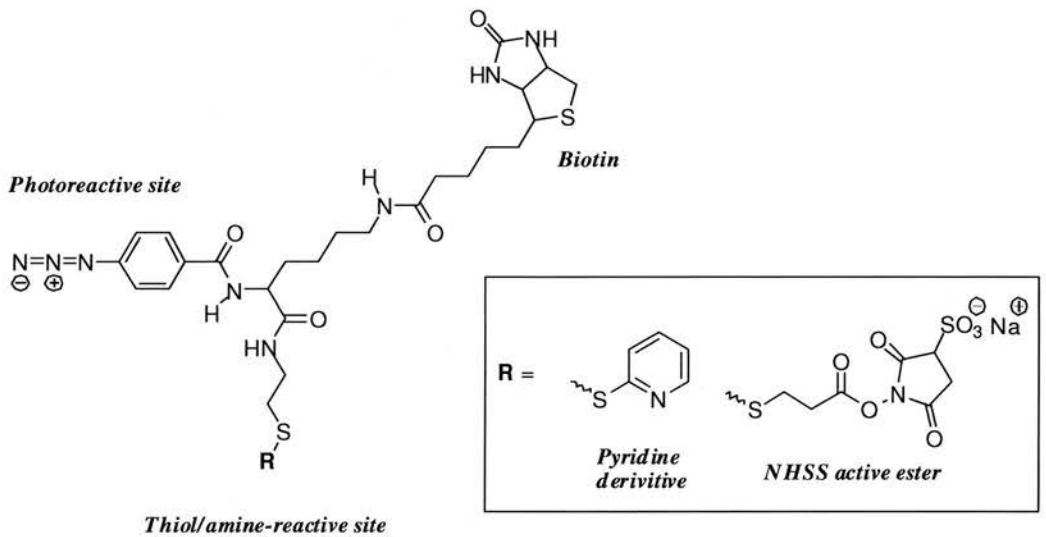

Figure 3.21 Biotin derivative trifunctional cross-linkers for enrichment. Amine reactive sulfo-SBED (sulfosuccinimidyl-2-[6-(biotinamido)-2-(*p*-azidobenzamido)hexanoamido]ethyl-1,3'-dithiopropionate and a thiol reactive derivative.

The great strength of the non-covalent interaction between avidin and biotin makes it extremely useful in bioconjugate chemistry, but its lack of reversible enrichment is its major downfall. Variations in buffer salt, pH, the presence of denaturants or detergents and extremes of temperature will not allow reversibility of the interaction. Another crudity with the avidin-biotin complex conjugation system is that it is

fundamentally based on the principle of using a huge protein to "fish-out" something that is relatively small. Another downside to these cross-linkers is that they are hydrophobic and relatively large, limiting their water-solubility. The reagents are soluble in solvents such as DMF and DMSO, but relatively insoluble under aqueous reaction conditions, which make them impractical for use with proteins in their native environment.

(ii). "Click Chemistry" based enrichment - The most recent advance in attempts to have practical cross-linked peptide enrichment is the introduction of so-called alkyne-azido click chemistry as the mechanism for selectively retrieving cross-linked peptides.[178]

The premier click reaction is undoubtedly the Huisgen 1,3-dipolar cycloaddition of alkynes and azides to yield triazoles (Figure 3.22),[179] which has been made more practical by the use of copper catalysis, reported by Meldal.[180]

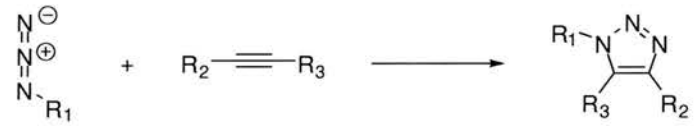

Figure 3.22 General Huisgen reaction. Cycloaddition of an azide with an alkyne, resulting in the formation of a triazole ring.

An azide containing cross-linker, BAMG (bis(succinimidyl)-3-azidomethyl glutarate), was first used as a marker tag in order to aid the identification and separation of cross-linked peptides from complex mixtures.[181]

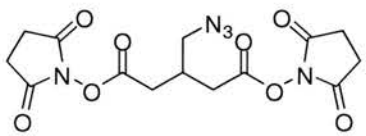

Figure 3.23 BAMG (bis(succinimidyl)-3-azidomethyl glutarate). An azide-containing homobifunctional cross-linker.

The reduction of the azide to primary amine competed with a chemo-selective peptide-bond cleavage at the site of the non-natural amino acid azidohomoalanine

with use of the reducing agent TCEP (tris(2-carboxyethyl)phosphine). The observation of both reactions was meant to facilitate cross-link identification from background protein because cross-linked products would have different retention times by reverse-phase HPLC than the parent compound cross-linked with an azide functionality present.

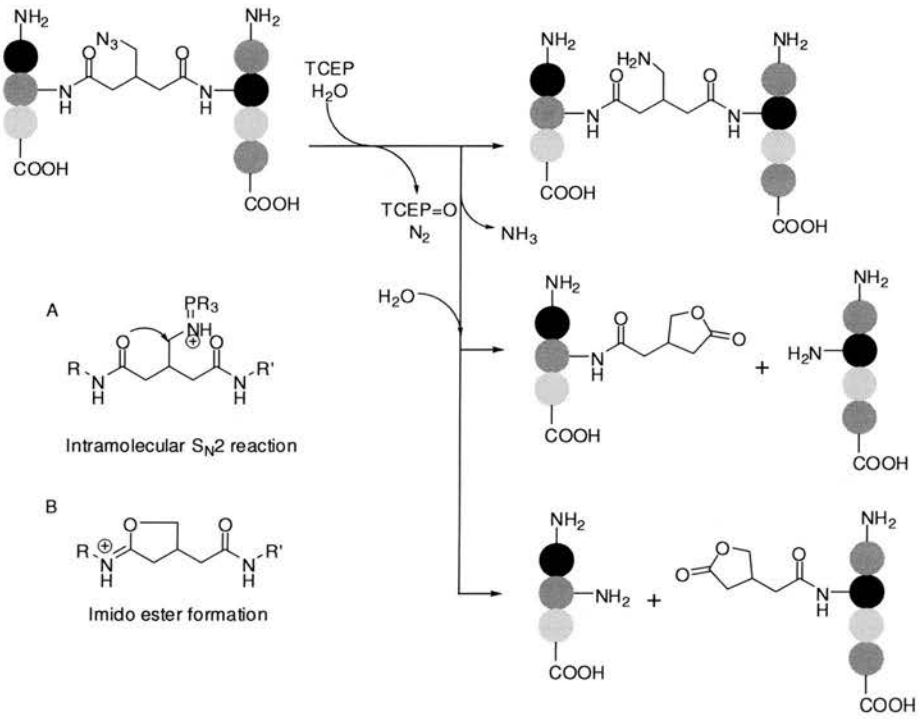

Figure 3.24 Phosphine induced reactions in BAMG cross-linked peptides. Two parallel reaction pathways occur in the presence of the phosphine reducing agent TCEP (tris(2-carboxyethyl)phosphine). TCEP either reduces the azido group to an amino group or to a leaving group that is displaced by one of the two amide groups by an intramolecular S_N2 reaction to form an imido ester, which is then hydrolysed to give a lactone. Both reactions are meant to aid in identification of cross-linked peptides.

In reality this approach was flawed because it over-complicates the range of cross-linked products that are obtained but more importantly it doesn't solve the problem of low abundance of cross-linked products. The principle relied on diagonal chromatography where huge losses of interesting species are made when only very small amounts of starting material are available.[181] Further problems with this strategy are that free cysteines are able to prematurely reduce and cleave BAMG cross-linked peptides and disulfide-linked peptides will also be reduced in the

presence of TCEP and will end up in shifted fractions after diagonal chromatography.

The BAMG cross-linker was used in a click-chemistry based enrichment system. Azide-containing cross-linked peptides were captured on resin *via* "strain-promoted" (3+2)-cycloaddition.[178] Following a washing step, peptide products were detached from the resin by reduction of the disulfide linker located between the solid-support and the solid-supported cyclooctyne responsible for capture of azide-modified peptides (Figure 3.25).

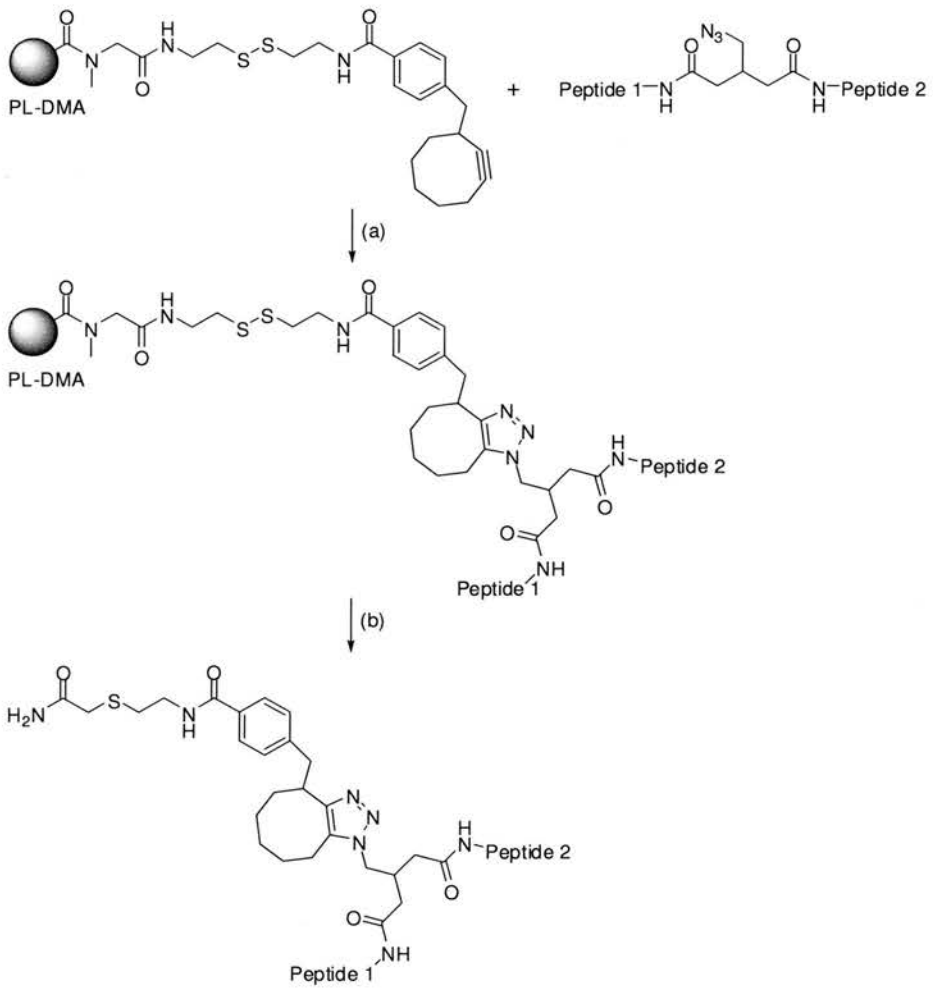

Figure 3.25 Click-chemistry based capture and release of azide containing cross-linked peptides. (a) Capture of azide containing cross-linked peptide products *via* a Huisgen reaction between the azide on the cross-linked peptides and solid-supported cyclooctyne (PL-DMA = polydimethylacrylamide resin), 72 h., 40 °C; (b) Release of captured peptides *via* reduction (i) 5 mM TCEP, 50 mM PBS pH 7.5, 1 h, rt; (ii) 55 mM iodoacetamide, 30 min, rt.

Although useful the method has numerous downfalls. The incubation time for capture was up to 72 hours and even after this time only 50% yield was achieved. Coupled with this is another major flaw in that the resulting peptides following cleavage from the resin have a massive hydrophobic modification, which causes quite heavy insolubility issues.

Chapter 4: *Boronate Ester Conjugate Enrichment*

4.1 Cross-linked peptide enrichment via boronate ester formation

Phenylboronic acids can form reversible, pH-dependent complexes with a variety of polar groups[182] such as dicarboxylic acids,[183,184] α-hydroxy carboxylic acids[185,186] and diols[187] to form boronate esters in aqueous media.[188] The most common complex is with 1,2- and 1,3-diols to form either 5- or 6-membered heterocycles (Figure 4.1). Reversible boronate ester chemistry with immobilised phenylboronates has already been exploited in affinity chromatographic purification of carbohydrates, glycoproteins, RNA,[189] AMP, glycated proteins (such as glycated haemoglobin found in diabetes) [190], and a range of small molecules containing 1,2- and 1,3-diols,[191,192] hydroxyl acids,[193] hydroxylamines, hydroxyamides[194] and hydroxyoximes, as well as various sugars containing these species. The interaction between catechol derivatives and phenylboronic acid has also been exploited in the development of an electrochemical dopamine sensor.[195]

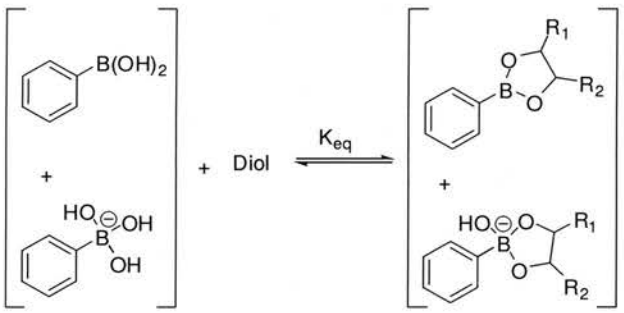

Figure 4.1 Boronate ester formation. Reaction between phenyl boronic acid and an unspecified 1,2-diol.

A whole range of solid-supports and linkers have been developed to provide a means for immobilising boronic acids, to facilitate purification and manipulation,[196,197] driven by the difficulties that are often encountered when isolating or removing boronic acids from aqueous and/or organic solvent systems (Figure 4.2).

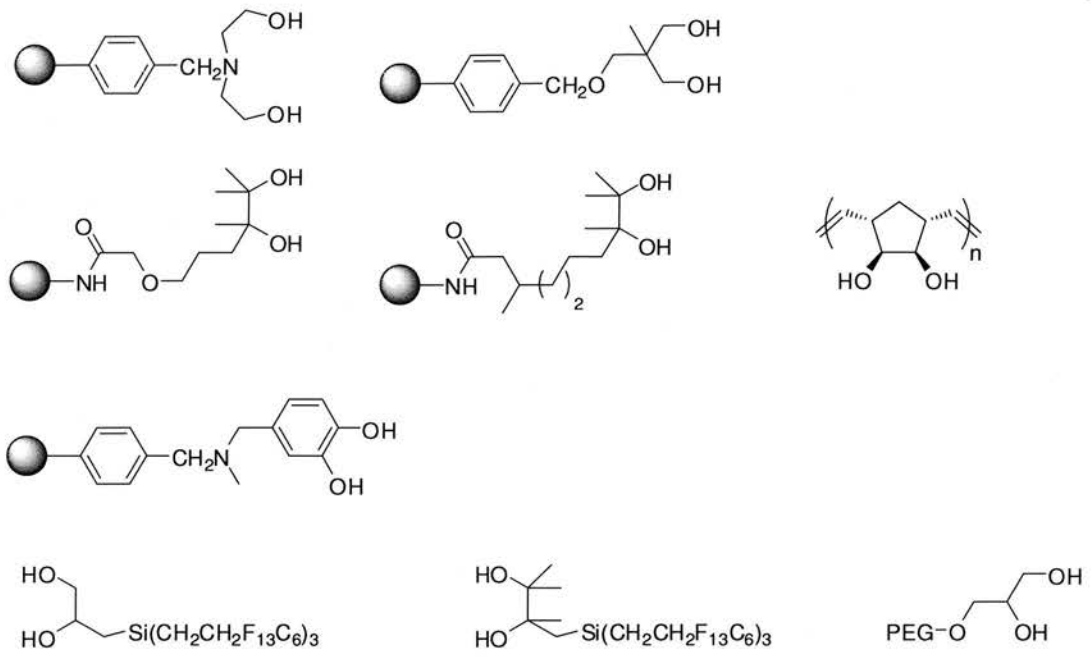

Figure 4.2 Solid-supported diols. A range of diols developed for the capture of boronic acids.

Boronic acid chemistry has been used for the manipulation of gold nanoparticles,[198] whereby a solid-supported boronic acid was used to attract gold nanoparticles *via* a thiol-derivatised catechol,[199] with thiols reacting with the surface of gold nanoparticles through Au-S interactions and the catechol forming a boronate ester with solid-supported boronic acid. More recently, boronic acid functionalised gold nanoparticles have been used to enrich *cis*-1,2- diol containing glycoproteins and glycopeptides.[200] Similarly a MALDI target plate was covered with an array of similar gold nanoparticles, allowing MALDI-TOF analysis of enriched glycopeptides directly from the plate.

The interaction between phenylboronic acid derivatives and diol-like systems occurs optimally in the pH range of 8-9 and is typically reversed at acidic pH or in the presence of a high concentration of a competing ligand (Figure 4.3). Stolowitz exploited the interaction potential in the design of a new chemoselective bioconjugation reagent pair consisting of a phenylboronic acid (PBA) on one reagent and a salicylhydroxamic acid (SHA) on a second.[201] Stolowitz proposed that each reactant of the pair could be used to modify biomolecules, surfaces or other compounds for subsequent conjugation or immobilisation through specific PBA-

SHA ring formation.[202] The major product of the reaction is a 6-membered ring, which is formed by the boron atom of PBA along with one of its oxygen atoms coordinated with the SHA's hydroxyl oxygen and hydroxamate nitrogen atoms. It is also possible to form a 5-membered ring structure with the boron interacting with the hydroxamate hydroxyl and carbonyl oxygens on the SHA but NMR has shown this to be a minor product.[203]

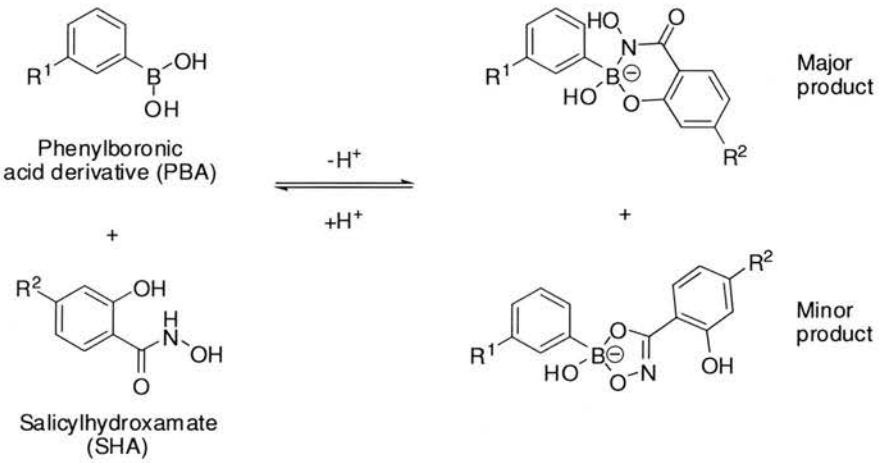

Figure 4.3 Boronate ester from salicylhydroxamic acid. Reaction between phenylboronic acid and a salicylhydroxamate.

Complex formation between the PBA group and SHA group occurs across a wide range of pHs (5 to 9) and high salt concentrations and can tolerate the presence of moderate quantities of water-miscible solvents, detergents, chaotropes and denaturing agents, such as are used when working with protein solutions. The interaction is reversed by lowering the pH, the value of which depends on the type of boronate ester involved. One study looking at pH dependence of boronic acid-diol affinity in aqueous solution found that complexation between phenylboronic acid and 4,5-dihydroxynaphthalene-2,7-disulfonate (as shown in Figure 4.4) even occurs at pH 1.[204]

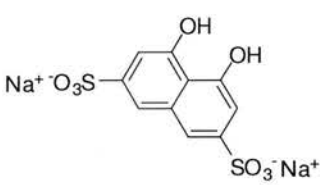

Figure 4.4 4,5-dihydroxynaphthalene-2,7-disulfonic acid disodium salt.

Interactions between solid supported SHA groups and ligands containing PBA groups have been investigated for immobilisation of antigen molecules for antibody protein purification.[205]

For the work in this chapter, a catechol derivative was selected as the 1,2-diol component for a boronate ester pairing along with a phenylboronic acid derivative because of their rigid planar structures.[206] Planarity leads to a stronger interaction with conjugation occurring due to overlap between the lone pair of electrons on the oxygen and the empty p-orbital on the boron.[207]

4.2 Aims

The aim of the work in this chapter was to develop novel peptide/protein reactive cross-linkers and tags that would allow the enrichment of cross-linked products from complex mixtures of peptides by exploiting the reversibility of boronate ester chemistry.

4.3 Overview

The enrichment concept is shown in Scheme 4.1. The initial idea was that either the boronic acid or the diol component could be immobilised onto a solid-support and the complimentary functionality incorporated onto either an amine-reactive tag or a protein cross-linker.

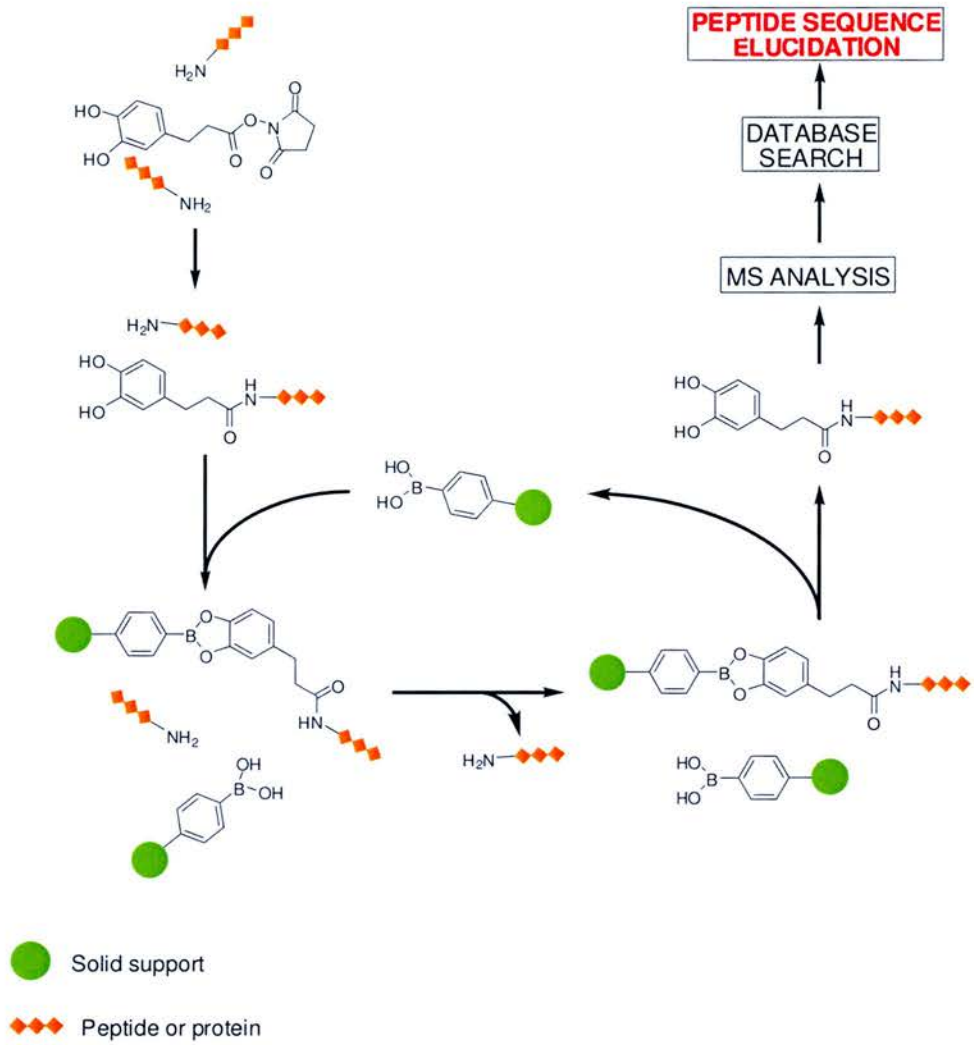

Scheme 4.1 Boronate ester based enrichment. Enrichment strategy exploiting boronate ester formation between a solid-supported phenylboronic acid and catechol tagged reaction products that result from a catechol *N*-hydroxysuccinimide (NHS) active ester reacting with a peptide or protein.

Scheme 4.1 shows an NHS-active-ester modified catechol reacting with free amino groups from a peptide or protein. The resulting mixture is then introduced to a solid-supported boronic acid at high pH, whereupon a boronate ester conjugate is formed. Unmodified material is then washed away, with only the modified material remaining attached to the solid support. When the pH is lowered, the diol-modified material is released from the solid-support and the 'enriched' material is then ready for MS analysis and subsequent data interpretation.

4.3.1 Synthesis of NHS activated esters

The NHS active ester of 3,4-dihydroxyhydrocinnamic acid was synthesised using an excess of NHS and the water-soluble coupling reagent 1-ethyl-3-(3-dimethylaminopropyl) carbodiimide hydrochloride) (EDC) (Scheme 4.2).

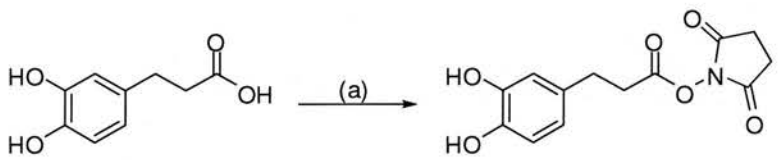

4.1

Scheme 4.2 Catechol tag NHS ester (4.1). Activation of 3,4-dihydroxyhydrocinnamic acid.
(a) 1.2 eq EDC, 1.5 eq NHS, DMF, 71%

To compliment this, an NHS active ester of 4-carboxyphenylboronic acid was also synthesised using the same conditions (Scheme 4.3).

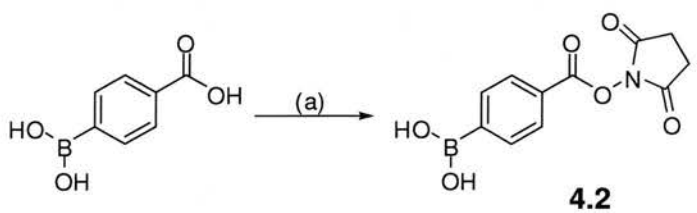

4.2

Scheme 4.3 Boronic acid tag NHS ester. Activation of 4-carboxyphenylboronic acid.
(a) 1.2 eq EDC, 1.5 eq NHS, DMF, 67%

4.3.2 Synthesis of solid-supported component

4.3.2.1 Choice of CPG as the solid support

For a study involving such a sensitive technique as mass spectrometry, any solid-support involved prior to analysis had to be resistant to leaching and give low background signals. The solid-support also had to be compatible with a wide range of aqueous buffers as well as organic solvents.

CPG or controlled pore glass is produced from borosilicate glass that has been held at a high temperature for a prolonged length of time, which results in separation of the borates from the silicates to give a rigid nonabsorptive matrix. Boronate, which is

soluble in acid, is leached from the material in a controlled process to create a silica glass with very uniform pores that have a narrow size distribution range, hence the use of the term "controlled-pore". CPG is stable to aggressive reagents and extremes of temperature and pressure that are often used in synthesis. The biocompatibility of CPG and its applicability with peptides and proteins has been proven.[208] It is particularly suitable for continuous flow synthesis because of the rigidity of its structure and it was decided that for these reasons, CPG would be the most suitable solid-support for this work.

Trisoperl supplied aminopropyl functionalised CPG of 50-100 μm diameter with 55 nm pore size (0.22 mmol/g free amino group loading). Experience in Professor Bradley's lab has indicated that functionalisation of aminopropyl CPG is sluggish. Initially a DIC/HOBt coupling protocol was employed for the coupling of 4-phenylboronic acid to aminopropyl CPG. Reactions were monitored by a ninhydrin reaction[209] and repeated couplings were necessary before complete coupling was observed. Coupling with HBTU were also attempted but there was no increase in reaction efficiency. Coupling with IIDQ gave greater coupling efficiency and could be forced with gentle microwave heating.[210]

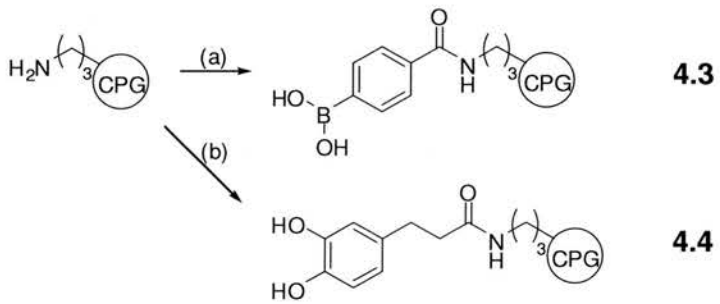

Scheme 4.4 CPG supported components. Coupling of either 4-phenylboronic acid or 3,4-dihydroxyhydrocinnamic acid to aminopropyl functionalised CPG using IIDQ.

(a) 3 eq 4-phenylboronic acid, 3.3 eq IIDQ, acetonitrile;

(b) 3 eq 3,4-dihydroxyhydrocinnamic acid, 3.3 eq IIDQ, acetonitrile.

4.3.3 Synthesis of modified peptides for a model system

Peptides were initially assembled *via* solid phase synthesis using the Wang linker resin and Fmoc-protected amino acids and consisted of a control peptide with no

modification **4.7**, a boronic acid modified peptide **4.8,** a catechol-modified peptide **4.9** and a derivative containing a salicylhydroxamic acid group **4.10** (Scheme 4.5). The peptide sequence in each case was LLEYLKR. The sequence was chosen from a range of peptides used in an earlier study that were most easily identified as being synthetic peptides after having been spiked into protein digests, run on the mass spectrometer and processed with a database searching program.

Initial loading of the resin was achieved by forming a symmetrical anhydride with DIC/DMAP and Fmoc-Arg(Pbf)-OH. Following an Fmoc test to assess the degree of loading, the Fmoc group was removed using 20% piperidine in DMF to give **4.5**. Subsequent synthesis was achieved using HBTU-mediated coupling cycles, which has been shown to facilitate rapid reaction times and produce clean products with even very difficult to synthesise sequences.[211] 4-Carboxyphenylboronic acid was coupled to the N-terminus of **4.6** using HBTU coupling chemistry to achieve a boronic acid modified peptide **4.8** and with 3,4-dihydroxyhydrocinnamic acid to achieve the catechol modification **4.9**.

The salicylhydroxamic acid peptide derivative **4.10** was generated by coupling the commercially available NHS-active ester-THP-protected salicylhydroxamic acid derivative (SHA(THP)-X-NHS) **4.11** under basic condtions.

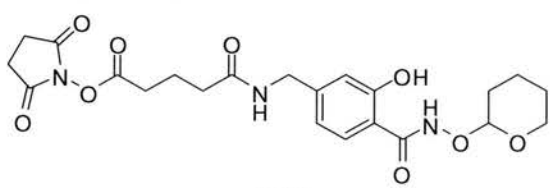

4.11

Figure 4.5 SHA(THP)-X-NHS 4.11. Structure of 4-(3-hydroxy-4-(tetrahydro-pyran-2-ylcarbamoyl)-benzylcarbamoyl)-butyric acid 2,5-dioxo-pyrrolidin-1-yl ester.

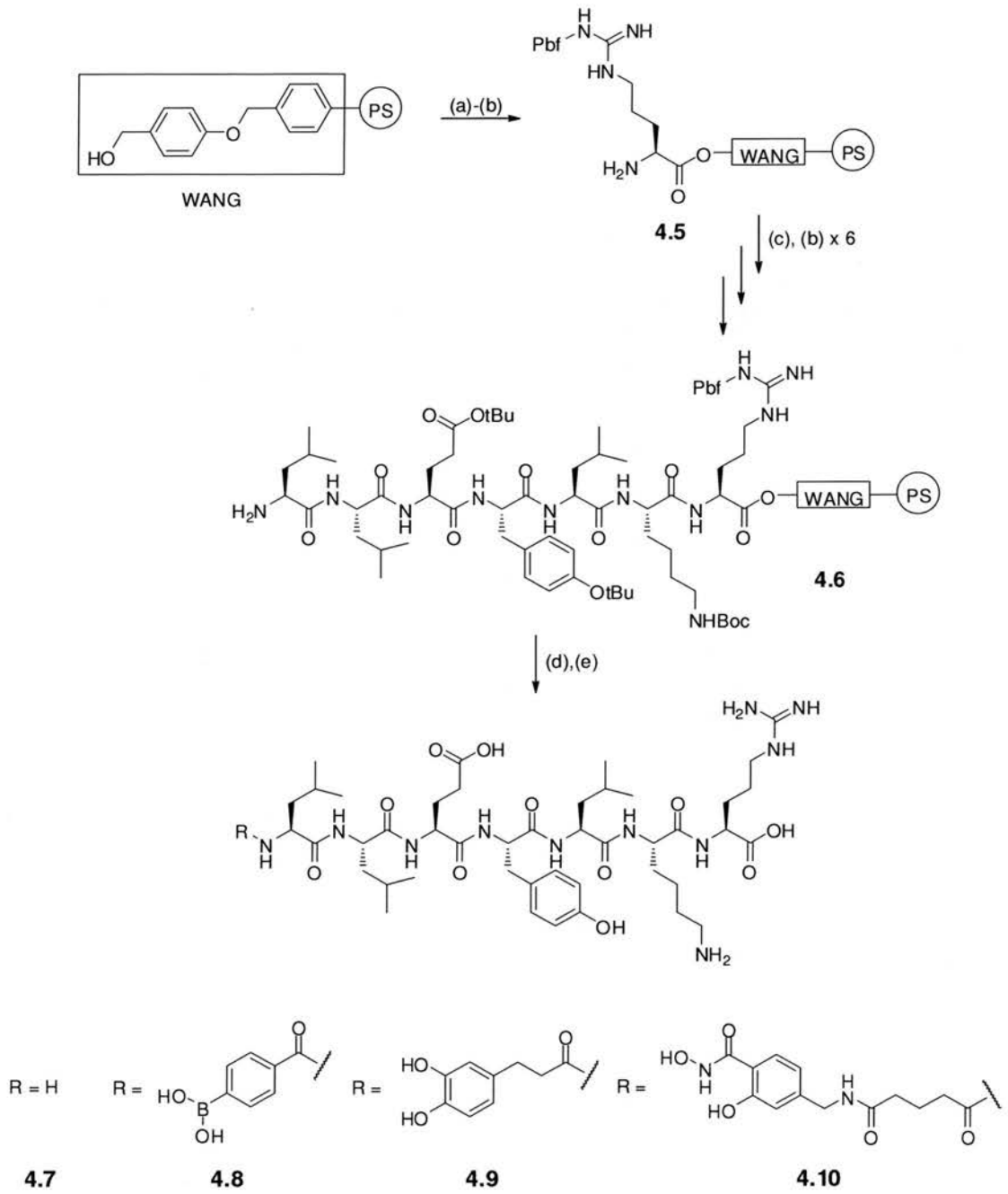

Scheme 4.5 Solid-phase synthesis of tagged peptides.

(a)(i) 10 eq Fmoc-Arg(Pbf)-OH, 5 eq DIC, 0.1 eq DMAP, 2 h; (b) 20% piperidine in DMF, 2 cycles of 10 min; (c) 5 eq Fmoc-AA-OH, 5 eq HBTU/HOBt, DMF (0.2 M), 10 eq DIPEA, 1 h; (d)(i) When R = boronic acid or catechol, 5 eq 4-carboxyphenylboronic acid or 3,4-dihydroxyhydrocinnamic acid, 5 eq HBTU/HOBt, DMF (0.2 M), 10 eq DIPEA, 1 h, followed by an additional step when R = catechol, 20% piperidine/DMF, 10 min; (ii) When R = salicylhydroxamic acid derivative, 2 eq SHA(THP)-X-NHS, 5% DIPEA in DMF (0.2 M); (g) TFA/TIS/H_2O (95:2.5:2.5), 2 h;

All peptides were released from the resin using a solution of TFA/TIS/H_2O (95:2.5:2.5) for 2 h, which simultaneously removed all protecting groups and cleaved the peptides from the resin.

4.4 Behaviour of catechol functionalised peptides on phenylboronic acid functionalised controlled pore glass (PBA-CPG)

Decomposition of all catechol derivatives under basic, aqueous conditions was a common feature, whether the catechol was present as an NHS-ester tag, a cross-linker or a direct peptide modification. Degradation was rapid and the degree of decomposition could be ascertained by analytical HPLC (Figure 4.6).

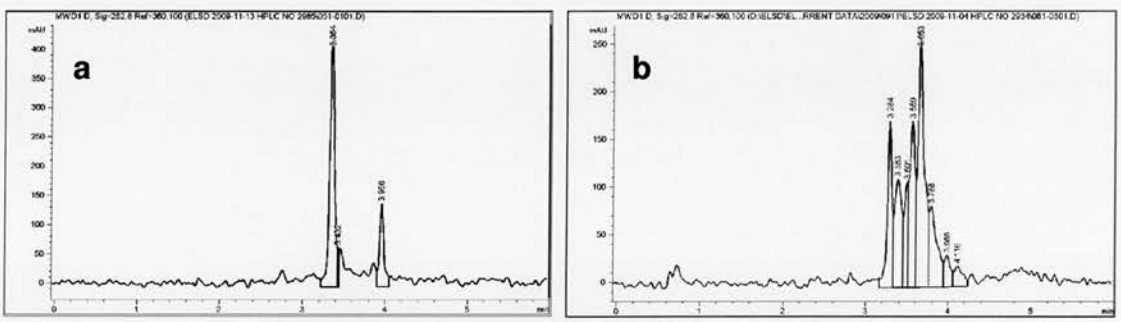

Figure 4.6 HPLC chromatograms. a. Crude catechol derivative peptide **4.9**; **b.** Decomposition of crude catechol derivative peptide following 30 minutes in 100 mM (pH 8.4) PBS.

The addition of 2 equivalents of dithiothreitol (DTT) relative to peptide **4.9**, in pH 8.4 buffer, slowed the rate of decomposition but after 24 hours all catechol modified peptide had fully decomposed. Stability of the catechol was achieved following addition of 5 mM *tris*(2-carboxyethyl)phosphine (TCEP) and working with a 0.6 mM peptide concentration, with the pH of the solution lowered to 7.60.

Capture of catechol modified peptide **4.9** was ascertained by measuring the UV absorbance of peptide that remained in solution following addition of PBA-CPG **4.3** and converted into a percentage based on the absorbance of peptide in the input solution (Figure 4.7). 20 equivalents of PBA-CPG **4.3** resulted in almost complete capture of peptide **4.9**.

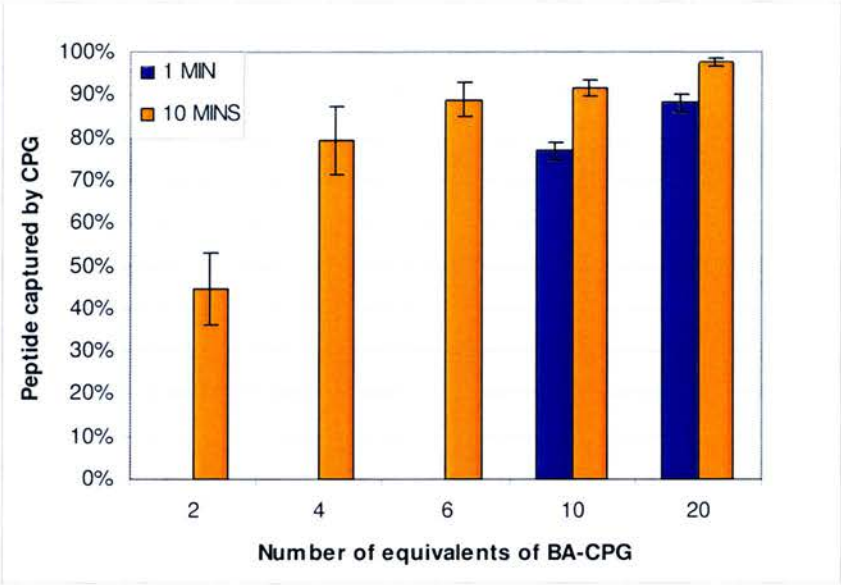

Figure 4.7 Peptide uptake. Percentage of peptide **4.9** remaining in solution following either 1 or 10 minutes exposure to varying equivalents of boronic acid-supported CPG **4.3**.

A study of the relationship between mixing time and number of equivalents of PBA-CPG **4.3** showed that the level of uptake was high (>77% with 10 equivalents PBA-CPG **4.3**) after only 1 minute of mixing (Figure 4.7).

This suggested that boronate ester formation was fast and the rate limiting factor was mixing and diffusion of the peptide solution. After 10 minutes mixing with 20 equivalents of PBA-CPG **4.3** the amount of peptide **4.9** remaining in solution was negligible (<3%) and uptake could be considered complete.

Elution of catechol derivatised peptide **4.9** from PBA-CPG **4.3** was achieved using 1% TFA in water (pH 1) and was assessed by measuring the absorbance (282 nm) of catechol derivatised peptide **4.9** released (Figure 4.8).

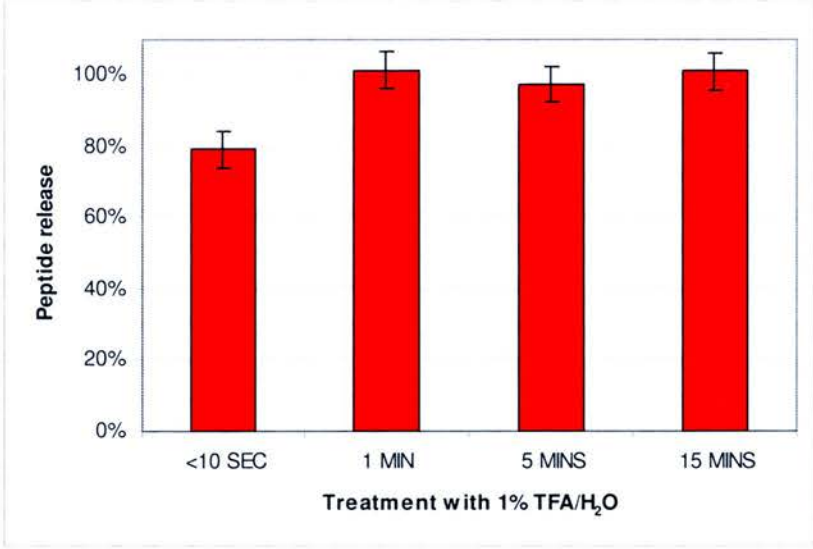

Figure 4.8 Peptide elution. Absorbance of peptide **4.9** eluted from boronate conjugated CPG **4.3** using 1% TFA in H_2O for varying lengths of time.

Peptide elution from boronate conjugated CPG using 1% TFA in water was rapid, with maximal release observed after only 1 minute of mixing time and less than 10 seconds required to achieve 80% release. Furthermore, peptide released from the PBA-CPG **4.3** was very clean with respect to the crude catechol derivatised peptide **4.9** that had been introduced as the input solution (Figure 4.9).

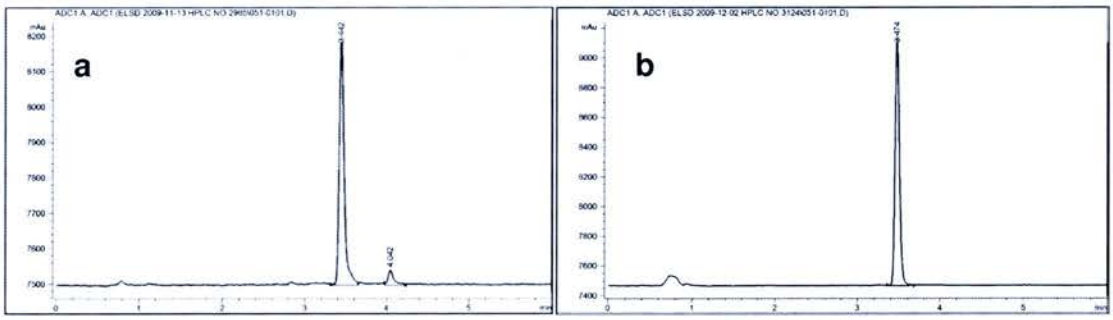

Figure 4.9 HPLC chromatograms. a. Crude catechol derivative peptide **4.9**; **b.** Recovered catechol derivative peptide **4.9** following 1% TFA elution from PBA- CPG **4.3**.

Full elution of peptide **4.9** was achieved with two successive 1 minute treatments with 1% TFA in water.

4.4.1 Enrichment of a tagged peptide in a complex mixture

Tagging and enrichment of a peptide using the catechol NHS ester tag (**4.1**) from a complex mixture was carried out by Lau Sennels in the Wellcome Trust Centre for Cell Biology in the School of Biological Sciences, University of Edinburgh. A crude synthetic peptide (H-EFYEKPTTER-OH **4.12**, 30 pmol) was labelled with **4.1** to give peptide derivative **4.13** and spiked into 1 μg of *E.coli* extract (*E.coli* lysate in 2 M urea was reduced with DTT and cysteines carbamidomethylated with iodoacetamide, followed by overnight incubation with trypsin (1 μg trypsin to 20 μg protein) at 37 °C). Enrichment of crude-labelled peptide **4.13** from the *E.coli* extract was carried out by incubating the peptide/digest mixture in loading buffer (25 mM TEAB, 20% acetonitrile) for 15 minutes along with 20 mg of boronic acid-functionalised CPG **4.3**. The CPG was washed three times with loading buffer. Elution of labelled peptide from the CPG was carried out using aqueous 1% TFA in 20% aq acetonitrile. Eluted fractions were desalted with a C18 stage tip and injected into the mass spectrometer *via* an online nano-LC and compared with injections of crude-labelled peptide **4.13** (control) and the labelled peptide in the *E.coli* extract mixture (Figure 4.10).

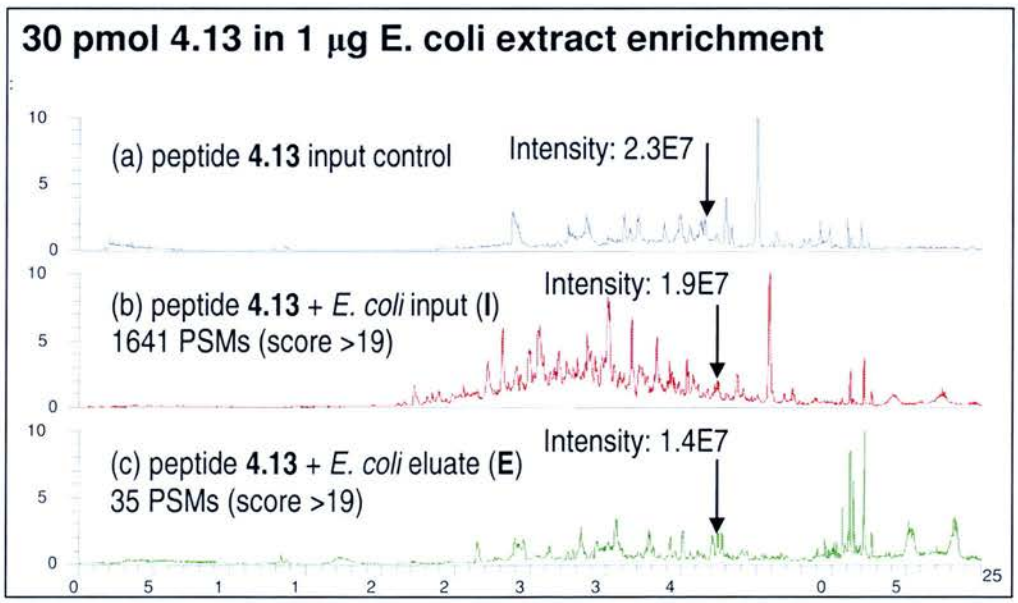

Figure 4.10 NanoLC traces showing catechol tag modified peptide 4.13 enrichment using CPG supported boronic acid 4.3. (a) Crude peptide **4.12** after modification with **4.1** (peptide **4.13**). (b) 30 pmol of peptide **4.13** spiked into 1 μg *E. coli* extract. (c) Eluate from CPG **4.3** after enrichment from *E. coli* extract.

Following analysis using in-house database search software Xi, the **4.1**-labelled peptide **4.13**/*E.coli* extract mixture yielded 1641 peptide sequence matches with high confidence. Following enrichment there were only 35 peptide sequence matches, which demonstrated that the enrichment system could be successfully applied to a complex biological mixture.

4.5 Cross-linkers

The next goal was to develop cross-linkers with built in enrichment functionality, as shown in Scheme 4.6.

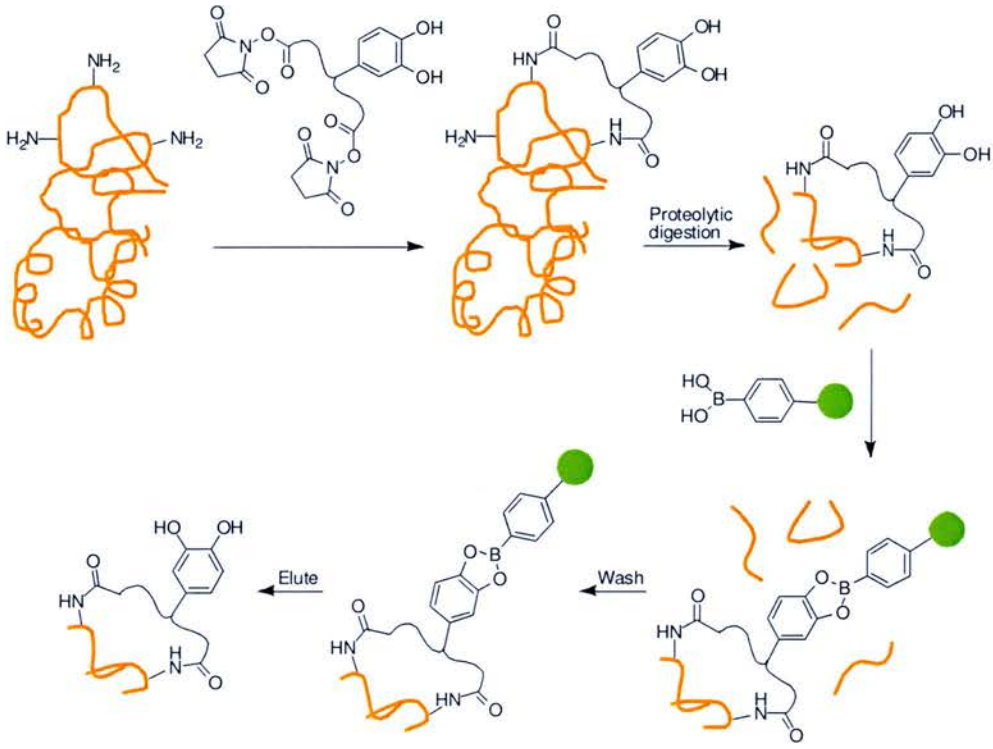

Scheme 4.6 Boronate ester conjugate enrichment of a cross-linked protein. A boronate ester would be formed between a solid supported boronic acid and peptides cross-linked with a catechol functionalised cross-linker. Unmodified peptides would be washed away leaving only cross-linked peptides. Elution from the solid support would allow analysis of cross-linked peptides.

The concept was that a homo-bifunctional amine-reactive NHS ester cross-linker would be introduced into a protein or protein complex, followed by proteolytic digestion using trypsin. The resulting mixture of peptide products would then be

exposed to the solid-supported capture tag followed by washing steps and finally elution of cross-linker modified peptides and MS analysis.

4.5.1 Initial attempts at solid-phase cross-linker synthesis

I decided to pursue a catechol-boronic acid conjugate approach for cross-linker synthesis after the promising results achieved in the tagging.

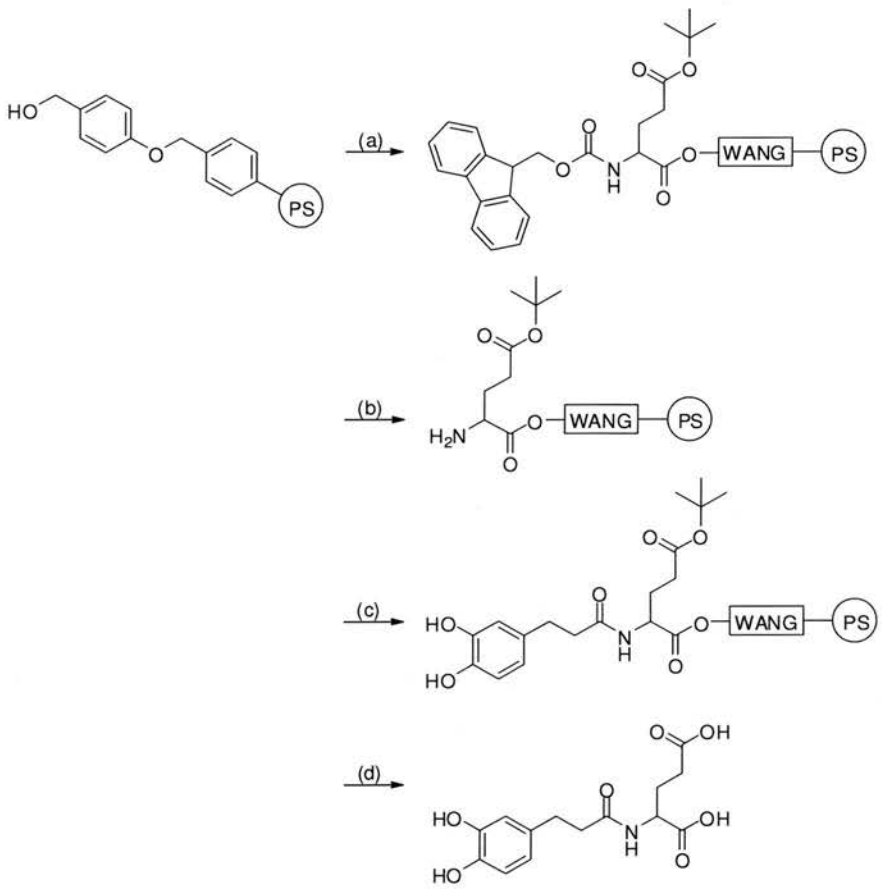

4.14

Scheme 4.7 Solid-phase synthesis of a glutamic acid-based catechol derivative diacid 4.14.
(a) 10 eq Fmoc-Glu(O^{t}Bu)-OH, 5 eq DIC, 0.1 eq DMAP, 2 h; (b) 20% piperidine/DMF, 2 cycles of 10 min; (c) 3 eq 3,4-dihydroxyhydrocinnamic acid, 3.3 eq EEDQ, 2 h; (d) 4 M HCl in dioxane, 1.5 h;

Synthesis was achieved by making an ester linkage between Wang linker and Fmoc-protected glutamic acid with a *t*Bu-protected side chain (Scheme 4.7). Fmoc deprotection gave the free amine onto which the catechol derivative, 3,4-

dihydroxyhydrocinnamic acid was coupled and cleavage from the resin was achieved following treatment of the resin with acid to give diacid **4.14**.

Generally, the solid-phase approach for synthesis of catechol derivative cross-linkers was unsuccessful. TFA (in CH_2Cl_2) cleavage from resin, with and without scavengers (H_2O and triisopropyl silane (TIS)) produced very messy results, and little or no product could be observed by LC-MS. Relatively clean HPLC product traces were generally achieved using 4 M HCl in dioxane for resin cleavage. Use of Fmoc-Asp(O^{t}Bu)-OH in place of Fmoc-Glu(O^{t}Bu)-OH resulted in failure to achieve the desired products as did use of more acid-labile 4-chlorotrityl polystyrene resin rather than Wang linker polystyrene resin.

The failure of the solid-phase approach led to several efforts to achieve the glutamic acid derivative cross-linker *via* solution phase reactions, firstly by forming a mixed anhydride with isobutyl chloroformate (and *N*-methylmorpholine (NMM))[212] and also by exploiting the NHS-active ester of the catechol derivative.

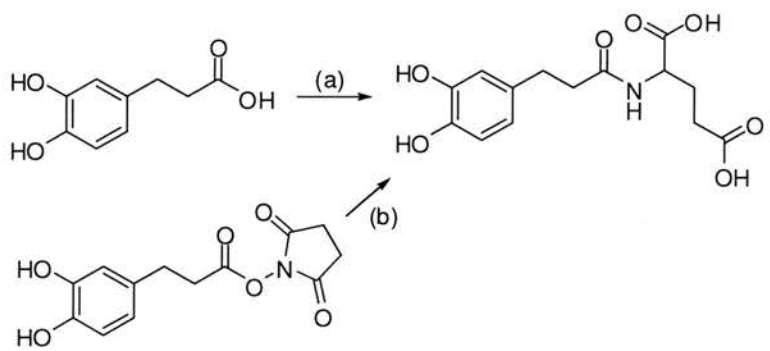

Scheme 4.8 Solution-phase synthetic attempts at a glutamic acid-based catechol derivative cross-linker.

(a)(i) Isobutyl chloroformate, NMM, THF; (ii) L-glutamic acid, Et_3N, DMF;

(b) L-glutamic acid, Et_3N, DMF;

The conclusion drawn from this work was that the inherent instability of the catechol derivative (which was also observed with catechol peptide **4.9** (Figure 4.6)) and its tendency to decompose under basic conditions meant that an alternative functionality was required.

4.5.2 Boronic acid cross-linker synthesis

Because of the problems incurred during synthesis of a catechol-modified cross-linker it was decided to use a reverse system whereby a solid-supported diol could be used to enrich a boronic-acid functionalised cross-linker.

Fujii reported a novel homobifunctional amine reactive cross-linker with a biotin functionality, with the advantages of having a symmetrical backbone with bifunctional amine reactivity, built around a central amide core (Figure 4.11).[213] The addition of a hydrophilic PEG linker greatly increases the water-solubility of the cross-linker. The strategy has the benefit of allowing the backbone length to be varied, which means that a range of different cross-linker lengths could be produced.

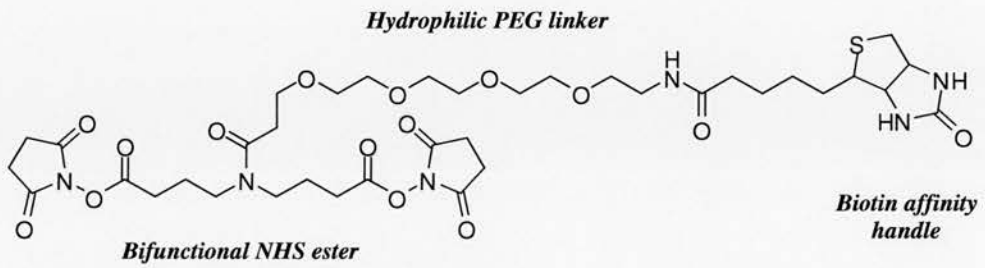

Figure 4.11 Hydrophilic biotin tagged cross-linker.[213]

The principles behind this synthetic strategy were taken and used to produce the boronic-acid containing cross-linker **4.19** (Scheme 4.9).

A dialkylation reaction between benzylamine and ethyl 4-bromobutyrate gave **4.15** in good yield. The de-benzylation proceeded readily with hydrogen and palladium but the reaction was much cleaner and time efficient when the H-Cube Tutor was employed, which generates hydrogen *in situ* and relies on a flow-reaction rather than a batch approach. The resulting secondary amine **4.16** was coupled to 4-carboxyphenylboronic acid and a number of coupling strategies were tested, HBTU with DIPEA, solid-supported (polystyrene) cyclohexylcarbodiimide (PS-DCC) and EDC. The best results were achieved using EDC to give **4.17**. Saponification yielded the diacid compound **4.18**, which was activated with PS-DCC and *N*-

hydroxysulfosuccinimide (NHSS) to give cross-linker **4.19**. The sulfonate group on the active ester significantly enhances cross-linker water solubility.

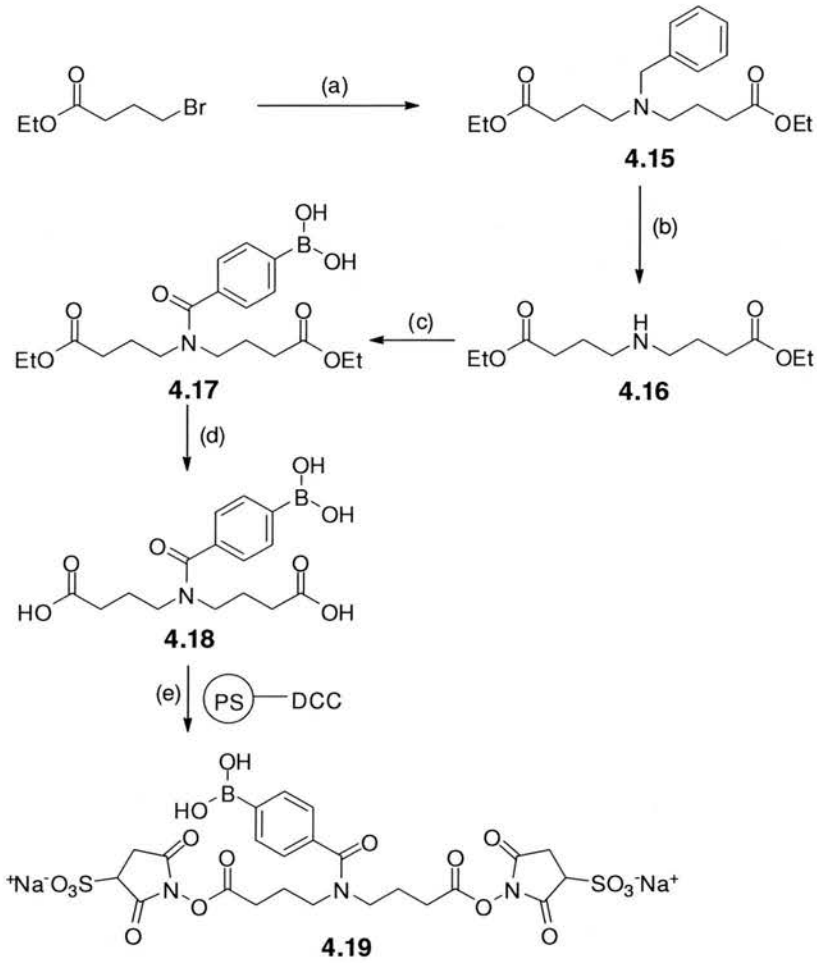

Scheme 4.9 Boronic acid functionalised cross-linker 4.19.

(a) Benzylamine, K_2CO_3, DMF, 40 °C, 20 h, 77 %; (b) H-Cube Tutor 10 % Pd/C/H_2, MeOH, 100 %; (c) 4-carboxyphenylboronic acid, EDC, HOBt, DMF, 18 h, 53 %; (d) NaOH aq, MeOH, 18 h, 40 %; (e) NHSS, DMF, 24 h, 100 %.

4.5.2.1 Conclusion from boronic acid derivative cross-linking

Cross-linked protein was observed following application of the boronic acid derivative NHSS active ester **4.19**, which was indicated by gel electrophoresis (Figure 4.12). However following tryptic digestion of gel bands containing cross-linked protein, there was an absence of detectable modified peptides.

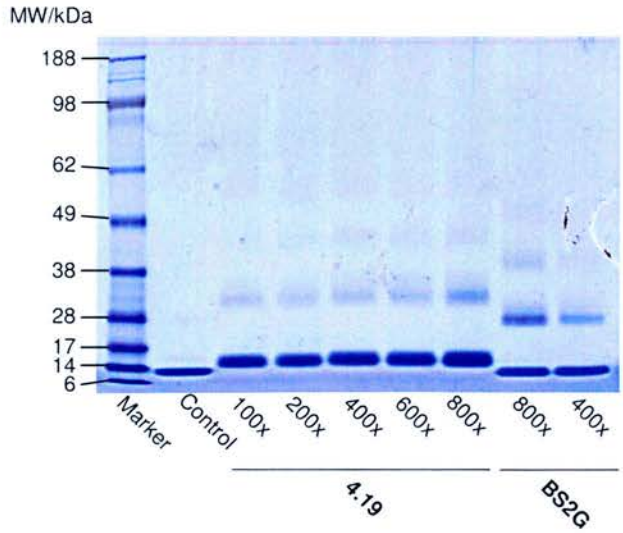

Figure 4.12 Gel electrophoresis of 4.19 cross-linked protein. Chicken lysozyme cross-linked with **4.19** (equivalents used: 100x, 200x, 400x, 600x and 800x) and BS2G (equivalents used: 400x and 800x). Control = no cross-linker.

Trypsin is a serine protease and peptide boronic acids have been shown to be potent inhibitors of this particular class of enzyme.[214] In view of this it is possible that digestion of boronic acid modified cross-linked peptides using trypsin would not be possible with the boronic acid in an unprotected state. This was confirmed using boronic acid modified peptide **4.8**. Boronic acid modified peptide **4.8** in the presence of trypsin resulted in inhibition of protein digestion, which indicated that it was the free boronic acid moiety that was responsible for the lack of observable boronic acid-modified cross-linked peptides in the cross-linking experiments. Simple arylboronic acids by themselves have been found to be inhibitors of serine proteases.[215]

Preliminary experiments with boronic acid supported CPG (PBA-CPG) **4.3** and the catechol and salicylhydroxamic acid modified peptides (**4.9** and **4.10** respectively) showed that conjugates could be formed readily with both moieties. Due to the stability problems previously encountered with catechol derivatives, it was decided to pursue salicylhydroxamic acid derivatives as the cross-linker affinity tag.

4.6 Hydroxamic acid chemistry

4.6.1 Synthesis of salicyl hydroxamic acid moiety as a conjugation reagent

Stolowitz *et al.* reported the ability to manipulate phenylboronic acid and salicylhydroxamic acid bioconjugates for protein immobilisation (Scheme 4.10). Protein modification reagents were synthesised from 3-aminophenylboronic acid to prepare phenylboronic acid bioconjugates that have affinity for a support-bound phenylboronic acid complexing reagent derived from salicylhydroxamic acid.[203]

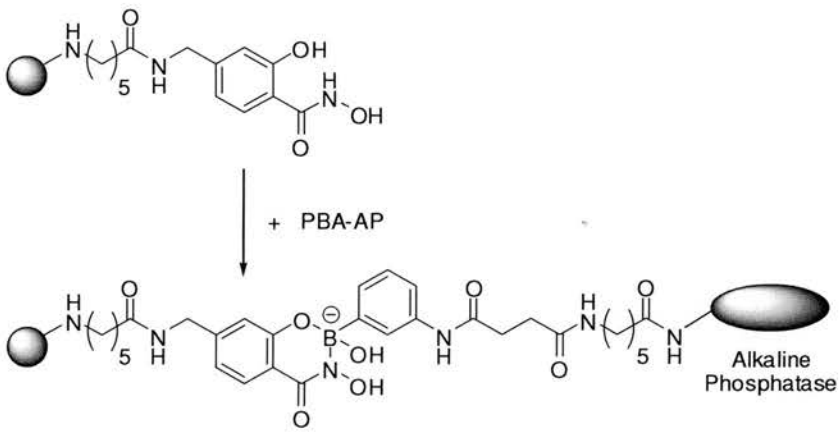

Scheme 4.10 Boronate ester conjugate *via* salicylhydroxamic acid. Immobilisation of phenylboronic acid (PBA) derivatised alkaline phosphatase (AP) by salicylhydroxamic acid modified sepharose. The illustration represents an oversimplification due to the fact that immobilisation may result from interaction involving several boronic acid complexes.

Hydroxamic acids can be readily synthesised from their corresponding methyl esters.[216]

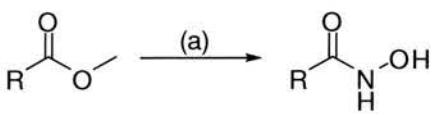

Scheme 4.11 Synthesis of hydroxamic acids from methyl esters.

(a) 50 % NH_2OH in H_2O, MeOH

A synthetic strategy based on the conversion of methyl esters to hydroxamic acids was developed that provide a salicylhydroxamic acid derivative that could be built into a cross-linker.

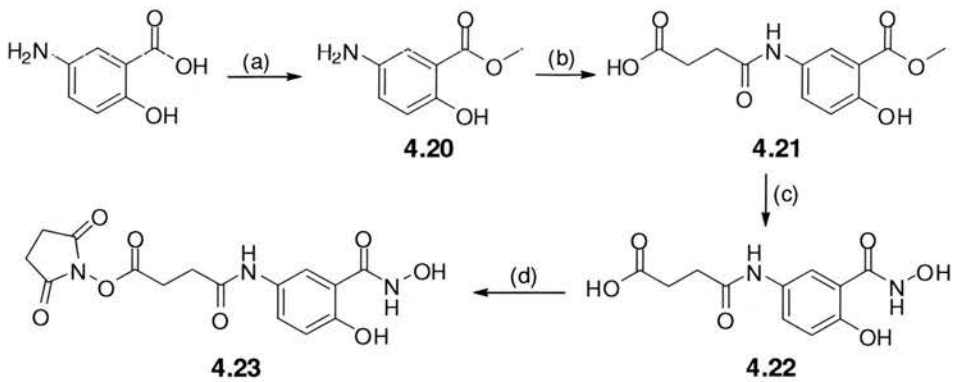

Scheme 4.12 Salicylhydroxamic acid NHS ester derivative 4.23 synthesis.

(a) MeOH, 1.5 eq H_2SO_4 conc., μwave 130 °C, 1 h, 75 %; (b) succinic anhydride, CH_2Cl_2, μwave 100 °C, 10 min, 94 %; (c) 50 % NH_2OH/H_2O, MeOH, 18 h, 98 %; (d) 1.5 eq NHS, 1.2 eq EDC, DMF, 18 h, 44 %.

Methyl ester protection of 5-aminosalicylic acid was followed by conversion of the amine group of **4.20** *via* reaction with succinic anhydride to provide the acid **4.21**. Conversion of the methyl ester of **4.21** to give the hydroxamic acid was achieved using a 50% aqueous solution of hydroxylamine. Over-exposure of the hydroxamic acid to basic conditions resulted in hydrolysis to the carboxylic acid.

4.6.2 Synthesis of salicylhydroxamic acid modified test-model peptides

The methyl ester tag **4.21** was added to the previously synthesised peptide sequence **4.6** (see section 4.3.3). Clean conversion of the methyl ester derivative **4.24** to a functional hydroxamic acid moiety was achieved as before using a 50% aqueous hydroxylamine solution at room temperature. The reaction was monitored by ELSD-HPLC; a 1 Da mass increase according to LC-MS confirmed the conversion to hydroxamic acid **4.25** while excess hydroxylamine could be removed by lyophilisation.

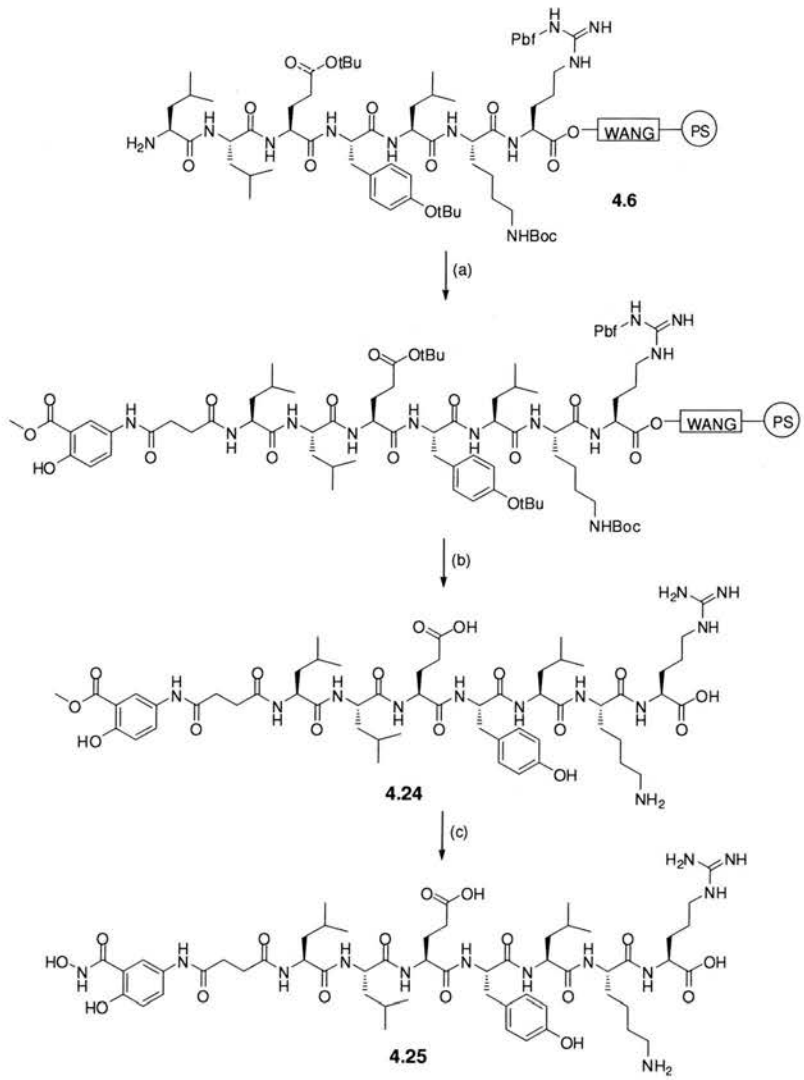

Scheme 4.13 Solid-phase synthesis of salicylhydroxamic acid modified peptide 4.25.

(a) 5 eq 4-{(4-hydroxy-3-(methoxycarbonyl)phenyl]amino}-4-oxobutanoic acid **4.21**, 5 eq HBTU/HOBt, DMF (0.2 M), 10 eq DIPEA, 1 h; (b) TFA/TIS/H_2O (95:2.5:2.5), 2 h; (c) 50% hydroxylamine/H_2O, 24 h;

4.6.2.1 Enrichment of a salicylhydroxamic acid peptide by a CPG-supported boronic acid

Binding of hydroxamic modified peptide **4.25** to PBA-CPG **4.3** (Figure 4.13) was demonstrated in a set of studies using varying equivalents of PBA-CPG **4.3** in one experiment (Figure 4.14) and using fixed quantities of PBA-CPG **4.3** for different time periods (Figure 4.15).

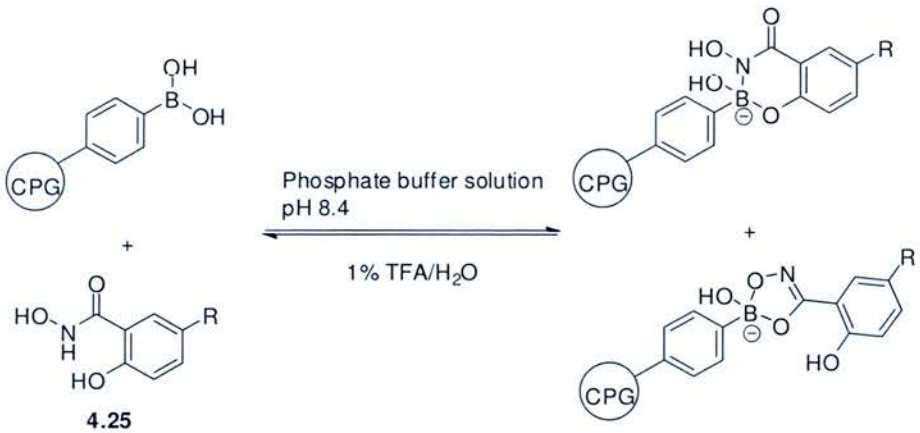

Figure 4.13 Boronate ester *via* hydroxamic acid. Formation of a boronate ester between a controlled pore glass supported boronic acid and a hydroxamic acid.

Uptake was determined by measuring the UV absorbance of peptide **4.25** that remained in solution following addition of PBA-CPG **4.3** (Figure 4.14). When 5 equivalents of PBA-CPG **4.3** were used 98% uptake was achieved.

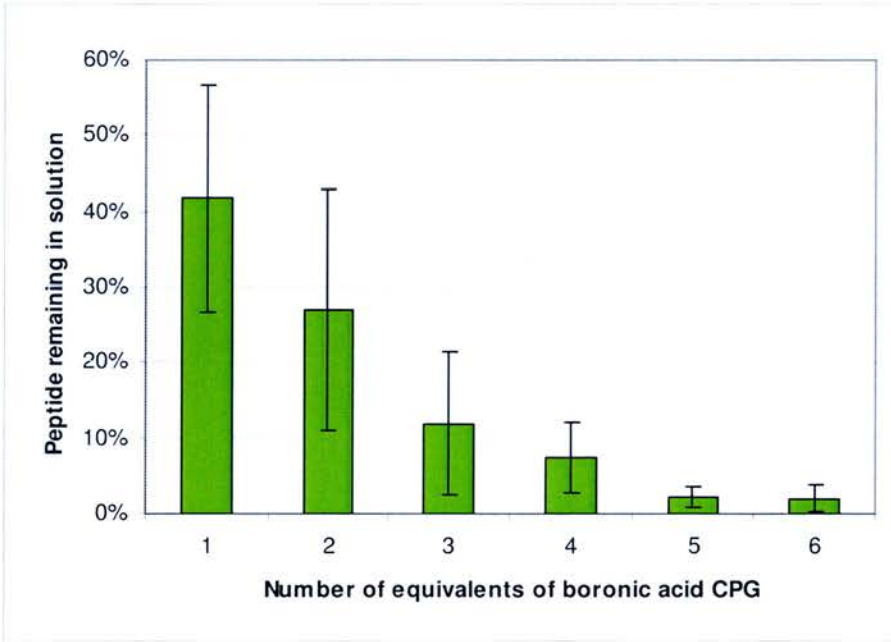

Figure 4.14 Peptide 4.25 uptake. Percentage of peptide **4.25** remaining in solution after 30 minutes with varying numbers of equivalents of PBA-CPG **4.3** resin (n=3).

Results indicate that there is a gradual decrease in peptide **4.25** that remains in the solution as the number of equivalents of boronic acid increased.

The relationship between number of equivalents of PBA-CPG **4.3** and mixing time was investigated by using three different numbers of equivalents, (4, 10 and 20) and applying peptide **4.25** solution, again in PBS buffer at pH 8.4, after 0.5, 1, 2, 4, 10 and 30 minutes (Figure 4.15). Using higher boronic acid equivalents resulted in close to 99% uptake onto the CPG beads after 30 minutes.

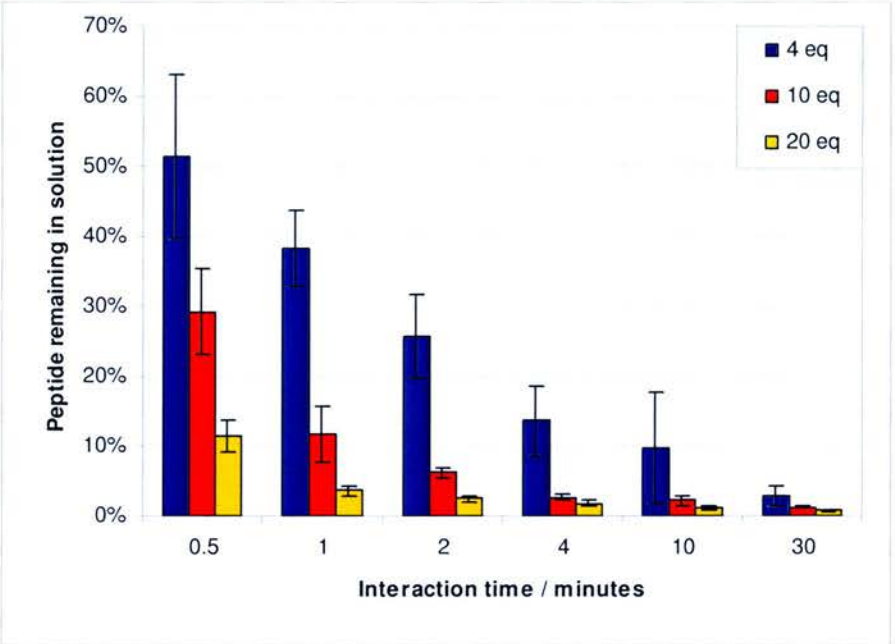

Figure 4.15 Peptide 4.25 uptake. Percentage of peptide **4.25** remaining in solution after different interaction times with various numbers of equivalents of PBA-CPG **4.3** (n=3).

Significantly when 20 equivalents of boronic acid were used, only 11% of peptide **4.25** remained in solution after just 30 seconds of mixing, and after 1 minute, only 4% of peptide remained in solution showing that boronate ester formation is rapid.

The study suggests that the enrichment process could be suited to a continuous flow system rather than the batch-wise system that was under investigation here. PBA-CPG **4.3** could be packed into columns which would reduce the errors associated with handling batches of loose beads.

4.6.2.2 Elution of salicylhydroxamic acid functionalised peptides from PBA-CPG

Elution of bound hydroxamic acid modified peptide **4.25** was achieved by adding 1% TFA in water (pH 1) to the CPG beads and mixing for 25 minutes at room temperature. TFA was removed by evaporation and 9.29 μmol of peptide **4.25**, was retrieved by lyophilisation (from an initial theoretical loading of 14 μmol), equating to an effective working capacity for the PBA-CPG **4.3** of 66%.

4.6.3 Synthesis of salicylhydroxamic acid modified cross-linker

The incorporation of a base-sensitive methyl ester head-group onto the cross-linker backbone rather than a boronic acid meant that an alternative protecting group strategy was needed for the carboxylic acid groups that would become active esters. Thus the carboxylic acid groups of the cross-linker arms were protected with the *tert*-butyl protecting group, which could be removed under acidic conditions.

Protection of the carboxylic acid group of 4-bromobutyric acid was achieved using trifluoroacetic anhydride and *tert*-butyl alcohol using the method of Patel to give **4.26** (Scheme 4.14).[217]

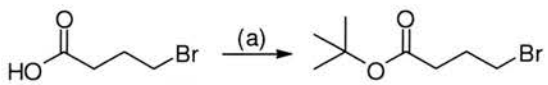

4.26

Scheme 4.14 Synthesis of tert-butyl protected cross-linker arm 4.26.[217]
(a) THF, $(CF_3CO)_2O$, *tert*-butyl alcohol, 16 h, 90%;

The synthesis of methyl-ester derivative cross-linker was essentially the same as the previous synthesis (Scheme 4.15). Dialkylation of benzylamine with *tert*-butyl-4-bromobutyrate **4.26** gave **4.27**. De-benzylation (Pd/H_2) gave the secondary amine **4.28**, onto which the methyl ester protected salicylic acid derivative **4.21** was coupled using a water-soluble carbodiimide EDC and HOBt.

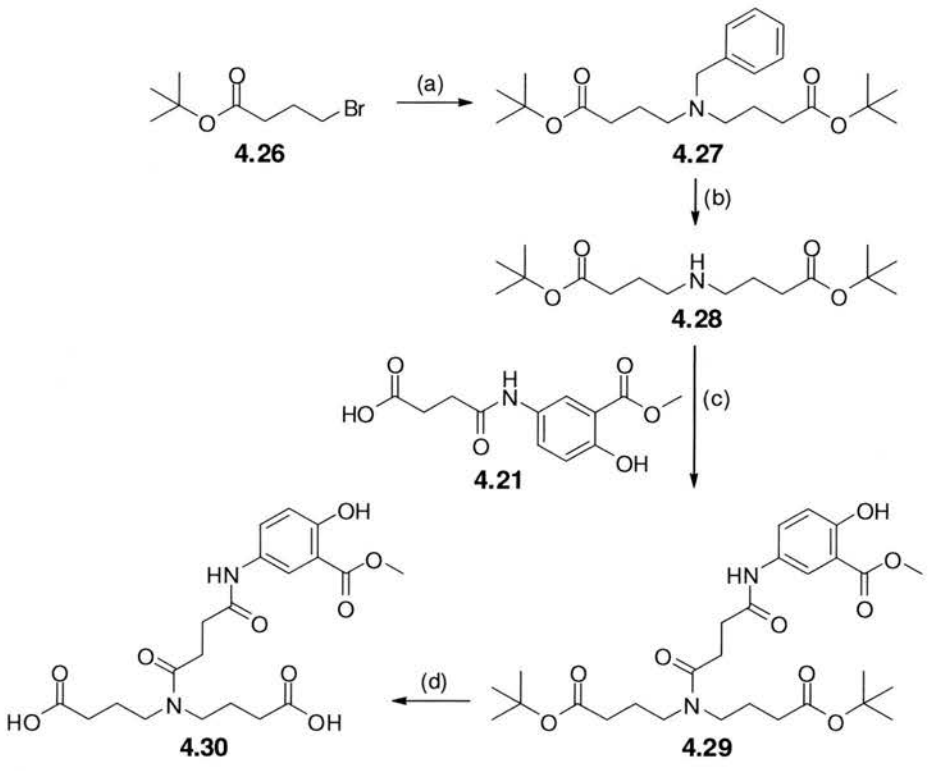

Scheme 4.15 Methyl ester protected salicylic acid functionalised diacid 4.30.

(a) benzylamine, K_2CO_3, DMF, 60 °C, 20 h, 47 %; (b) 10 % Pd/C/H_2, MeOH, 90 %; (c) **4.21**, EDC, HOBt, DMF, 18 h, 22 %; (d) TFA/CH_2Cl_2/TIS/H_2O (47.5:47.5:2.5:2.5) 2 h, 48 %;

The coupling of the methyl ester derivative **4.21** and cross-linker backbone **4.28** resulted in a very poor yield for **4.29**. Coupling reactions involving secondary amines are generally more sluggish than with primary amines but the most significant limiting factor here was deemed to be the succinic spacer group undergoing intramolecular ring formation before coupling could be achieved. This was routinely observed by LC-MS as a major side product during coupling. The carboxylic acid groups of **4.30** were cleanly revealed following treatment at room temperature with a cocktail of TFA in dichloromethane along with triisopropylsilane and water acting as scavengers. The *tert*-butyl protecting groups could also be removed using an equimolar amount of sulphuric acid but the reaction was slower and not as clean as with the TFA cocktail. The methyl ester dicarboxylic acid derivative **4.30** was purified by Prep HPLC and lyophilised to produce a fluffy white lyophilisate.

Conversion of the methyl ester **4.30** to hydroxamic acid **4.31** was achieved with a 50% aqueous hydroxylamine solution (Scheme 4.16).

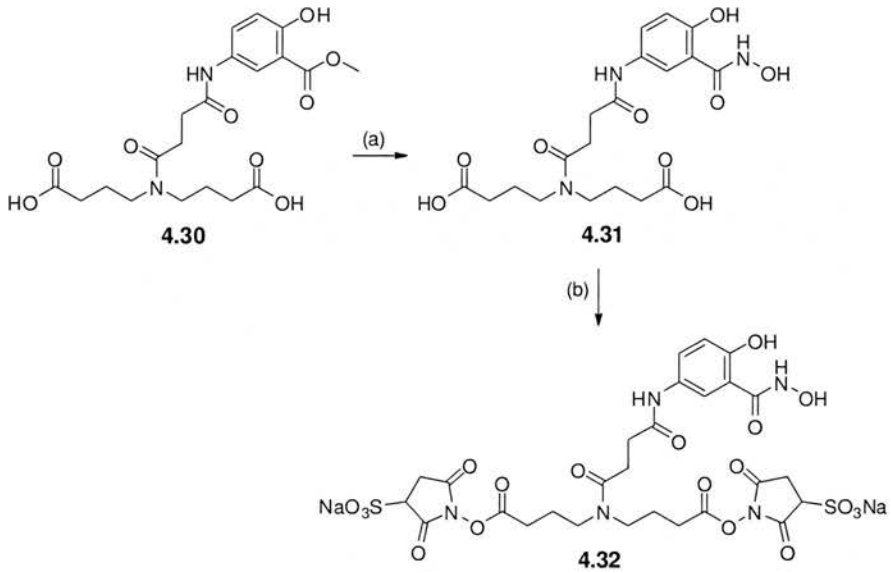

Scheme 4.16 Salicylhydroxamic acid cross-linker 4.32 synthesis. Conversion of methyl ester **4.30** to hydroxamic acid derivative **4.31** followed by activation to cross-linker **4.32**.
(a) 50% hydroxylamine in H_2O, rt, 24 h, 100 %; (b) PS-DCC, NHSS, DMF, 24 h, 100%.

Conversion was monitored by analytical HPLC (Figure 4.16) and was shown to be complete with very few side reactions. Attempts to speed up the reaction by applying microwave heating led to ester hydrolysis. The hydroxamic acid derivative **4.31** could be isolated by Prep-HPLC, however there were indications that the compound was not stable and was prone to decomposition, indicated by the appearance of impurities following HPLC purification and lyophilisation.

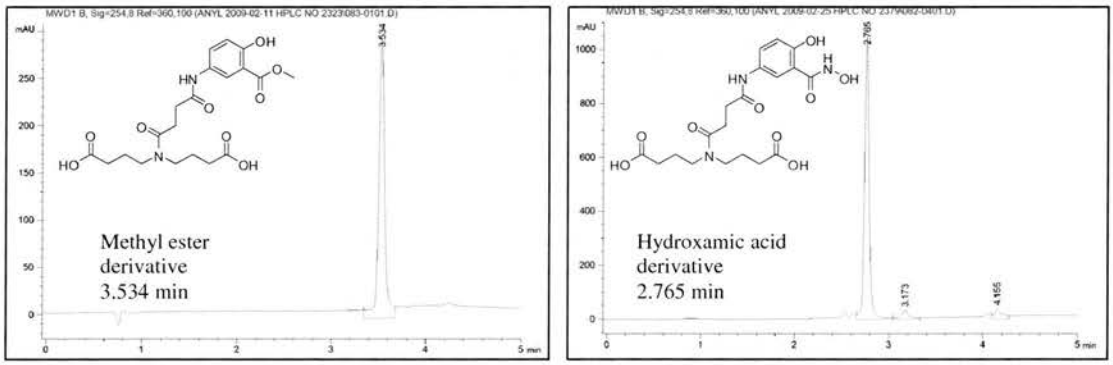

Figure 4.16 HPLC chromatograms. Conversion of the methyl ester derivative **4.30** to the corresponding hydroxamic acid derivative **4.31**.

Following solid-supported DCC mediated NHSS ester activation using the previously applied method, the resulting activated cross-linker **4.32** was applied to the previously synthesised peptide, H_2N-LLEYLKR-OH **4.7**, under basic conditions. The resulting mixture was analysed by LC-MS but the predominant product corresponded to internally cross-linked peptide **4.33** with the hydroxamic acid group hydrolysed back to the carboxylic acid. It is likely that the cross-linking conditions used are basic enough to cause hydrolysis of the hydroxamic acid. During the conversion step it seems most likely that the methyl ester group is converted to a hydroxamic acid and is then hydrolysed back to a carboxylic acid rather than the occurrence of hydrolysis of the methyl ester.

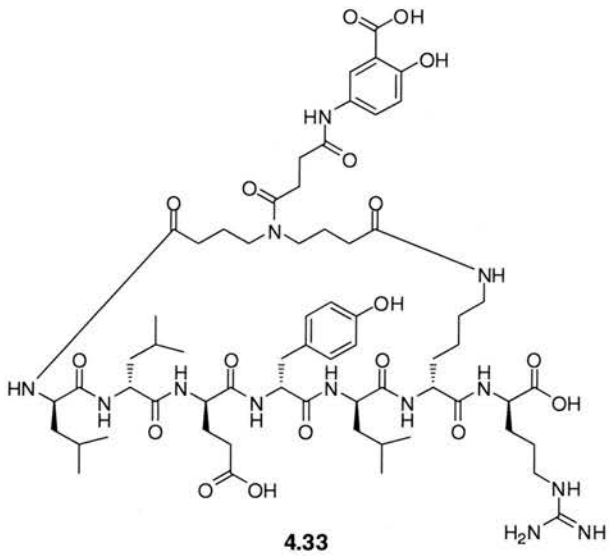

4.33

Figure 4.17 Intrapeptide cross-link. Synthetic test peptide modified with an internal cross-link and hydrolysis of the affinity tag to a non-binding carboxylic acid derivative **4.33**.

Another major concern involved with NHS ester activation of a hydroxamic acid containing derivative is that hydroxamic acids are capable of reacting readily with dicyclohexyl carbodiimide to form a bimolecular "anhydride".[218] Yet another issue is that of the hydroxamic acid undergoing an intramolecular nucleophilic attack on the activated NHSS esters. Following cross-linking experiments on proteins, protein dimers were observed according to gel electrophoresis of cross-linking products but cross-linked peptides with a hydroxamic acid modification could not be identified.

At this stage the cross-linking strategy was reconsidered. Attempts to synthesise activated hydroxamic acid derivative cross-linker **4.32** and perform cross-linking experiments were abandoned in favour of synthesising the stable activated ester of the methyl ester cross-linker derivative **4.34** (Scheme 4.17) using solid-supported DCC and *N*-hydroxysulfosuccinimide.

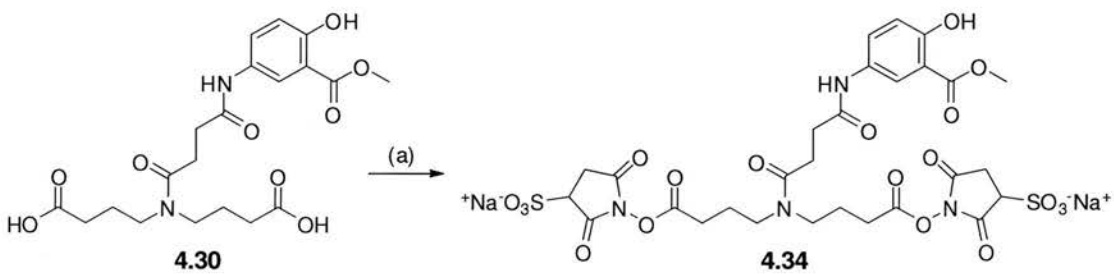

Scheme 4.17 Activation of methyl ester derivative 4.30 with PS-DCC and NHSS to produce cross-linker 4.34.

(a) PS-DCC, NHSS, DMF, 24 h, 100 %.

4.6.3.1 Cross-linking experiments with methyl ester derivative 4.34

Following a 2 hour cross-linking reaction with the activated NHSS ester of the methyl ester derivative **4.34**, cross-linked beta-lactoglobulin was identified by gel electrophoresis and subjected to overnight protease digestion in-solution using trypsin. Cross-linked peptide products were treated with a 50% aqueous hydroxylamine solution and peptides were analysed by mass spectrometry before and after treatment, revealing a mass difference following conversion of 1 Da, indicating conversion of the cross-linker tagging group of **4.34** to the corresponding hydroxamic acid. Data was analysed using the computer software programs Mascot and an in-house developed software Xi and detected cross-linked peptides were visualised and validated using the in-house developed software program Xaminatrix (Figure 4.18). Beta-lactoglobulin peptide 155-164 was found cross-linked to another beta-lactoglobulin peptide 155-164; an example of an intermolecular cross-link.

(a)

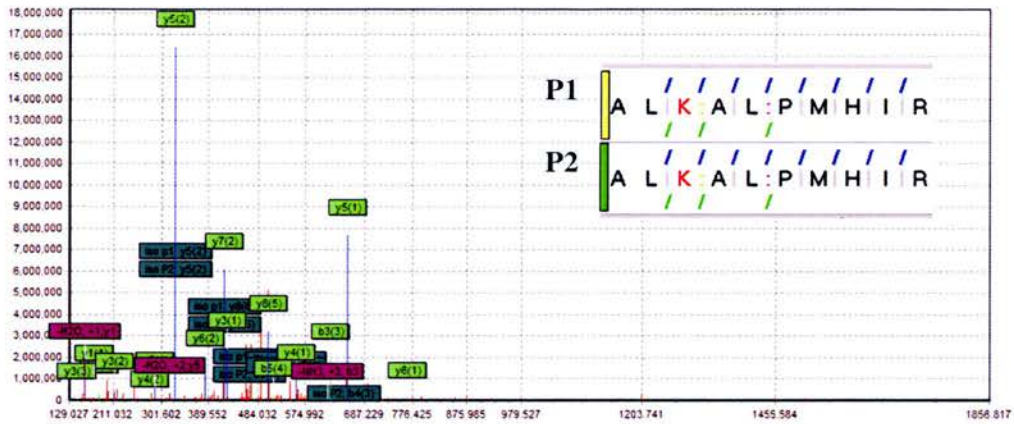

(b)

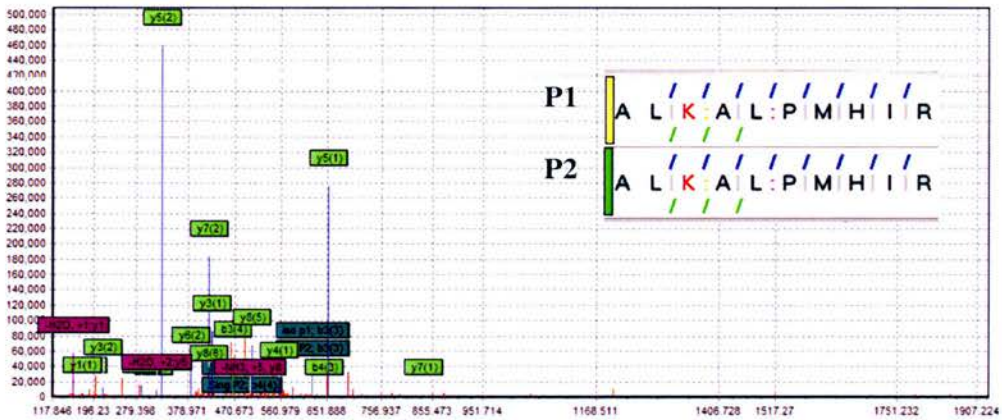

Figure 4.18 Cross-linked peptide analysis. Output from Xaminatrix software showing analysis of fragmented cross-linked peptide (a) modified with methyl ester derivative cross-linker **4.34** and (b) following conversion of the methyl ester of **4.34** to the corresponding hydroxamic acid derivative. Residues denoted in red have reacted with cross-linker. Blue markers indicate the positions of y ions, which are represented on the chart with the corresponding peptide number (P1 or P2) shown in parentheses. Green markers indicate the positions of b ions.

4.6.4 Synthesis of methyl ester derivative active ester tag

The relative stability of the methyl ester derivative **4.34** led to the synthesis of an NHS active ester tag that could be used as part of the dual tagging system rather than the hydroxamic acid. Having an active ester of the methyl ester derivative, effectively an affinity tag precursor, also carries the advantage that following dual tagging with a complimentary affinity tag, the first enrichment step can be performed while the second affinity tag is effectively inert. The methyl ester derivative tag is

"activated" by conversion with hydroxylamine to give a hydroxamic acid that will bind with solid-supported boronic acid with strong affinity.

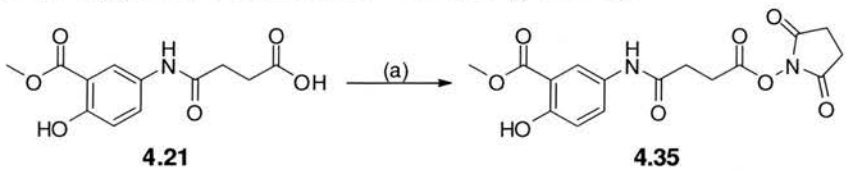

4.21 **4.35**

Scheme 4.18 NHS ester activation of 4.21 to give methyl ester protected salicyclic acid tag 4.35.
(a) 1.2 eq EDC, 1.5 eq NHS, DMF, 79%.

4.6.5 Next generation cross-linker – solutions to hydrophobicity

Precipitation of cross-linked peptides due to hydrophobicity was a major concern and cause of sample loss during cross-linking experiments. An improved cross-linker was sought that would give better cross-linking efficiency.

4.6.5.1 Synthesis of a novel methyl ester derivative

Due to intramolecular ring formation occurring when activating methyl ester **4.21**, an alternative was sought. Astles *et al.*[219] had previously demonstrated that selective modification of 2,4-dihydroxy benzoic acid at the *para* hydroxyl group could be achieved *via* methyl ester protection of the acid followed by benzylation under Finkelstein conditions. Initial attempts at alkylation using Cs_2CO_3 and *tert*-butyl bromoacetate resulted in a mixture of both regio-isomers (proven by NOESY experiments). Alkylation using Finkelstein conditions and microwave heating resulted in modification of the desired *para*-OH group (Scheme 4.19).

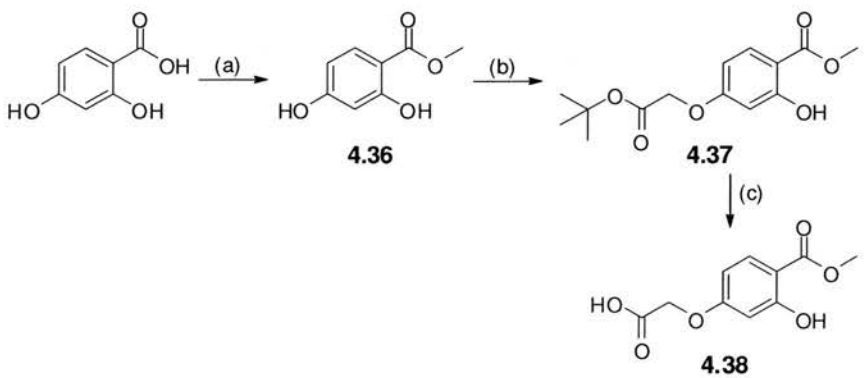

4.36 **4.37** **4.38**

Scheme 4.19 Alkylation *via* a methyl ester derivative
(a) MeOH, conc. H_2SO_4, reflux, 66 h, 96 %; (b) *tert*-butyl bromoacetate, K_2CO_3, KI, TBA-Cl, acetone, μwave 90 °C, 75 min, 74%; (c) TFA/CH_2Cl_2/TIS/H_2O, 1 h, 89%.

Removal of the *tert*-butyl protecting group was carried out with TFA along with TIS and water as scavengers. In most cases the acid could be obtained cleanly, simply by removing the TFA *in vacuo* followed by lyophilisation.

4.6.5.2 Synthesis of an Fmoc-protected PEG spacer

PEG groups are frequently used to increase hydrophilicity of surfaces[220] and small molecules.[221] Synthesis of an Fmoc-protected PEG amino acid **4.43** was straightforward and carried out as *per* Visintin *et al* (Scheme 4.20).[222] The PEG spacer was chosen because it could be conveniently inserted between the cross-linker backbone and affinity tag without changing the existing synthetic strategy.

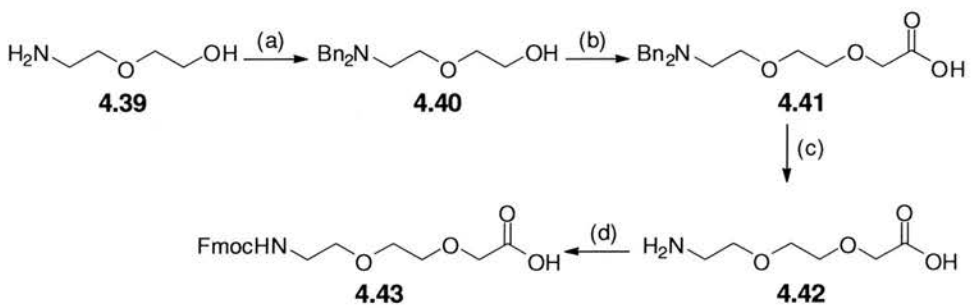

Scheme 4.20 Fmoc-8-amino-3,6-dioxaoctanoic acid 4.43 synthesis.
(a) 2 eq BnBr, 2.5 eq K_2CO_3, CH_3CN, 90 °C, 50 h, 85%; (b) 4 eq NaH, 1.5 eq α-bromoacetic acid, dry THF, 0 °C to rt, 16 h, 80%; (c) 10% Pd/C/H_2, MeOH, rt, 1 atm, 20 h, 98%; (d) 2 eq K_2CO_3, 1 eq Fmoc-OSu, H_2O, 43%.

The amino group of the amino acid **4.39** was protected by dibenzylation using benzyl bromide and potassium carbonate as base, followed by alkylation of the hydroxyl group with α-bromoacetic acid to provide a terminal carboxylic acid group to yield **4.41**. The amine was revealed by Pd/H_2 and re-protected with an Fmoc group to give **4.43**.

4.6.5.3 Synthesis of novel methyl ester derivative NHS ester tag

The NHS ester active ester **4.44** of the methyl ester derivative **4.38** was made using the established method involving the water-soluble carbodiimide EDC and NHS, which were easily removed following reaction with a quick basic and acidic wash.

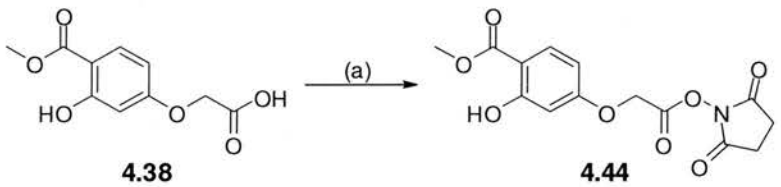

4.38 **4.44**

Scheme 4.21 Synthesis of methyl ester salicylic acid derivative NHS active ester tag 4.44.
(a) 1.2 eq EDC, 1.5 eq NHS, DMF, 87%.

*4.6.5.4 Synthesis of a novel hydrophilic methyl ester derivative NHSS active ester cross-linker – **4.49***

Synthesis of a second generation cross-linker with increased hydrophilicity started with an amide forming coupling, mediated with HBTU, between the secondary amino backbone **4.28** used in the previous cross-linker and the Fmoc-protected amino acid PEG spacer compound **4.43**. This was followed by removal of the Fmoc protecting group using piperidine in DMF to reveal a free amine **4.46**, onto which was coupled the novel methyl ester derivative **4.38** developed previously. Removal of the *tert*-butyl protecting groups was achieved using a cocktail of TFA/CH_2Cl_2 along with H_2O and TIS acting as scavengers. The resulting diacid **4.48** was purified by Prep-HPLC and then activated to give **4.49** using solid-supported DCC along with *N*-hydroxysulfosuccinimide.

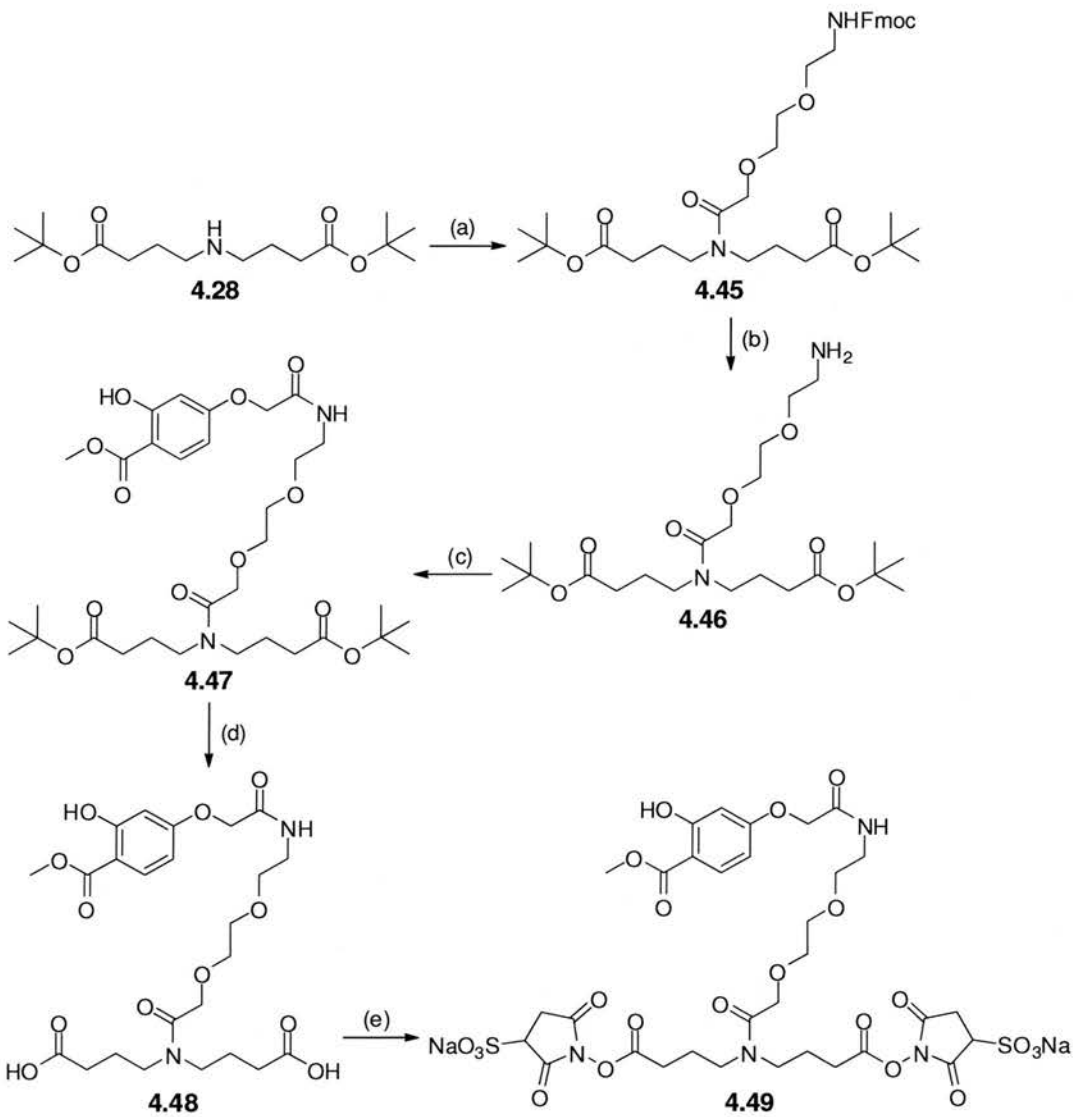

Scheme 4.22 Methyl ester derivative 4.49 synthesis.

(a) {2-[2-(Fmoc-amino)ethoxy]ethoxy}acetic acid **4.43**, HBTU, DIPEA, DMF, 1.5 h, 67%; (b) 20% piperidine in DMF, 40 min, 100%; (c) [3-hydroxy-4-(methoxycarbonyl)phenoxy]acetic acid **4.38**, HBTU, DIPEA, DMF, 1.5 h, 86%; (d) TFA/CH_2Cl_2/TIS/H_2O (47.5:47.5:2.5:2.5) 2 h, 30%; (e) PS-DCC, NHSS, DMF, 24 h, 100 %;

*4.6.5.5 Cross-linking experiments with methyl ester derivative **4.49***

Cross-linking and cross-linked peptide enrichment was carried out by Lau Sennels in the Wellcome Trust Centre for Cell Biology in the School of Biological Sciences, University of Edinburgh.

Beta-lactoglobulin was cross-linked with the hydrophilic methyl ester derivative cross-linker **4.49** using the same cross-linking protocol that was used for **4.34**. Cross-linked products were identified by gel electrophoresis as before (Figure 4.19).

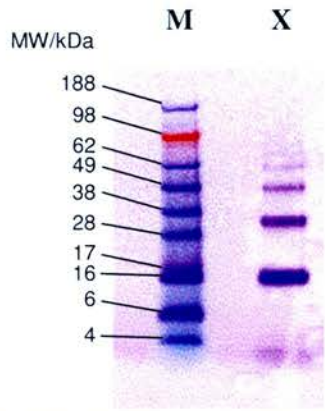

Figure 4.19 Gel electrophoresis. Beta-lactoglobulin cross-linked with **4.49** (X) ran against a marker lane (M).

Following separation of cross-linked protein by gel electrophoresis, protein bands were excised from the gel and digested with trypsin. The resulting peptides were analysed by mass spectrometry as for **4.34** cross-linked peptides. Interestingly, the intermolecular cross-linked peptide sequence (ALKALPMHIR) observed using **4.34** was also observed with **4.49** (Figure 4.20). Five cross-linked peptides from beta-lactoglobulin were observed, consistent with the distance constraints between lysines present in the protein. The methyl ester tag of **4.49** cross-linked peptide products was converted using hydroxylamine solution to give hydroxamic acid modified cross-linked peptides ready for enrichment (as with **4.34** cross-linked peptide products). Hydroxamic acid modified cross-linked peptides in PBS (pH 8.4) were bound to phenylboronic acid CPG **4.3**, unbound material was filtered from the resin and enriched peptides were eluted from the resin using 1% TFA/H_2O. Unbound material was analysed by HPLC and mass spectrometry and compared with peptides that had been bound and released from CPG **4.3** (Figure 4.21). The result was enrichment of cross-linker modified peptides from a mixture of unmodified peptides.

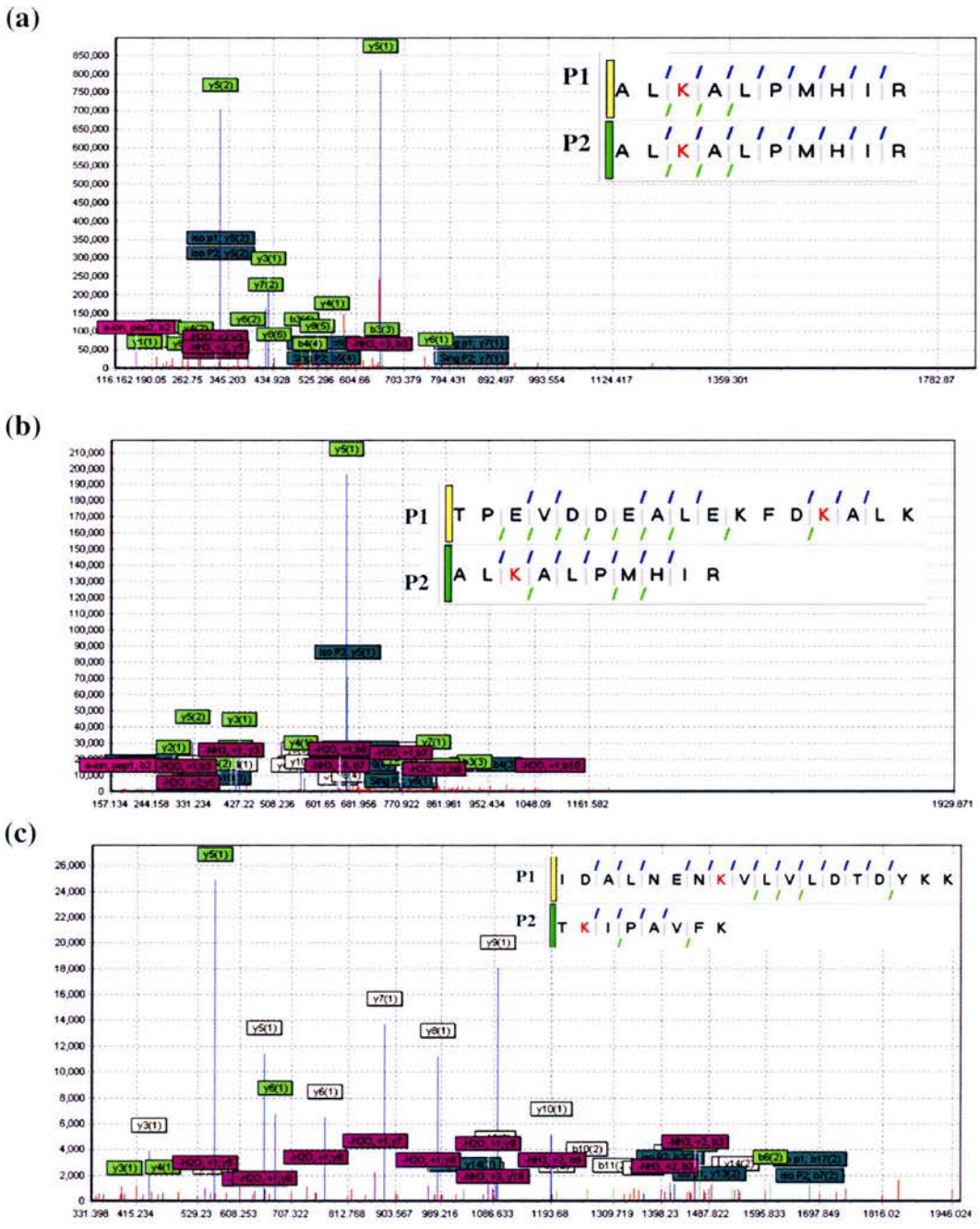

Figure 4.20 Cross-linked peptide analysis. Output from Xaminatrix software showing analysis of three identified fragmented cross-linked peptides (a)-(c) modified with methyl ester derivative cross-linker **4.49**. Residues denoted in red have reacted with cross-linker. Blue markers indicate the positions of y ions, which are represented on the chart with the corresponding peptide number (P1 or P2) shown in parentheses. Green markers indicate the positions of b ions.

4.7 Conclusions

A functional system for enrichment of tagged and cross-linked peptides and proteins *via* boronate ester chemistry has been demonstrated. A set of modified peptides were synthesised and enabled a study showing the reversibility of interactions occurring between a solid-supported phenylboronic acid and a 1,2-diol system. Capture and release of modified peptides *via* boronate ester chemistry was shown to be quick and effective. A series of affinity tag labelled cross-linkers have been synthesised and used to cross-link model proteins allowing selective enrichment of cross-linked and modified peptides from mixtures.

In conclusion, the preliminary cross-linking experiments conducted have shown that enrichment of cross-linked peptides *via* boronate ester chemistry holds great promise as a tool for the study of proteins.

Chapter 5: *Experimental*

5.1 General information

5.1.1 Equipment

UV-visible spectrophotometer: Agilent 8453 UV (Agilent Technologies)

BioAnalyzer 4F/4S white light scanner and FIPS software (LaVision BioTech)

Biosafety cabinet: HERAsafe KS 18 class II (Heraeus)

Incubator: HERAcell 150 (Heraeus)

Vacuum oven: Vacutherm VT6025 (Heraeus)

Europlasma NV Junior System

K Control Coater (R K Print-Coat Instruments Ltd.)

Autodrop inkjet printing system (Microdrop Technology, Norderstedt, Germany)

The Smith Synthesiser (Personal Chemistry), Initiator^{TM} (Biotage) and Sanyo EM-S1553 were used to perform microwave irradiations.

Dry solvents were obtained by passing through an alumina column. Reagents were used as purchased from commercial sources unless otherwise specified. TLC analysis was carried out using foil-backed sheets coated with silica gel (0.25 mm). Flash column chromatography was performed, on Sorbsil C60, 40-60 mesh silica.

Amino acids were of the L-configuration unless otherwise stated.

All buffers were prepared using commercial reagent grade chemicals.

RP-HPLC was performed on an Agilent 1100 Chemstation analytical system with a Supelco Discovery® C18 ODS, 5 μm, 50 mm x 4.6 mm i.d. column coupled to a Polymer Laboratories 100 ES evaporative light scattering detector. The following eluents were used: (A) H_2O + 0.1% TFA; (B) CH_3CN + 0.04% TFA; (C) H_2O + 0.1% FA; (D) MeOH + 0.1% FA. HPLC grade eluents were employed at a flow rate of 1 mL min^{-1} with samples prepared to a concentration of about 1 mg mL^{-1} and filtered prior to injection.

The following methods were used:

Method 1: (6 min) 90% (A) to 10% (A) in (B) over 3 min, then 10% (A) in (B) over 1 min, then 10% (A) in (B) to 90% (A) over 1 min, then 90% (A) over 1 min, detection by UV at 230, 254, 260 and 280 nm.

Method 2: (6 min) 95% (C) to 5% (C) in (D) over 3 min, then 5% (C) in (D) over 1 min, then 5% (C) in (D) to 95% (C) over 1 min, then 95% (C) over 1 min, detection by UV at 230, 254, 260 and 280 nm and ELSD (evaporative light scattering detection).

Method 3: (10 min) 95% (C) to 5% (C) in (D) over 6 min, then 5% (C) in (D) over 3 min, then 5% (C) in (D) to 95% (C) over 0.05 min, then 95% (C) over 0.95 min, detection by UV at 230, 254, 260 and 280 nm and ELSD (evaporative light scattering detection).

LC-MS were carried out on an Agilent LCMSD 1100 equipped with an Supelco Discovery® C18 ODS, 5 μm, 50 mm x 4.6 mm i.d. column, flow rate: 1 mL min^{-1} as *per* Method 3.

LRES mass spectra were recorded using a VG Platform Quadrupole Electrospray Ionisation mass spectrometer, measuring monoisotopic masses.

HRES mass spectra were recorded using an LTQ-Orbitrap Classic (ThermoElectron, Germany) mass spectrometer.

Preparative RP-HPLC was performed on an Agilent Technologies HP1100 Chemstation eluting with (A) H_2O + 0.1% TFA and (B) CH_3CN + 0.1% TFA on a Phenomenex (Prodigy) ODS-3 column (250 mm x 10 mm i.d., 5 μm), at a flow rate

of 5 mL min^{-1}, using the methods below. Fractions were collected using an Agilent 1200 Series Fraction Collector.

Method 4: (35 min) 95% (A) to 50% (A) in (B) over 20 min, then 50% (A) in (B) to 5% (A) in (B) over 5 min, then 5% (A) in (B) over 3 min, then 5% (A) in (B) to 95% (A) over 2 min, then 95% (A) over 5 minutes, detection by UV at 230, 254, 260 and 280 nm.

Method 5: (33 min) 100% (A) to 60% (A) over 5 min, 60% (A) to 30% (A) in (B) over 20 min, 30% (A) in (B) to 100% (B) over 4 min, 100% (B) to 100% (A) over 4 minutes, detection by UV at 214, 254 and 440 nm.

^{1}H NMR and **^{13}C NMR** spectra were recorded on Bruker ARX-250 (250 and 63 MHz respectively), DPX-360 (360 and 90 MHz respectively) and AVA-800 (800 and 200 MHz respectively). Chemical shifts (δ), referenced to the residual protonated solvent as an internal standard, are quoted in ppm, coupling constants (J) are reported in Hz.

IR spectra were recorded on a Fourier transform IR Bruker Tensor 27 Spectrometer (FTS) fitted with a Specac single reflection diamond attenuated total reflection (ATR) Golden Gate. All samples were run neat, frequencies are reported in cm^{-1} and only frequencies corresponding to significant functional groups are reported.

Microscopy and **Confocal microscopy** were performed on a Zeiss Axiovert 200M pseudo confocal microscope with a 100 W Hg lamp or a Leica Inverted Confocal Microscope with a DM IRE2 microscope stand and analysed using Improvision Volocity acquisition software.

Microarray imaging was carried out on a BioAnalyzer 4F/4S white light scanner (LaVision Bio Tech) equipped with Cy3, Cy5 and FITC filters. The BioAnalyzer was capable of imaging a standard microscopy slide (26x76 mm) in a single scan. Fluorescence intensity was integrated over a circular area of diameter 250 μm.

Melting points were determined using a Gellenkamp melting point apparatus.

Inkjet printing was carried out using an Autodrop inkjet printing system (Microdrop Technology, Norderstedt, Germany), using (unless specified) the following printing parameters: 120 V, 28 μs and 100 Hz with a AK-501 micropipette (70 μm nozzle).

5.2 General resin procedures

5.2.1 Calculation of theoretical loading

The theoretical loading of a resin after a reaction was calculated using Equation 5.1:

$$\textbf{New loading (mmol/g)} = \textbf{[Old loading /(1+(Old loading x Mass added x } 10^{-3}\textbf{)]}$$

Equation 5.1. Theoretical loading of a resin following a reaction, Where: "old loading" is the loading of the starting resin (mmol/g) and "mass added" is the mass of compound added onto the resin.

5.2.2 Quantitative ninhydrin test

A known mass of resin (*ca.* 5 mg) in a small test tube was treated with 6 drops of reagent A (preparation described below) and 2 drops of Reagent B (preparation described below) and heated in an oil bath at 110 °C for 10 min. The test tube was cooled and 60% aqueous EtOH (2 mL) added to the mixture. The resin was removed by filtration through glass wool and the deep blue filtrate collected in a 25 mL volumetric flask. The resin was washed with a solution of Et_4NCl (0.5 M in CH_2Cl_2, 2 x 0.5 mL) and the sample made up to 25 mL with 60% aqueous EtOH. The absorbance at 570 nm was then measured against a reagent blank using a spectrophotometer. The level of amine present was calculated using Equation 5.2:

$$\textbf{Amount of amine present (mmol/g)} = [(A_{570} \times V) / (\varepsilon_{570} \times W)] \times 10^3$$

Equation 5.2. Analysis of amine loading, where:

A_{570} = Recorded absorbance at 570 nm (arbitrary units)

V = Volume of combined solution (mL)

ε_{570} = Average molar extinction coefficient suitable for most peptides with the value 15000 $M^{-1}cm^{-1}$

W = Weight of the resin sample (mg).

Ninhydrin Reagent A:

Solution 1 – Reagent grade phenol (40.0 g) was dissolved in absolute EtOH (10 mL) with warming and then stirred over Amberlite mixed-bed resin MB-3 (4.0 g) for 45 min. The mixture was then filtered.

Solution 2 – Potassium cyanide (65 mg) was dissolved in H_2O (100 mL). A 2 mL aliquot of this solution was diluted with pyridine (38 mL, freshly distilled from ninhydrin) and stirred over Amberlite mixed-bed resin MB-3 (4.0 g). The solution was filtered and mixed with Solution 1 to give Reagent A.

Ninhydrin Reagent B:

Ninhydrin (2.5 g) was dissolved in absolute EtOH (50 mL).

5.2.3 TNBS test (2,4,6-trinitrobenzensulfonic acid)[223]

A few beads were suspended in 2 drops of a solution of 10% DIPEA in DMF and 2 drops of a solution of 1% TNBS in DMF (commercially available). After a few minutes, the beads were washed with DMF to remove the red solution. A positive test was indicated by red beads and confirmed the presence of primary amines.

5.2.4 Estimation of level of first residue attachment – Quantitative Fmoc Test[224]

To a known mass of dry Fmoc amino acid-resin (approximately 5 μmol with respect to Fmoc, (*e.g.* 5 mg)) was added a solution of 20% piperidine in DMF (1 mL), and the mixture was shaken for 5 min. The cleavage solution was added to a 10 mL

volumetric flask and the volume was made up to 10 mL with a solution of 20% piperidine in DMF. The absorbance at 302 nm of the liberated dibenzofulvene-piperidine adduct was measured twice against a blank solution of 20% piperidine in DMF and the average value was used. The loading was calculated according to Equation 5.3:

$$\textbf{Loading (mmole/g)} = [(A_{302} \times V)/(\varepsilon_{302} \times m)] \times 10^3$$

Equation 5.3. Analysis of amine loading, where "A_{302}" is the recorded absorbance at 302 nm, "V" is the diluted volume (10 mL), "ε_{302}" is the extinction coefficient of the dibenzofulvene-piperidine adduct (7800 M^{-1} cm^{-1}) and "m" is the mass of resin (mg).

5.3 General methods for solid phase peptide synthesis

1 mL of solvent per gram of resin was used for the following procedures.

5.3.1 Method A: Solid phase peptide coupling conditions – DIC/HOBt

Resin was swollen in a minimum amount of CH_2Cl_2. *N*-Fmoc-amino acid (2 eq) and HOBt (2 eq) were dissolved in CH_2Cl_2 with a few drops of DMF and stirred for 10 min. DIC (2.2 eq) was added and the mixture stirred for 10 min before addition to the resin. The resin was agitated for 1 h to effect coupling. The resin was washed with DMF (x3), CH_2Cl_2 (x3), MeOH (x3), Et_2O (x2) and dried under vacuum for 30 min.

5.3.2 Method B: Solid phase peptide coupling conditions – HBTU/DIPEA

Resin was swollen in a minimum amount of CH_2Cl_2. *N*-Fmoc-amino acid (5 eq) and HBTU (4.9 eq) were dissolved in DMF (0.1 M). DIPEA (10 eq) was added and the resulting mixture was immediately added to the resin. The resin was agitated for 40 minutes to affect coupling. The resin was washed with DMF (x3), CH_2Cl_2 (x3), MeOH (x3), Et_2O (x2) and dried under vacuum for 30 min.

5.3.3 Method C: *N*-terminal Fmoc removal

Fmoc removal was performed using 20% piperidine in DMF with two sequential treatments of 20 min. The resin was then filtered and washed with DMF (x3), CH_2Cl_2 (x3), MeOH (x3), Et_2O (x2) and dried under vacuum for 30 min.

5.3.4 Method D: Cleavage of peptides from resin

Resin was swollen in a minimum of CH_2Cl_2. TFA/TIS/H_2O (95/2.5/2.5) was added and the resin agitated for 2h. The TFA solution was removed, concentrated to *ca.* 1 mL and added to cold (4 °C) Et_2O in a centrifuge tube. The resulting precipitate was collected by centrifugation and washed with Et_2O (x4).

5.3.5 Method E: Intra-resin disulfide bond formation[77]

ArCONH-Cys(Trt)-Rink amide resin was shaken with a solution of iodine (10 eq) in DMF for 1.5 h. The resin was then washed with DMF (10 mL x 5), CH_2Cl_2 (10 mL x 5), MeOH (10 mL x 5) and Et_2O (10 mL x 3).

5.3.6 Method F: Attachment of Fmoc amino acids to Wang linker resin

Resin was swollen in a minimum of DMF for 30 min. Fmoc amino acid (10 eq) was dissolved in dry CH_2Cl_2 and a solution of DIC (5 eq) in dry CH_2Cl_2 was added. The mixture was stirred for 20 min at 0 °C, followed by removal of the CH_2Cl_2 *in vacuo*. The residue was dissolved in the minimum of DMF and the solution added to the swollen resin. DMAP (0.1 eq) in DMF was added to the resin mixture, which was agitated for 2 h. The resin was then filtered and washed with DMF (x3), CH_2Cl_2 (x3), MeOH (x3), Et_2O (x2) dried under vacuum for 30 min and the level of attachment estimated using the quantitative Fmoc test (Section 5.2.4).

5.4 General cell procedures

5.4.1 Cell culture

HeLa cells were cultivated in T-75 flasks (Nunc) to 70% confluency in Roswell Park's Memorial Institute (RPMI-1640, Sigma-Aldrich) medium supplemented with 10% foetal bovine serum (FBS, Biosera), 100 U/mL penicillin and streptomycin and 4 mM L-glutamine (Gibco) at 37 °C / 5% CO_2. At this time, the old growth media was removed and the cells were washed with PBS (10 mL) and harvested *via* trypsination (trypsin (0.050% w/v)/EDTA (0.20% w/v), Gibco) (1 mL) at 37 °C. Detached cells were collected in fresh growth media (4 mL) and diluted using more fresh growth media to give the appropriate cell density for experiments.

5.4.2 Haemocytometry

Haemocytometry was used to determine cell densities. An aliquot (10 μL) of cells detached from a T-75 flask and collected in growth media (total volume: 5 mL) was mixed with 0.2% trypan blue (40 μL, Sigma-Aldrich) and pipetted into a Bright Line™ haemocytometer (an etched glass device with an H-shaped moat forming two cell-counting areas (with 4 quadrants in each area), with surface features enhanced by Neubauer rulings, Sigma-Aldrich). Cell concentration and the densities required for experiments were determined by Equations 5.4 and 5.5 respectively.

$$\textbf{Concentration (cell/mL)} - \textbf{(N / Q) x } 5x10^4$$

Equation 5.4. Concentration of cell/mL by haemocytometry, where "N" is the total number of cells counted and "Q" is the number of quadrants counted.

$$V_{Exp}\ \textbf{(mL)} = (V_{Tot} \textbf{ x } C_{Well}) \textbf{ x } (1000 / V_{Well}) / C_{Tot}$$

Equation 5.5. Volume of cells detached from T-75 flask "V_{Exp}" required in an experiment, a total medium volume of "V_{Tot}" and a concentration per well of "C_{Well}". "V_{Well}" is the volume required per well and "C_{Tot}" is the concentration of cells/mL as calculated in Equation 5.4.

5.5 Experimental for Chapter 2

5.5.1 Synthesis of compounds

Fmoc-Rink-PS (2.2)

Amino polystyrene resin (5.00 g, 8.00 mmol, 1 eq) was coupled to Fmoc-Rink amide linker (8.11 g, 16.0 mmol, 2 eq) using *Method A* (Section 5.3.1). Qualitative ninhydrin test negative.

H-Rink-PS (2.3)

Resin **2.2** was Fmoc-deprotected using *Method C* (Section 5.3.3). Qualitative ninhydrin test positive.

H-Cys(Trt)-Rink-PS (2.4)

Resin **2.3** (3.58 g, 2.40 mmol, 1 eq) was coupled to Fmoc-Cys(Trt)-OH (2.81 g, 4.80 mmol, 2 eq) using *Method A* (Section 5.3.1). Qualitative ninhydrin test negative. Quantitative Fmoc test gave a loading of 0.608 mmol/g. Resin was deprotected using *Method C* (Section 5.3.3). Qualitative ninhydrin test positive.

Cystine diamides (2.6-2.12)

Resin **2.4** (0.427 g, 0.300 mmol, 1 eq) was coupled to carboxylic acids (**2.5**) according to *Method A* (Section 5.3.1). Qualitative ninhydrin test negative. Resins were treated according to *Method E* (Section 5.3.5) and cleaved with *Method D* (Section 5.3.4).

***N,N'*-Di(benzoyl)-L-cystine diamide (2.6)[34]**

Yield: 95%; **RP-HPLC** (λ_{254}): 7.0 min (100%) (Method 3); ***m/z*** (ES^+): 447.0 $(M+H)^+$, 469.0 $(M+Na)^+$; **^{1}H-NMR** (DMSO-d_6, 250 MHz): δ 8.65 (d, 2H, J = 8 Hz, N*H*), 7.95 (dd, 4H, ^3J = 6.8 Hz, 2Ar*H*-2 + 2Ar*H*-6), 7.65-7.50 (m, 8H, NH_2 + 2Ar*H*-3 + 2Ar*H*-4 + 2Ar*H*-5), 7.30 (s, 2H, NH_2), 4.83-4.72 (m, 2H, C*H*), 2.60-2.55 (m, 4H, Cystine-$CH_{2\alpha}$ + Cystine-$CH_{2\beta}$).

***N,N'*-Di(2-naphthoyl)-L-cystine diamide (2.7)[34]**

Yield: 92%; **LCMS** (λ_{254}): 8.4 min (100%) (Method 3); ***m/z*** (ES^+): 569.3 $(M+Na)^+$; **^{1}H-NMR** (DMSO-d_6, 250 MHz): δ 8.85 (d, 2H, J = 8 Hz, N*H*), 8.58 (s, 2H, 2Ar*H*-2), 8.09-8.00 (m, 8H, 2Ar*H*-4 + 2Ar*H*-5 + 2Ar*H*-6 + 2Ar*H*-7), 7.72-7.68 (m, 6H, NH_2 + 2Ar*H*-9 + 2Ar*H*-10), 7.38 (br s, 2H, NH_2), 4.95-4.85 (m, 2H, C*H*), 3.25-3.15 (m, 2H, Cystine-$CH_{2\alpha}$), 2.60-2.55 (m, 2H, Cystine-H_β)

***N,N'*-Di(*p*-fluorobenzoyl)-L-cystine diamide (2.8)[34]**

Yield: 75%; **LCMS** (λ_{254}): 6.9 min (100%) (Method 3); ***m/z*** (ES^+): 483.0 $(M+H)^+$, 505.0 $(M+Na)^+$; ***R_f*:** 0.44 ($CHCl_3$/MeOH, 9/1); **IR** (neat): ν_{max}: 1688, 1636, 1602 cm^{-1}; **^{1}H-NMR** (DMSO-d_6, 250 MHz): δ 8.61 (d, 2H, J = 8.5 Hz, N*H*), 7.95 (dd, 4H, J = 9 Hz, $^4J_{HF}$ = 5 Hz, 2Ar*H*-2 + 2Ar*H*-6), 7.60 (br s, 2H, NH_2), 7.28-7.24 (m, 6H, 2Ar*H*-3 + 2Ar*H*-5 + NH_2), 4.72-4.68 (m, 2H, Cystine-$H_{2\alpha}$), 3.30 (dd, 2H, J = 4 Hz, Cystine-$H_{2\beta}$).

***N,N'*- Di(*p*-bromobenzoyl)-L-cystine diamide (2.9)[34]**

Yield: 52%; **LCMS** (λ_{254}): 8.4 min (100%) (Method 3); ***m/z*** (ES^+): 627.2.0 $(M+Na)^+$

***N,N'*-Di(*p*-anisoyl)-L-cystine diamide (2.10)**

Yield: 35%; **LCMS** (λ_{254}): 7.1 min (100%) (Method 3); ***m/z*** (ES^+): 529.3 $(M+Na)^+$

***N,N'*-Di(butyryl)-L-cystine diamide (2.11)**

Yield: 75%; **LCMS** (λ_{254}): 5.5 min (100%) (Method 3); ***m/z*** (ES^+): 401.2 $(M+Na)^+$

benzyl (2*R*,2*R*)-3,3'-disulfanediylbis(1-amino-1-oxopropane-3,2-diyl)dicarbamate (2.12)

Yield: 91%; **LCMS** (λ_{254}): 8.0 min (100%) (Method 3); ***m/z*** (ES^+): 507.0 $(M+H)^+$, 529.0 $(M+Na)^+$

Synthesis of *N,N'*-(2,2'-(2*R*,2'*R*)-3,3'-disulfanediylbis(1-amino-1-oxopropane-3,2-diyl)bis(azanediyl)bis(2-oxoethane-2,1-diyl))di-2-napthamide (2.13)

Resin **2.4** (0.427 g, 0.300 mmol, 1 eq) was coupled to Fmoc-Gly-OH (0.179 g, 0.600 mmol, 2 eq) according to *Method A* (Section 5.3.1) followed by Fmoc deprotection according to *Method C* (Section 5.3.3). 2-napthoic acid (0.103 g, 0.600 mmol, 2 eq) was coupled according to *Method A* (Section 5.3.1) and the resulting resin was treated according to *Method E* (Section 5.3.5) and cleaved with *Method D* (Section 5.3.4). Couplings and deprotections were monitored by qualitative ninhydrin test. **Yield:** 56%; **LCMS** (λ_{254}): 7.6 min (100%) (Method 3); ***m/z*** (ES^+): 661.1 $(M+H)^+$

Synthesis of *N,N'*-(3,3'-(2*R*,2'*R*)-3,3'-disulfanediylbis(1-amino-1-oxopropane-3,2-diyl)bis(azanediyl)bis(3-oxoethane-3,1-diyl))di-2-napthamide (2.14)

Synthesis was as for cystine **2.13** but Fmoc-β-Ala-OH (0.186 g, 0.600 mmol, 2 eq) was coupled using *Method A* (Section 5.3.1) instead of Fmoc-Gly-OH. **Yield:** 77%; **LCMS** (λ_{254}): 7.4 min (100%) (Method 3); ***m/z*** (ES^+): 689.0 $(M+H)^+$

Synthesis of *N,N'*-Di(napthoyl)-L-cystine *N'',N'''*-Di(glycine) diamide (2.15)

Resin **2.3** (0.427 g, 0.300 mmol, 1 eq) was coupled to Fmoc-Gly-OH (0.178 g, 0.600 mmol, 2 eq) using *Method A* (Section 5.3.1). Resin was deprotected using *Method C* (Section 5.3.3) and then coupled to Fmoc-Cys(Trt)-OH (0.352 g, 0.600 mmol, 2 eq). This was followed with Fmoc-deprotection according to *Method C* (Section 5.3.3) and capping with 2-napthoic acid (0.103 g, 0.600 mmol, 2 eq) using *Method A* (Section 5.3.1). Couplings and deprotections were monitored by qualitative ninhydrin test. Resin was treated according to *Method E* (Section 5.3.5) and cleaved with *Method D* (Section 5.3.4). **Yield:** 37%; **LCMS** (λ_{254}): 7.5 min (100%) (Method 3); ***m/z*** (ES^+): 661.0 $(M+H)^+$, 883.0 $(M+Na)^+$

Synthesis of *N,N'*-Di(napthoyl)-L-cystine *N'',N'''*-Di(phenylalanine) diamide (2.16) Synthesis was as for **2.15** except Fmoc-Phe-OH was coupled rather than Fmoc-Gly-OH. **Yield:** 43%; **LCMS** (λ_{254}): complex mixture, ***m/z*** (ES^+): 841.2 $(M+H)^+$, 863.2 $(M+Na)^+$

Synthesis of *N,N'*-Di(benzoyl)-L-cystine *N'',N'''*-Di(glycine) diamide (2.17) Synthesis was as for **2.15** except benzoic acid was used as a capping group rather than 2-napthoic acid. **Yield:** 100%; **LCMS** (λ_{254}): 5.5 min (100%) (Method 3); ***m/z*** (ES^+): 561.0 $(M+H)^+$, 583.0 $(M+Na)^+$

Synthesis of *N,N'*-Di(benzoyl)-L-cystine *N'',N'''*-Di(phenylalanine) diamide (2.18) Synthesis was as for **2.15** except Fmoc-Phe-OH was coupled rather than Fmoc-Gly-OH and benzoic acid was used as a capping group rather than 2-napthoic acid. **Yield:** 100%; **LCMS** (λ_{254}): complex mixture, ***m/z*** (ES^+): 741.1 $(M+H)^+$

Synthesis of *N,N'*-Di(*p*-fluorobenzoyl)-L-cystine *N'',N'''*-Di(glycine) diamide (2.19) Synthesis was as for **2.15** except 4-fluorobenzoic acid was used as a capping group rather than 2-napthoic acid. **Yield:** 79%; **LCMS** (λ_{254}): 6.6 min (91%) (Method 3); ***m/z*** (ES^+): 597.0 $(M+H)^+$, 619.0 $(M+Na)^+$

Synthesis of *N,N'*-Di(*p*-fluorobenzoyl)-L-cystine *N'',N'''*-Di(phenylalanine) diamide (2.20) Synthesis was as for **2.15** except Fmoc-Phe-OH was coupled rather than Fmoc-Gly-OH and 4-fluorobenzoic acid was used as a capping group rather than 2-napthoic acid. **Yield:** 85%; **LCMS** (λ_{254}): 7.0 min (100%) (Method 3); ***m/z*** (ES^-): 777.1 $(M+H)^+$, 799.1 $(M+Na)^+$

Synthesis of *N,N'*-Di(2-naphthoyl)-L-cystine (2.21) Fmoc-Cys(Trt)-OH (2.694 g, 4.6 mmol, 10 eq) was loaded onto polystyrene Wang linker resin (0.92 mmol/g, 0.46 mmol, 0.500 g, 1eq) using *Method F* (Section 5.3.6). An Fmoc deprotection according to *Method C* (Section 5.3.3) was followed by coupling of 2-napthoic acid using *Method A* (Section 5.3.1). Resin was treated according to *Method E* (Section 5.3.5) and cleaved with *Method D* (Section 5.3.4). **Yield:** 96%; **LCMS** (λ_{254}): 6.2 min (83%) (Method 3); ***m/z*** (ES^-): 547.0 $(M-H)^-$

Synthesis of *N,N'*-Di(benzoyl)-L-cystine *N'',N'''*-Di(glycine) (2.22) Fmoc-Gly-OH (6.00 mmol, 1.784 g, 10 eq) was loaded onto polystyrene Wang linker resin (0.92 mmol/g, 0.60 mmol, 0.652 g) using *Method F* (Section 5.3.6). An Fmoc

deprotection according to *Method C* (Section 5.3.3) was followed by coupling of Fmoc-Cys(Trt)-OH (0.703 g, 1.2 mmol, 2 eq) using *Method A* (Section 5.3.1). Fmoc deprotection as before was followed by coupling of benzoic acid (0.147 g, 1.2 mmol, 2 eq) according to *Method A* (Section 5.3.1). Resin was treated according to *Method E* (Section 5.3.5) and cleaved with *Method D* (Section 5.3.4). **Yield:** 75%; **LCMS** (λ_{254}): 6.7 min (100%) (Method 3); ***m/z*** (ES^-): 561.0 $(M-H)^-$

Synthesis of *N,N'*-Di(benzoyl)-L-cystine *N'',N'''*-Di(phenylalanine) (2.23) Synthesis was as for **2.22** except Fmoc-Phe-OH was coupled instead of Fmoc-Gly-OH. **Yield:** 73%; **LCMS** (λ_{254}): 9.8 min (100%) (Method 3); ***m/z*** (ES^-): 741 $(M-H)^-$

Synthesis of *N,N'*-Di(*p*-fluorobenzoyl)-L-cystine *N'',N'''*-Di(glycine) (2.24) Synthesis was as for **2.22** except 4-fluorobenzoic acid was coupled instead of benzoic acid. **Yield:** 75%; **LCMS** (λ_{254}): 7.2 min (100%) (Method 3); ***m/z*** (ES^-): 597.0 $(M-H)^-$

Synthesis of *N,N'*-Di(*p*-fluorobenzoyl)-L-cystine *N'',N'''*-Di(phenylalanine) (2.25) Synthesis was as for **2.22** except Fmoc-Phe-OH was coupled instead of Fmoc-Gly-OH and 4-fluorobenzoic acid was coupled instead of benzoic acid. **Yield:** 62%; **LCMS** (λ_{254}): 7.0 min (100%) (Method 3); ***m/z*** (ES^-): 777.0 $(M-H)^-$

Synthesis of *N*-*p*-bromobenzoyl-*N'*-benzoyl-L-cystine diamide (2.26) Synthesis was as for cystine diamides (**2.6-2.12**) except a mixture of 4-bromobenzoic acid (1 eq) and benzoic acid (1 eq) was coupled as capping groups. **Yield:** 78%; **LCMS** (λ_{254}): 7.0 min (50%, dibenzoyl derivative) and 7.6 min (50%, **2.26**) (Method 3); ***m/z*** (ES^+): 469.0 $(M+Na)^+$ (dibenzoyl derivative), 547 $(M+Na)^+$ product.

5.5.3 Gelation in well plate and seeding with HeLa cells

In a typical experiment, gel was broken up inside microwave vials by 30 seconds of vigorous shaking. "Gel solutions" were then added to polystyrene 96-well plates (Nunc) (two volumes were used: 50 and 100 μL). The well plates were then covered using well plate covers, irradiated with microwaves (Sanyo EM-S1553) at 800 W for 15 s and left to stand for 10 min. Gel formation was confirmed principally by well plate inversion. Cells were cultured as described (Section 5.4.1) and seeded directly onto the surface of gels at a density of 1 x 10^4 cells/well (volume per well: 100 μL). The last row of every well plate was used as a blank (no gel). Cells were incubated (37 °C/5% CO_2) and well plates were examined after 24 and 48 h by microscopy.

5.5.4 Gelation on glass slides

In a typical experiment, glass slides spotted/printed with DMSO gelator solutions were introduced to a 10-slide capacity chamber (Genetix; Product No. X2530), along with H_2O (2 mL) added to the base well, which was sealed and heated in an oven at 80 °C for 1 h. The chamber was removed from the oven and allowed to cool to room temperature undisturbed. Slides were then scanned using a BioAnalyzer 4F/4S white light scanner and the data analysed using FIPS software (LaVision BioTech).

5.5.5 Glass slide treatment and masking

Tridecafluoro-1,1,2,2-tetrahydroocctyldimethylchlorosilane (TFCS) was supplied by Gelest. Standard microscope slides (76×26 mm) were used from Menzel GmbH. Glass slides were initially rinsed in various solvents (hexane, DMF, acetone and MeOH) to remove manufacturing grease and residues. The glass slides were then etched using oxygen plasma, from a Europlasma NV Junior System (Frequency: 50 Hz, Rf Power: 100 W, stabilising time: 30 seconds), for 2 minutes at 200 mTr, rotating after 1 minute. A 40% w/v sucrose masking solution was prepared by dissolving sucrose in water. The solutions were printed on the glass surface using an Autodrop inkjet printing system (Microdrop Technology, Norderstedt, Germany).

This consists of an automated XYZ stage and a stroboscopic video camera. The diameter of the nozzle used was 70 μm.

Table 5.1 shows the printing parameters used to produce sucrose squares with the following diameters: 4.5 mm (30 x 30 spots/square), 3 mm (20 x 20 spots/square), 1.5 mm (10 x 10 spots/square) and 0.75 mm (5 x 5 spots/square):

Spots/square	Distance between squares (mm)	No. drops printed at each position	Spots printed/square	Maximum no. squares/slide
30 x 30	1.4	4	3600	36
20 x 20	1.6	4	1600	80
10 x 10	1.8	4	400	132
5 x 5	1.8	4	100	261

Table 5.1. Printing parameters used to print sucrose squares onto glass slides.

After printing, sucrose masked slides were dried in 60 °C for 1 h, allowed to cool to room temperature and then coated with Tridecafluoro-1,1,2,2-tetrahydrooctyl)dimethylchlorosilane (TFCS) (4 μL per slide) using a K Hand Bar Coater (bar of 4.5 mm diameter with a 0.05 mm diameter wire and coating speed 2.5 cm/s). Finally, the slides were washed in water (3 x 200 mL) to remove the mask and excess TFCS, and dried under a stream of nitrogen. The result was hydrophobic patterned slides consisting of different sized arrays of hydrophilic features.

5.5.6 Gelator deposition using inkjet printing

Printing different concentrations of *N,N'*-Di(2-naphthoyl)-L-cystine diamide

0.5 μM Rhodamine B DMSO solutions containing different concentrations (0, 1, 2, 3, 4, 5, 7.5, 10, 20, 30, 40 and 50 mM) of *N,N'*-Di(2-naphthoyl)-L-cystine diamide were prepared. Each concentration was deposited onto a slide patterned with a 1.5 x 1.5 mm hydrophilic feature array by piezo jet-printing 350 drops (0.4 μL) onto each

defined hydrophilic feature using the printing parameters 115 V, 28 μs and 200 Hz. Each concentration was printed in triplicate.

Mixed gelators printed on an array

35 mM solutions of gelators used in this study (**2.6**-**2.10**) were prepared in DMSO and deposited in defined positions onto 1.5 x 1.5 mm hydrophilic features in an array by piezo jet-printing 100 drops (0.11 μL) of each gelator solution. Each gelator solution was printed in 5 positions on the array. The printing parameters were 115 V, 28 μs and 200 Hz. The printing pipette was cleaned between each gelator to avoid contamination. The cleaning protocol involved filling the micropipette with DMSO, applying an impulse (12500 Hz) frequency to the micropipette for 5 s and emptying the micropipette. 100 drops of each 35 mM gelator solutions were then printed onto the first set of printed gelators such that 25 different gelator combinations were achieved. This was followed by printing 100 drops of 210 mM DTT solution prepared in DMSO onto every gelator mixture combination and then printing 50 drops of 3.5 μM Rhodamine B in DMSO. Each gelator combination with DTT and Rhodamine B was printed in triplicate on one slide. Gelation was induced according to Section 5.4.4.

Mixed gelators printed on an array without DTT

The printing procedure was repeated as in the previous experiment but instead of printing 100 drops of 210 mM DTT solution in DMSO, 100 drops of DMSO only was printed along with gelator/Rhodamine B mixtures. Gelation was induced according to Section 5.4.4.

Mixed gelators printed on an array and 6 day incubation

The printing procedure was repeated as in the previous experiment but gelation was induced by holding the incubation chamber containing printed slides at 80 °C for 6 days before allowing it to cool.

5.5.7 Gel degradation study

In a typical gel degradation experiment, **2.6** hydrogel (2 mM) was formed by heating **2.6** solid (10 μmol, 4.5 mg) in H_2O (5 mL) in the microwave at 180 °C for 5 min and allowing the resulting gelator solution to rest and cool down for 15 min. A steel ball bearing (diameter = 4 mm, 84 mg) was carefully placed on the centre of the gel surface (diameter = 12 mm) and the movement of the steel ball over time and distance measured. Gel degradation was studied following addition of 300 μL of each of H_2O, 100 mM TEAA buffer (pH 8.15), 1 M DTT (0.3 mmol, 46.2 mg) in 100 mM TEAA buffer (pH 8.15) and 4 M DTT (1.2 mmol, 185 g) in 100 mM TEAA buffer (pH 8.15).

A steel ball bearing (diameter = 4 mm, 84 mg) was carefully placed on the centre of the gel surface (diameter = 12 mm) of **2.15** hydrogel (5 mL, 10 μmol, 2 mM), which was treated with 300 μL bovine trypsin (1 mg/mL) in PBS (pH 7.4) and the movement of the steel ball over time and distance measured.

5.6 Experimental for Chapter 4

5.6.1 Synthesis of compounds

1-{[3-(3,4-dihydroxyphenyl)propanoyl]oxy}pyrrolidine-2,5-dione (4.1)

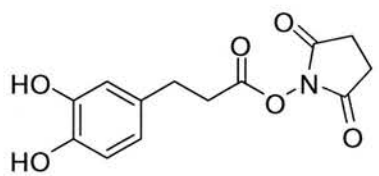

3,4-dihydroxyhydrocinnamic acid (0.50 g, 2.75 mmol) and *N*-hydroxysuccinimide (0.475 g, 4.13 mmol) were dissolved in DMF (28 mL), followed by addition of EDC (0.63 g, 3.30 mmol). The mixture was stirred for 24 h at rt. The solvent was evaporated *in vacuo* and the solid was dissolved in EtOAc (40 mL), which was then washed with sat. $NaHCO_3$ (3 x 25 mL), 10% citric acid (3 x 25 mL), brine (2 x 25 mL), dried ($MgSO_4$) and evaporated *in vacuo* to yield a straw-coloured solid (0.541 g, 1.94 mmol, 71%). **^{1}H-NMR** (250 MHz, $(CD_3)_2SO$): δ_H 8.70-8.30 (m, 2H, 2CO*H*), 6.79-6.20 (m, 3H, 3Ar*H*), 2.80-2.30 (m, 8H, ($CH_2CH_2C(O)$ and ($CH_2CH_2C(O)$ and

2NC(O)CH_2); **^{13}C-NMR** (63 MHz, $(CD_3)_2SO$): δ_C 170.54 (CH_2CH_2C(O)), 168.73 (N*C*(O)), 145.40 (Ar-5-*C*OH), 144.07 (Ar-4-*C*OH), 130.56 (*C*), 119.22 (Ar-2-*C*H), 116.15 (Ar-3-*C*H), 115.78 (Ar-6-*C*H), 32.50 (CH_2CH_2C(O)), 29.60 (CH_2CH_2C(O)), 25.77 (NC(O)CH_2); **HRMS** (ES^-) for $C_{13}H_{12}NO_6$ $(M-H)^-$: calcd 278.0665, found 278.0668; **R_f** 0.39 (10% MeOH/CH_2Cl_2, $KMnO_4$).

4-phenylboronic acid *N*-hydroxysuccinimide ester (4.2)

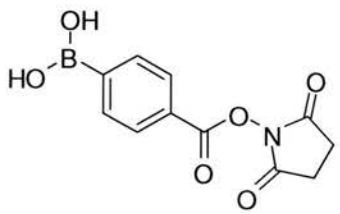

4-carboxyphenylboronic acid (0.20 g, 1.21 mmol) and *N*-hydroxysuccinimide (0.21 g, 1.81 mmol) were dissolved in DMF (12 mL), followed by addition of EDC (0.28 g, 1.45 mmol). The mixture was stirred for 24 h at rt. The solvent was evaporated *in vacuo* and the solid was dissolved in EtOAc (30 mL), which was then washed with sat. $NaHCO_3$ (3 x 20 mL), 10% citric acid (3 x 20 mL), brine (2 x 20 mL), dried ($MgSO_4$) and evaporated *in vacuo* to yield a straw-coloured solid (0.211 g, 0.80 mmol, 67%). **^{1}H-NMR** (250 MHz, $(CD_3)_2SO$): δ_H 8.06-8.05 (m, 2H, $_2$(HO)B-Ar-*o*-C*H*), 8.03-8.02 (m, 2H, $_2$(HO)B-Ar-*m*-C*H*), 2.91 (s, 4H, 2CH_2); **^{13}C-NMR** (63 MHz, $(CD_3)_2SO$): δ_C 173.50 (2N*C*(O)), 165.10 (C(O)), 145.63 ($_2$(HO)B*C*), 137.93 ($_2$(HO)B-Ar-*o*-*C*H), 131.88 ($_2$(HO)B-Ar-*m*-*C*H), 128.67 (*C*C(O)O), 28.68 (CH_2); **HRMS** (ES^-) for $C_{11}H_9NO_6B$ $(M-H)^-$: calcd 262.0523, found 262.0523; **R_f** 0.37 (10% MeOH/CH_2Cl_2).

4-(propylcarbamoyl)phenylboronic acid CPG (4.3)

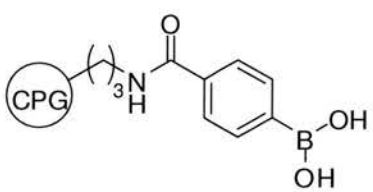

Trisoperl CPG (500 mg, 0.22 mmolg^{-1}, 110 μmol) in acetonitrile (4 mL) was treated with 4-carboxyphenylboronic acid (164 mg, 990 μmol) and IIDQ (323 μL, 1090 μmol) and was heated at 60 °C for 2 h. The resin was drained, rinsed with acetonitrile, DMF, CH_2Cl_2 and MeOH (3 x 10 mL each) and vacuum dried. **Ninhydrin test:** negative, **Theoretical loading:** 0.21 mmolg^{-1}.

3-(3,4-dihydroxyphenyl)-*N*-propylpropanamide CPG (4.4)

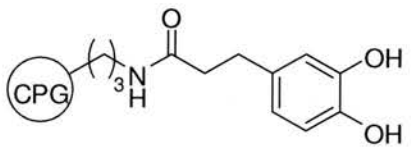

Trisoperl CPG (500 mg, 0.22 mmolg^{-1}, 110 μmol) in acetonitrile (4 mL) was treated with 3,4-dihydroxyhydrocinnamic acid (180 mg, 990 μmol) and IIDQ (323 μL, 1090 μmol) and was heated at 60 °C for 2 h. The resin was drained, rinsed with acetonitrile, DMF, CH_2Cl_2 and MeOH (3 x 10 mL each) and vacuum dried. **Ninhydrin test:** negative, **Theoretical loading:** 0.21 mmolg^{-1}.

H-Arg(Pbf)-Wang linker polystyrene resin (4.5)

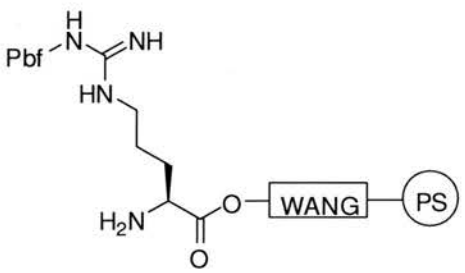

Fmoc-Arg(Pbf)-OH (2.00 mmol, 1.30 g, 10 eq) was loaded onto polystyrene Wang linker resin (0.92 mmol/g, 0.200 mmol, 0.220 g) using *Method F* (Section 5.3.6). An Fmoc deprotection according to *Method C* (Section 5.3.3) gave resin **4.5**. Quantitative Fmoc test gave a loading of 0.768 mmol/g.

H-Leu-Leu-Glu(tBu)-Tyr(tBu)-Leu-Lys(Boc)-Arg(Pbf)-Wang linker polystyrene resin (4.6)

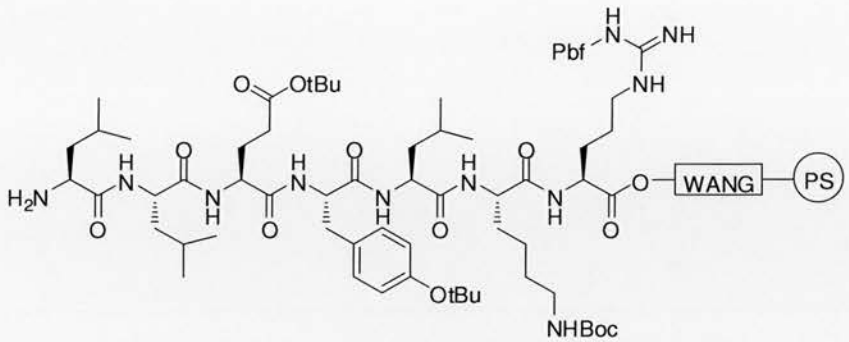

Resin **4.5** was coupled to a succession of Fmoc protected amino acids (1.00 mmol, 5 eq): Fmoc-Lys(Boc)-OH, Fmoc-Leu-OH, Fmoc-Tyr(^{t}Bu)-OH, Fmoc-Glu(^{t}Bu)-OH and 2x Fmoc-Leu-OH using *Method B* (Section 5.3.2) with Fmoc deprotection after every coupling using *Method C* (Section 5.3.3). The completion of each coupling was verified using the qualitative ninhydrin test. If needed, an extended cycle was repeated until completion of the reaction. Quantitative Fmoc test gave a loading of 0.385 mmol/g.

H-Leu-Leu-Glu-Try-Leu-Lys-Arg-OH (4.7)

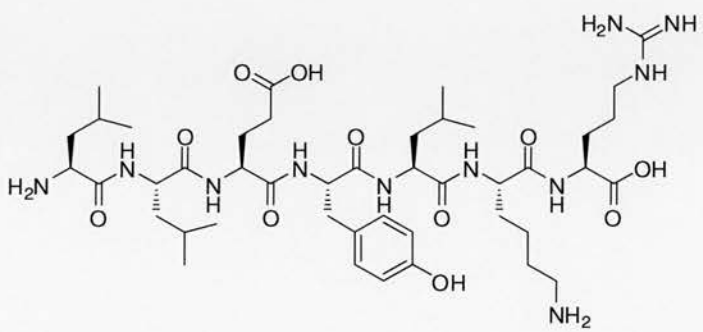

Resin **4.6** (0.0846 mmol, 79 mg) was cleaved using *Method D* (Section 5.3.4) and lyophilised to afford **4.7** as a white solid (29 mg, 95% (based on **4.5**)). ***m/z*** (ES^+): 934.5 $(M+H)^+$, 467.8 $(M+2H)^{2+}$ (100%); **HRMS** (ES+) for $C_{44}H_{76}N_{11}O_{11}$ $(M+H)^+$: calcd 934.57203, found 934.57251; **RP-HPLC** (λ_{254}): 2.36 min (100%) (Method 1).

4-carbamoylphenylboronic acid-Leu-Leu-Glu-Try-Leu-Lys-Arg-OH (4.8)

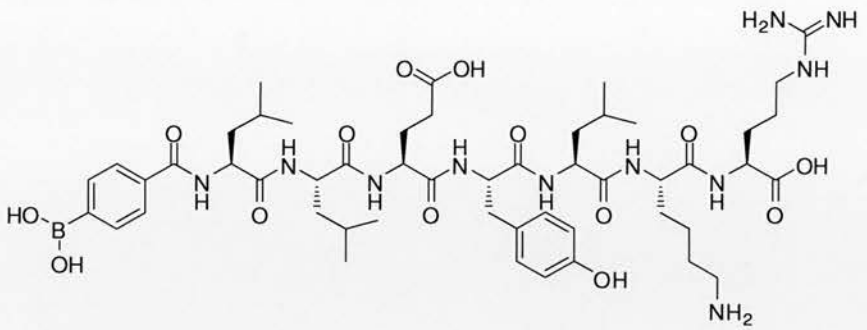

4-carboxyphenylboronic acid (0.185 mmol, 31 mg, 5 eq) was coupled to resin **4.6** (0.0370 mmol, 91 mg, 1 eq) using *Method B* (Section 5.3.2). Coupling was confirmed using qualitative ninhydrin test. Peptide **4.8** was cleaved using *Method D* (Section 5.3.4) and lyophilised to afford white solid (37 mg, 92% (based on **4.5**). ***m/z*** (ES^+): 1082.5 $(M+H)^+$, 541.7 $(M-2H)^{2+}$ (100%); **HRMS** (ES^+) for $C_{51}H_{81}BN_{11}O_{14}$ $(M+H)^+$: calcd 1082.6058, found 1082.6058; **RP-HPLC** (ELSD): 3.49 min (100%) (Method 2).

3-(3,4-dihydroxyphenyl)propanamide-Leu-Leu-Glu-Try-Leu-Lys-Arg-OH (4.9)

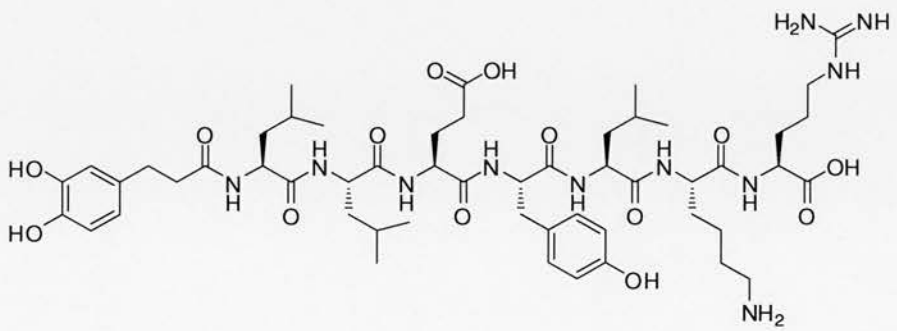

3,4-dihydroxyhydrocinnamic acid (0.182 mmol, 33 mg, 5 eq) was coupled to resin **4.6** (0.0364 mmol, 90 mg, 1 eq) using *Method B* (Section 5.3.2) followed by treatment with 20% piperdine in DMF for 10 min and washing with DMF (3 x 1 mL), CH_2Cl_2 (3 x 1 mL) and Et_2O (2 x 1 mL). Coupling was confirmed using qualitative ninhydrin test. Peptide **4.9** was cleaved using *Method D* (Section 5.3.4) and lyophilised to afford white solid (51 mg, 92% (based on **4.5**). ***m/z*** (ES^+): 1096.6 $(M-H)^-$, 547.7 $(M-2H)^{2-}$; **HRMS** (ES^+) for $C_{53}H_{84}BN_{11}O_{14}$ $(M+H)^+$: calcd 1098.6199, found 1098.6206; **RP-HPLC** (λ_{254}): 2.77 min (100%) (Method 1).

***N*-(3-hydroxy-4-(hydroxycarbamoyl)benzyl)glutaramide-Leu-Leu-Glu-Try-Leu-Lys-Arg-OH (4.10)**

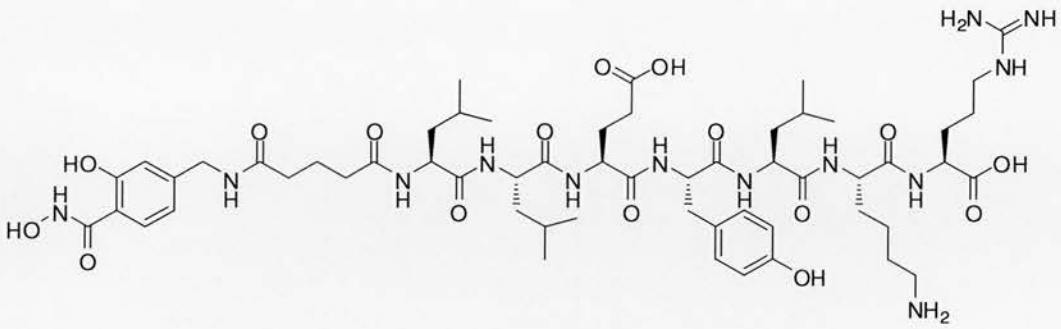

4-(3-hydroxy-4-(tetrahydro-pyran-2-ylcarbamoyl)-benzylcarbamoyl)-butyric acid 2,5-dioxo-pyrrolidin-1-yl ester (12.6 μmol, 6 mg, 2 eq) in DMF/DIPEA (200 μL, 95:5) was coupled to resin **4.6** (6.3 μmol, 16 mg, 1 eq) with mixing for 2 h. Peptide **4.10** was cleaved using *Method D* (Section 5.3.4) and lyophilised to afford white solid (12 mg, 75% (based on **4.5**). ***m/z*** (ES^+): calcd 1212.7, found 1212.5 $(M+H)^+$, 606.8 $(M+2H)^{2+}$; **RP-HPLC** (λ_{254}): 2.68 min (Method 1).

2-(3-(3,4-dihydroxyphenyl)propanamido)pentanedioic acid (4.14)

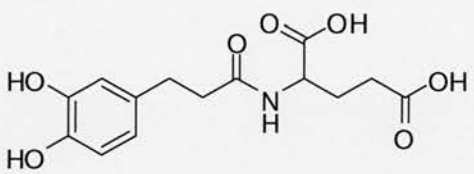

Fmoc-Glu(O^{t}Bu)-OH (9.20 mmol, 4.08 g, 10 eq) was coupled to polystyrene Wang linker resin (0.92 mmol, 1.00 g, 1 eq) using *Method F* (Section 5.3.6). A quantitative Fmoc test revealed the loading to be 0.595 mmol/g. The Fmoc group was removed using *Method C* (Section 5.3.3). 3,4-dihydroxyhydrocinnamic acid (2.87 mmol, 0.523 g, 3 eq) in DMF (5 mL) was added to the resin along with EEDQ (2.87 mmol, 0.711 g, 3 eq) and the resin was shaken overnight, after which the reaction mixture was removed by filtration and the resin was washed with DMF (3 x 5 mL), CH_2Cl_2 (3 x 5 mL), MeOH (3 x 5 mL) and Et_2O (2 x 1 mL). A negative ninhydrin result indicated that coupling was complete. The resin was treated with 4 M HCl in dioxane (3 mL) for 4 h, which was removed by filtration and evaporated *in vacuo*. The residue was purified using silica gel chromatography eluted with 3-10 %

MeOH/CH_2Cl_2 to yield a pale-yellow oil (180 mg, 0.579 mmol, 70%). **^{1}H-NMR** (250 MHz, CD_3OD): δ_H 6.66-6.54 (m, 2H, Ar-*o*-C*H* and Ar-*m*-C*H*), 6.44-6.40 (m, 1H, *o*-C*H*), 4.35-4.30 (m, 1H, NC*H*), 2.65 (t, *J* = 7.5 Hz, 2H ($CH_2CH_2C(O)NH$)), 2.41 (t, *J* = 7.5 Hz, 2H, ($CH_2CH_2C(O)NH$)), 2.18 (t, *J* = 7.5 Hz, 2H ($CH_2CH_2C(O)OH$)), 2.05-1.70 (m, ($CH_2CH_2C(O)OH$)); **^{13}C-NMR** (63 MHz, CD_3OD): δ_C 176.20 (*C*(O)NH), 175.19 (CH*C*(O)OH), 173.91 ($CH_2CH_2C(O)OH$), 146.61 (Ar-5-*C*OH), 145.08 (Ar-4-*C*OH), 121.04 (Ar-2-*C*H), 116.99 (Ar-3-*C*H), 116.77 (Ar-6-*C*H), 53.38 (*C*HC(O)OH), 39.26 ($CH_2CH_2C(O)$), 32.62 ($CH_2CH_2C(O)OH$), 31.25 ($CH_2CH_2C(O)$), 27.96 ($CH_2CH_2C(O)OH$); ***m/z*** (ES^-): 310.0 $(M-H)^-$ (100%); **RP-HPLC** (λ_{254}): 3.08 min (Method 1).

4-[Benzyl-(3-ethoxycarbonyl-propyl)-amino]-butyric acid ethyl ester (4.15)[213]

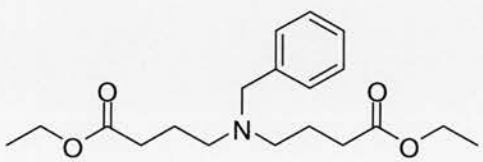

A mixture of ethyl 4-bromobutyrate (2.0 mL, 14.0 mmol, 1.94 eq), benzylamine (0.760 mL, 7.20 mmol) and potassium carbonate (5.8 g, 42.0 mmol, 5.82 eq) in DMF (30 mL) was stirred at 40 °C for 20 h. The majority of the DMF was then removed *in vacuo* and the reaction mixture was then diluted with water (20 mL) and extracted with ethyl acetate (3 x 30 mL). The pooled extracts were dried over $MgSO_4$, evaporated and purified by silica gel chromatography with EtOAc in hexane (7:1 v/v) to give the title compound (1.86 g, 5.55 mmol, 77% yield). **^{1}H-NMR** (500 MHz, $CDCl_3$): δ_H 7.32-7.19 (m, 5H, Ar-*H*), 4.12 (q, *J* = 7.0 Hz, 4H, $CH_3CH_2O(O)C$ and $C(O)OCH_2CH_3$), 3.54 (s, 2H, NCH_2Ar), 2.43 (t, *J* = 7.0 Hz, 4H, $CH_3CH_2O(O)CCH_2CH_2CH_2N$ and $NCH_2CH_2CH_2C(O)OCH_2CH_3$), 2.30 (t, *J* = 7.5 Hz, 4H, $CH_3CH_2O(O)CCH_2CH_2CH_2N$ and $NCH_2CH_2CH_2C(O)OCH_2CH_3$), 1.81 (quint, *J* = 7.2 Hz, 4H, $CH_3CH_2O(O)CCH_2CH_2CH_2N$ and $NCH_2CH_2CH_2C(O)OCH_2CH_3$), 1.26 (t, *J* = 7.1 Hz, 6H, $CH_3CH_2O(O)CCH_2CH_2CH_2N$ and $NCH_2CH_2CH_2C(O)OCH_2CH_3$); **^{13}C-NMR** (150 MHz, $CDCl_3$): δ_C 176.3 ($CH_3CH_2O(O)C$ and $C(O)OCH_2CH_3$), 131.6 (*o*-*C*H), 131.3

(*o*-*C*H), 131.2 (*C*), 130.9 (*m*-*C*H), 130.2 (*m*-*C*H), 129.6 (*p*-*C*H), 63.2 (N*C*H_2C), 61.1 (CH_3CH_2O(O)C and C(O)OCH_2CH_3), 55.3 ($CCH_2CH_2CH_2N$ and $NCH_2CH_2CH_2C$), 34.6 ($CCH_2CH_2CH_2N$ and $NCH_2CH_2CH_2C$), 24.9 ($CCH_2CH_2CH_2N$ and $NCH_2CH_2CH_2C$), 16.9 (CH_3); ***m/z*** (ES^+): 336.1 $(M+H)^+$ (100%); **RP-HPLC** (ELSD): 3.21 min (Method 2); $\mathbf{R_f}$ 0.75 (10% MeOH/CH_2Cl_2, Ninhydrin).

4-(bis(4-ethoxy-4-oxobutyl)carbamoyl)phenylboronic acid (4.17)

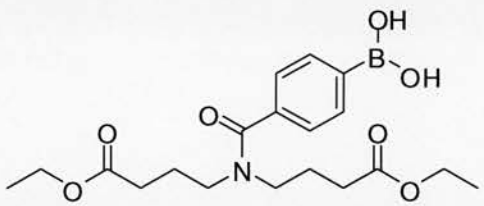

4.15 (285 mg, 0.851 mmol) was dissolved in MeOH (60 mL) and passed through a 10 % Pd/C/H_2 column on an H-Cube Tutor at 40 °C at 1 mL/min. The solvent was removed *in vacuo* and the crude residue was re-dissolved in DMF (3 mL) and treated with 4-carboxyphenylboronic acid (170 mg, 1.02 mmol, 1.2 eq) and EDC (212 mg, 1.11 mmol, 1.3 eq) and stirred for 18 h at rt. The DMF was evaporated *in vacuo* and the resulting residue was dissolved in saturated $NaHCO_3$ solution (20 mL) and extracted with EtOAc (3 x 15 mL). The organic layer was washed with $KHSO_4$ (20 mL) and brine (20 mL) and dried over $MgSO_4$ followed by evaporation *in vacuo*. The resulting dark yellow oil was purified by silica gel chromatography eluted with 3-10 % MeOH/CH_2Cl_2 to yield a pale-yellow oil (177 mg, 0.450 mmol, 53%). **^{1}H-NMR** (250 MHz, $(CD_3)_2SO$): δ_H 8.12-8.06 (m, 2H, 2 x *o*-C*H*), 7.50-7.45 (m, 2H, 2 x *m*-C*H*), 4.17-4.10 (m, 4H, CH_3CH_2O and OCH_2CH_3), 3.38-3.29 (m, 4H, $NCH_2CH_2CH_2$ and $CH_2CH_2CH_2N$), 3.17-3.13 (m, 2H, $NCH_2CH_2CH_2$), 2.35-2.30 (m, 4H, $NCH_2CH_2CH_2$ and $CH_2CH_2CH_2N$), 1.90-1.84 (m, 4H, $NCH_2CH_2CH_2$ and $CH_2CH_2CH_2N$), 1.28-1.25 (m, 6H, CH_3CH_2O and OCH_2CH_3); **^{13}C-NMR** (63 MHz, CD_3OD): δ_C 172.10 (*C*(O)O), 168.91 (N*C*(O)), 135.63 (NC(O)*C*), 128.83 (2 x *o*-*C*H), 98.61 (2 x *m*-*C*H), 60.13 (*C*(O)OCH_2CH_3), 48.80 ($NCH_2CH_2CH_2$), 46.55 ($NCH_2CH_2CH_2$), 32.40 (O(O)CCH_2CH_2), 24.51 (O(O)CCH_2CH_2), 14.06 (*C*(O)OCH_2CH_3); ***m/z*** (ES^+): 394.1 $(M+H)^+$ (100%); **HRMS** (ES^+) for $C_{19}H_{29}BNO_7$

$(M+H)^+$: calcd 394.2032, found 394.2033; **RP-HPLC** (λ_{254}): 2.79 min (100 %) (Method 1).

4,4'-(4-boronobenzoylazanediyl)dibutanoic acid (4.18)

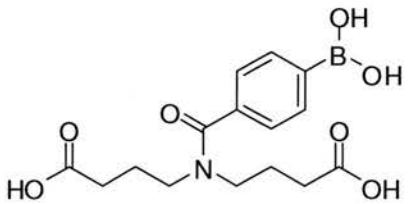

A mixture of **4.17** (177 mg, 0.450 mmol), MeOH (5.5 mL) and 1 N aqueous NaOH solution (1.3 mL) was stirred at 45 °C for 18 h. The reaction mixture was carefully acidified to pH 3-4 with 1N HCl and extracted with EtOAc (3 x 10 mL). The pooled extracts were washed with water (15 mL) and brine (15 mL) and dried ($MgSO_4$) and evaporated *in vacuo* to yield an off-white coloured gum (60 mg, 0.18 mmol, 40%). **^{1}H-NMR** (250 MHz, CD_3OD): δ_H 7.60 (d, J = 7.5 Hz, 2H, 2 x *o*-C*H*), 7.18 (d, J = 7.5 Hz, 2H, 2 x *m*-C*H*), 3.40 (t, J = 7.5 Hz, 2H, NCH_2CH$_2$CH$_2$), 3.17-3.13 (m, 2H, NCH_2CH$_2$CH$_2$), 2.44 (t, J = 7.5 Hz, 2H, NCH$_2$CH$_2$CH_2), 1.95 (t, J = 7.5 Hz, 2H, NCH$_2$CH$_2$CH_2), 1.86-1.82 (m, 2H, NCH$_2$CH_2CH$_2$), 1.65 (t, J = 7.5 Hz, 2H, NCH$_2$CH_2CH$_2$); **^{13}C-NMR** (63 MHz, CD_3OD): δ_C 180.40 (*C*(O)OH), 169.81 (N*C*(O)), 148.36-145.55 ((OH)$_2$B*C*), 137.48 (NC(O)*C*), 129.43 (2 x *o*-*C*H), 99.45 (2 x *m*-*C*H), 48.75 (N*C*H$_2$CH$_2$CH$_2$), 46.50 (N*C*H$_2$CH$_2$CH$_2$), 34.70 (HO(O)C*C*H$_2$CH$_2$), 24.61 (HO(O)CCH$_2$*C*H$_2$); ***m/z*** (ES^+): 336.0 $(M-H)^-$ (100%); **RP-HPLC** (λ_{254}): 2.61 min.

5-aminosalicylic acid methyl ester (4.20)

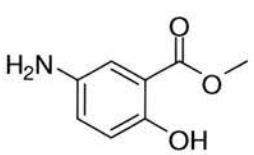

5-aminosalicylic acid (3.06 g, 20.0 mmol) in MeOH (40 mL) was treated with conc. H_2SO_4 (1.6 mL) and heated in the microwave at 120 °C for 1.5 h. The reaction was

neutralised by adding $NaHCO_3$ powder and evaporated *in vacuo*. H_2O (100 mL) was added and extracted into CH_2Cl_2 (150 mL). The CH_2Cl_2 layer was washed with brine (100 mL), dried ($MgSO_4$) and evaporated *in vacuo* to yield an off-white powder (2.65 g, 15.9 mmol, 80%). **^{1}H-NMR** (250 MHz, $CDCl_3$): δ_H 10.20 (br signal, 1H, *o*-O*H*), 7.14 (d, *J* = 2.8 Hz, 1H, *o*-C*H*), 6.89 (m, 2H, *m*-C*H* and *p*-C*H*), 3.91 (s, 3H, CH_3), 3.32 (br signal, 2H, NH_2); **^{13}C-NMR** (63 MHz, $CDCl_3$): δ_C 170.8 (*C*O), 155.2 (*C*OH), 138.7 (*C*NH_2), 124.7 (*o*-*C*H), 118.6 (*p*-*C*H), 115.1 (*m*-*C*H), 112.6 (*C*), 52.6 (*C*H_3); ***m/z*** (ES^+): 168.0 $(M+H)^+$ (100%); **RP-HPLC** (λ_{220}): 0.87 min; **R_f** 0.71 (10% MeOH/CH_2Cl_2, Ninhydrin).

4-{(4-hydroxy-3-(methoxycarbonyl)phenyl]amino}-4-oxobutanoic acid (4.21)

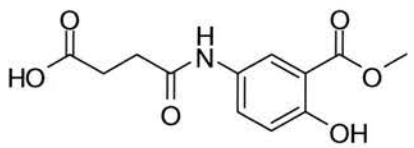

4.20 (0.334 g, 2.00 mmol) in CH_2Cl_2 (2.5 mL) was added to succinic anhydride (0.180 g, 1.80 mmol) in CH_2Cl_2 (2.5 mL). The reaction mixture was irradiated at 100 °C for 10 min and the resulting solid was filtered and re-crystallised in MeOH to give the title compound as a pale-brown solid (0.455 g, 1.70 mmol, 94%). **^{1}H-NMR** (250 MHz, $(CD_3)_2SO$): δ_H 10.24 (s, 1H, *o*-O*H*), 9.94 (s, 1H, C(O)O*H*), 8.14 (d, *J* = 2.8 Hz, 1H, *m*-C*H*), 7.59 (dd, *J* = 9.0, 2.8 Hz, 1H, *p*-CH_3), 6.90 (d, *J* = 9.0 Hz, 1H, *o*-C*H*), 3.67 (s, 3H, CH_3), 2.52-2.48 (m, 4H, HO(O)CCH_2CH_2C(O) and HO(O)CCH_2CH_2C(O)); **^{13}C-NMR** (63 MHz, $CDCl_3$): δ_C 174.2 (*C*(O)OH), 170.2 (*C*(O)OCH_3), 169.5 (NH*C*(O)), 156.2 (*C*OH), 131.6 (*C*NH), 127.5 (*o*-*C*H), 120.2 (*p*-*C*H), 117.9 (*m*-*C*H), 112.7 (*C*C(O)OCH_3), 52.8 (*C*H_3), 31.2 (HO(O)C*C*H_2CH_2C(O)), 29.1 (HO(O)CCH_2CH_2C(O)); ***m/z*** (ES^-): 266.0 $(M-H)^-$ (100%); **HRMS** (ES^+) for $C_{12}H_{14}NO_6$ $(M+H)^+$: calcd 268.0816, found 268.0817 ; **RP-HPLC** (λ_{254}): 2.62 min (100 %) (Method 1).

4-({4-hydroxy-3-[(hydroxyamino)carbonyl]phenyl}amino)-4-oxobutanoic acid (4.22)

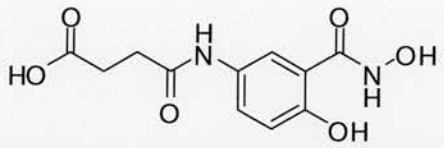

4.21 (0.100 g, 0.375 mmol) in MeOH (9.4 mL) was treated with 50% hydroxylamine/H_2O (5.3 mL) and stirred overnight at rt, after which MeOH was removed *in vacuo* and the remaining aqueous solution was acidified to pH 3-4 with 1 N HCl, followed by extraction with EtOAc (3 x 25 mL). The combined EtOAc extractions were washed with brine (2 x 20 mL), dried over $MgSO_4$ and the solvent removed *in vacuo* followed by purification by Prep HPLC to yield a cream solid (38 mg, 0.142 mmol, 38%). **^{1}H-NMR** (800 MHz, $(CD_3)_2SO$): δ_H 12.22 (br signal, 1H, C(O)N*H*OH), 11.51 (s, 1H, *o*-O*H*), 11.21 (s, 1H, C(O)NHO*H*), 9.91 (s, 1H, C(O)O*H*), 7.94 (d, J = 2.4 Hz, *m*-C*H*), 7.57 (dd, J = 8.8, 2.4 Hz, 1H, *p*-CH_3), 6.93 (d, J = 8.8 Hz, 1H, *o*-C*H*), 2.60-2.59 (m, 4H, HO(O)CCH_2CH_2C(O) and HO(O)CCH_2CH_2C(O)); **^{13}C-NMR** (200 MHz, $(CD_3)_2SO$): δ_C 177.0 (*C*(O)OH), 173.0 (*C*(O)NHOH), 168.4 (HO(O)CCH_2CH_2*C*(O)NH), 156.9 (*C*OH), 133.9 (*C*NH), 128.1 (*o*-*C*H), 122.4 (*p*-*C*H), 120.0 (*m*-*C*H), 118.6 (*C*C(O)NHOH), 33.9 (HO(O)C*C*H_2CH_2C), 31.9 (HO(O)CCH_2*C*H_2C); ***m/z*** (ES^-): 267.0 $(M-H)^-$ (100%); **HRMS** (ES^+) for $C_{11}H_{13}N_2O_6$ $(M+H)^+$: calcd 269.0768, found 269.0768; **RP-HPLC** (λ_{254}): 2.38 min (100 %) (Method 1).

5-({4-[(2,5-dioxopyrrolidin-1-yl)oxy]-4-oxobutanoyl}amino)-*N*,2-dihydroxybenzamide (4.23)

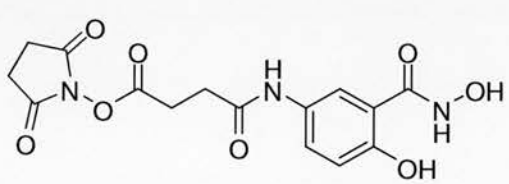

4.22 (0.093 g, 0.347 mmol) and *N*-hydroxysuccinimide (0.060 g, 0.521 mmol) were dissolved in DMF (3.5 mL), followed by addition of EDC (0.080 g, 0.416 mmol).

The mixture was stirred for 24 h at rt. The solvent was evaporated *in vacuo* and the solid was dissolved in EtOAc (10 mL), which was then washed with sat. $NaHCO_3$ (3 x 5 mL), 10% citric acid (3 x 5 mL), brine (2 x 5 mL), dried ($MgSO_4$) and evaporated *in vacuo* to yield a straw-coloured solid (55 mg, 0.151 mmol, 44%). **^{1}H-NMR** (800 MHz, $(CD_3)_2SO$): δ_H 7.38 (d, J = 8.8 Hz, 1H, *o*-C*H*), 7.02 (d, J = 2.4 Hz, 1H, *m*-CH_3), 6.96 (dd, J = 8.8, 2.4 Hz, *p*-CH_3), 2.77 (s, 4H, 2CH_2C(O)NO(O)C), 2.66-2.63 (m, 4H, NO(O)CCH_2CH_2C(O) and NO(O)CCH_2CH_2C(O); **^{13}C-NMR** (200 MHz, $(CD_3)_2SO$): δ_C 180.1 (NO(O)*C*), 177.8 (*C*(O)NO(O)C), 174.4 (*C*(O)NHOH), 165.5 (NO(O)CCH_2CH_2*C*(O), 157.6 (*C*OH), 133.7 (*C*NH), 131.5 (*C*C(O)NHOH), 124.2 (*p*-*C*H), 112.7 (*o*-*C*H), 112.2 (*m*-*C*H), 45.9 (2*C*H_2C(O)NO(O)C), 31.6 (NO(O)CCH_2*C*H_2C); **HRMS** (ES^-) for $C_{15}H_{14}N_3O_8$ $(M-H)^-$: calcd 364.0781, found 364.0781; **R_f** 0.44 (10% MeOH/CH_2Cl_2, $KMnO_4$).

Methyl 2-hydroxy-5-(4-oxobutanamide)benzoate-Leu-Leu-Glu-Try-Leu-Lys-Arg-OH (4.24)

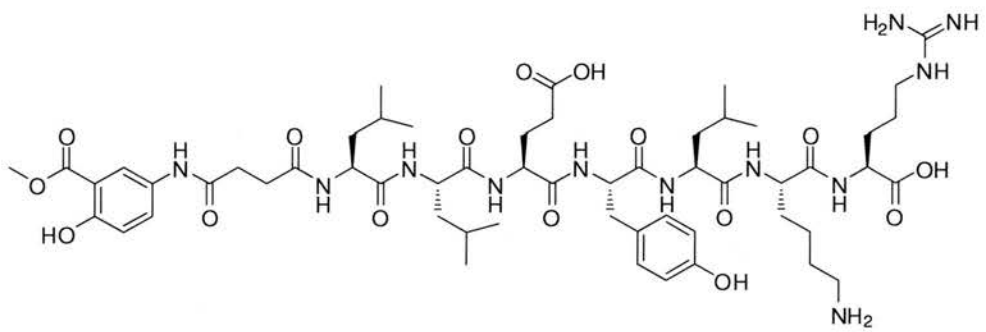

Synthesis of peptide **4.24** was as peptide **4.7** but with additional coupling of **4.21** using *Method B* (Section 5.3.2). Cleavage from resin using *Method D* (Section 5.3.4) resulted in peptide **4.24** as a white solid (227 mg, 96%). **HRMS** (ES^+) for $C_{56}H_{87}N_{12}O_{16}$ $(M+H)^+$: calcd 1183.6358, found 1183.6358; **RP-HPLC** (ELSD): 3.52 min (100 %) (Method 2).

***N*, 2-dihydroxy-5-(4- oxobutanamide)benzoate-Leu-Leu-Glu-Try-Leu-Lys-Arg-OH (4.25)**

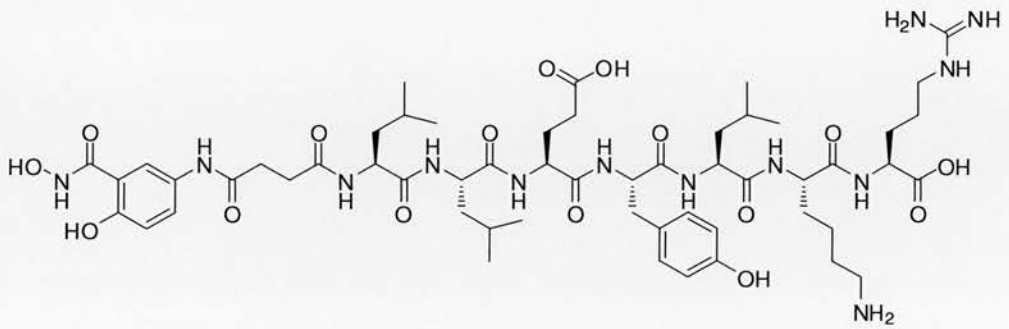

Peptide **4.24** (0.0676 mmol, 80 mg) was treated with 50% NH_2OH/H_2O (1.5 mL) for 24 h. Solvent was removed *in vacuo* and the residue was dissolved in 50% CH_3CN/H_2O and lyophilised to quantitatively yield **4.25** as a white solid. **HRMS** (ES^+) for $C_{55}H_{86}N_{13}O_{16}$ $(M+H)^+$: calcd 1184.6310, found 1184.6310; **RP-HPLC** (ELSD): 3.74 min (100 %) (Method 2).

***tert*-butyl 4 bromobutanoate (4.26)[225]**

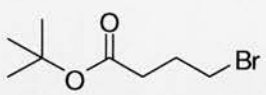

Concentrated sulphuric acid (0.235 mL, 4.41 mmol) was added to a vigorously stirred suspension of anhydrous magnesium sulphate (2.12 g, 17.65 mmol) in CH_2Cl_2 (18 mL). The mixture was stirred for 15 min, after which 4-bromobutyric acid (0.74 g, 4.41 mmol) was added. *tert*-Butanol (2.07 mL, 22 mmol) was added last. The mixture was stoppered tightly and stirred under argon at 25 °C for 48 h. The reaction mixture was quenched with saturated sodium bicarbonate solution (35 mL) and stirred until all magnesium sulphate had dissolved. The organic layer was separated, washed with H_2O, dried ($MgSO_4$) and then evaporated to afford, after purification by column chromatography (silica; MeOH/ CH_2Cl_2), the *tert*-butyl 4-bromobutyrate as a pale-yellow oil (0.41 g, 1.86 mmol, 42%). **IR** (neat) 2973, 2927, 1727 (C=O), 1364, 1156, 842 cm^{-1}; **^{1}H-NMR** (250 MHz, $CDCl_3$): δ_H 3.52 (t, J = 6.8 Hz, 2H, CH_2Br),

2.34 (t, J = 7.2 Hz, 2H, C(O)CH_2), 2.00 (q, J = 6.8 Hz, 2H, $CH_2CH_2CH_2$), 1.40 (s, 9H, $(CH_3)_3C$); **^{13}C-NMR** (63 MHz, $CDCl_3$): δ_C 170.8 (*C*O), 155.2 (*C*OH), 138.7 (*C*NH_2), 124.7 (*o*-*C*H), 118.6 (*p*-*C*H), 115.1 (*m*-*C*H), 112.6 (*C*), 52.6 (CH_3); ***m/z*** (ES^-): 166.9 $(M-H)^-$ (100%).

tert-butyl _N_-benzyl _N_(4-butyryloxy _tert_-butyl)-4-amino butyrate (4.27)

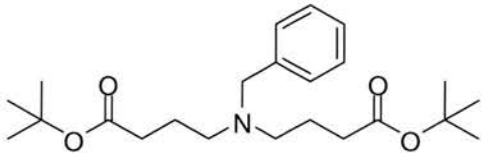

A mixture of *tert*-butyl-4-bromobutyrate (0.81 g, 3.63 mmol, 1.94 eq), benzylamine (0.205 mL, 1.87 mmol) and potassium carbonate (1.5 g, 10.9 mmol, 5.82 eq) in DMF (8.6 mL) was stirred at 40 °C for 20 h. The majority of the DMF was then removed *in vacuo* and the reaction mixture was then diluted with water (15 mL) and extracted with ethyl acetate (3 x 20 mL). The pooled extracts were dried over $MgSO_4$, evaporated and purified by silica gel chromatography with EtOAc in hexane (7:1 v/v) to give the title compound (0.389 g, 0.995 mmol, 53% yield). **^{1}H-NMR** (250 MHz, $CDCl_3$): δ_H 7.36-7.20 (m, 5H, Ar-C*H*), 2.42 (t, J = 7.5 Hz, 4H, (O)$CCH_2CH_2CH_2N$), 2.21 (t, J = 7.5 Hz, 4H, (O)$CCH_2CH_2CH_2N$), 1.79 (dt, J = 7.5 Hz, 4H, (O)C-$H_2CH_2CH_2N$), 1.41 (s, 18H, $C(CH_3)_3$); **^{13}C-NMR** (63 MHz, $CDCl_3$): δ_C 173.5 ($(CH_3)_3CO(O)CCH_2CH_2CH_2N$), 129.2 (*o*-*C*H), 129.1(*o*-*C*H), 129.0 (*m*-*C*H), 127.9 (*m*-*C*H), 127.2 (*p*-*C*H), 80.4 ($(CH_3)_3CO(O)CCH_2CH_2CH_2N$), 58.9 ($NCH_2C$), 53.1 ($CCH_2CH_2CH_2N$), 33.6 ($CCH_2CH_2CH_2N$), 28.5 ($CH_3$), 25.0 ($CCH_2CH_2CH_2N$), 22.8 ($CCH_2CH_2CH_2N$); ***m/z*** ($ES^+$): 392.2 $(M+H)^+$ (100%); **HRMS** (ES^+) for $C_{23}H_{38}NO_4$ $(M+H)^+$: calcd 392.2795, found 392.2798; **RP-HPLC** (λ_{280}): 3.23 min (100 %) (Method 2).

***tert*-butyl *N*(4-{(4-hydroxy-3-(methoxycarbonyl)phenyl]amino}-4-oxobutanoic acid) *N*(4-butyryloxy *tert*-butyl)-4-amino butyrate (4.29)**

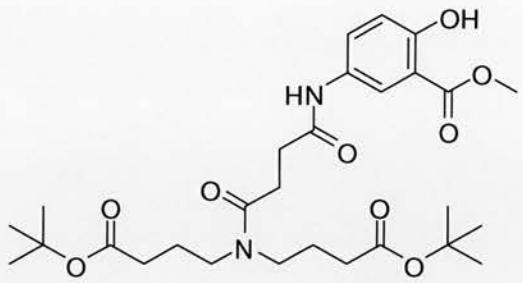

4.27 (0.582 g, 1.49 mmol) was dissolved in MeOH (15 mL) followed by the introduction of 10% Pd/C (48 mg) and a H_2 balloon. The reaction was stirred for 24 h at rt, after which the Pd was removed by filtration over celite, and the MeOH was removed *in vacuo*. The crude residue was re-dissolved in DMF (15 mL) and treated with **4.21** (0.479 g, 1.79 mmol), EDC (0.372 g, 1.94 mmol) and HOBt (0.275 g, 1.79 mmol) and stirred overnight at rt. The DMF was evaporated *in vacuo* and the resulting residue was dissolved in saturated $NaHCO_3$ solution (20 mL) and extracted with EtOAc (3 x 15 mL). The organic layer was washed with $KHSO_4$ (20 mL) and brine (20 mL) and dried over $MgSO_4$ followed by evaporation *in vacuo*. The resulting dark yellow oil was purified by silica gel chromatography eluted with 1-5 % MeOH/CH_2Cl_2 to yield yellow oil (178 mg, 0.324 mmol, 22%). **^{1}H-NMR** (250 MHz, $CDCl_3$): δ_H 10.57 (s, 1H, ArO*H*), 8.66 (s, 1H, N*H*), 8.06 (d, J = 2.8 Hz, 1H, Ar*H*-2), 7.49 (dd, J = 9.0, 2.8 Hz, 1H, Ar*H*-4), 6.89 (d, J = 9 Hz, 1H, Ar*H*-5), 3.92 (s, 3H, $COOCH_3$), 3.41-3.27 (m, 4H, (O)C$CH_2$$CH_2$$CH_2$N and N$CH_2$$CH_2$$CH_2$C(O)), 2.80-2.65 (m, 4H, (O)CCH_2CH$_2$CH$_2$N and NCH$_2$CH_2CH$_2$C(O)), 2.26-2.17 (m, 4H, (O)CCH_2CH$_2$C(O) and (O)CCH$_2$CH_2C(O)), 1.92-1.73 (m, 4H, (O)CCH$_2$CH$_2$CH_2N and NCH_2CH$_2$CH$_2$C(O)), 1.68 (s, 9H, C(CH_3)$_3$); **^{13}C-NMR** (63 MHz, $CDCl_3$): δ_C 172.7 (N*C*(O)CH$_2$CH$_2$C(O)NH), 172.5 ((CH$_3$)$_3$CO(O)*C*CH$_2$CH$_2$CH$_2$N), 172.2 (NCH$_2$CH$_2$CH$_2$*C*(O)OC(CH$_3$)$_3$), 171.2 (C*C*(O)OCH$_3$), 170.8 (NC(O)CH$_2$CH$_2$*C*(O)NH), 158.4 (*o*-*C*OH), 130.6 (*m*-*C*NH), 128.7 (*p*-*C*H), 121.3 (*o*-*C*H), 118.0 (*m*-*C*H), 112.3 (*C*C(O)OCH$_3$), 81.3 ((CH$_3$)$_3$*C*O(O)C), 80.8 (C(O)O*C*(CH$_3$)$_3$), 52.7 (CC(O)O*C*H$_3$), 47.6 (N*C*H$_2$CH$_2$CH$_2$C(O)OC(CH$_3$)$_3$), 45.8 ((CH$_3$)$_3$CO(O)CCH$_2$CH$_2$*C*H$_2$N), 33.1 ((CH$_3$)$_3$CO(O)C*C*H$_2$CH$_2$CH$_2$N and (NCH$_2$CH$_2$*C*H$_2$C(O)OC(CH$_3$)$_3$), 33.0 (NC(O)CH$_2$*C*H$_2$C(O)NH), 32.6

(NC(O)CH_2CH_2C(O)NH), 28.5 ((CH_3)$_3$CO(O)C and C(O)OC(CH_3)$_3$), 24.3 ((CH_3)$_3$CO(O)C$CH_2CH_2CH_2$N), 23.5 (N$CH_2CH_2CH_2$C(O)OC(CH_3)$_3$); ***m/z*** (ES^+): 551.2 $(M+H)^+$, 573.1 $(M+Na)^+$; **HRMS** (ES^+) for $C_{28}H_{43}N_2O_9$ $(M+H)^+$: calcd 551.29631, found 551.29688; **RP-HPLC** (λ_{280}): 3.12 min (100 %) (Method 2).

4,4'-(4-(4-hydroxy-3-(methoxycarbanoyl)phenylamino)-4-oxobutanoylazanediyl)dibutanoic acid (4.30)

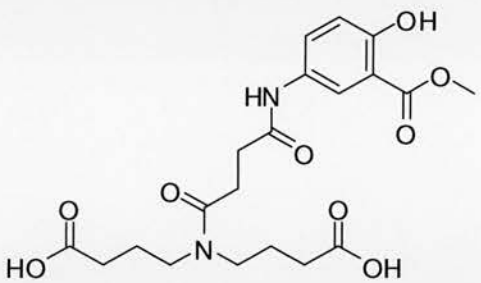

4.29 (0.178 g, 0.324 mmol) was treated with a cocktail of TFA/CH_2Cl_2/TIS/H_2O (47.5:47.5:2.5:2.5) (2 mL) and stirred for 2 h at rt. The cleavage cocktail was removed *in vacuo* and the resulting residue was re-dissolved in 30% acetonitrile/70% H_2O (10 mL) and freeze-dried prior to purification by Prep-HPLC to yield a colourless oil (68 mg, 0.155 mmol, 48%). **^{1}H-NMR** (800 MHz, CD_3OD): δ_H 7.90 (d, *J* = 2.8 Hz, 1H, Ar*H*-2), 7.54 (dd, *J* = 8.9, 2.8 Hz, 1H, Ar*H*-4), 7.13 (d, *J* = 8.9 Hz, 1H, Ar*H*-5), 4.00 (s, 3H, C(O)OCH_3), 3.41-3.35 (m, 4H, CH_2N and NCH_2), 2.69 (t, *J* = 7.91 Hz, 2H, (O)CC$H_2$$CH_2$C(O)), 2.62 (t, *J* = 6.9 Hz, 2H, (O)CCH_2CH_2C(O)), 2.41 (t, *J* = 7.0 Hz, 2H, HO(O)CCH_2), 2.31 (t, *J* = 7.0 Hz, 2H, CH_2C(O)OH), 1.92 (dt, *J* = 14.9, 7.1 Hz, 2H, HO(O)C$CH_2CH_2CH_2$N), 1.82 (dt, *J* = 14.6, 7.3 Hz, 2H, N$CH_2CH_2$$CH_2$C(O)OH); **^{13}C-NMR** (200 MHz, CD_3OD): δ_C 176.6 (*C*(O)OH), 176.4 (HO(O)*C*), 175.2 (N*C*(O)), 174.5 (C*C*(O)OCH$_3$), 171.7 (*C*(O)N-Ar), 163.9 (*o*-COH), 132.6 (*m*-*C*NH), 126.9 (*p*-*C*H), 124.5 (*o*-*C*H), 121.8 (*m*-*C*H), 115.8 (*C*C(O)OCH$_3$), 54.7 (CC(O)O*C*H$_3$), 49.4 (N$CH_2CH_2CH_2$C(O)OH), 47.5 (HO(O)C$CH_2CH_2$$CH_2$N), 33.2 (HO(O)C$CH_2CH_2CH_2$N), 32.7 (N$CH_2CH_2$$CH_2$C(O)OH), 31.4 (NC(O)$CH_2$$CH_2$C(O)NH), 30.1 (NC(O)$CH_2CH_2$C(O)NH), 26.0 (HO(O)C$CH_2$$CH_2CH_2$N), 25.2 (N$CH_2$$CH_2CH_2$C(O)OH); ***m/z*** ($ES^+$): 438.0 $(M+H)^+$ (100%); **HRMS** (ES^+) for

$C_{20}H_{27}N_2O_9$ $(M+H)^+$: calcd 439.17111, found 439.17105; **RP-HPLC** (λ_{254}): 3.5 min (100 %) (Method 1).

Methyl 5-({4-[(2,5-dioxopyrrolidin-1-yl)oxy]-4-oxobutanoyl}amino)-2-hydroxybenzoate (4.35)

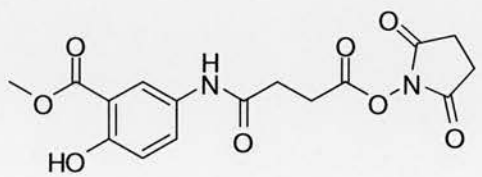

4.21 (0.500 g, 1.87 mmol) and *N*-hydroxysuccinimide (0.323 g, 2.81 mmol) were dissolved in CH_3CN (19 mL), followed by addition of EDC (0.431 g, 2.25 mmol). The mixture was stirred for 24 h at rt. The solvent was evaporated *in vacuo* and the solid was dissolved in EtOAc (10 mL), which was then washed with sat. $NaHCO_3$ (3 x 5 mL), 10% citric acid (3 x 5 mL), brine (2 x 5 mL), dried ($MgSO_4$) and evaporated *in vacuo* to yield a white solid (0.540 g, 1.48 mmol, 79%). **^{1}H-NMR** (800 MHz, $(CD_3)_2SO$): δ_H 7.38 (d, J = 8.8 Hz, 1H, *o*-C*H*), 7.02 (d, J = 2.4 Hz, 1H, *m*-CH_3), 6.96 (dd, J = 8.8, 2.4 Hz, *p*-CH_3), 2.77 (s, 4H, 2CH_2C(O)NO(O)C), 2.66-2.63 (m, 4H, NO(O)CCH_2CH_2C(O) and NO(O)CCH_2CH_2C(O); **^{13}C-NMR** (200 MHz, $(CD_3)_2SO$): δ_C 180.1 (NO(O)*C*), 177.8 (*C*(O)NO(O)C), 174.4 (*C*(O)NHOH), 165.5 (NO(O)CCH_2CH_2*C*(O), 157.6 (*C*OH), 133.7 (*C*NH), 131.5 (*C*C(O)NHOH), 124.2 (*p*-*C*H), 112.7 (*o*-*C*H), 112.2 (*m*-*C*H), 45.9 (2*C*H_2C(O)NO(O)C), 31.6 (NO(O)CCH_2*C*H_2C); ***m/z*** (ES^-): 365.0 $(M+H)^+$, 387.0 $(M+Na)^+$ (100%), 751.1 $(2M+Na)^+$; **HRMS** (ES^-) for $C_{16}H_{15}N_2O_8$ $(M-H)^-$: calcd 363.0828, found 363.0830; **R_f** 0.54 (10% $MeOH/CH_2Cl_2$, $KMnO_4$).

Methyl 2,4-dihydroxybenzoate (4.36)

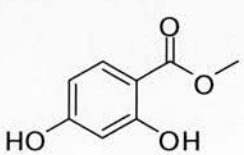

2,4-dihydroxybenozic acid (10.0 g, 0.065 mol) in MeOH (75 mL) was treated with conc. H_2SO_4 (2.5 mL) and refluxed at 70 °C for 66 h. The reaction was cooled to rt, neutralised by adding $NaHCO_3$ powder and evaporated *in vacuo*. H_2O (250 mL) was added and extracted into CH_2Cl_2 (300 mL). The CH_2Cl_2 layer was washed with brine (250 mL), dried ($MgSO_4$) and evaporated *in vacuo* to yield an off-white powder (10.5 g, 0.062 mol, 96%) **mp** 113-114 °C (aq MeOH), *lit.*[226]116-117 °C (benzene), **IR** (neat) 3331 (m), 3176 (m), 1741 (w), 1637 (s), 1615 (s), 1434 (s), 1145 (s), 1095 (s) cm^{-1}; **^{1}H-NMR** (250 MHz, CD_3CN): δ_H 10.86 (s, 1H, *o*-O*H*), 7.69 (d, J = 8.7 Hz, 1H, *o*-C*H*), 6.40-6.33 (m, 2H, *m*-C*H*), 3.86 (s, 3H, CH_3); **^{13}C-NMR** (63 MHz, CD_3CN): δ_C 170.0 (*C*=O), 163.2 (*C*OH), 131.4 (*o*-*C*H), 107.0 (*m*-*C*H), 104.7 (*C*), 102.2 (*m*-*C*H), 51.4 (*C*H_3); ***m/z*** (ES$^-$): 166.9 (M-H)$^-$; **R_f** 0.62 (10% MeOH/CH_2Cl_2, $KMnO_4$).

Methyl 4-(2-tert-butoxy-2-oxoethoxy)-2-hydroxybenzoate (4.37)

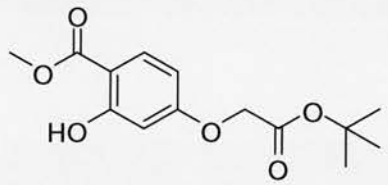

In a method adapted from Astles *et al.*,[219] phenol **4.32** (1.00 g, 5.95 mmol) dissolved in acetone (7 mL), treated with KI (0.51 g, 3.07 mmol), Bu_4NCl (11 mg, 38 μmol), K_2CO_3 (0.94 g, 6.83 mmol) and *tert*-butyl bromoacetate (0.870 mL, 5.88 mmol), was irradiated at 90 °C in a microwave for 75 min. The mixture was filtered and the filtrate evaporated *in vacuo*. The residue was purified by column chromatography eluted with 1% MeOH/CH_2Cl_2 to give a white powder (1.25 g, 4.42 mmol, 74% yield). **mp** 73 °C; **^{1}H-NMR** (250 MHz, $CDCl_3$): δ_H 11.20 (s, 1H, O*H*), 7.96 (d, J = 7.5 Hz, 1H, *o*-C*H*), 6.70-6.51 (m, 2H, 2 x *m*-C*H*), 4.74 (s, 2H, OCH_2C(O)O), 4.03 (s, 3H, C(O)OCH_3), 1.70 (s, 9H, C(O)OC(CH_3)$_3$); **^{13}C-NMR** (63 MHz, $CDCl_3$): δ_C 170.7 (*C*(O)OCH$_3$), 167.6 (*C*OH), 164.0 (*C*(O)OC(CH$_3$)$_3$), 131.8 (*o*-*C*H), 108.1 (*m*-*C*H), 106.6 (*C*C(O)OCH$_3$), 101.9 (*m*-*C*H), 83.2 (*C*(CH$_3$)$_3$), 65.8 (*C*H$_2$), 52.4 (C(O)O*C*H$_3$), 28.4 (C(O)OC(*C*H$_3$)$_3$); ***m/z*** (ES$^+$): 283.0 (M+H)$^+$ (100%), 587.1 (2M+Na)$^+$; **HRMS** (ES$^+$) for $C_{14}H_{19}O_6$ (M+H)$^+$: calcd 283.1176, found 283.1178;

RP-HPLC (λ_{282}) t_R 4.30 min (100 %) **ELSD** t_R 4.38 min (100 %) (Method 2); $\mathbf{R_f}$ 0.82 (10% $MeOH/CH_2Cl_2$, $KMnO_4$).

[3-hydroxy-4-(methoxycarbonyl)phenoxy]acetic acid (4.38)

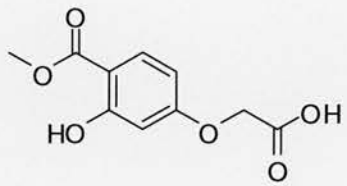

4.33 (0.500 g, 1.77 mmol) was treated with a cocktail of $TFA/CH_2Cl_2/TIS/H_2O$ (47.5:47.5:2.5:2.5) (10 mL) and stirred for 1 h at rt. The cleavage cocktail was removed *in vacuo* and the resulting residue was re-dissolved in 30% acetonitrile/70% H_2O (10 mL) and freeze-dried to yield a fluffy white lyophilisate (0.356 g, 1.58 mmol, 89%). **^{1}H-NMR** (500 MHz, CD_3OD): δ_H 7.78 (d, J = 9 Hz, 1H, *o*-C*H*), 6.53 (dd, J = 2.5 Hz, 9 Hz, 1H, *m*-C*H*), 6.45 (d, J = 2.5 Hz, 1 H, *m*-C*H*), 4.71 (s, 2H, $OCH_2C(O)O$), 3.91 (s, 3H, $C(O)OCH_3$); **^{13}C-NMR** (125 MHz, CD_3OD): δ_C 171.9 ($C(O)OCH_3$), 171.6 (*C*OH), 165.4 (*C*(O)OH), 164.8 (CH_2OC), 132.6 (*o*-*C*H), 108.5 (*m*-*C*H), 107.3 ($CC(O)OCH_3$), 102.7 (*m*-*C*H), 65.8 (CH_2), 52.6 ($C(O)OCH_3$); ***m/z*** (ES^-): 225.0 $(M-H)^-$; **HRMS** (ES^+) for $C_{10}H_{11}O_6$ $(M+H)^+$: calcd 227.0550, found 227.0547; **RP-HPLC** (λ_{282}) t_R 3.69 min (100 %) **ELSD** t_R 3.77 min (100 %) (Method 2).

2-[(Dibenzylamino)ethoxy]ethanol (4.40)

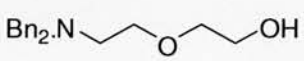

Using a procedure by Visintin *et al.*,[222] a mixture of 2-(aminoethoxy)ethanol (5.00 g, 47.5 mmol), potassium carbonate (16.4 g, 119 mmol) and benzyl bromide (11.3 mL, 95 mmol) in acetonitrile (250 mL) was stirred at 50 °C for 20 h. The solid was filtered and the solvent was evaporated from the filtrate *in vacuo*. The residue was dissolved in HCl (0.1 M) and washed with EtOAc (2 x 50 mL). The aqueous layer was then made basic with NaOH (1 M) and extracted with CH_2Cl_2 (4 x 50 mL). The solvent was dried ($MgSO_4$) and removed *in vacuo*, to give the product, which was

used in the next reaction without further purification (11.53 g, 40.4 mmol, 85%). **^{1}H-NMR** (250 MHz, $CDCl_3$): δ_H 7.40-7.20 (m, 10H, Ph-*H*), 3.70-3.60 (m, 6H, PhCH_2 and NCH_2), 3.57 (t, *J* = 7.5 Hz, 2H, NCH_2CH_2O), 3.46 (t, *J* = 7.5 Hz, 2H, OCH_2CH_2OH), 2.69 (t, *J* = 10 Hz, 2H, OCH_2CH_2OH); **^{13}C-NMR** (63 MHz, $CDCl_3$): δ_C 139.8 (Ph-C), 129.3 (Ph-CH), 128.7 (Ph-CH), 127.4 (4-Ph-*C*H), 72.5 (OCH_2CH_2OH), 70.0 (NCH_2CH_2O), 62.3 (OCH_2CH_2OH), 59.4 (PhCH_2), 53.4 (NCH_2CH_2O); ***m/z*** (ES^+): 286.1 $(M+H)^+$ (100%); **RP-HPLC** (ELSD): 2.78 min (100 %) (Method 2).

2-[(Dibenzylaminoethoxy)ethoxy]acetic acid (4.41)

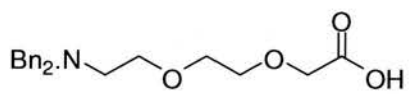

Using a procedure by Visintin *et al.*,[222] **4.40** (11.53 g, 40.5 mmol) was dissolved in dry THF (90 mL) and cooled at 0 °C, then NaH (5.44 g, 162 mmol; 60% dispersion in oil) was added in portions followed by α bromo acetic acid (8.46 g, 61 mmol). The suspension was refluxed overnight under nitrogen. Water (3.5 mL) was added carefully and then stirred for 5 minutes, then more water (100 mL) was added and the aqueous layer washed with a mixture of hexane/Et_2O 1:1 (2 x 50 mL). The aqueous solution was acidified to pH 2-3 with HCl (1 M) and washed with Et_2O (3 x 50 mL), then neutralised to pH 6/7 with NaOH (1 M). Solid sodium chloride was added and the mixture was extracted with CH_2Cl_2 (5 x 75 mL). The solvent was dried ($MgSO_4$) and removed *in vacuo*. The crude product was used in the next reaction without further purification (11.17 g, 32.6 mmol, 80%). **^{1}H-NMR** (250 MHz, $CDCl_3$): δ_H 7.44-7.10 (m, 10H), 3.88 (s, 2H), 3.68 (s, 4H), 3.61-3.34 (m, 4H); **^{13}C-NMR** (63 MHz, $CDCl_3$): δ_C 137.53, 129.84, 128.78, 127.93, 71.39, 70.33, 69.69, 69.34, 59.14, 52.63; ***m/z*** (ES^-): 342.1 $(M-H)^-$ (100%); **RP-HPLC** (ELSD): 3.02 min (100 %) (Method 2).

[2-(2-Aminoethoxy)ethoxy]acetic acid (4.42)

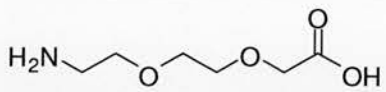

Using a procedure by Visintin *et al.*,[222] **4.41** (11.17 g, 32.6 mmol) was dissolved in MeOH (150 mL) and palladium (2.79 g, 10% on carbon) was added. The mixture was stirred under a hydrogen atmosphere (760 mm Hg) at rt for 24 h. The catalyst was removed by filtration through celite and the solvent removed *in vacuo*. The residue was triturated with diethyl ether (100 mL) to give the title compound **4.42** (5.22 g, 32 mmol, 98%). **^{1}H-NMR** (250 MHz, CD_3OD): δ_H 3.98 (s, 2H, $CH_2C(O)OH$), 3.89-3.72 (m, 6H, H_2NCH_2CH2 and OCH_2CH_2 and OCH_2CH_2), 3.22-3.19 (m, 2H, NCH_2CH_2O); **^{13}C-NMR** (63 MHz, CD_3OD): δ_C 173.66, 72.07, 71.69, 71.53, 68.36, 40.85; ***m/z*** (ES^+): 164.1 $(M+H)^+$; **RP-HPLC** (ELSD): 0.87 min (100 %) (Method 2).

{2-[9H-Fluoren-9-ylmethoxycarbonylamino)-methoxy]-ethoxy}-acetic acid (4.43)

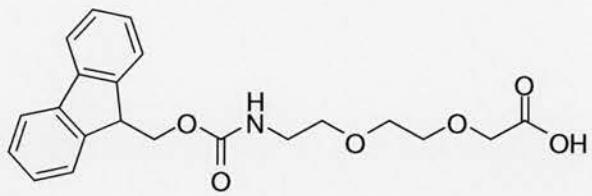

Using a procedure by Visintin *et al.*,[222] crude [2-(2-Aminoethoxy)ethoxy]acetic acid **4.42** (5.10 g, 31.3 mmol) was suspended in H_2O (50 mL) and K_2CO_3 (8.65 g, 62.6 mmol) and stirred at rt for 10 minutes. *N*-(9-fluorenylmethoxycarbonyl) succinimide (10.55 g, 31.3 mmol) was added to the mixture and stirred for 16 h. The reaction mixture was then washed with diethyl ether (2 x 30 mL). The aqueous solution was acidified to pH 1-2 with HCl, concentrated and extracted with CH_2Cl_2 (5 x 30 mL). The solvent was dried ($MgSO_4$) and removed *in vacuo*. The obtained product was crystallised from acetonitrile to give the title compound **4.43** (5.76 g, 15.0 mmol, 43%). **^{1}H-NMR** (250 MHz, $CDCl_3$): δ_H 7.89 (d, J = 7.0 Hz, 2H), 7.79-7.68 (m, 2H), 7.55-7.39 (m, 4H), 4.50 (d, J = 7.5 Hz, 2H), 4.37-4.31 (m, 1H), 4.31 (s, 2H), 3.86-3.84 (m, 2H), 3.79-3.77 (m, 2H), 3.73-3.69 (m, 2H), 3.59-3.50 (m, 2H); **^{13}C-NMR**

(90 MHz, $CDCl_3$): δ_C 173.2 (*C*), 156.5 (*C*), 143.8 (*C*), 141.1 (*C*), 127.5 (*C*H), 126.9 (*C*H), 125.0 (*C*H), 119.8 (*C*H), 71.0 (CH_2), 70.1 (CH_2), 69.9 (CH_2), 68.3 (CH_2), 66.6 (CH_2), 47.0 (*C*H), 40.6 (CH_2); ***m/z*** (ES^+): 386.0 $(M+H)^+$, 408.0 $(M+Na)^+$; **RP-HPLC** (ELSD): 4.28 min (100 %) (Method 2).

Methyl 4-(2-[(2,5-dioxopyrrolidin-1-yl)oxy]-2-oxoethoxy)-2-hydroxybenzoate (4.44)

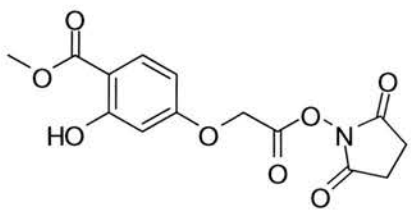

4.34 (0.150 g, 0.663 mmol) and *N*-hydroxysuccinimide (0.115 g, 0.995 mmol) were dissolved in CH_3CN (7 mL), followed by addition of EDC.HCl (0.153 g, 0.995 mmol). The mixture was stirred for 24 hours at room temperature. The solvent was evaporated *in vacuo* and the residue was dissolved in EtOAc (30 mL), which was then washed with sat. $NaHCO_3$ (3 x 15 mL), 10% citric acid (3 x 15 mL), brine (2 x 15 mL), dried ($MgSO_4$) and evaporated *in vacuo* to yield an off-white solid (0.187 g, 0.579 mmol, 87%). **^{1}H-NMR** (250 MHz, $(CD_3)_2SO$): δ_H 10.50 (s, 1H, O*H*), 7.87-7.66 (m, 1H, *o*-C*H*), 6.70-6.52 (m, 2H, 2 x *m*-C*H*), 5.35 (s, 2H, $OCH_2C(O)O$), 3.80 (s, 3H, $C(O)OCH_3$), 2.76 (s, 4H, $2CH_2$); **^{13}C-NMR** (63 MHz, $(CD_3)_2SO$): δ_C 170.3 ($C(O)OCH_3$), 169.5 (*C*(O)ON), 165.4 (N*C*(O)), 163.0 (*C*OH), 162.7 (Ar-OCH_2), 131.9 (*o*-*C*H), 108.0 (*m*-*C*H), 106.9 (164.0 ($C(O)OC(CH_3)_3$), 131.8 (*o*-*C*H), 108.0 (*m*-*C*H), 106.9 (*C*C(O)OCH_3), 102.4 (*m*-*C*H), 63.2 (CH_2), ($C(CH_3)_3$), 52.7 ($C(O)OCH_3$), 25.8 ($2CH_2$); $\mathbf{R_f}$ 0.71 (10% $MeOH/CH_2Cl_2$, $KMnO_4$).

Tert-butyl 13-(4-_tert_-butoxy-4-oxobutyl)-1-(9_H_-fluoren-9-yl)-3, 12-dioxo-2,7,10-trioxa-4, 13-diazaheptadecan-17-oate (4.45)

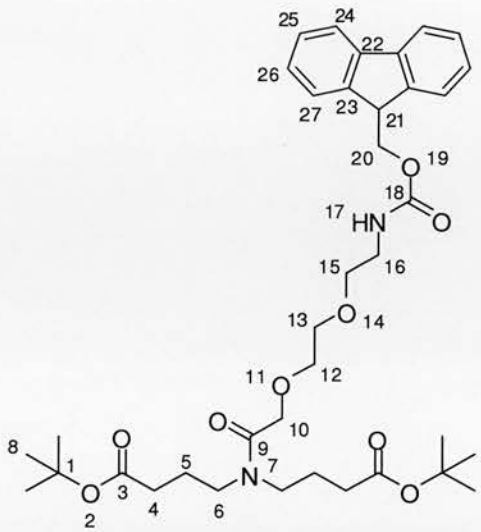

4.27 (83 mg, 0.272 mmol) was dissolved in EtOH (10 mL) followed by the introduction of 10% Pd/C (15 mg) and a H_2 balloon. The reaction was stirred for 24 h at rt, after which the Pd was removed by filtration over celite, and the MeOH was removed *in vacuo*. The crude residue was re-dissolved in DMF (1.5 mL) and treated with **4.43** (100 mg, 0.259 mmol) and HBTU (134 mg, 0.354 mmol) in DMF (1 mL), followed by addition of DIPEA (0.180 mL, 1.03 mmol) and stirred overnight at rt. The DMF was evaporated *in vacuo* and the residue re-dissolved in EtOAc (10 mL) and washed with H_2O (2 x 10 mL) and brine (10 mL). The EtOAc was then dried over $MgSO_4$ and removed *in vacuo*. The resulting residue was purified by silica gel chromatography eluted with 1-10 % MeOH/CH_2Cl_2 to yield colourless oil (116 mg, 0.173 mmol, 67%). **^{1}H-NMR** (250 MHz, $CDCl_3$): δ_H 7.60 (d, J = 7.5 Hz, 2H, Fmoc-*H*-24), 7.45 (d, J = 7.5 Hz, 2H, Fmoc-*H*-27), 7.24-7.10 (m, 4H, Fmoc-*H*), 4.21 (d, J = 7.5 Hz, 2H, C*H*$_2$-20), 4.10-4.08 (m, 3H, NC(O)C*H*$_2$O and *H*-21), 3.54-3.44 (m, 4H, OC*H*$_2$CH$_2$O and OCH$_2$C*H*$_2$O), 3.26-3.05 (m, 6H, O(O)CCH$_2$CH$_2$C*H*$_2$N and OC*H*$_2$CH$_2$NH and OCH$_2$C*H*$_2$NH), 2.09-2.02 (m, 4H, O(O)CC*H*$_2$CH$_2$CH$_2$N), 1.68-1.63 (m, 4H, O(O)CCH$_2$C*H*$_2$CH$_2$N), 6.70-6.52 (m, 2H, 2 x *m*-C*H*), 5.35 (s, 2H, OC*H*$_2$C(O)O), 3.80 (s, 3H, C(O)OC*H*$_3$), 1.29 (s, 9H (C*H*$_3$)$_3$CO(O)C), 1.27 (s, 9H, (C*H*$_3$)$_3$CO(O)C); **^{13}C-NMR** (63 MHz, $CDCl_3$): δ_C 172.6 (C-3), 172.1 (C-9), 155.4 (C-18), 148.7 (C-23), 127.2 (C-25), 126.2 (C-26), 124.1 (C-27), 120.0 (C-24), 79.2 (C-1), 72.6 (C-15), 69.7 (C-13), 67.9 (C-12), 66.4 (C-10), 47.1 (C-21), 46.4 (C-6),

37.9 (C-16), 33.1 (C-4), 27.7 (C-8), 23.6 (C-5); ***m/z*** (ES^+): 669.3 $(M+H)^+$; **HRMS** (ES^+) for $C_{37}H_{53}N_2O_9$ $(M+H)^+$: calcd 669.3746, found 669.3749; **RP-HPLC** (ELSD) t_R 4.83 min (100 %) (Method 2); $\mathbf{R_f}$ 0.47 (5% $MeOH/CH_2Cl_2$, $KMnO_4$).

***Tert*-butyl 12-(4-*tert*-butoxy-4-oxobutyl)-1-(4-hydroxy-3-(methoxycarbonyl)phenoxy)-2,11-dioxo-6,9-dioxa-3,12-diazapentadecane-15-carboxylate (4.47)**

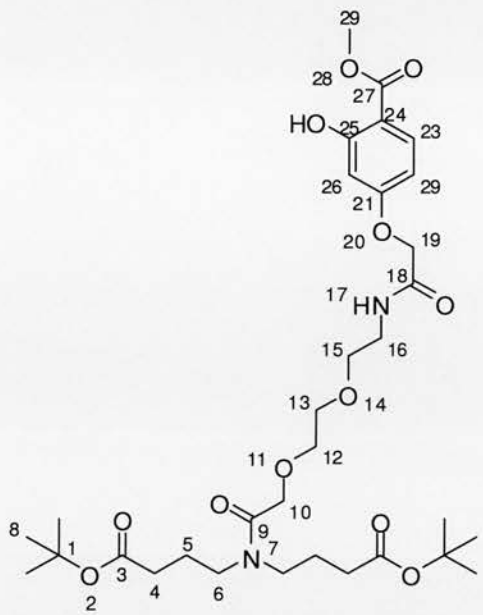

4.45 (115 mg, 0.172 mmol) was treated with 20% piperidine in DMF for 40 min at rt, after which the solvent removed *in vacuo*. The crude residue was re-dissolved in DMF (1.4 mL) along with **4.38** (37 mg, 0.163 mmol) and HBTU (85 mg, 0.224 mmol) followed by addition of DIPEA (0.113 mL, 0.648 mmol). The reaction mixture was stirred for 2 hours at rt, after which the solvent was removed *in vacuo*. The residue was re-dissolved in EtOAc (5 mL), which was washed with H_2O (2 x 5 mL) and brine (5 mL), dried over $MgSO_4$ and the solvent removed *in vacuo* before being purified by silica gel chromatography eluted with 1-10 % $MeOH/CH_2Cl_2$ to give the title compound **4.47** (92 mg, 0.141 mmol, 86%). **^{1}H-NMR** (250 MHz, $CDCl_3$): δ_H 11.80 (s, 1H, O*H*-25), 8.50 (s, 1H, N*H*-17), 7.98-7.91 (m, 1H, *H*-23), 6.73-6.62 (m, 2H, *H*-26 and *H*-29), 4.72-4.63 (m, 4H, 10-CH_2 and 19-CH_2), 4.12 (s, 3H, 29-CH_3), 4.02-3.80 (m, 4H, 12-CH_2 and 13-CH_2), 3.69 (t, J = 5.5 Hz, 2H, 16-CH_2), 3.57-3.20 (m, 6H, 15-CH_2 and 2 x 6-CH_2), 2.47-2.41 (m, 4H, 2 x 4-CH_2), 2.02-1.91 (m, 4H, 2 x 5-CH_2), 1.65 and 1.64 (2 x s, 2 x 9H, 2 x (8-CH_3)$_3$); **^{13}C-NMR** (63

MHz, $CDCl_3$): δ_C 172.6 (C-18), 172.3 (C-3), 170.6 (C-9), 163.7 (C-27), 163.1 (C-21), 161.3 (C-25), 132.1 (C-23), 107.7 (C-29), 107.0 (C-24), 102.4 (C-26), 81.2 (C-1), 70.4 (C-15), 69.5 (C-19), 68.0 (C-13), 67.5 (C-12), 65.0 (C-10), 52.5 (C-29), 47.3 (C-6), 46.7 (C-6), 41.0 (C-16), 32.8 (C-4), 32.1 (C-4), 28.4 (C-8), 26.9 (C-5), 25.5 (C-5); ***m/z*** (ES^+): 655.2 $(M+H)^+$ (100%), 677.2 $(M+Na)^+$; **HRMS** (ES^+) for $C_{32}H_{51}N_2O_{12}$ $(M+H)^+$: calcd 655.3437, found 655.3437; **RP-HPLC** (ELSD) t_R 4.58 min (100 %) (Method 2); $\mathbf{R_f}$ 0.38 (5% $MeOH/CH_2Cl_2$, $KMnO_4$).

12-(3-carboxypropyl)-1-(4-hydroxy-3-(methoxycarbonyl)phenoxy)-2,11-dioxo-6,9-dioxa-3,12-diazahexadecan-16-oic acid (4.48)

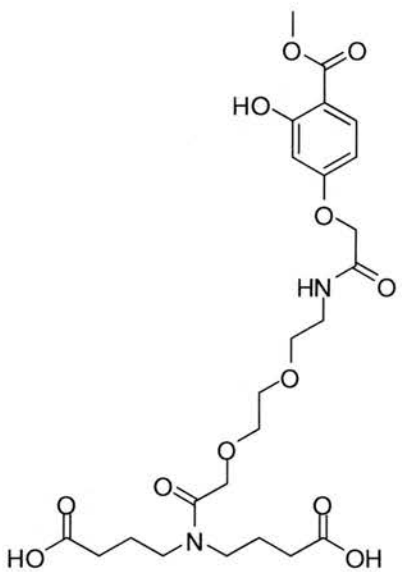

4.47 (45 mg, 68.7 μmol) was treated with a cocktail of $TFA/CH_2Cl_2/TIS/H_2O$ (47.5:47.5:2.5:2.5) (1 mL) and stirred for 1 h at rt. The cleavage cocktail was removed *in vacuo* and the resulting residue was re-dissolved in 30% acetonitrile/70% H_2O (10 mL) and freeze-dried prior to purification by Prep-HPLC to yield a white lyophilisate (11.6 mg, 21.2 μmol, 31%). **^{1}H-NMR** (250 MHz, CD_3OD): δ_H 7.70 (d, *J* = 7.5 Hz, 1H, *o*-C*H*), 6.51-6.42 (m, 2H, *m*-C*H*), 4.49 (s, 2H, NHC(O)CH_2O-Ar), 4.18 (s, 2H, NC(O)CH_2), 3.83 (s, 3H, C(O)OCH_3), 3.56-3.26 (m, 12H, OCH_2CH_2O and OCH_2CH_2O and OCH_2CH_2NH and OCH_2CH_2NH and $HO(O)CCH_2CH_2CH_2N$), 2.24-2.17 (m, 4H, $HO(O)CCH_2$), 1.79-1.71 (m, 4H, $HO(O)CCH_2CH_2CH_2N$); **^{13}C-NMR** (90 MHz, CD_3OD): δ_C 174.9 (C(O)OH), 174.5 (N*C*(O)CH_2O-Ar), 169.7 (N*C*(O)CH_2O), 168.6 (*C*(O)OCH_3), 163.1 (*C*OH), 130.8 (*o*-*C*H), 106.7 ($CH_3O(O)C$-

Ar), 105.6 (*m*-*C*H), 101.1 (*m*-*C*H), 69.8 (O*C*H_2CH_2NH), 69.3 (NHC(O)*C*H_2O-Ar), 68.5 (OCH_2*C*H_2O), 68.4 (O*C*H_2CH_2O), 66.2 (NC(O)*C*H_2O), 50.8 (C(O)O*C*H_3), 45.3 (HO(O)CCH$_2$CH$_2$*C*H_2N), 44.2 (HO(O)CCH$_2$CH$_2$*C*H_2N), 38.2 (OCH_2*C*H_2NH), 30.2 (HO(O)C*C*H_2CH$_2$CH$_2$N), 29.6 (HO(O)C*C*H_2CH$_2$CH$_2$N), 22.9 (HO(O)CCH$_2$*C*H_2CH$_2$N), 21.9 (HO(O)CCH$_2$*C*H_2CH$_2$N); ***m/z*** (ES^-): 541.2 $(M-H)^-$ (100%); **HRMS** (ES^+) for $C_{24}H_{35}N_2O_{12}$ $(M+H)^+$: calcd 543.2185, found 543.2185; **RP-HPLC** (λ_{282}) t_R 3.56 min (100 %) **ELSD** t_R 3.64 min (100 %) (Method 2).

5.6.2 Binding and elution studies

Catechol modified peptide (4.9) - Binding

In a typical experiment, boronic acid modified CPG **4.3** was placed into a Supelco Filtration Tube and washed in MeOH (3x), H_2O (3x) and 100 mM PBS (pH 7.6) with 5 mM TCEP (3x). 0.6 mM peptide **4.9** solution was prepared in 100 mM PBS (pH 7.6) with 5 mM TCEP and mixed with varying equivalents (relative to peptide) of boronic acid modified CPG **4.3** for either 1 min (10 and 20 eq) or 10 min (2, 4, 6, 10 and 20 eq). Peptide solution was removed from the boronic acid modified CPG **4.3** by vacuum filtration and eluate (100 µL) was injected onto an analytical HPLC running *Method 2* (General methods) with detection at 282 nm. The area under the HPLC chromatogram peak was integrated using Agilent Chemstation software. All experiments were carried out in triplicate.

Catechol modified peptide (4.9) - Elution

Boronic acid modified CPG **4.3** (6.3 µmol, 30 mg, theoretical loading = 0.21 mmol/g) was placed into a Supelco Filtration Tube and washed in MeOH (3x), H_2O (3x) followed by addition of peptide **4.9** (5 mM) in 5% DIPEA in DMF with 20 mM TCEP with mixing for 10 min. Peptide solution was removed by vacuum filtration and the resin was washed with MeOH (2 x 0.5 mL), 5% DIPEA in DMF with 20 mM TCEP (2 x 0.5 mL) and Et_2O (3 x 1 mL) followed by drying of the resin in a vacuum oven at 40 °C for 1 h. Loaded resin (2 mg) was treated with 1% TFA/H_2O (1 mL) for various lengths of time (<10 s and 1, 5, 10 and 15 min) before applying vacuum filtration to the resin. Eluates were analysed by injecting onto an analytical HPLC

running *Method 2* (General methods) with detection at 282 nm. The area under the HPLC chromatogram peak was integrated using Agilent Chemstation software. All experiments were carried out in triplicate.

Hydroxamic acid modified peptide (4.25) - Binding

Binding of peptide **4.25** to boronic acid modified CPG **4.3** was carried out in a similar manner to binding of peptide **4.9** except that 0.6 mM peptide **4.25** solution was made in 100 mM PBS (pH 8.4). 1-6 eq of boronic acid CPG **4.3** were mixed with peptide **4.25** solution for 30 min. In another study either 4, 10 or 20 eq of boronic acid CPG **4.3** were mixed with peptide **4.25** solution for the following times: 0.5, 1, 2, 4, 10 and 30 min.

Hydroxamic acid modified peptide (4.25) - Elution

Saturation of CPG **4.3** with peptide **4.25** and elution was achieved using the same method as with peptide **4.9** except the binding buffer used was 100 mM PBS (pH 8.4).

5.6.3 Tagging and enrichment studies

In a typical tagging experiment, peptide (1 mg/mL) in 50% CH_3CN/50% 100 mM TEAA pH 8.0 buffer was labelled with NHS-ester tag (3 eq) with mixing for 2 h (TCEP (20 mM) was used when tagging with **4.1**). Enrichment of tagged peptides was carried out as in Section 5.6.2. Enriched tagged peptide mixtures were separated online by nano-LC on a 25 min gradient (5-80% phase B, CH_3CN + 0.5% acetic acid), on-line separated on C18-packed picotip emitter (Proxeon) and analysed on an LTQ-Orbitrap Classic (ThermoElectron, Germany) mass spectrometer.

5.6.4 NHSS cross-linker activation

In a typical NHSS activation reaction, diacid cross-linker (10 mg, 1eq) in dry DMF (0.1 M) was added to polystyrene supported DCC (2.6 eq) along with NHSS (2.4 eq). The resin mixture was stirred gently under nitrogen for 24 h, after which the resin

was filtered and solvent removed *in vacuo*. The resulting NHSS ester was used directly for protein cross-linking without further purification. Cross-linking was confirmed by gel electrophoresis of cross-linked protein.

5.6.5 Cross-linking studies

Protein cross-linking studies were carried out at the Wellcome Trust Centre for Cell Biology in the University of Edinburgh by Lau Sennels. In a typical (10 μL) experiment, protein (0.8 μg/μL) in cross-linker buffer (10 mM HEPES pH 8.0, 200 mM potassium acetate) was mixed with NHS/NHSS activated cross-linker (in protein/cross-linker ratios of 1:100-1:1000, final concentration = 1 mM) and incubated on ice for 2 h. The reaction was stopped by addition of 2.5 M ammonium bicarbonate (1 μL) for 45 min on ice. Gel electrophoresis of cross-linked proteins was carried out using Invitrogen Pre-Cast 3-12% polyacrylamide gel using MES running buffer and Coomassie blue stain. Bands from the SDS-PAGE gel corresponding to cross-linked complexes were excised and the proteins reduced/alkylated and digested using trypsin following standard protocols. Cross-linked peptide mixtures were separated online by nano-LC on either 25 min or 95 min gradients (5-80% phase B, CH_3CN + 0.5% acetic acid), on-line separated on C18-packed picotip emitter (Proxeon) and analysed on an LTQ-Orbitrap Classic (ThermoElectron, Germany) mass spectrometer. Raw data was acquired in cycles of 1 FT-MS (30000 resolution) and top 6 data-dependent IT-MS2 (7500 resolution), singly-charged precursors excluded. Raw data was processed into peak lists using MaxQuant (Cox and Mann, 2008) and searched against protein sequence databases using in-house written software Xi. MS2 data was validated using the in-house Xaminatrix program, which sorted data into high and low confidence.

References

[1] Graham, T. *Phil. Trans. Roy. Soc.*, **1861**, *151*, 183-224.

[2] Lloyd, D. J. *Colloid Science*; Alexander, J., Ed.; The Chemical Catalog Co.; NY, **1926**, *1*, 767

[3] Flory, P. *J. Discuss. Faraday Soc.* **1974**, *57*, 7-18.

[4] (a) van Bommel, K. J. C.; Friggeri, A.; Shinkai, S. *Angew. Chem. Int. Ed.* **2003**, *42*, 980-999. (b) Jung, J. H.; Kobayashi, H.; van Bommel, K. J. C.; Shinkai, S.; Shimizu, T. *Chem. Mater.* **2002**, *14*, 1445-1447. (c) Sugiyasu, K.; Fujita, N.; Shinkai, S. *J. Mater. Chem.* **2005**, *15*, 2747-2754. (d) Xue, P.; Lu, R.; Huang, Y.; Jin, M.; Tan, C.; Bao, C.; Wang, Z.; Zhao, Y. *Langmuir* **2004**, *20*, 6470-6475.

[5] (a) Murdan, S.; Gregoriadis, G.; Florence, A. T. *J. Pharm. Sci.* **1999**, *88*, 608-614. (b) Motulsky, A.; Lafleur, M.; Couffin-Hoarau, A. C.; Hoarau, D.; Boury, F.; Benoit, J.-P.; Leroux, J. C. *Biomaterials* **2005**, *26*, 6242-6253. (c) Friggeri, A.; Feringa, B. L.; van Esch, J. *J. Controlled Release* **2004**, *97*, 241-248.

[6] Jain, A.; Kim, Y. T.; McKeon, R. J.; Bellamkonda, R. V. *Biomaterials*, **2006**, *27*, 497-504.

[7] (a) Walter, A.; Hannich, M.; Schmich, B.; Loifenfeld, M. *Eur. Pat. Appl.* **2007** EP 1792640; (b) Warr, J.; Fraser, S.; Aussant, E.; Masakatsu, U. *Eur. Pat. Appl.* **2007** EP 1767185

[8] Jenning, V.; Gysler, A.; Schäfer-Korting, M.; Gohla, S. H. *Eur. J. Pharm. Biopharm.* **2000**, *49*, 211-218.

[9] Gong, J. P. *Soft Matter* **2006**, *2*, 544-552.

[10] (a) Madamwar, D.; Thakar, A. *Appl. Biochem. Biotechnol.* **2004**, *118*, 361-369. (b) Delimitsou, C.; Zoumpanioti, M.; Xenakis, A.; Stamatis, H. *Biocatal. Biotransform.* **2002**, *20*, 319-327. (c) Fadnavis, N. W.; Koteshwar, K. *Biotechnol. Prog.* **1999**, *15*, 98-104.

[11] Mizrahi, S.; Gun, J.; Kipervaser, Z. G.; Lev, O. *Anal. Chem.* **2004**, *76*, 5399-5404.

[12] Abdallah, D. J.; Weiss, R. G. *Adv. Mater.* **2000**, *12*, 1237-1247.

[13] Cushing, M. C.; Anseth, K. S. *Science* **2007**, *316*, 1133-1134.

[14] (a) Estroff, L. A.; Hamilton, A. D. *Chem. Rev.* **2004**, *104*, 1201-1218. (b) Yong, K.; Mooney, D. J. *Chem. Rev.* **2001**, *101*, 1869-1880. (c) Tiller, J. C. *Angew. Chem.* **2003**, *115*, 3180. (d) Tiller, J. C. *Angew. Chem. Int. Ed.* **2003**, *42*, 3072-3075. (e)

Van Bommel, K. J. C.; van der Pol, C.; Muizebelt, I.; Friggeri, A.; Meetsma, A.; Feringa, B. L.; van Esch, J. *Angew. Chem. Int. Ed.* **2004**, *43*, 1663-1667.

[15] Sangeetha, N. M.; Maitra, U. *Chem. Soc. Rev.* **2005**, *34*, 821-836.

[16] (a) Li, X.; Wu, W.; Wang, J.; Duan, Y. *Carbohydr. Polym.* **2006**, *66*, 473-479. (b) Bajpai, A. K.; Giri, A. *Carbohydr. Polym.* **2003**, *53*, 271-279. (c) Yoshida, M.; Koumura, N.; Misawa, Y.; Tamaoki, N.; Matsumoto, H.; Kawanami, H.; Kazaoui, S.; Minami, N. *J. Am. Chem. Soc.* **2007**, *129*, 11039-11041.

[17] Wichterle, O.; Lim, D. *Nature* **1960**, *185*, 117-118.

[18] Guven, O.; Sen, M.; Karadag, E.; Saraydin, D. *Radiation Phys. Chem.* **1999**, *56*, 381-386.

[19] Schneider, G. B.; English, A.; Abraham, M.; Zaharias, R.; Stanford, C.; Keller, J. *Biomaterials*, **2004**, *25*, 3023-3028.

[20] Hoffman, A. S. *Adv. Drug Deliv. Rev.*, **2002**, *43*, 3-12.

[21] Lai, Y-C. *J. Appl. Polym. Sci.*, **1997**, *66*, 1475-1484.

[22] (a) Guner, A.; Kara, M. *Polymer*, **1998**, *39*, 1569-1572. (b) Lopergolo, L. C.; Lugao, A. B.; Catalani, L. H. *Polymer*, **2003**, *44*, 6217-6222. (c) Stammen, J. A.; Williams, S.; Ku, D. N.; Guldberg, R. E. *Biomaterials*, **2001**, *22*, 799-806.

[23] Lugao, A. B.; Rogero, S. O.; Malmonge, S. M. *Radiation Phys. Chem.* **2002**, *63*, 543-546.

[24] Chuang, W-Y.; Young, T-H.; Yao, C-H.; Chiu, W-Y. *Biomaterials*, **1999**, *20*, 1479-1487.

[25] Chen, P.; Zhang, W.; Luo, W.; Fang, Y. *J. Appl. Poly. Sci.* **2004**, *93*, 1748-1755.

[26] Venkatesh, S.; Sizemore, S. P.; Byrne, M. E. *Biomaterials*, **2007**, *28*, 717-724.

[27] Walton, D.; Lorimer, P. "Polymers", Oxford University Press, 2000, pp. 76-79.

[28] Xuequan, L.; Maolin, Z.; Jiuqiang, L.; Hongfei, H. *Radiation Phys. Chem.* **2000**, *57*, 477-480.

[29] Liu, Y.; Chan-Park, M. B. *Biomaterials* **2009**, *30*, 196-207.

[30] Weiss, R. G.; Terech, P. *Chem. Rev.* **1997**, *97*, 3133-3159.

[31] Lin, Y-C.; Weiss, R. G. *Macromolecules* **1987**, *20*, 414-417.

[32] Uhrich, K. E.; Cannizzaro, S. M; Langer, R. S. *Chem. Rev.* **1999**, *99*, 3181-3198.

[33] Xing, B.; Yu, C-W.; Chow, K-H.; Ho, P-L.; Fu, D.; Xu, B. *J. Am. Chem. Soc.* **2002**, *124*, 14846-14847.

[34] Menger, F. M.; Caran, K. L. *J. Am. Chem. Soc.* **2000**, *122*, 11679-11691.

[35] Bradford, S. C. *Biochem. J.* **1921**, *15*, 553-563.

[36] Keller, A. *Faraday Discuss. Chem. Soc.* **1995**, *101*, 1-49.

[37] Wang, R.; Geiger, C.; Chen, L.; Swanson, B.; Whitten, D. G. *J. Am. Chem. Soc.* **2000**, *122*, 2399-2400.

[38] Terek, P.; Furman, I.; Weiss, R. G. *J. Phys. Chem.* **1995**, *99*, 9558-9566.

[39] Krieg, E.; Shirman, E.; Weissman, H.; Shimoni, E.; Wolf, S. G.; Pinkas, I.; Rybtchinski, B. *J. Am. Chem. Soc.* **2009**, *131*, 14365-14373.

[40] Simmons, B. A.; Taylor, C. E.; Landis, F. A.; John, V. T.; McPherson, G. L.; Schartz, D. K; Moore, R. *J. Am. Chem. Soc.* **2001**, *123*, 2414-2421.

[41] Aggeli, A.; Nyrkova, I. A.; Bell, M.; Harding, R.; Carrick, L.; McLeish, T. C. B.; Semenov, A. N.; Boden, N. *Proc. Natl. Acad. Sci.* **2001**, *98*, 11857-11862.

[42] Fenniri, H.; Mathivanan, P.; Vidale, K. L.; Sherman, D. M.; Hallenga, K.; Wood, K. V.; Stowell, J. G. *J. Am. Chem. Soc.* **2001**, *123*, 3854-3855.

[43] Xing, B.; Choi, M-F.; Xu, B. *Chem. Commun.* **2002**, 362-363.

[44] Fuhrhop, J. H.: *Chem. Rev.* **1993**, *93*, 1565-1582.

[45] Lu, L.; Cocker, T. M.; Bachman, R. E.; Weiss, R. G. *Langmuir* **2000**, *16*, 20-34.

[46] Mukkamala, R.; Weiss, R. G. *Langmuir* **1996**, *12*, 1474-1482.

[47] Estroff, L. A.; Hamilton, A. D. *Angew. Chem. Int. Ed.* **2000**, *39*, 3447-3450.

[48] Schonbeek, F. S.; vanEsch, J. H.; Hulst, R.; Kellog, R. M.; Feringa, B. L. *Chem. Eur. J.* **2000**, *6*, 2633-2643.

[49] Menger, F. M.; Venkatasubban, K. S. *J. Org. Chem.* **1978**, *43*, 3413-3414.

[50] Yoza, K.; Amanokura, N.; Ono, Y.; Akao, T.; Shinmori, H.; Takeuchi, M.; Shinkai, S.; Reinhoudt, D. N. *Chem. Eur. J.* **1999**, *5*, 2722-2729.

[51] (a) Furman, I.; Weiss, R. G.; *Langmuir* **1993**, *9*, 2084-2088; (b) Lin, X.-C.; Kachar, B.; Weiss, R. G. *J. Am. Chem. Soc.* **1989**, *111*, 5542-5551.

[52] Jayawarna, V.; Ali, M.; Jowitt, T. A.; Miller, A. F.; Saiani, A.; Gough, J. E.; Ulijn, R. V. *Adv. Mater.* **2006**, *18*, 611-614.

[53] (a) Gronwald, O.; Snip, E.; Shinkai, S. *Curr. Opin. Colloid Interface Sci.* **2002**, *7*, 148-156; (b) Sakurai, K.; Ono, Y.; Jung, J. H.; Okamoto, S.; Sakurai, S.; Shinkai, S. *J. Chem. Soc., Perkin Trans. 2* **2001**, 108-112.

[54] Binder, W. H.; Smrzka, O. W. *Angew. Chem. Int. Ed.* **2006**, *45*, 7324-7328.

[55] Huang, X.; Terech, P.; Raghavan, S. R.; Weiss, R. G. *J. Am. Chem. Soc.* **2005**, *127*, 4336-4344.

[56] Liu, X. Y.; Sawant, P. D.; Tan, W. B.; Noor, B. M.; Pramesti, C.; Chen, B. H. *J. Am. Chem. Soc.* **2002**, *124*, 15055-15063.

[57] Yang, Z.; Liang, G.; Ma, M.; Gao, Y.; Xu, B. *J. Mater. Chem.* **2007**, *17*, 850-854.

[58] Takahashi, A.; Sakai, M.; Kato, T. *Polym. J.* **1980**, *12*, 335-341.

[59] Ratner, B. D.; Hoffman, A. S. "Synthetic Hydrogels for Biomedical Applications", American Chemical Society, 1976, pp. 1-36.

[60] Nicolson, P. C.; Vogt, J. *Biomaterials* **2001**, *22*, 3273-3283.

[61] Akin, F.; Spraker, M.; Aly, R.; Leyden, J.; Raynor, W.; Landin, W. *Pediatr. Dermatol.* **2001**, *18*, 282-290.

[62] Kioussis, D. R.; Wheaton, F. W.; Kofinas, P. *Aquacult. Eng.* **1999**, *19*, 163-178.

[63] Kulawardana, E. U.; Neckers, D. C. *J. Polym. Sci., Part A: Polym. Chem.* **2010**, *48*, 55-62.

[64] Karim, A. A.; Bhat, R. *Trends Food Sci. Tech.* **2008**, *19*, 644-656.

[65] Helling, R. B.; Goodman, H. M.; Boyer, H. W. *J. Virol.* **1974**, *14*, 1235-1244.

[66] Petersen, O. W.; Ronnov-Jessen, L.; Howlett, A. R.; Bissell, M. J. *Proc. Natl. Acad. Sci.* **1992**, *89*, 9064-9068.

[67] Hui, L.; Krishnendu, R. *Tissue Eng.* **2005**, *11*, 319-330.

[68] Reichardt, L. F. *Phil. Trans. R. Soc. B* **2006**, *361*, 1545-1564.

[69] Luboradzki, R.; Gronwald, O.; Ikeda, M.; Shinkai, S.; Reinhoudt, D. N. *Tetrahedron* **2000**, *56*, 9595-9599.

[70] Ostuni, E.; Kamaras, P.; Weiss, R. G. *Angew. Chem. Int. Ed.* **1996**, *35*, 1324-1326.

[71] Kiyonaka, S.; Shinkai, S.; Hamachi, I. *Chem. Eur. J.* **2003**, *9*, 976-983.

[72] Nakano, K.; Hishikawa, Y.; Sada, K.; Miyata, M.; Hanabusa, K. *Chem. Lett.* **2000**, 1170-1171.

[73] Gortner, R. A.; Hoffman, W. F. *J. Am. Chem. Soc.* **1921**, *43*, 2199.

[74] Menger, F. M.; Yamasaki, Y.; Catlin, K. K.; Nishimi, T. *Angew. Chem. Int. Ed.* **1995**, *34*, 585-586.

[75] Wolf, C. G. L.; Rideal, E. K. *Biochem. J.* **1922**, *16*, 548.

[76] Matteucci, M.; Bhalay, G.; Bradley, M. *J. Peptide Sci.* **2004**, *10*, 318-325.

[77] Kamber, B.; Hartmann, A.; Eisler, K.; Riniker, B.; Rink, H.; Sieber, P.; Rittel, W. *Helv. Chim. Acta* **1980**, *63*, 899-915 and references therein.

[78] Schanche, J.-S. *Mol. Diversity* **2003**, *7*, 287-291.

[79] Dallinger, D.; Kappe, O. C. *Chem. Rev.* **2007**, *107*, 2563-2591.

[80] Krammer, P.; Mittelstadt, S.; Vogel, H. *Chem. Eng. Technol.* **1999**, *22*, 126-130.

[81] Yang, Z.; Liang, G.; Ma, M.; Gao, Y.; Xu, B. *J. Mater. Chem.* **2007**, *17*, 850-854.

[82] Diaz-Mochon, J. J.; Tourniaire, G.; Bradley, M. *Chem. Soc. Rev.* **2006**, *36*, 449-457.

[83] Diaz-Mochon, J. J.; Bialy, L.; Keinicke, L.; Bradley, M. *Chem. Commun.* **2005**, 1384-1386.

[84] Deegan, R. D.; Bakajin, O.; Dupont, T. F.; Huber, G.; Nagel, S. R.; Witten, T. A. *Nature*, **1997**, *389*, 827-829.

[85] Stryer, L. *Science*, **1968**, *162*, 526-533.

[86] DeToma, R. P.; Easter, J. H.; Brand, L. *J. Am. Chem. Soc.* **1976**, *98*, 5001-5007.

[87] Das, D.; Dasgupta, A.; Roy, S.; Mitra, R. N.; Debnath, S.; Das, P. K. *Chem. Eur. J.* **2006**, *12*, 5068-5074.

[88] Suzuki, M.; Yumoto, M.; Kimura, M.; Shirai, H.; Hanabusa, K. *Chem. Eur. J.* **2003**, *9*, 348-354.

[89] Mathias, J. H.; Rosen, M. J.; Davenport, L. *Langmuir*, **2001**, *17*, 6148-6154.

[90] Cull, T. R.; Goulding, M. J.; Bradley, M. *Adv. Mater.* **2007**, *19*, 2355-2359.

[91] De Gans, B. J.; Schubert, U. S. *Macromol. Rapid Commun.* **2003**, *24*, 659-666.

[92] zur Hausen, H. *Nat. Rev. Cancer* **2002**, *2*, 342-350.

[93] You, J.; Croyle, J. L.; Nishimura, A.; Ozato, K.; Howley, P. M. *Cell* **2004**, *117*, 349-360.

[94] Ryan, D. P.; Matthews, J. M. *Curr. Opin. Struct. Biol.* **2005**, *15*, 441-446.

[95] Schwarz-Linek, U.; Werner, J. M.; Pickford, A. R.; Gurusiddappa, S.; Kim, J. H.; Pilka, E. S.; Briggs, J. A. G.; Gough, T. S.; Höök, M.; Campbell, I. D.; Potts, J. R. *Nature* **2003**, *423*, 177-181.

[96] Bach, I. *Mech. Develop.* **2000**, *91*, 5-17.

[97] Hacein-Bey-Abina, S.; Von Kalle, C.; Schmidt, M.; McCormack, M. P.; Wulffraat, N.; Leboulch, P.; Lim, A.; Osborne, C. S.; Pawliuk, R.; Morillon, E.; Sorensen, R.; Forster, A.; Fraser, P.; Cohen, J. I.; de Saint Basile, G.; Alexander, I.; Wintergerst,

U.; Frebourg, T.; Aurias, A.; Stoppa-Lyonnet, D.; Romana, S.; Radford-Weiss, I.; Gross, F.; Valensi, F.; Delabesse, E.; Macintyre, E.; Sigaux, F.; Soulier, J.; Leiva, L. E.; Wissler, M.; Prinz, C.; Rabbitts, T. H.; Le Deist, F.; Fischer, A.; Cavazzana-Calvo, M. *Science* **2003**, *302*, 415-419.

[98] Zhao, L.; Chmielewski, J. *Curr. Opin. Struct. Biol.* **2005**, *15*, 31-34.

[99] Sali, A. *Structure* **2003**, *11*, 1043-1047.

[100] Yee, A.; Pardee, K.; Christendat, D.; Savchenko, A.; Edwards, A. M.; Arrowsmith, C. H. *Acc. Chem. Res.* **2003**, *36*, 183-189.

[101] Yates, J. R. *Trends in Genetics* **2000**, *16*, 5-8.

[102] Zhang, Z.; Smith, D. L. *Protein Sci.* **1993**, *2*, 522-531.

[103] Pramanik, B. N.; Bartner, P. L.; Mirza, U. A.; Liu, Y. H.; Ganguly, A. K. *J. Mass Spectrom.* **1998**, *33*, 911-920.

[104] Farmer, T. B.; Caprioli, R. M. *J. Mass Spectrom.* **1998**, *33*, 697-704.

[105] Young, M. M.; Tang, N.; Hempel, J. C.; Oshiro, C. M.; Taylor, E. W.; Kuntz, I. D.; Gibson, B. W.; Dollinger, G. *Proc. Natl. Acad. Sci.* **2000**, *97*, 5802-5806.

[106] Tang, X.; Munske, G. R.; Siems, W. F.; Bruce, J. E. *Anal. Chem.* **2005**, *77*, 311-318.

[107] Lee, Y. J. *Mol. Biosyst.* **2008**, *4*, 816-823.

[108] Quiocho, F. A.; Richards, F. M. *Proc. Natl. Acad. Sci. USA* **1964**, *52*, 833-839.

[109] Zahn, H.; Meienhofer, J. *Makromol. Chem.* **1958**, *26*, 153-166.

[110] Hartman, F. C.; Wold, F. *J. Am. Chem. Soc.* **1966**, *88*, 3890-3891.

[111] Davies, G. E.; Stark, G. R. *Proc. Natl. Acad. Sci.* **1970**, *66*, 651-656.

[112] Patterson, S. D.; Aebersold, R. *Electrophoresis* **1995**, *16*, 1791-1814.

[113] Rappsilber, J.; Siniossoglou, S.; Hurt, E. C.; Mann, M. *Anal. Chem.* **2000**, *72*, 267-275.

[114] Bennett, K. L.; Kussmann, M.; Björk, P.; Godzwon, M.; Mikkelsen, M.; Sørensen, P.; Roepstorff, P. *Protein Sci.* **2000**, *9*, 1503-1518.

[115] Sinz, A.; Wang, K. *Biochemistry*, **2001**, *40*, 7903-7913.

[116] Müller, D. R.; Schindler, P.; Towbin, H.; Wirth, U.; Voshol, H.; Hoving, S.; Steinmetz, M. O. *Anal. Chem.* **2001**, *73*, 1927-1934.

[117] Cai, K.; Itoh, Y.; Khorana, H. G. *Proc. Natl. Acad. Sci.* **2001**, *98*, 4877-4882.

[118] Itoh, Y.; Cai, K.; Khorana, H. G. *Proc. Natl. Acad. Sci.* **2001**, *98*, 4883-4887.

[119] Back, J. W.; Sanz, M. A.; de Jong, L.; de Koning, L. J.; Nijtmans, L. G. J.; de Koster, C. G.; Grivell, L. A.; van der Spek, H.; Muijsers, A. O. *Protein Sci.* **2002**, *11*, 2471-2478.

[120] Lanman, J. L.; Lam, T. T.; Barnes, S.; Sakalian, M.; Emmett, M. R.; Marshall, A. G.; Prevelige Jr, P. E. *J. Mol. Biol.* **2003,** *325*, 759-772.

[121] Davidson, W. S.; Hilliard, G. M. *J. Biol. Chem.* **2003**, *278*, 27199-27207.

[122] Wine, R. N.; Dial, J. M.; Tomer, K. B.; Borchers, C. H. *Anal. Chem.* **2002**, *74*, 1939-1945.

[123] Taverner, T.; Hall, N. E.; O'Hair, R. A. J.; Simpson, R. J. *J. Biol. Chem.* **2002**, *277*, 46487-46492.

[124] Back, J. W.; Notenboom, V.; de Koning, L. J.; Muijsers, A. O.; Sixma, T. K.; de Koster, C. G.; de Jong, L. *Anal. Chem.* **2002**, *74*, 4417-4422.

[125] D'Ambrosio, C.; Talamo, F.; Vitale, R. M.; Amodeo, P.; Tell, G.; Ferrara, L.; Scaloni, A. *Biochemistry*, **2003**, *42*, 4430-4443.

[126] Trester-Zedlitz, M.; Kamada, K.; Burley, S. K.; Fenyö, D.; Chait, B. T.; Muir, T. W. *J. Am. Chem. Soc.* **2003**, *125*, 2416-2425.

[127] Pearson, K. M.; Pannell, L. K.; Fales, H. M. *Rapid Commun. Mass Spectrom.* **2002**, *16*, 149-159.

[128] Dihazi, G. H.; Sinz, A. *Rapid Commun. Mass Spectrom.* **2003**, *17*, 2005-2014.

[129] Kruppa, G. H.; Schoeniger, J.; Young, M. M. *Rapid Commun. Mass Spectrom.* **2003**, *17*, 155-162.

[130] Chen, X.; Chen, Y. H.; Anderson, V. E. *Anal. Biochem.* **1999**, *273*, 192-203.

[131] Chen, X.; Eswaran, D.; Smith, M. A.; Perry, G.; Anderson, V. E. *Bioconjugate Chem.* **1999**, *10*, 112-118.

[132] Back, J. W.; Hartog, A. F.; Dekker, H. L.; Muijsers, A. O.; de Koning, L. J.; de Jong, L. *J Am. Chem. Soc. Mass Spectrom.* **2001**, *12*, 222-227.

[133] Karas, M.; Hillenkamp, F. *Anal. Chem.* **1988**, *60*, 2299-2301.

[134] Fenn, J. B.; Mann, M.; Meng, C. K.; Wong, S. F.; Whitehouse, C. M. *Science*, **1989**, *246*, 64-71.

[135] Karas, M.; Krüger, R. *Chem. Rev.* **2003**, *103*, 427-439.

[136] Dreisewerd, K. *Chem. Rev.* **2003**, *103*, 395-425.

[137] Knochenmuss, R.; Zenobi, R. *Chem. Rev.* **2003**, *103*, 441-452.

[138] Chang, W. C.; Huang, L. C. L.; Wang, Y. S.; Peng, W. P.; Chang, H. C.; Hsu, N. Y.; Yang, W. B.; Chen, C. H. *Anal. Chim. Acta* **2007**, *582*, 1-9.

[139] Beavis, R. C.; Chait, B. T.; Fales, H. M. *Rapid Commun. Mass Spectrom.* **1989**, *3*, 436-439.

[140] Beavis, R. C.; Chait, B. T.; Standing, K. G. *Rapid Commun. Mass Spectrom.* **1989**, *3*, 432-435.

[141] Strupat, K.; Karas, M.; Hillenkamp, F. *Int. J. Mass Spectrom. Ion Processes* **1991**, *72*, 89-102.

[142] Spengler, B. *J. Mass Spectrom.* **1997**, *32*, 1019-1036.

[143] (a) Chang, Z.; Kuchar, J.; Hausinger, R. P. *J. Biol. Chem.* **2004**, *279*, 15305-15313. (b) Giron-Monzon, L.; Manelyte, L.; Ahrends, R.; Kirsch, D.; Spengler, B.; Friedhoff, P. *J. Biol. Chem.* **2004**, *279*, 49338-49345. (c) Onisko, B.; Fernández, E. G.; Freire, M. L.; Schwarz, A.; Baier, M.; Camiña, F.; García, J. R.; Villamarín, S. R. S.; Requena, J. R. *Biochemistry* **2005**, *44*, 10100-10109.

[144] Wilm, M.; Mann, M. *Anal. Chem.* **1996**, *68*, 1-8.

[145] Holland, L. A.; Jorgenson, J. W. *Anal. Chem.* **1995**, *67*, 3275-3283.

[146] Jonscher, K. R.; Yates, J. R. *Anal. Biochem.* **1997**, *244*, 1-15.

[147] Silva, R. A. G. D.; Hilliard, G. M.; Fang, J.; Macha, S.; Davidson, W. S. *Biochemistry* **2005**, *44*, 2759-2769.

[148] Füzesi, M.; Gottschalk, K. E.; Lindzen, M.; Shainskaya, A.; Küster, B.; Garty, H.; Karlish, S. J. D. *J. Biol. Chem.* **2005**, *280*, 18291-18301.

[149] Gardner, M. W.; Brodbelt, J. S. *J. Am. Soc. Mass Spectrom.* **2008**, *19*, 344-357.

[150] Sinz, A. *J. Mass Spectrom.* **2003**, *38*, 1225-1237.

[151] Hermanson, G. T. "Bioconjugate Techniques", 2nd Edition Elsevier, 2008.

[152] Ghosh, S. S.; Kao, P. M.; McCue, A. W.; Chappelle, H. L. *Bioconjugate Chem.* **1990**, *1*, 71-76.

[153] Kalkhof, S.; Ihling, C.; Mechtler, K.; Sinz, A. *Anal. Chem.* **2005**, *77*, 495-503.

[154] Bragg, P. D.; Hou, C. *Arch. Biochem. Biophys.* **1975**, *167*, 311-321.

[155] Lomont, A. J.; Fairbanks, G. *J. Mol. Biol.* **1976**, *104*, 243-261.

[156] Cuatrecasas, P.; Parikh, I. *Biochemistry* **1972**, *11*, 2291-2299.

[157] Swaim, C. L.; Smith, J. B.; Smith, D. L. *J. Am. Chem. Soc. Mass Spectrom.* **2004**, *15*, 736-749.

[158] Leavell, M. D.; Novak, P.; Behrens, C. R.; Schoeniger, J. S.; Kruppa, G. H. *J. Am. Chem. Soc. Mass Spectrom.* **2004**, *15*, 1604-1611.

[159] Mädler, S.; Bich, C.; Touboul, D.; Zenobi, R. *J. Mass Spectrom.* **2009**, *44*, 694-706.

[160] Lynch, B. A.; Koshland, D. E. *Proc. Natl. Acad. Sci. USA* **1991**, *88*, 10402-10406.

[161] Byrne, M. P.; Broomfield, C. A.; Stites, W. E. *J. Protein Chem.* **1996**, *15*, 131-136.

[162] (a) Smyth, D. G.; Blumenfeld, O. O.; Konigsberg, W. *Biochem. J.* **1964**, *91*, 589-595. (b) Gorin, G.; Martic, P. A.; Doughty, G. *Arch. Biochem. Biophys.* **1966**, *115*, 593-597. (c) Heitz, J. R.; Anderson, C. D.; Anderson, B. M. *Arch. Biochem. Biophys.* **1968**, *127*, 627-636. (d) Partis, M. D.; Griffiths, D. G.; Roberts, G. C.; Beechey, R. B. *J. Protein Chem.* **1983**, *2*, 263-277.

[163] Brewer, C. F.; Riehm, J. P. *Anal. Biochem.* **1967**, *18*, 248-255.

[164] Gilchrist, T. L.; Rees, C. W. "Carbenes, Nitrenes, and Arynes (Studies in Modern Chemistry)", Nelson Publishers, London, 1969, pp. 131.

[165] (a) Keana, J. F. W.; Cai, S. X. *J. Org. Chem.* **1990**, *55*, 3640-3647. (b) Cai, S. X.; Glenn, D. J.; Gee, K. R.; Yan, M.; Cotter, R. E.; Reddy, N. L.; Weber, E.; Keana, J. F. W. *Bioconj. Chem.* **1993**, *4*, 545-548. (c) Schnapp, K. A.; Platz, M. S. *Bioconj. Chem.* **1993**, *4*, 178-183. (d) Soundararajan, N.; Liu, S. H.; Soundrararajan, S.; Platz, M. S. *Bioconj. Chem.* **1993**, *4*, 256-261. (e) Schnapp, K. A.; Poe, R.; Leyva, E.; Soundararajan, N.; Platz, M. S. *Bioconj. Chem.* **1993**, *4*, 172-177. (f) Yan, M.; Cai, S. X.; Wybourne, M. N.; Keana, J. F. W. *Bioconj. Chem.* **1994**, *5*, 151-157.

[166] Smith, R. A. G.; Knowles, J. R. *J. Am. Chem. Soc.* **1973**, *95*, 5072-5073.

[167] Brunner, J. *Annu. Rev. Biochem.* **1993**, *62*, 483-514.

[168] Collioud, A.; Clémence, J. F.; Sänger, M.; Sigrist, H. *Bioconj. Chem.* **1993**, *4*, 528-536.

[169] Suchanek, M.; Radzikowska, A.; Thiele, C. *Nat. Meth.* **2005**, *2*, 261-267.

[170] Walling, C.; Gibian, M. J. *J. Am. Chem. Soc.* **1965**, *87*, 3361-3364.

[171] (a) Dormán, G.; Prestwich, G. D. *Biochemistry* **1994**, *33*, 5661-5673. (b) Egnaczyk, G. F.; Greis, K. D.; Stimson, E. R.; Maggio, J. E. *Biochemistry*, **2001**, *40*, 11706-11714. (c) Junge, H. J.; Rhee, J.S.; Jahn, O.; Varoqueaux, F.; Spiess, J.; Waxham, M. N.; Rosenmund, C.; Brose, N. *Cell*, **2004**, *118*, 389-401.

[172] Åhrman, E.; Lambert, W.; Aquilina, J. A.; Robinson, C. V.; Emanuelsson, C. S. *Protein Sci.* **2007**, *16*, 1464-1478.

[173] Peterson, J. J.; Young, M. M.; Takemoto, L. J. *Molecul. Vision* **2004**, *10*, 857-866.

[174] King, G. J.; Jones, A.; Kobe, B.; Huber, T.; Mouradov, D. *Anal. Chem.* **2008**, *80*, 5036-5043.

[175] Green, N. *Biochem. J.* **1963**, *89*, 585-591.

[176] Alley, S. C.; Ishmael, F. T.; Jones, A. D.; Benkovic, S. J. *J. Am. Chem. Soc.* **2000**, *122*, 6126-6127.

[177] Sinz, A.; Kalkhof, S.; Ihling, C. *J. Am. Soc. Mass Spectrom.* **2005**, *16*, 1921-1931.

[178] Nessen, M. A.; Kramer, G.; Back, J.; Baskin, J. M.; Smeenk, L. E.; de Koning, L. J.; van Maarseveen, J. H.; de Jong, L.; Bertozzi, C. R.; Hiemstra, H.; de Koster, C. G. *J. Proteome Res.* **2009**, *8*, 3702-3711.

[179] Huisgen, R. "1,3-Dipolar Cycloaddition Chemistry (Vol. 1)", Wiley, 1984, pp. 1-176.

[180] Tornøe, C. W.; Christensen, C.; Meldal, M. *J. Org. Chem.* **2002**, *67*, 3057-3064.

[181] Kasper, P. T.; Back, J. W.; Vitale, M.; Hartog, A. F.; Roseboom, W.; de Koning, L. J.; van Maarseveen, J. H.; Muijsers, A. O.; de Koster, C. G.; de Jong, L. *Chembiochem* **2007**, *8*, 1281-1292.

[182] Eggert, H.; Frederiksen, J.; Morin, C.; Norrild, J. C. *J. Org. Chem.* **1999**, *64*, 3846-3852.

[183] Friedman, S.; Pizer, R. *J. Am. Chem. Soc.* **1975**, *97*, 6059-6062.

[184] Pizer, R.; Selzer, R. *Inorg. Chem.* **1984**, *23*, 3023-3026.

[185] Kustin, K.; Pizer, R. *J. Am. Chem. Soc.* **1969**, *91*, 317-322.

[186] Babcock, L.; Pizer, R. *Inorg. Chem.* **1980**, *19*, 56-61.

[187] Lorand, J. P.; Edwards, J. O. *J. Org. Chem.* **1959**, *24*, 769-774.

[188] Pizer, R.; Tihal, C. *Inorg. Chem.* **1992**, *31*, 3243-3247.

[189] Weith, H. L.; Wiebers, J. L.; Gilham, P. T. *Biochemistry* **1970**, *9*, 4396-4401.

[190] Klenk, D. C.; Hermanson, G. T.; Krohn, R. I.; Fujimoto, E. K.; Mallia, A. K.; Smith, P. K.; England, J. D.; Wiedmeyer, H. M.; Little, R. R.; Goldstein, D. E. *Clin. Chem.* **1982**, *28*, 2088-2094.

[191] Gamoh, K.; Brooks, C. J. W. *Anal. Sci.* **1993**, *9*, 549-552.

[192] Tucker, J. L.; Couturier, M.; Leeman, K. R.; Hinderaker, M. P.; Andresen, B. M. *Org. Proc. Res. Dev.* **2003**, *7*, 929-932.

[193] Higa, S.; Kishimoto, S. *Anal. Biochem.* **1986**, *154*, 71-74.

[194] Leonard, W. R.; Belyk, K. M.; Conlon, D. A.; Bender, D. R.; DiMichele, L. M.; Liu, J.; Hughes, D. L. *J. Org. Chem.* **2007**, *72*, 2335-2343.

[195] Strawbridge, S. M.; Green, S. J.; Tucker, J. H. R. *Chem. Commun.* **2000**, 2393-2394.

[196] (a) Hall, D. G.; Tailor, J.; Gravel, M. *Angew. Chem. Int. Ed.* **1999**, *38*, 3064-3067. (b) Arimori, S.; Hartley, J. H.; Bell, M. L.; Oh, C. S.; James, T. D. **2000**, *41*, 10291-10294. (c) Gravel, M.; Thompson, K. A.; Zak, M.; Bérubé, C.; Hall, D. G. *J. Org. Chem.* **2002**, *67*, 3-15. (d) Carboni, B.; Pourbaix, C.; Carreaux, F.; Deleuze, H.; Maillard, B. *Tet. Lett.* **1999**, *40*, 7979-7983.

[197] (a) Li, W.; Burgess, K. *Tet. Lett.* **1999**, *40*, 6527-6530. (b) Dunsdon, R. M.; Greening, J. R.; Jones, P. S.; Jordan, S.; Wilson, F. X. *Bioorg. Med. Chem. Lett.* **2000**, *10*, 1577-1579. (c) Arnauld, T.; Barrett, A. G. M.; Seifried, R. *Tet. Lett.* **2001**, *42*, 7899-7901. (d) Yang, W.; Gao, X.; Springsteen, G.; Wang, B. *Tet. Lett.* **2002**, *43*, 6339-6342.

[198] Abed, O.; Vaskevich, A.; Arad-Yellin, R.; Shanzer, A.; Rubinstein, I. *Chem. Eur. J.* **2005**, *11*, 2836-3841.

[199] Abed, O.; Wanunu, M.; Vaskevich, A.; Arad-Yellin, R.; Shanzer, A.; Rubinstein, I. *Chem. Mater.* **2006**, *18*, 1247-1260.

[200] Tang, J.; Liu, Y.; Qi, D.; Yao, G.; Deng, C.; Zhang, X. *Proteomics* **2009**, *9*, 5046-5055.

[201] Stolowitz, M. L.; Kaiser, R. J.; Lund, K. P. *U.S. Pat. Appl. Publ.* **1998** US Patent No. 5594111

[202] Springer, A. L.; Gall, A. S.; Hughes, K. A.; Kaiser, R. J.; Li, G.; Lucas, D. D.; Lund, K. P.; Spicer, D. A.; Wiley, J. **2002** *Affinity-Based Immobilization Tools for Functional Genomics.* Presented at Transcriptome 2002: From Functional to Systems Biology, Seattle, WA, March 10-13, 2002.

[203] Stolowitz, M. L.; Ahlem, C.; Hughes, K. A.; Kaiser, R. J.; Kesicki, E. A.; Li, G.; Lund, K. P.; Torkelson, S. M.; Wiley, J. P. *Bioconj. Chem.* **2001**, *12*, 229-239.

[204] Sienkiewicz, P. A.; Roberts, D. C. *J. Inorg. Nucl. Chem.* **1980**, *42*, 1559-1575.

[205] Wiley, J. P.; Hughes, K. A.; Kaiser, R. J.; Kesicki, E. A.; Lund, K. P.; Stolowitz, M. L. *Bioconj. Chem.* **2001**, *12*, 240-250.

[206] Niu, W.; Smith, M. D.; Lavigne, J. J. *J. Am. Chem. Soc.* **2006**, *128*, 16466-16467.

[207] Hall, L. W.; Odom, J. D.; Ellis, P. D. *J. Am. Chem. Soc.* **1975**, *97*, 4527-4531.

[208] Kress, J.; Zanaletti, R.; Amour, A.; Ladlow, M.; Frey, J. G.; Bradley, M. *Chem. Eur. J.* **2002**, *8*, 3769-3772.

[209] Yan, B. "Analytical methods in combinatorial chemistry", CRC Press, 1999, pg. 131.

[210] Fara, M. A.; Díaz-Mochón, J. J.; Bradley, M. *Tetrahedron Lett.* **2006**, *47*, 1011-1014.

[211] Lee, J.; Griffin, J. H. *J. Org. Chem.* **1996**, *61*, 3983-3986.

[212] Chehade, K. A. H.; Baruch, A.; Verhelst, S. H. L.; Bogyo, M. *Synthesis* **2005**, *2*, 240-244.

[213] Fujii, N.; Jacobsen, R. B.; Wood, N. L.; Schoeniger, J. S.; Guy, R. K. *Bioorg. Med. Chem. Lett.* **2004**, *14*, 427-429.

[214] Kettner, C. A.; Shenvi, A. B. *J. Biol. Chem.* **1984**, *259*, 15106-15114.

[215] Philipp, M.; Bender, M. L. *Proc. Natl. Acad. Sci.* **1971**, *68*, 478-480.

[216] Reddy, A. S.; Kumar, M. S.; Reddy, G. R. *Tetrahedron Lett.* **2000**, *41*, 6285-6288.

[217] Patel, R. N.; Goswami, A.; Chu, L.; Donovan, M. J.; Nanduri, V.; Goldberg, S.; Johnston, R.; Siva, P. J.; Nielsen, B.; Fan, J.; He, W.; Shi, Z.; Wang, K. Y.; Eiring, R.; Cazzulino, D.; Singh, A.; Mueller, R. *Tetrahedron: Asymmetry* **2004**, *15*, 1247-1258.

[218] Nagarajan, K.; Rajappa, S.; Iyer, V. S. *Tetrahedron* **1967**, *23*, 1049-1054.

[219] Astles, P. C.; Brown, T. J.; Handscombe, C. M.; Harper, M. F.; Harris, N. V.; Lewis, R. A. *Eur. J. Med. Chem.* **1997**, *32*, 409-423.

[220] Chen, H.; Chen, Y.; Sheardown, H.; Brook, M. A. *Biomaterials* **2005**, *26*, 7418-7424.

[221] Liu, W.; Howarth, M.; Greytak, A. B.; Zheng, Y.; Nocera, D. G.; Ting, A. Y.; Bawendi, M. G. *J. Am. Chem. Soc.* **2008**, *130*, 1274-1284.

[222] Visintin, C.; Aliev, A. E.; Riddall, D.; Baker, D.; Okuyama, M.; Hoi, P. M.; Hiley, R.; Selwood, D. L. *Org. Lett.* **2005**, *7*, 1699-1702.

[223] Hancock, W. S.; Battersby, J. E. *Anal. Biochem.* **1976**, *71*, 260-264

[224] Gude, M.; Ryf, J.; White, P. D. *Lett. Pept. Sci.* **2002**, *9*, 203-206

[225] Chaleix, V.; Sol, V.; Huang, Y.; Guilloton M.; Granet, R.; Blais, J. C.; Krausz, P. *Eur. J. Org. Chem.* **2003**, 1486-1493.

[226] Thomas, E. W.; Cromwell, T. I. *J. Org. Chem.* **1972**, *37*, 744-747.